# Modeling the Earth System in the Mission to Planet Earth Era

***July 1993***



*Prepared by*

**Sushel Unninayar**

**Kenneth H. Bergman**

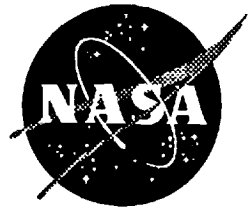

# *Table of Contents*

# *Foreword*

This report provides a broad overview of global Earth system modeling in the Mission to Planet Earth (MTPE) era to the multidisciplinary audience encompassed by the Global Change Research Program (GCRP). This audience includes physical scientists, social scientists, and policy-level managers.

Brevity has been somewhat sacrificed in favor of retaining background material so that a soil scientist, biologist, chemist, or economist may obtain a reasonable grasp of how the atmosphere, the ocean, or radiative processes are handled in a global model—without having to read a large collection of reference material. Thus, the individual specialist may find certain sections overly familiar. This multidisciplinary coverage should provide the necessary impetus toward a fuller participation by the scientific disciplines involved in and required for the development of the next-generation global Earth systems models.

The Earth Observing System (EOS)—the centerpiece of MTPE—is covered in some depth to provide the reader with a feel for the next-generation space-based instruments, and what they are intended to deliver. Other operational and planned observing systems, which together with EOS comprise MTPE, have only been mentioned briefly, with references provided to details in other documents. Requirements for observations and long-term monitoring are covered throughout the report. The term "MTPE era" is used in a generic sense to refer to the need for global observational coverage with long-term time continuity and a heavy reliance on remote sensing to fulfill this need; of course, independent supporting, ground-based observations are needed to complement the space-based components of Mission to Planet Earth.

This review is based on presentations and discussions held during the NASA Climate Modeling Workshop of November 13-15, 1991, in Alexandria, Virginia, and on an extensive survey of available scientific literature. Over 50 national and international experts representing virtually all scientific disciplines participated in the workshop, as well as representatives of most major research institutions and Federal agencies.

The efforts of NASA's Office of Mission to Planet Earth and the Earth Science Support Office in organizing the workshop and in preparing and publishing this report are gratefully acknowledged.

# *Executive Summary*

A major part of the "global Earth system" is composed of the *atmosphere* (troposphere, stratosphere, and mesosphere), the *hydrosphere* (oceans and other important elements of the hydrological cycle such as lakes, rivers, and subterranean waters), the *land surface* and *biosphere* (soils, vegetation cover, continental fauna and flora, and fauna of the oceans), the *cryosphere* (the ice fields of Greenland and the Antarctic, other continental glaciers, snow fields, and sea ice), and the *geosphere/lithosphere* (continents and their topography, ocean bottoms, the Earth's crust and molten core, gravitational fields, geomagnetics, Earth rotation, volcanic and earthquake processes, etc.). Recent additions to this list are the *chemosphere* (chemical constituents and exchanges) and the *technosphere* (technology, anthropogenic forcing, etc.). The system is in a continual state of flux, with parts of the system leading and others lagging in time. The highly nonlinear interactions between the subsystems tend to occur on many time and space scales; therefore, the subsystems are not always in equilibrium with each other, and not even necessarily in internal equilibrium.

Time scales of global system fluctuation and change are described in Section 2. It should be noted that as the characteristic time scale of a global system event or feature increases, so does the space scale. Correspondingly, more and more components and subsystems are involved physically and interactively in defining the state of the composite system, which imposes more comprehensive and stringent requirements on global monitoring systems and on global models.

Section 3 provides a rubric for modeling the global Earth system, as presently understood. Deficiencies in observations and monitoring strategies and the limitations of the present generation of global models are highlighted at the end of each major subsection. Given the dynamic and interactive nature of the actual physical global Earth system, one may deem the subdivision of this section to be somewhat arbitrary. For example, clouds and water vapor, radiative processes, greenhouse gases, ozone, aerosols, and dust are treated separately, even though they are an integral part of the atmosphere and processes within the atmosphere that control or modulate the global Earth system. This is partly because of the historical evolution of science and the current separation found in scientific specialization. No doubt, their boundaries will dissolve in the future, but they have not (generally) yet. On account of the complexity of the Earth system, it is generally felt that a hierarchical set of models is needed, with complementary resolutions and functional capabilities. Eventually, they all need to be interlinked to perform as an emsemble that emulates nature. The critical issue of the parameterization of physical processes also receives attention in this section.

The ability of models to predict the future state of the global Earth system and the extent to which their predictions are reliable are covered in Sections 4 and 5. Although substantial progress has been made over the past 10 or 20 years, an equally substantial research effort is required over the next decade or two to reduce the uncertainties in predictions and to improve the mathematical (model) representation of physical processes.

The "engineering" use of global system models (and predictions) is covered in Section 6. The term "engineering" implies that an absolutely accurate mathematical depiction of the global system is not possible at this time, and that the various simplifications are necessary to approximate the real physical system. These approximations will presumably undergo improvement and changes with more research. Such improvements can only arise through much better and comprehensive observational methods and monitoring; thus, the need for a stable and true global Earth observing system receives emphasis. Even with the deficiencies of present models of the global system, they provide a framework for future policy planning if used correctly and pragmatically in an "engineering" sense. Prior to such application, it would be essential that existing global model prediction capabilities be explained and defined exactly, together with assumptions and limitations, in a language understandable to a lay user of model-generated information. These individuals need not fall within the bounds of the modeling community. The interaction between global models (i.e., predictions) and impact assessment and policy guidance are also briefly covered in this section. Until absolutely correct predictions can be attained, all future scenarios of the state of the global system or its "climate" will need to be updated and revised regularly (operationally) to guide policy decisions.

With the advent of satellite remote sensing and true global coverage, but not necessarily (directly) the geophysical parameters needed for monitoring and modeling, there is an increasing need for improved transform algorithms and better methods to assimilate this information into global models. Some of these aspects are covered in Section 7. Of particular importance, perhaps, is the need to improve data assimilation schemes so that data sets are available for research purposes and for the initialization of prediction models.

Future monitoring and data requirements are detailed in Section 8. As improvements are made in both models and observing system technology, these requirements may change, but it is felt that fundamental requirements are already reasonably well-known, even if the corresponding

data are not presently collected. Global coverage and long-term data continuity must be secured.

Section 9 covers the NASA-initiated concept "Mission to Planet Earth," which employs space- and ground-based measurement systems to provide the scientific basis for understanding global change. The centerpiece of Mission to Planet Earth—the Earth Observing System—includes a series of polar-orbiting and low-inclination satellites to provide long-term observations of the land surface, biosphere, solid Earth, atmosphere, and oceans. In tandem with NASA's EOS Program, the polar-orbiting and mid-inclination platforms from Europe, Japan, and the U.S. National Oceanic and Atmospheric Administration (NOAA) form the basis for a comprehensive International Earth Observing System (IEOS). EOS instruments are also briefly described in this section to give the reader a feel for the range and scope of the next-generation satellite platforms and what they are expected to deliver.

Section 10 concludes this review with general remarks concerning the state of global system modeling and observing technology and the need for future research. Specific recommendations for research are contained under subject titles throughout the report. Key areas for research and development include the following:

- **Modeling and Data**—A comprehensive observational database for initializing and validating model predictions is needed. This includes paleoclimatic data for validating model predictions of past climatic states as well as currently observed data. Long-term records of key climate parameters are needed in order to properly validate model integrations for periods of several years. Observed data also have an important role in the development and improvement of model parameterizations of subgrid-scale climatic processes.
- **Space- and Ground-Based Research**—*In situ* and theoretical studies of physical, chemical, biological, and geological processes must be complemented by comprehensive spaced-based observations to provide global coverage of key environmental parameters. Processes such as air-sea interaction, atmosphere-biosphere interaction, convective and precipitation processes, and cloud-radiation feedback need special attention in order to improve key parameterizations and to facilitate interactive coupling of model components. Long-term monitoring is essential to describe the dynamic and changing nature of the global system.
- **Data Assimilation**—Obtaining information from a complex suite of observing systems in a usable form for modeling requires the development and application of a model-based data assimilation methodology to produce research-quality data sets. These data sets will incorporate model dynamics and physics to get the best possible and most consistent fit of variable fields to the observed data. As such, they will represent value added to data sets of the original observations, and are expected to form the database for most modeling development and applications.
- **Parameterization and Scaling**—A major component of required research involves development of improved parameterizations of subgrid-scale processes. Such parameterizations include convective clouds and precipitation, cloud-radiation interaction, land surface hydrology and its interaction with the atmosphere, air-sea interaction processes, atmosphere-biosphere coupling, and subgrid-scale sea-ice dynamics. As model resolution is increased, some parameterizations can be replaced with explicit formulations, and other parameterizations can be made more physically realistic.
- **Computers**—The availability of greatly increased computer resources, with speeds and capacities up to 1,000 times those of present-generation systems, will be essential for further significant progress in global climate/Earth system modeling. Hopes are focused on massive parallel supercomputer systems, but they will require complex software code development. The Government-wide high performance computing initiative is directed towards maximizing efficient use of state-of-the-art computational architectures.
- **Total Earth System Modeling**—The ultimate goal is to develop a comprehensive dynamically, thermally, and chemically interactive model of the physical-biological Earth system. Such a total Earth system model would be driven by only two truly external forces—solar radiation and gravity—although anthropogenic influences such as atmospheric and oceanic pollutants and changes in the land surface could be treated as variable "scenarios" that would have the effect of external forcings. The choice of scenarios would likely continue to be determined by policy considerations. Although the physical-dynamical parts of an Earth system model either already exist or are well along in development, the chemical and biological components are less advanced and will require focused effort in the next several

years. Recent evidence linking the climate of the Earth with solar fluctuations and solid Earth geology need to be explicitly incorporated into Earth system models. Increased remotely sensed and other observations will be needed, along with pertinent field experiments, in order to improve understanding and modeling of these components and their coupling to physical and dynamical components.

- **Future Research Framework for Earth System Modeling**—Although substantial progress has been made over the last decade in modeling the Earth system, each incremental improvement has led to expanded requirements for observational data, field experiments, process studies, and improved model numerics. To the extent that these ancillary requirements are met, the next decade should witness significant progress in model development and predictive capability. Future models should substantially reduce uncertainties of present prediction models and should provide much clearer guidance for policymakers. In conjunction with the improved monitoring capability provided by EOS and other observing systems and improved computational power, these future models will provide a more precise basis for determining the impact of environmental change on the world's socio-economic activities.

# 1. Introduction: The Global System

A major part of the "global Earth system" consists of the physical system—that is, the *atmosphere* (troposphere, stratosphere, and the mesosphere), *hydrosphere* (oceans and other elements of the hydrological cycle such as lakes, rivers and subterranean waters), the *land surface* and *biosphere* (the soils, vegetation cover, continental and oceanic fauna and flora), the *cryosphere* (the ice fields of Greenland and the Antarctic, other continental glaciers, snow fields, and sea ice), and the *geosphere/lithosphere* (continents and their topography, ocean bottoms, the Earth's crust and molten core, the gravity field, as well as mantle convection and tectonic crust deformation, geomagnetic flow patterns in the liquid core, mantle-core interaction, gravity field changes due to mass movements, volcanic and earthquake processes, Earth rotation, etc.) (ICSU 1987). Recent additions to this list are the *chemosphere* (chemical constituents and exchanges) and the *technosphere* (technology, anthropogenic activity, etc.). The system is in a continual state of flux, with parts of the system leading and others lagging in time. The highly nonlinear interactions between the subsystem tend to occur on many time and space scales. Therefore, the subsystems are not always in equilibrium with each other, and not even necessarily in internal equilibrium. Due to the complexity and interactive nature of the global system, it has been convenient to select a combination of its components and define this set as the "internal" system, considering the remaining components as the "external" system (Peixóto and Oort 1984). By and large, the separation is made on the basis of the characteristic time scales of change of individual components of the system. The precise selection of components forming the internal system often depends on the ability to model the system, including interactions between subsystems, as well as the "objective" of the model. Currently, the "climate system" represents the closest global models have come to approximating the actual total global Earth system. Details are presented in this report.

Figure 1 illustrates several of the components and interactions involved in the global system. The atmosphere is the fastest changing component of the global system and also the most responsive. In the past, the atmosphere alone was regarded as the prominently dynamic, and changing, part of the global climate system. The other components of the global system were thought to be more static, thereby external in a global model; they were involved only in the specification of boundary conditions. However, the strong coupling between the atmosphere and oceans has forced the recognition that both subsystems must be considered as a more complete internal system. Climate variability during the recent history of the planet has demonstrated that the cryosphere needed to be included in the internal system. This introduced the notion of the global system wherein the atmosphere, hydrosphere (especially oceans), and the cryosphere were defined as internal interacting physical components of the system and the lithosphere, biosphere, and geosphere as external components. These external components are now beginning to be recognized as critical and interactive parts of the global system that must be modeled adequately (especially interacting with the atmosphere) before prediction is possible. To the above, simplified definition of the global system must be added anthropogenic forcing and other influences due to changes in solar output and orbital fluctuations. Furthermore, when studying or modeling the physical processes that link any two components of the global system, elements of other components of the system are inextricably involved. For example, atmosphere-hydrosphere coupling must include processes involving moisture recycling through vegetation and the upper layers of the land surface/soil.

Though somewhat arbitrary, the above distinctions have had an important impact on the evolution of how the global system is mathematically modeled and how the models are used for prediction purposes. These distinctions have been influenced strongly by the characteristic time scales of variability of the various components and subsystems of the global system.

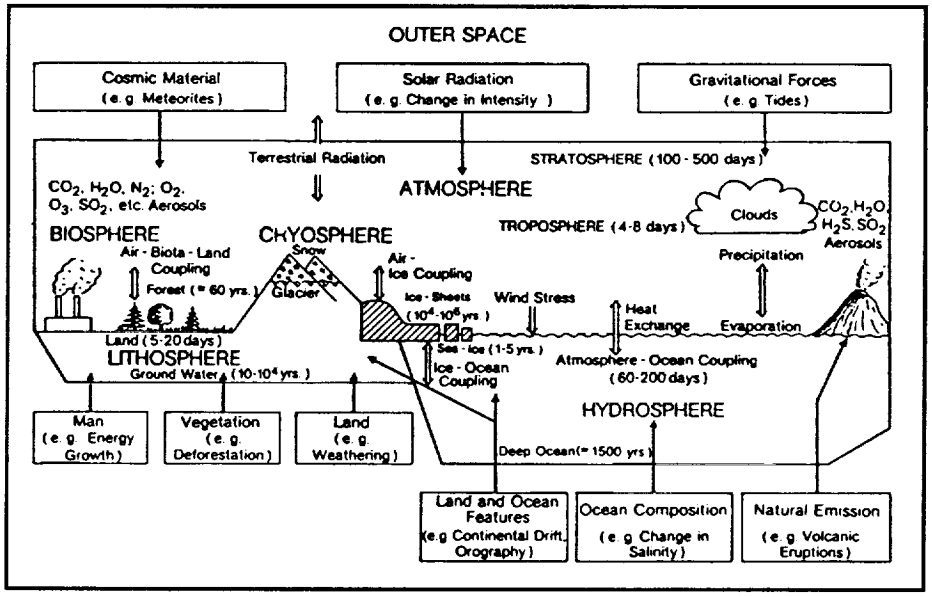


*Figure 1. Schematic illustration of various components and interactions in the climate system. Source: Bach 1984.*

# 2. *Time Scales of Fluctuation and Change*

A linear separation of phenomena according to time scale (for discussion purposes) does not preclude significant interaction between them. Slowly varying global fluctuations can modulate higher frequency phenomena and should be regarded as large-scale constraints or forcings on the coupled global system and the characteristics and distribution of the system's "weather" and "climate." This implies that even if specific events cannot be fully predicted, it would still be useful to be able to predict the average limits or thresholds between which the ensemble system fluctuates. An *in situ* (space or time) extrapolation may then be made to transform the predicted information into something useful, such as the distribution of events occurring within the system. Detailed knowledge would, however, be required of the structure of the ensemble of finer space and time scale phenomena, as well as an accurate specification and/or classification of the state of the slowly varying components of the global Earth system.

Fluctuations of the global system and their consequences on time scales, from weeks to decades and longer, are briefly described below to provide perspective to aspects of the system's variability (adapted from Unninayar 1986):

- **1 Day to a Few Weeks**—Weather, the effects of which are immediately felt, is but a short-time atmospheric system fluctuation due to internal instability processes that aim to reestablish mass, momentum, or heat balance on certain space-time scales. Social and economic impacts due to extreme weather events can be great but are usually localized (e.g., wind bursts, flash floods, tornadoes, hurricanes). On a synoptic scale, atmospheric models can make predictions up to about a week. Beyond a few weeks, boundary conditions or coupling with the land and ocean surface become important. Partial, longer term atmospheric memory may exist indirectly through long-wave systems in the atmosphere that are geographically positioned for dynamic and thermodynamic reasons. At present, initialization and other errors in numerical models of the atmosphere, which grow at each integration time step, degrade daily weather forecasting skills beyond a few weeks.
- **Months to 1 Year**—The annual cycle is strongest in this time range and is determined largely by the orbital position of the Earth with respect to the Sun. The change from summer to winter due to the tilt of the Earth's axis from its orbital plane and the climate system's responding to this annual fluctuation in solar radiation are well-known facts. Predicting the severity (cold/hot, wet/dry) of the next season, however, is not simple. Processes that integrate recent history (e.g., months to a year) with present system state need to be taken into account; atmosphere-ocean and atmosphere-land surface/biosphere interactions are important. Also important are 30- to 60-day fluctuations that modulate surface weather as the waves propagate around the globe. Effects are larger—entire national economies can be affected—and the space scale is regional or global.
- **1 to 10 Years**—Interannual variability involves more components and processes of the global system. Atmosphere-ocean coupling is of particular significance [e.g., warm Pacific sea surface temperature (SST) anomalies and the occurrence of El Niño/southern oscillation (ENSO) phenomena]. Anomalies associated with ENSO can be persistent (12 to 18 months) and affect large areas of the world (WMO/UNEP 1986, 1987). The recurrence period of ENSO events is between 2 and 7 years. The El Niño signature is also apparent in changes in the Earth's angular momentum (rotation speed/day length) (Rosen et al. 1983). Thus atmosphere/ocean-solid body (Earth) interactions are likely to be important, involving momentum exchange processes in which tectonic plate movements and earthquakes may participate (Oort 1985). Economic impact can be substantial (estimated at over $10 billion for the 1982-83 El Niño event) and of global scale.
- **10 to 100 Years**—Changes in this time scale are usually designated as long-term trends. Fluctuations of significance are interactions and external influences that modulate the atmosphere and the ocean circulation. For example, there is evidence that the difference in SST anomalies between the Northern Hemisphere oceans and Southern Hemisphere oceans are related to the long time scale (greater than 15 years) fluctuation in the rainfall over the Sahel (Folland and Parker 1985). The physical mechanism for this relationship is hypothesized to be the effect of the global distribution of SST on boundary layer moisture convergence and the intertropical

convergence zone (ITCZ). Greenhouse gases (GHGs) and atmosphere-cryosphere and atmosphere/biosphere land surface interaction are likely to play a part in determining variability in the decadal time scale. Also of relevance are ocean-ice interaction, especially in the Antarctic (Gordon and Comiso 1988), and the exchange of angular momentum between the solid Earth and the atmosphere (Oort 1985). Solar activity and lunar effects (gravitational) also show relationships to wet/drought sequences of fairly long duration (Mitchel 1976) and other atmospheric and surface climate features (Van Loon and Labitske 1990). The situation is complicated by interaction between climate changes and social practice (e.g., overgrazing, deforestation, desertification), which could affect surface albedo, moisture-recycling mechanisms, radiation balance, and, consequently, climate. If present trends continue, the combined concentration of atmospheric $CO_2$ and other GHGs are radiatively equivalent to a doubling of $CO_2$ from preindustrial levels, possibly as early as the 2030s, accompanied by an increase in global mean temperature between 1.5 and 4.5°C and a sea level rise of 20 to 140 cm (Houghton et al., IPCC 1990, 1992). Impacts are likely to be substantial—widespread disruption and dislocation of societies can occur if "anomalous" conditions persist for many years. Even if $CO_2$ levels are reduced drastically, 10- to 100-year time lags introduced by the ocean would ensure persistence.

- **100 to 1,000s of Years**—History documents rather drastic consequences of climatic fluctuations in this time scale. Entire civilizations have been forced to relocate or have been eliminated because of climate change. Historical evidence points to major sea level changes and large-scale floods, or mini ice ages. Ice-ocean and ocean-atmosphere interaction processes appear to play a dominant role, as do changes in greenhouse gas concentrations ($CO_2$, $CH_4$, etc.), solar activity, and orbital parameter fluctuations. Changes in the frequency of volcanic activity, tectonic plate movements, and Earth mantle-core interactions are also likely factors.
- **10,000 to 1,000,000 Years**—Climate variations in this time scale include the major glacial/interglacial cycles during the Quaternary period that are believed to have been initiated by changes in the Earth's orbital parameters, which in turn influence the latitudinal and seasonal variation of solar energy received by the Earth (the Milankovitch Effect) (Berger 1980). All components of the climate system interact on this time scale. Some interactions could lead to abrupt change of much shorter time scale, even though the processes leading to the abrupt change are of longer time scale. An example is the Younger Dryas cold episode, which involved an abrupt reversal of the general warming trend in progress around 10,500 BP as the last episode of continental glaciation came to a close. The event was of global significance, though the signal was the strongest around the northern Atlantic Ocean. Broecker et al. (1989) suggest that the large-scale melting of the Laurentian ice sheet resulted in the influx of huge amounts of low-density freshwater into the northern Atlantic Ocean, which reduced deep water production there. Consequently, the thermohaline circulation, involving a northward flow of water near the ocean surface sinking in the subarctic region, and return flow at depth was affected, altering sea surface temperatures globally (Street-Perrott and Perrott 1990; Houghton et al., IPCC 1990). Thus, fluctuations in the hydrological cycle involving the atmosphere, cryosphere, the oceans, and land surface/biosphere are also important. Impacts are worldwide and large, including large changes in sea level of perhaps 1,000 m or more as implied in Sumerian and Biblical records. Though the 10,000- to 100,000-year time scale appears at first glance to be irrelevant for a 100-year forecast, it would be important to know exactly where in this long-term system fluctuation the planet is in at the present time.
- **Millions of Years**—Fossil and paleoclimatic records point to catastrophic changes approximately every 25 to 30 million years that were involved with the mass extinction of entire species on the Earth. For example, the dinosaurs that dominated the world for over 100 million years were rather abruptly terminated; a lack of intelligence for survival is an unacceptable and somewhat arrogant concoction. Humankind (including homonids, etc.) has thus far managed a mere 5 million years. Several theories exist: Most refer to impacts by large comets or asteroids (detected by an abnormal enrichment in iridium or other noble metals) that caused a terrestrial dust cloud of such extent that sunlight was blocked out, or that an unseen companion star to the Sun (an as yet undetected black hole or brown dwarf in a highly eccentric orbit) initiated intense comet

showers. Some evidence (e.g., mammoths that were instantly frozen and recently excavated in a frozen, not fossilized, state) points to abrupt shifts of the Earth's axis. A third scenario refers to the large rise and fall of sea level (along with changes in ice cover/extent), which is supported by evidence of extensive black shale deposits made possible through the extinction of biota by anoxia.

***Conclusions/Recommendations.*** *As the characteristic time scale of a global system event or feature increases, so does the space scale. Correspondingly, more and more components and subsystems are interactively involved in defining the state of the system. This imposes special requirements in monitoring systems and models. Slowly varying components of the global system (e.g., the middle and the deep ocean) can modulate the frequency and distribution of more rapidly changing components (e.g., the atmosphere).*

# 3. *Modeling the Global Earth System*

Prior to modeling, or in fact monitoring the global system, the goals or objectives of the exercise must be defined and specified. If a range of prediction time scales are chosen (e.g., 2 weeks, 1 year, 10 years, and 100 years), then a range of models would usually be required of differing complexity, resolution, and scope. That is, it would be pointless for a model designed to predict a mesoscale event, such as a localized thunderstorm, to concurrently contain the mathematics (and subsystem components) necessary to predict tectonic plate motion or deep ocean circulation. The converse is also true, unless significant interaction occurs between the subsystems involved. In a model, all subsystems not explicitly (i.e., mathematically) included must be incorporated in the specification of boundary conditions, initial conditions, or forcing functions; this would require a continual global monitoring of the state of these subsystems. As the prediction objective expands in scope to include longer and longer time scales, the prediction model must include interaction with more and more components of the global Earth system.

For example, for forecasting weather (a time scale of a few days), the ocean surface temperatures may be regarded as constant over "weather" time scales. Similarly, the amount of solar radiation reaching the Earth, the distribution of vegetation and soil, and so forth, may be assumed or prescribed as fixed. A prediction model designed and developed to address an objective of predicting the state of the global system 3 days ahead needs to be primarily concerned with the changes within the atmosphere, though interaction with the land and ocean surface needs to be taken into account. On seasonal and interannual time scales, fluctuation in at least the upper layers of the ocean needs to be taken into account; thus, coupled models need to include the thermodynamics of the upper ocean circulation and interactions at the atmosphere-ocean interface. On longer time scale (e.g., 100 years) the entire ocean circulation must be modeled in any prediction scheme as well as a dynamically interactive land surface and biosphere. Using similar arguments, variations in orbital parameters may be assumed to be constant, on a 1- to 10-year time scale but not so on a 100- to 1,000-year time scale. For a full comprehension of the carbon cycle and atmospheric $CO_2$, the carbonate-silicate geochemical cycle is involved where atmospheric $CO_2$ dissolves in rainwater, forming carbonic acid ($H_2CO_3$) which erodes surface rock, releasing calcium and bicarbonate ions into the groundwater flowing into the ocean.

Ideally, observations commensurate with the time scales involved are required to understand the physics and chemistry involved in the forces acting on the system and the interactive feedback processes taking place within and between component subsystems. The luxury of a complete observational record of all components and processes of the global system is presently not available to science despite ingenious methods of reconstructing the history of the planet from paleo and proxy records. Advances in modeling and monitoring will at each step be constrained by the existing (at any point in time) understanding of processes, available computer power, and observational technology, leading, by necessity, to approximations and assumptions. These constraints would impose limits on the theoretically possible "model" Earth system's prediction time and space scales—limits that introduce uncertainties in the future state of the system predicted by the model.

***Conclusions/Recommendations.*** *It is presently impractical, if not impossible, to construct the ideally required global Earth system model of very high resolution (possibly 100 m to 0.5 km) with all components dynamically interacting with one another. Advantage needs to be taken of the differences in the characteristic time scales of change between the various components and processes of the global system in order to construct a viable engineering approximation for the components and processes of practical and specific interest. To do this, the modeling objective in terms of its prediction time range should be specified. A hierarchical set of models of differing complexity and resolution may be required to address global system prediction objectives of short to very long ranges. Observational records corresponding to the space and time scale of the features of the global system being modeled are required for monitoring, process studies, model initialization, and validation.*

*Given the complexity of the global system, a long-term and substantive effort is required in comprehensive observational field experiments and in improved global monitoring and modeling technology. Concurrently, analysis and diagnostic research is required to verify and validate the capabilities of Earth system models; for this, past (including paleo), present, and future observational data are required.*

*In order to simulate or predict events or the future state of the system, more and more components and interactions need to be explicitly modeled as the prediction time range increases. Those components or processes not explicitly modeled must be monitored accurately in order to construct the specification of initial or boundary conditions to the partially modeled global system.*

## 3.1. *Types of Global System Models*

Possibly the most advanced mathematical-numerical models dealing with the global Earth system are those developed to investigate and predict the atmosphere's and the ocean's general circulation—climate and climate change. There are many other sophisticated models designed to simulate the dynamics of ecosystems, soil, ground hydrology, nutrient cycling, plant and animal populations, the transport of pollutants in the air and water, and so on, but they are typically applied to *in situ* or, at best, subregional (i.e., about 1 to 10 $km^2$) problems. One of the challenges in global Earth system modeling is to determine how these *in situ* processes are to be incorporated in global models with substantially larger space scales (10,000 to 62,500 or even 250,000 $km^2$). The inverse problem is just as acute—namely, how to improve the accuracy and representativeness of the output (predictions) of global models at the individual model grid-scale level, and the interpretation of model-simulated or predicted system state variables for *in situ* and subgrid-scale applications.

An elemental cubic volume of 250,000 $km^3$ that represents the algebraic/numerical approximation of an infinitesimal mathematical point in differential calculus is, indeed, a very large volume even if it is small relative to the size of the total Earth system. Even at this coarse resolution, many model computational grid points are required, as are observations to measure the actual global system. Much action and interaction takes place below this resolution (i.e., most weather); thus, there is the need to parameterize all small subgrid-scale processes (i.e., transport, transfer, and exchange processes) in terms of the large-scale variables explicitly resolved by the model. Common examples of parametric representations are the relation of the net turbulent and/or convective transport of heat, momentum, and moisture through the planetary boundary layer to conditions at the surface and at the top of the boundary layer. Another example is the parameterization of heat and moisture transport by deep moist convection in terms of resolvable vertical profiles of temperature and moisture.

There are two basic approaches to parameterization, namely inductive and deductive (Randall 1989). The inductive approach pioneered by Smagorinsky (1960), and recently pursued by Slingo (1980, 1987), in the context of cloud parameterization seeks to identify intuitively plausible relationships between unknowns (such as cloud amount) and known (or currently measured) variables of the problem, such as relative humidity, static stability, or vertical velocity (usually a kinematically computed, not measured, variable). The resulting parameterization is called "empirical" even though scatter diagrams or other systematic observational bases are often not presented. A disadvantage of the inductive approach is that it lacks the theoretical underpinnings and observational evidence that may indicate its limits of applicability. This statement should, perhaps, not be taken too seriously because even if theoretical bases are used in the initial conceptual formulation of a parameterization, the approximations and simplifications applied could render the final product just as obscure as an intuitive guess.

The deductive approach is based on the concept that the development of parameterizations should proceed, as far as possible, from general (and basic) physical principles. Thus, a deductive parameterization should provide a condensed representation of the important physical processes of interest, hence give physical insight into the phenomena being parameterized. The limits of applicability of such a parameterization can be inferred, *a priori*, from its physical basis. Due note should be taken of the phrase "important physical processes of interest" because the accuracy or representativeness of the parameterization depends on the present understanding of what these processes are, either through observational or other considerations. This definition is also constrained, usually by available computer power, because even if all physical processes were known, the resulting parameterization could be (and often is) computationally exorbitant, leading to simplifications that could dilute the formulating premise of the deductive approach.

The final parameterization, no matter whether it is inductively or deductively obtained is, *de facto*, an engineering approximation that can be tested only by comparison with observations of the processes being parameterized and its effect on overall system performance. Intellectually, the deductive approach has much appeal even though in reality it is not clear whether the two approaches yield substantial differences in performance. Performance, in this case, should only be determined on the basis of the true physical process or system under consideration and not the "consensus" view of how the system is anticipated to perform. Consensus views may be right, wrong, or indifferent, and could change with time.

Generally for investigations of the global system and global change, a hierarchy of "models" varying in both physical and mathematical exactness and complexity need to be used. Not all models require supercomputers, and some of the simpler or simplified models provide substantial physical insight into processes. In fact, sophisticated global coupled models are nearly as complex as the natural system, thus rendering cause-effect analysis difficult. That is, the diagnostic analysis of model output is required almost as

much as diagnostic studies of observational data in order to better understand global system processes. Often, simplified models are used to understand the sensitivity of the global system to intentionally isolated processes (including forcings and feedbacks) prior to incorporation in global models. Moreover, global models must parametrically include all important processes not resolved explicitly. High-resolution climate models treat the prediction problem essentially as an extension of numerical weather prediction schemes, but include additional factors (e.g., ice or ocean dynamics, thermodynamics, ice-albedo feedback, water vapor and cloud feedback, etc.).

At another level of parameterization, the transfer properties of the large-scale features are themselves parameterized. By this means, the ensemble statistics produced by repeated runs of the finer resolution models may be introduced at the outset and carried as dependent variables. The validity of this simplification depends on the realistic expression of these ensemble statistics in terms of larger scale variables. Such models are known as statistical-dynamical models. At an even higher level of parameterization the horizontal resolution can be reduced further to the extent that one point represents the entire globe, in which case only vertical profiles of system state parameters such as temperature, humidity, radiative flux, and so forth are produced. Examples of selected global models that include critical elements governing the dynamics of global change, ranging from the simplest parametric representation of the global system to the most complex, are briefly described below.

### 3.1.1. Radiative-Convective Models (RCMs)

Traditionally, the study of the thermal structure of planetary and stellar atmospheres begins with the computation of the radiative equilibrium (RE) temperature profile. A comparison of the RE temperature profile with the observed profile is a measure of the importance of other diabatic (e.g., convection) and dynamical processes. For many planetary atmospheres with strong, radiatively active trace gases (e.g., Mars, Venus, Earth), the computed profile yields a stably stratified region—the stratosphere—overlying a region that is unstable to convection—the troposphere. In 1953, Chandrasehkar suggested that an atmosphere with an initial superadiabatic lapse rate attains a final state of convective equilibrium (the criterion for which was originally defined by Lord Kelvin in 1862). Physically, convective equilibrium means that convection mechanically stirs the atmosphere until a uniform potential temperature is reached.

The radiative equilibrium assumption enables the reduction of the thermodynamic energy balance equation to a balance between the net (i.e., up minus down) radiative fluxes and the vertical heat flux that is the sum of the convective heat flux and the large-scale eddy heat flux transport component. In a moist atmosphere, the convective heat flux also includes the latent heat release term. At the top of the atmosphere, the upward and downward fluxes must be equal. That is, on the long-term average, the net solar radiation absorbed by the planet is in balance with the outgoing terrestrial radiation emitted by the surface-atmosphere system. The convective heat flux vanishes at the top of the troposphere.

The RCMs pioneered by Manabe and Stickler et al. (1965) are discussed extensively by Ramanathan and Coakley (1978). The RCMs represent the vertical structure of the atmosphere, but do not attempt to deal with horizontal variations. However, because many important physical processes occur primarily in vertical columns, in particular radiative transfer and buoyancy-driven natural convection, RCMs can include fairly elaborate process models. Most fully developed RCMs are, in fact, one-dimensional subsets of the complex three-dimensional climate models known as general circulation models (GCMs).

### 3.1.2. Energy Balance Models (EBMs)

EBMs have been developed and applied to a variety of climate change problems by Budyko (1969), Sellers (1969), and North et al. (1983). EBMs typically resolve variations with latitude but not with longitude or height. They do not explicitly simulate the effects of atmospheric motions, but include them very indirectly using mixing lengths or other comparably simplified approaches (Randall 1991). As recently reviewed by Lindzen (1990), EBMs have produced a number of interesting results, including evidence that the Earth's climate may have more than one stable equilibrium under some conditions. Nevertheless, EBMs are so drastically simplified that they can do little more than suggest possibilities for investigations with more complete models.

### 3.1.3. Global Climate Models (GCMs)

Most complex, high-resolution GCMs have been developed to represent the atmosphere (AGCMs) or the ocean (OGCMs). Global climate models usually incorporate coupling between the atmosphere and, at least, the upper layers of the ocean. In order to more correctly investigate the response of the coupled system to changes in "forcings," atmospheric models are asynchronously and dynamically coupled to more complete ocean models (Note: Such dynamically coupled model experiments are computationally expensive). Substantial research is also being carried out with models that couple atmospheric

GCMs with land-surface processes and the biosphere. Coupled models also include aspects of ocean-ice feedback, cloud-radiation feedback, water vapor feedback, soil moisture and ground hydrology, plant physiology, and other processes that need to be integrated into GCMs so that they contain at least the rudimentary elements of a future Earth system model.

Low-resolution GCMs achieve relatively high computational efficiency at the expense of crude resolution of synoptic eddies (atmosphere), ocean eddies (ocean), and processes. The GCMs are routinely used in runs of several decades' (or even 100 to 1,000s of years) duration, making them well-suited, albeit with deficiencies, for studies of interannual variability and long-range global change.

High-resolution GCMs are much better able to resolve atmospheric and oceanic eddies, and incorporate more realistic parameterizations of the hydrological cycle and interactive feedback processes. These GCMs demonstrate the limits of how well the Earth system can be simulated at the present time. Progress is rapid, but constrained by available computer technology, observations, and the accuracy of the mathematical or numerical representation of processes in parametric form.

### 3.1.4. Global Earth System Models (GEMs)

Developing complete Earth system models is a formidable task, given the complexities of the global system and the range of time and space scales that need to be handled. The term "Earth system model" cannot be arbitrarily used without first specifying the objective of the modeling exercise and, particularly, the space and time scales the model is expected to resolve, as well as the space and time scales of events or features the model is expected to predict. At present, models that include interactions between the atmosphere, the ocean, and land surface/vegetation are the most advanced available; they are generally referred to as "climate system models" because their primary application is in predicting global climate change. However, it is well recognized that they are inadequate for simulating or predicting a large number of effect and impact parameters, particularly on the regional scale. Moreover, even the best models incorporate only relatively short time scale interactions between the atmosphere and the land surface, the biosphere, and the geosphere. That is, the internal dynamics of several of these component subsystems are not included even if the exchange of momentum, heat, and moisture are. Advances are expected through improvements in subsystem component models followed by their linkage with existing climate system models. Significant experience has already been obtained in asynchronously running atmospheric and ocean models with inherently different time scales. With increasing computer speeds, experiments are beginning to be conducted with synchronously coupled atmosphere-ocean models, which in principle should more realistically simulate the natural system. More work needs to be done to incorporate the interaction between vastly different space scales involved in hydrological and ecological systems. Eventually, through a combination of higher resolution, faster computers, better observations, and improved parameterizations, global models are expected to evolve into viable approximations of the total Earth system.

***Conclusions/Recommendations.*** *Simplified global models such as energy balance models or radiative-convective models can be quite useful in studying several global climate system processes, including the response of the global system to changes in forcing functions; however, the models do not provide information on the regional scale, thus cannot be used to evaluate the impact of climate change on, for example, ecosystems or socio-economic activities.*

*More complex models of the global system involve the parameterization of a large number of interactions and processes. Both inductive and deductive approaches are used, but in either case interactively coupled global GCMs of the ocean and the atmosphere (which also include coupling with the biosphere and cryosphere) represent the limits of how well the Earth system can be simulated at the present time. Through a combination of higher resolution, faster computers, better global observations, and improved parameterizations, reasonable approximations to the total Earth system are anticipated.*

## 3.2. *Partitioning the System*

Because of the complexity of the global Earth system, it has to be mathematically treated as an ensemble of component systems or subsystems. A system may be defined within a thermodynamical framework as a finite region in space specified by a set of physical variables with additive or extensive properties. The variables could represent, for example, volume, internal energy, mass of individual components, and angular momentum (Peixóto and Oort 1984). A composite system is a conjunction of spatially disjointed simple systems separated by conceptual or real partitions or walls. The amount of any particular quantity (e.g., mass) for the global system is then the sum of that quantity for all subsystems. The set of all such quantities (i.e., mass, energy, momentum) specifies the state of the composite system. The laws of conservation dictate that variables with extensive properties (excluding the relativistic domain) are conservative. The amount of any quantity transferred between two adjacent subsystems represents a thermodynamic process. If no transfer is possible, the

wall is restrictive and the two systems uncoupled; otherwise the system is interactive or coupled.

Systems can also be classified in terms of their functions or internal complexity. When the boundary of the system is restrictive for all quantities, it is called an "isolated" system. When the boundary is restrictive only for matter, the system is closed (impermeable boundary). An open system is one in which the transfer of mass is allowed. A cascading system is composed of a chain of open subsystems that are linked dynamically by a cascade of mass or energy in such a way that the output of mass or energy from one subsystem becomes the input for the next subsystem. An open system can be decaying, cyclic, or haphazardly fluctuating.

The state of a system may also be specified by intensive properties that are independent of the total mass of the system and defined at a given point of the system at a given time. Intensive properties may change in time, hence are considered to define a field in the domain of the system. As such, they are not additive properties, which include temperature, pressure, densities, velocities, and so forth. For example, the arithmetic sum of all temperature values at all points within a system is not a conserved quantity. Similarly, the total number and density of a particular variety of plant, animal, or micro-organic species is not a conservative quantity, even if the total mass of the planet is.

In modeling the global Earth system, formulating equations are usually defined to describe nonconservative field variables at a point within the system; that is, the system is defined by such field variables as temperature, pressure, moisture, velocities, and so on. However, the equations need to be formulated in such a way that when integrated over all points of the system, such parameters as mass, energy, and momentum are conserved. The physical Earth system can be described by mathematical equations constructed upon the basis of the laws of physics. At present, the biological Earth system needs to be handled somewhat differently even though fundamental physical principles apply at the microphysical level. The integral constraints are not simple: The population density and distribution of any one particular species of plant, animal, or micro-organism will be constrained by ambient climate, nutrient supply, competition with other species, the abundance of predator species (both macro- and micro-organic), and genetic defense mechanisms. In very simplistic terms, the biosphere is a result of the conversion of inorganic to organic matter, involving a multitude of interactions between solar radiation, climate and weather, soil, water, chemistry, and biology. It would not be preposterous to state that we are only at the very beginning of modeling the complexities of the biosphere and ecosystems.

***Conclusions/Recommendations.*** *Because the global Earth system is complex and deals with components and processes of vastly differing space and time scales, ranging from the molecular to the planetary, it has to be treated mathematically as an ensemble of component systems or subsystems. The amount of any quantity transferred between adjacent subsystems represents a thermodynamic process. If no transfer is physically possible, the wall is restrictive and the two subsystems are uncoupled; otherwise, the subsystems are interactive or coupled. Models of the Earth system must explicitly account for such exchange processes so that the laws of conservation apply to the entire ensemble system. Many of the interactive and exchange processes need to be parameterized in terms of large-scale field variables. Biological systems require special handling and much more research and monitoring on account of the systems' complexity and a lack of understanding of their causative and response dynamics.*

## *3.3. Modeling Components and Processes of the Global Earth System*

### 3.3.1 The Atmosphere

The atmosphere comprising the Earth's gaseous envelope is the most variable part of the system. The troposphere, wherein lie most weather-producing processes, has a characteristic response time or thermal adjustment time on the order of 1 month. That is, the atmosphere, by transferring heat vertically and horizontally, will adjust to an imposed surface temperature distribution in about a month's time. Figure 2 is a schematic of a highly simplified model of the mechanisms that drive atmospheric motions and climate. The straight arrows represent the energy coming from the Sun, of which about 30 to 35 percent is reflected annually; the reflectivity is the Earth's albedo. The wavy arrows represent the outgoing planetary longwave or infrared radiation. The tropics are warm, because they receive more heat from the Sun than they emit as infrared radiation; the poles are cold, because they radiate more solar energy than they receive, which is due to a greater average solar zenith angle and the presence of more reflective ice and snow cover. This differential heating results in strong equator-to-pole temperature gradients—warm air rises in the tropics and moves poleward to cooler regions until a state of quasi-equilibrium is reached. Were it not for the general circulation of the atmosphere that conveys excess heat from low to high latitudes, the tropics would be much hotter and the polar regions much colder than they are. Owing to the rotation of the Earth, air motions are more complicated than in the case of a simple convective circulation (e.g., a bonfire). As an air parcel moves poleward its radial distance from the axis of the Earth decreases and it takes with it the fast rotational speeds of the equator, thus providing the

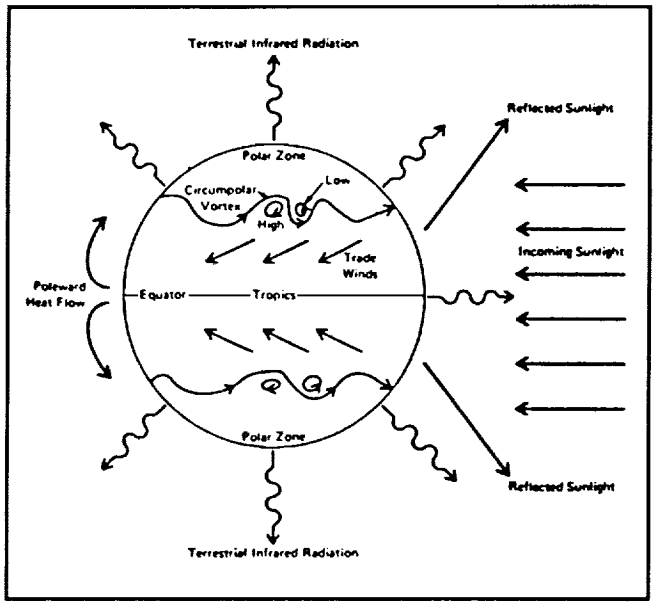


*Figure 2. Schematic illustration of how the major weather systems of the Earth are driven by the unequal heating between the equator and the poles. The tropics intercept a much larger fraction of the incoming solar energy than do the polar zones, thus giving rise to the motions that regulate climate. Source: S.H. Schneider and L. Temkin 1977.*

momentum that creates westerly winds in the mid-latitudes. Similarly, the return flows in the lower layers of the atmosphere become easterlies—hence, the trade winds.

Because of the tilt of the Earth's axis, the zone of maximum heating shifts north-south during the year, creating the summer-to-winter seasonal cycle; therefore, the system is always changing while attempting to reach an equilibrium. The availability of water, and the fact that it changes phase from liquid to gas over typical atmospheric temperature ranges, enhances the coupling between the atmosphere, the oceans, and land surface. Much of the heat redistribution is through the hydrological cycle, as in the sequence of evaporation-clouds-precipitation-runoff. Figure 3 shows the global water cycle and the contents of major reservoirs and rates of transfer between them. As will be seen from later sections, this cycling of water through the system has a pronounced impact on the atmospheric and oceanic general circulation, the radiation balance of the planet, and global and local average temperatures, as well as agricultural, industrial, and socio-economic activities.

Ultimately, at any given location, weather and climate are consequences of differential solar heating, flow instabilities, and interactions between the atmosphere and the underlying oceans, land surface (including vegetation), and snow/ice cover. At longer time scales, climate fluctuations influenced by changes in the radiation balance (i.e., solar input, effect of greenhouse gases, and other forcing factors) need to be taken into account.

Mathematically, the gaseous atmosphere, the liquid ocean, or any other fluid may be treated as an infinite number of fluid particles in four-dimensional motion. Depending on the nature of the fluid, these particles would obey various laws of physics and chemistry. Perhaps the most fundamental of these laws deal with motion and energy that link forces acting on a body with its mass, velocity, and acceleration. The forces are those of pressure, gravity, and friction in a "Newtonian" domain. Dealing with an infinite set of particles is numerically intractable; thus, the fluid atmosphere (and ocean) is represented by a finite number of elemental parcels or cubic volumes, as depicted in Figure 4. Similar algebraic approximations need to be made in time. The atmosphere is laterally unbounded while the oceans are surrounded by the continental land masses. Otherwise, the formulating equations are nearly identical even if atmospheric and oceanic motions and processes are somewhat different on account of the former being a gaseous fluid and the latter a liquid. The formal set of equations usually refer to "Lagrangian" motion—that is, the relationship between forces, time rates of change, etc., acting on and following a particle or element. The instantaneous rate of change of a physical variable or property following the motion of a parcel or particle may also be expressed as the local rate of change at a fixed location plus the change advected into or out of the same location by the ambient fluid motion. The local rate of change is related to physical processes occurring locally; thus, the condensation of moisture would release latent heat, which would increase local temperature. Advective change depends on motion and the local gradient, in space, of the parameter or variable under consideration. That is, if there is no field gradient between neighboring grid points, the advective change would be zero. These latter "Eulerian" expressions of the mathematical equations are customarily used so that a fixed set of grid points may be used to depict the global system. Figure 5 shows one example of a horizontal grid system that could be used in a global model as well as how horizontal and vertical partial derivatives are expressed in finite difference form.

The five basic sets of equations that describe the atmosphere follow. 1) The *three-dimensional momentum equations* relate the time rate of change in the velocity of an elemental parcel of air (i.e., acceleration) to forces acting on the parcel, namely pressure gradient, gravity, centrifugal forces, and friction. The coriolis or apparent force appears in the equations when a frame of reference relative to the Earth's surface is used instead of an absolute inertial coordinate system. The vertical component of the momentum equation is usually approximated for large-scale

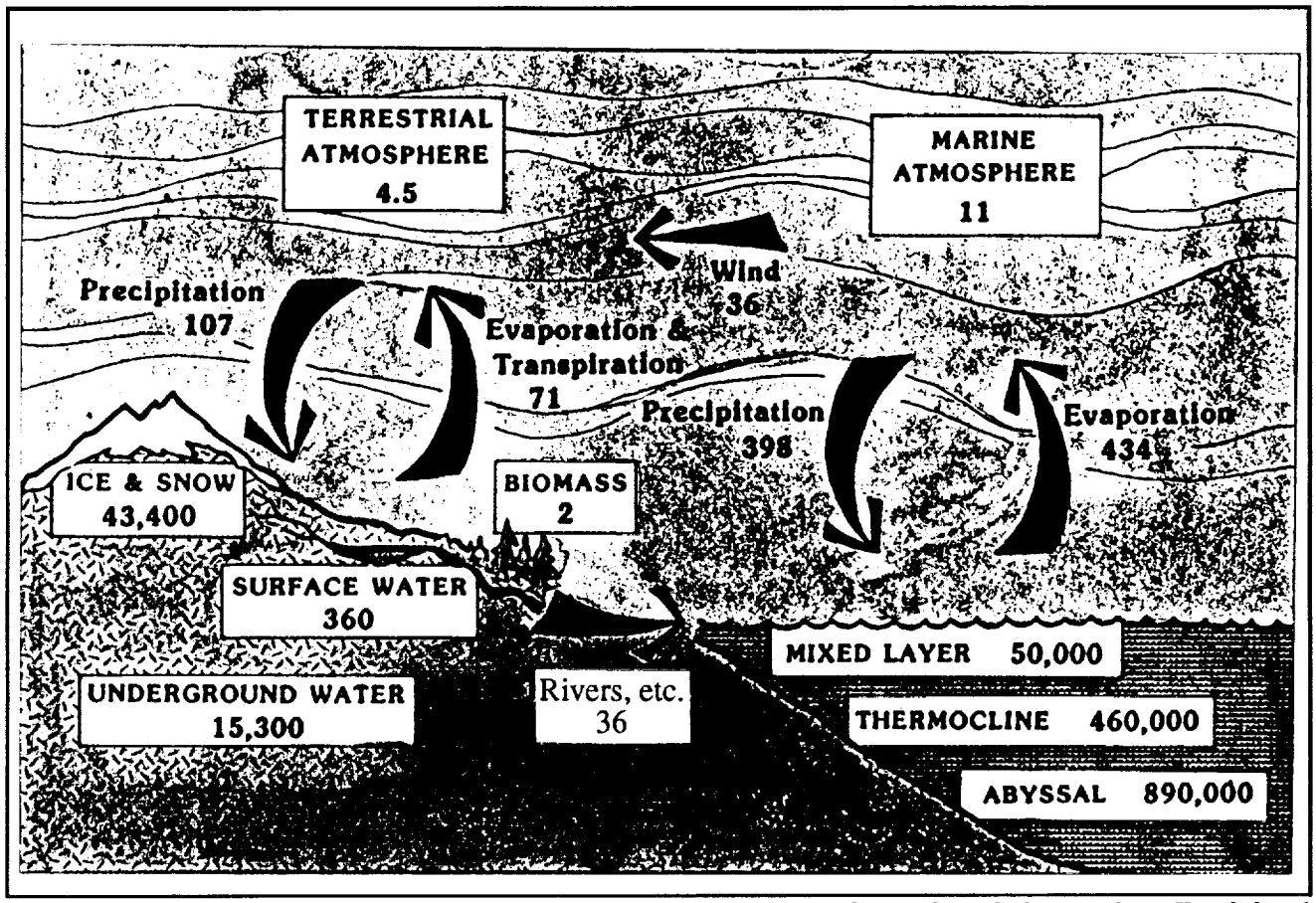


*Figure 3. The global water cycle, showing estimates of contents of major reservoirs and rates of transfer between them. Knowledge of water contained in the ground is particularly poor; this fundamental parameter is known to only a factor of 2 or perhaps 4. Source: Global Change in the Geosphere-Biosphere, NRC 1986.*

motions by the condition of hydrostatic balance, namely a balance between the vertical pressure gradient force and gravity. 2) The *equation of continuity*, derived from the law of conservation of mass, relates the local-time rate of change of density to the mass flux into or out of an elemental volume of the atmosphere. 3) The *first law of thermodynamics*, or *the law of the conservation of energy*, relates the time rates of change of temperature and pressure to heating or cooling. This equation links heating with pressure changes that are already linked to acceleration or retardation through pressure gradient forces in the momentum equations. 4) The *equation of state*, or the *gas law*, relates pressure and temperature. 5) The *equation of continuity for moisture and water substance* relates the local rate of change of moisture content to the flux divergence or convergence of moisture into/out of the elemental atmospheric volume and local sources and sinks of moisture—namely, the local rate of change of moisture owing to condensation (or freezing) and evaporation.

Figure 6 schematically depicts the mathematical simulation of the atmosphere and the manner in which the various time- and process-dependent equations interact with one another. For example, radiative heating or cooling alters pressure, therefore pressure gradient, which affects motion, which affects wind stress on the ocean, and so forth.

The set of equations is, in principle, solvable once the values of the various constants and heating, frictional forces, and precipitation/evaporation (usually computed separately) are known. Thus, the set of equations is not in itself mathematically closed (i.e., there are more variables than the number of equations). To obtain closure, the unknown parameters need to be expressed in terms of known dependent or independent variables. This is done through various parameterizations (of processes) and empirical formulations. The final set of equations is thus rendered solvable, albeit with assumptions (in regard to processes) and approximations (in regard to processes, time, space scales, etc.). Such terms as friction/dissipation, stresses, heating, evaporation, energy, moisture, and momentum fluxes are most important because they determine and describe how the atmosphere interacts with forcings (e.g., solar, GHGs) and with other components of

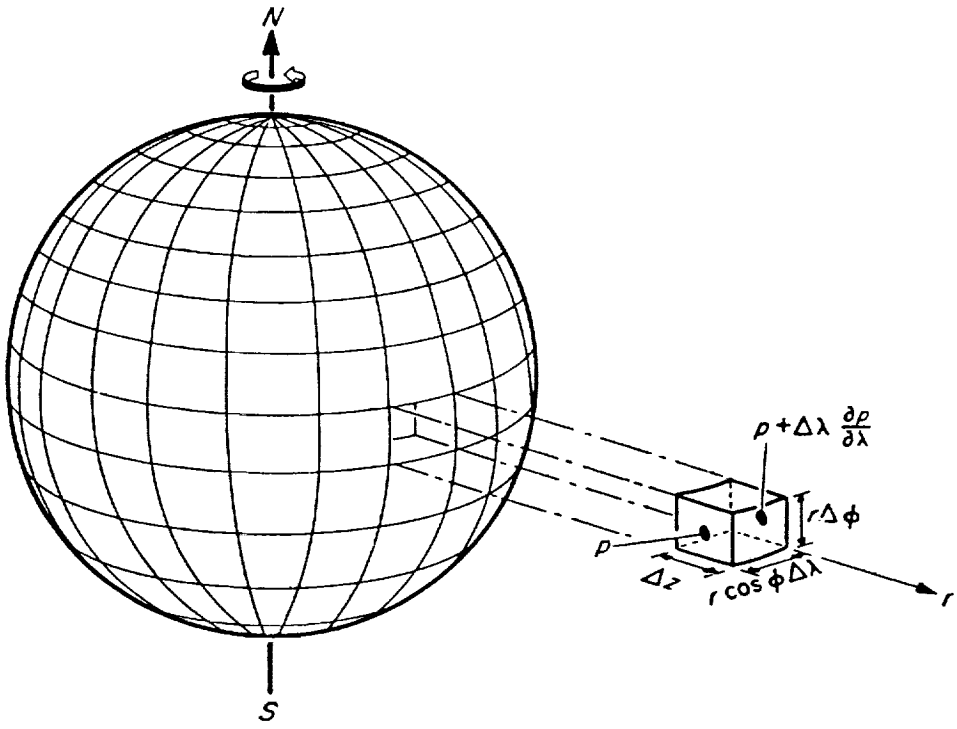


*Figure 4. Schematic of pressure forces on an imaginary volume of air. Source: Washington and Parkinson 1986.*

the global system (i.e., land surface, cryosphere, ocean, or vegetation).

### 3.3.1.1. Space and Time Discretization

Dividing global space into elemental volumes in order to solve the governing time-and space-dependent equations is termed the "finite difference" method. All models use finite difference discretization in the vertical—that is, vertical space divided into a specified number of layers. An alternative approach to horizontal discretization is the use of functional transforms. In this case, the dependent variables are expanded in terms of a complete set of basic functions, usually taken to be spherical harmonics. The expansion is truncated after a finite number of modes. The method may be termed "spectral discretization." Figure 7 shows the global patterns for a typical spherical function with a latitudinal mode of 5 and longitudinal wave number varying from 0 to 5. Choosing the correct combination of amplitudes for each wave number would reproduce the structure of the original spatially continuous field. The degree of exactness in the representation of detail depends on the spectral truncation wave number. Figure 8 shows the equivalent grid point representations for a selection of truncated spectral representations.

An advantage of the "spectral" method is that linear wave propagation is represented exactly on a mode-by-mode basis so that, for example, the linear phase speeds of individual modes are obtained without any error whatsoever (Note: Finite difference methods result in a "physical" mode and a spurious "computational" mode, which travels in the opposite direction and changes phase at every integration time step). When the wavelength of the disturbance or "field" structure is large compared with the grid length, the amplitude of the physical mode will be nearly that of the analytic wave and the amplitude of the computational mode will be small (Lindzen 1989). Special numerical techniques and time-averaging need to be applied to reduce or eliminate the computational mode. Nonlinear instability, arising from "aliasing," can lead to the erroneous amplification of very short waves (Phillips 1959). This type of computational instability is controlled in a GCM by periodical spatial smoothing of the prognostic field to remove wavelengths smaller than four times the grid length. They can also be removed by temporal smoothing and by the inclusion of diffusion terms in the predictive equations, or by a proper choice of certain finite difference schemes that have implicit smoothing or selective damping. The direct calculation of nonlinear processes in the spectral wave number domain is computationally expensive, especially at grid resolution better than about 50 km. For this reason, variables in a spectral model are usually transformed into a grid for the purpose of evaluating all nonlinear processes, including the advection terms and physical parameterizations. The computed fields or terms are then converted back into spectral form before proceeding with the time integration of the model. This process explicitly introduces spatial smoothing of the nonlinear terms by eliminating wavelengths smaller than the specified spectral resolution of the model.

The use of smoothing and damping (especially diffusive damping) within models serves to decrease horizontal resolution. The use of a fourth-order horizontal diffusion in the European Centre for Medium Range Weather Forecasting (ECMWF) model, for example, provides

$$\frac{\partial \psi}{\partial x} = \frac{\psi_{i+1,j,k} - \psi_{i-1,j,k}}{2\Delta x},$$

$$\frac{\partial \psi}{\partial y} = \frac{\psi_{i,j+1,k} - \psi_{i,j-1,k}}{2\Delta y},$$

$$\frac{\partial \psi}{\partial z} = \frac{\psi_{i,j,k+1} - \psi_{i,j,k-1}}{2\Delta z}.$$

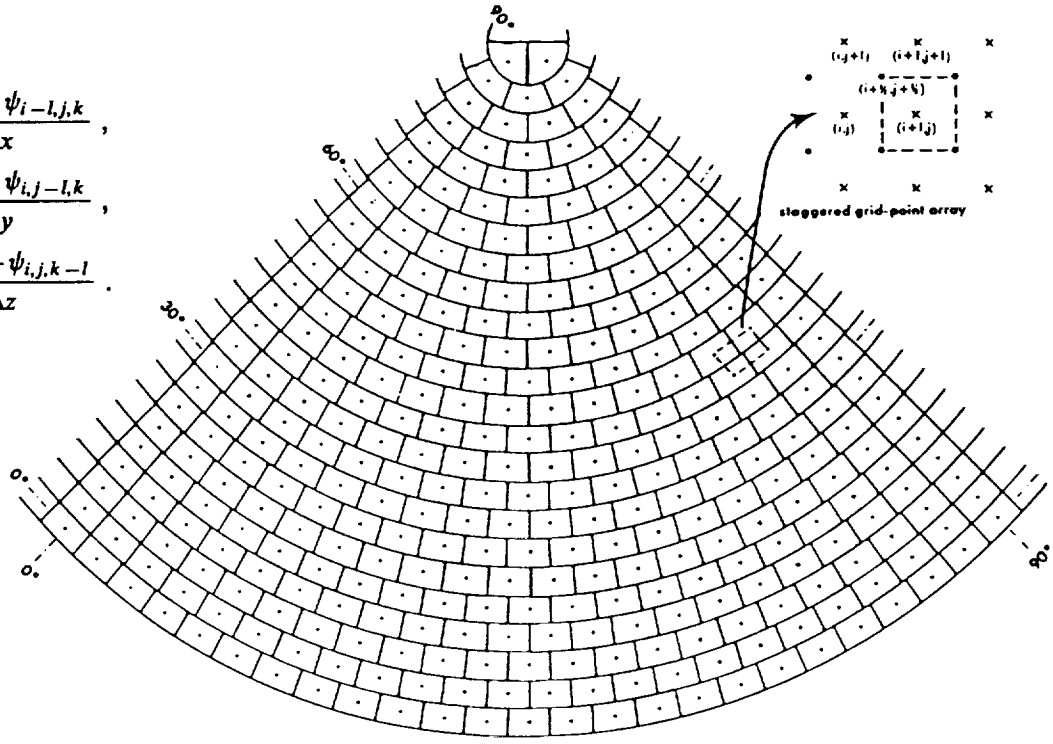


*Figure 5. An example of horizontal grid system (the so-called Kurihara grid) with 24 grid points between the pole and equator, used in general circulation model experiments (only 1/8 of globe is shown). A staggered grid-point array for performing the needed finite difference computations is shown as an inset in the top righthand corner. Other systems in use are regular latitude-longitude grids and various spherical harmonic systems. Source: Peixóto and Oort.*

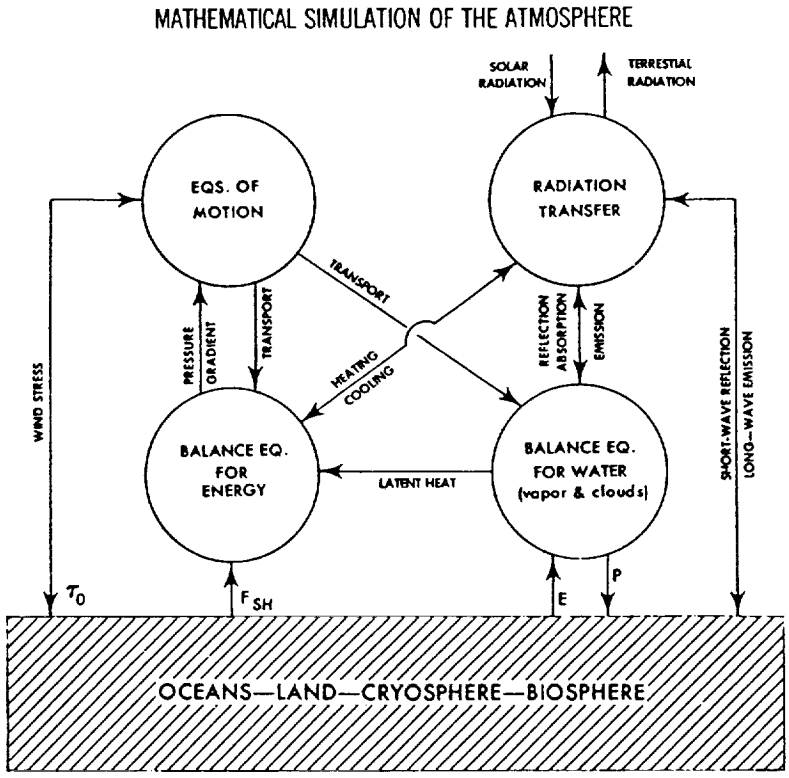


*Figure 6. Major components of the mathematical simulation of climate. Source: Peixóto and Oort.*

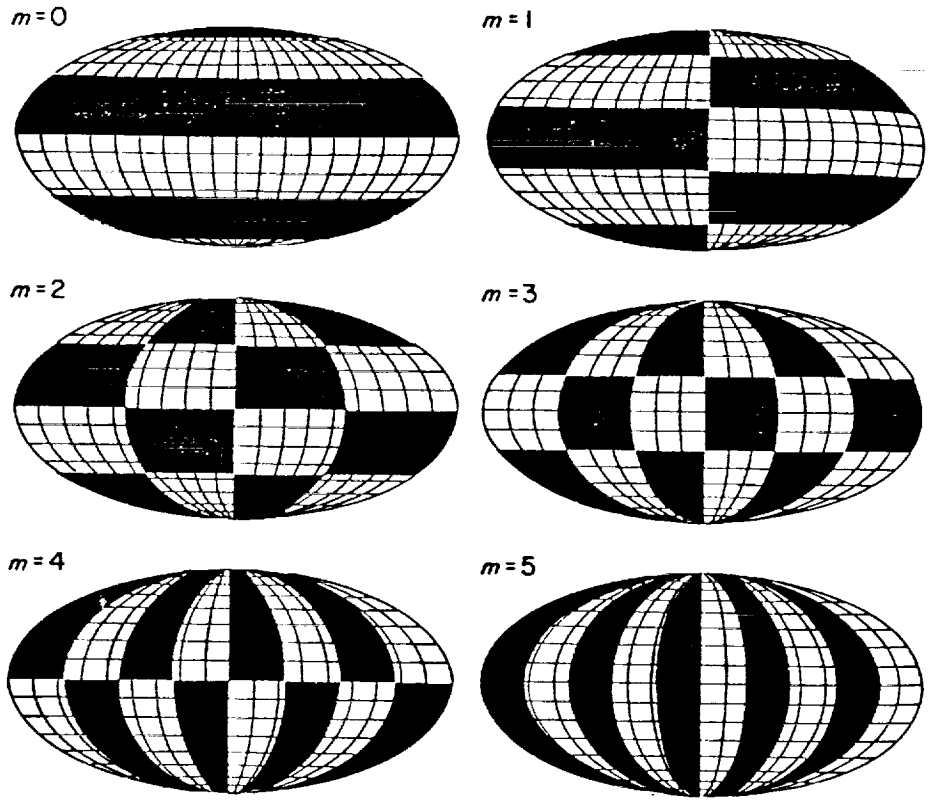


*Figure 7. Alternating patterns of positives and negatives for spherical functions with l = 5 and m = 0,1,2,...,5. Source: Baer 1972.*

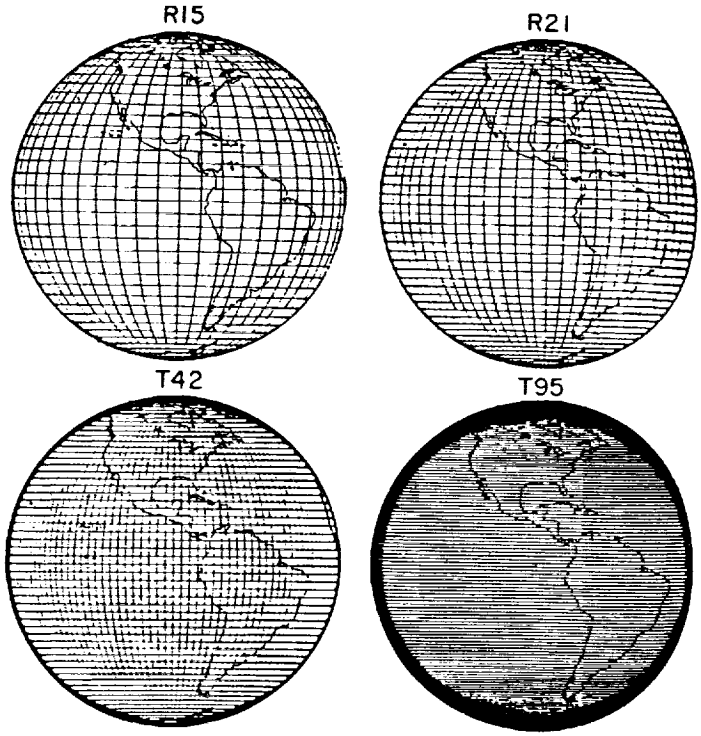


| | LAT. | LONG. | TOTAL |
|---|---|---|---|
| R15 | 40 | 48 | 1920 |
| R21 | 54 | 64 | 3456 |
| T42 | 64 | 128 | 8192 |
| T95 | 144 | 288 | 41472 |

*Figure 8. Gaussian grid on the globe for various resolutions: Rhomboidal, R15 and R21, and triangular, T42 and T95. Source: Williamson 1983.*

substantial damping for scales less than 500 km, even though the model's stated or nominal resolution is ~100 km. Thus, the effective resolution of any model depends on both the specified mathematical grid or spectral resolution and, importantly, the damping and smoothing functions applied, for one reason or another, when integrating the model equations.

Generally, the discretization of the equations of motion in existing global models is based on either a Eulerian or semi-Lagrangian approach. In the Eulerian approach, all derivatives following particles are expressed in terms of partial derivatives in time and space; in the semi-Lagrangian approach, particle derivatives are retained, and the equations are discretized along the trajectories of particles that arrive at a fixed array of regularly spaced grid points each time step (Bates 1990). In either case, the spatial discretization can be based on finite differences or on a spectral expansion where each field is expressed as a series of spherical harmonic functions. There are four basic categories of models: 1) Eularian spectral [e.g., the National Meteorological Center (NMC) operational model; Sela 1980], 2) semi-Lagrangian spectral (e.g., the Canadian and ECMWF models; Ritchie 1991), 3) Eulerian finite difference [e.g., the United Kingdom Meteorological Office (UKMO) model; Cullen 1991], and 4) semi-Lagrangian finite difference (e.g., the Goddard Laboratory for Atmospheres model; Bates et al. 1992). Spectral models have held a dominant position in global modeling for the past decade, but their poor representation of rapidly varying quantities such as water vapor (giving appreciable negative values of moisture in some regions and false supersaturation in others) is seen as a serious defect (Williamson 1990; Rasch and Williamson 1990). This has led to the abandonment of the spectral representation of water vapor in the National Center for Atmospheric Research (NCAR) Community Climate Model Version 2 (CCM2) and its replacement by a semi-Lagrangian grid point formulation (Bates 1992, personal communication). A major advantage that spectral models previously enjoyed relative to finite difference models was the absence of numerical problems associated with the polar singularity in the spherical coordinate system. Semi-Lagrangian discretization, with the momentum equation discretized in vector form, serves to eliminate this defect in finite difference models. Because of the absence of the stability criteria in semi-Lagrangian models, large time steps can be chosen that allow these models to be integrated with increased efficiency.

With semi-Lagrangian methods, the integration time step may be increased from 10 or 15 minutes to about 1 hour without significant degradation of the resultant prognostic fields. A smaller number of time steps during an integration also results in a reduced cumulative effect of truncation and round-off errors produced per time step, leading to better numerical accuracy. Though not unique to semi-Lagrangian models, there is the lack of mass conservation in using this approach. While this is not very serious for short- to medium-range forecasting applications, it could pose problems for very long-range time integrations typical in climate predictions. A possible solution to this problem has been suggested by Rancic (1992), where a mass conservative semi-Lagrangian scheme is derived as a semi-Lagrangian extension of the piecewise parabolic method (PPM), first developed by Colella and Woodard (1984) and suggested for meteorological application by Carpenter et al. (1990).

In the vertical, the atmosphere is divided into "sigma" layers as shown in Figure 9. Here, the vertical dimension is the ratio of pressure to surface pressure, rather than height, in order to account for such surface topographical variations as mountains. Basically, global models use about 10 to 20 layers in the vertical (to delineate the troposphere and stratosphere up to about 20 km) and between 2.5° to 5.0° latitude, and 2.5° to 10° longitude grids in the horizontal.

Attempts have been and are being made to improve model performance by using different vertical coordinate systems that better account for mountains. In this regard, significant improvements are reported by Mesinger and Black (1992) when using an "eta" versus "sigma" vertical coordinate system in high-resolution, nested grid models. Improvements are attributed to the "eta" system's ability to better resolve the boundary layer and reduce the "slope"-related pressure gradient and other problems of the sigma coordinate system. The isentropic "theta" coordinate system is considered more appropriate for the stratospheric circulation (Anderson 1992). The most recent variant to modeling the vertical structure of the atmosphere suggests the use of a multi-coordinate system in the vertical—namely, eta in the lower layers, sigma in the middle atmosphere, and theta in the upper atmosphere.

Lindzen and Fox-Rabinovitz (1989) contend that in global atmospheric models, increased horizontal resolution without a corresponding and carefully matched vertical resolution can lead to increased model "noise" rather than improved accuracy. They also contend that virtually all large-scale models (i.e., GCMs) and observing systems have inadequate vertical resolution. It has been known for a while that a given spatial resolution demands a minimum time resolution to avoid computational instability (Courant et al. 1928). The instability arises when the spatial resolution defines modes whose time scale is too short to be resolved with the existing time step. Hong and Lindzen (1976) suggest that a similar consistency requirement exists between vertical and horizontal resolution. Excessive horizontal resolution could resolve modes whose vertical wavelength might be too small

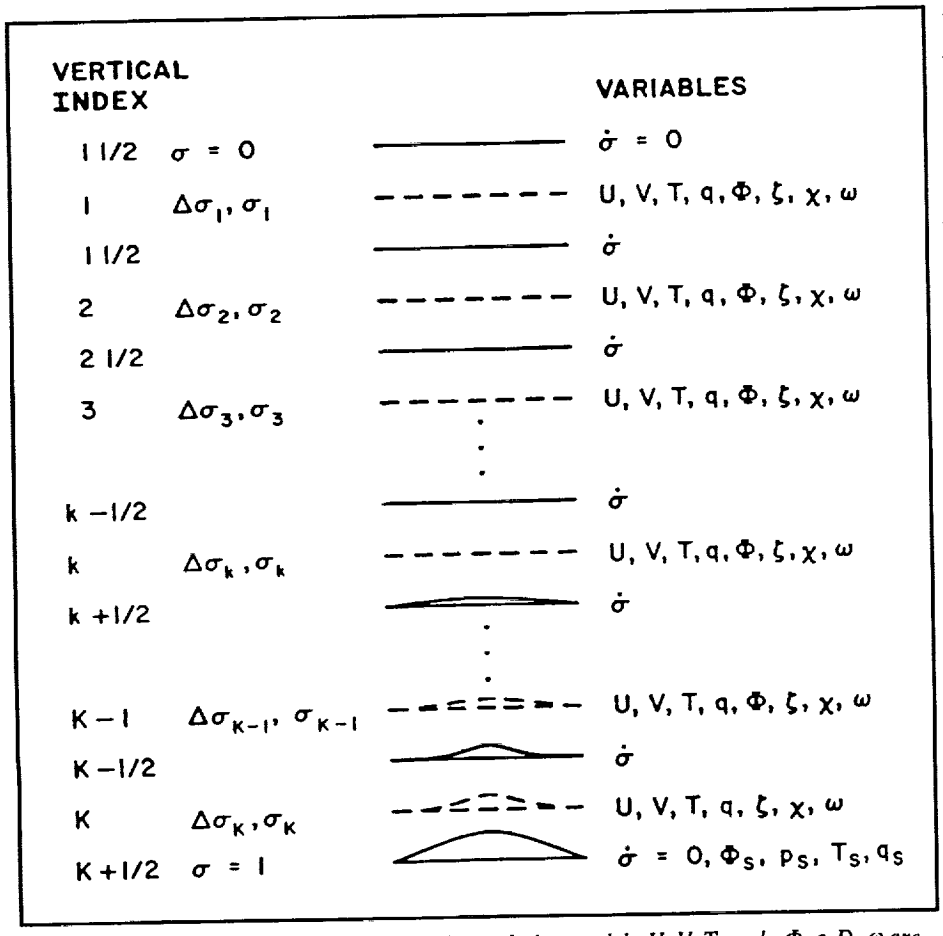


*Figure 9. Vertical structure of a general circulation model. U, V, T, and qΦ, ς D, ω are computed at the dashed-line locations, and σ is computed at the solid-line locations. Source: Williamson 1983.*

to be resolved with the existing vertical resolution, leading to spatial instability, and, when spurious growth cannot manifest itself (due to too few levels), one could obtain incorrect solutions (Lindzen 1970; Lindzen et al. 1968). Furthermore, the vertical-to-horizontal resolution dependence is different from equatorial to mid- and higher latitude regions because of differences in the structure of the energetically dominant systems in these latitudes.

***Conclusions/Recommendations.*** *Research and improvements are required in several areas, such as the parameterization of physical processes. Details on convective, precipitation, and radiative processes are covered in the sections dealing with those subjects. This section deals more with the dynamic and kinematic aspects of the atmospheric general circulation.*

*Substantial improvements are required in the parameterization of boundary layer processes and turbulence. This is important because the "free" atmosphere interacts with the land and ocean surface through the boundary layer via the exchange of fluxes of momentum, heat, and moisture.*

*Higher horizontal resolution is required to enable a better match between atmospheric and surface processes such as hydrology. Also, this would greatly help in the incorporation of results from subcomponent land surface models in GCMs.*

*More research is required into the relationships between horizontal and vertical resolution. Based on the analysis of simplified atmospheric models, evidence indicates that there is a mismatch between the two at present. Arbitrarily increasing horizontal resolution without a carefully matched vertical resolution can lead to increased model noise rather than increasing accuracy. Increased model resolution has not necessarily led to better model performance. This has also been the experience with weather forecast models at NMC and ECMWF. Advances in model physics have led to more improvements than refined resolution.*

*More research is required into the numerical treatment of the vertical structure of the atmosphere and the vertical coordinate system used. Experimental model comparisons suggest that the eta coordinate system better resolves surface topographical and other surface processes (F. Messinger). Hybrid "isentropic-sigma" coordinate models perform better than sigma models (even those with higher resolution) in the transport of water vapor, the simulation of equivalent potential temperature, and the prediction of the timing, location, and amount of precipitation. Research is ongoing in using hybrid eta-sigma-theta vertical coordinate models.*

*Short -term (e.g., day-to-day weather) forecasts are very sensitive to initial error. For seasonal and longer term forecasts, the initial error growth rate is not as important as the saturation value of the error.*

*Tropical-extratropical interactions need to be investigated more, in particular tropical intraseasonal (30-to 60-day) oscillations.*

*Methods need to be developed in the use of improved satellite observations (e.g., tropical rainfall, moisture, winds) in the initialization of atmospheric models.*

*Many of the improvements in models attributable to increases in resolution are due to better resolution of gravity waves. Gravity waves are a crucial part of exchange processes and the climate of a model, and should not be eliminated by filtering or smoothing techniques. They need to be better and explicitly accounted for.*

*The use of fourth-order horizontal diffusion in models (e.g., ECMWF) introduces substantial damping for scales of less than about 500 km, even though the nominal model resolution is 100 km. Thus, the effective resolution of any model depends on both the specified grid or spectral resolution and the damping and smoothing procedures applied to eliminate spurious computational modes to account for the energy cascade to scales smaller than that resolved by the model grid or to prevent the growth of model-generated gravity waves.*

*Further research is required in the use of semi-Lagrangian techniques in the integration of climate models. The technique, which is inherently computationally stable and permits the use of much larger integration time steps, is already operational in data assimilation and weather forecast models (e.g., the United Kingdom, Canada, and Ireland).*

*The spectral form serves to eliminate the polar singularity in finite difference models, and, because of the absence of stability criteria, large time steps can be chosen that allow them to be integrated with increased efficiency, thus compete more effectively with spectral models. For these reasons, a reassessment of the situation with regard to the methods of horizontal discretization in global models is currently warranted.*

*There is a need to improve experience with massive parallel processor computers. In the future, substantial improvements in speeds, as well as numerical approaches to modeling, are likely with parallel processing.*

### 3.3.1.2. The Stratosphere

The stratosphere [i.e., the layer of the atmosphere above the troposphere from about 10 km (~200 mb) to 50 km] is treated separately here for two reasons: 1) Historically, the stratosphere has been neglected in atmospheric GCMs and in diagnostic studies partly because of a paucity of data and partly because of the emphasis placed on the troposphere and the weather, thus GCMs typically have very few vertical layers to represent the stratosphere; and 2) stratospheric chemistry has become rather crucial in climate system modeling on account of ozone ($O_3$) generation and depletion processes that can affect the temperature structure, the chemical and radiative effects of chlorofluorocarbons (CFCs), and the cooling effect of stratospheric aerosols injected by volcanic eruptions. These items effectively and directly couple the lithosphere with the stratosphere and climate change. Other important aspects that need to be monitored and modeled as well are stratospheric water vapor and its consequent greenhouse effect on the climate system. The stratosphere has also been the subject of investigations on the effect of enhanced GHGs (i.e., the detection of the GHG signal, models predicting stratospheric cooling). Among the parameters being sought are stratospheric temperature change in radiative fluxes out of the troposphere and change in convective depth (Rood 1992).

Most short-term solar fluctuation-climate interactions have been observed to be most pronounced in the stratosphere (Van Loon and Labitzke 1991), and, in order to investigate surface impacts, stratosphere-troposphere exchanges need to be better understood. Other features of interest are the quasi-biennial oscillation (QBO), observed for many years with 30-mbar winds at Balboa, and generally ignored until recently when correlations emerged with ENSO, surface weather, and so on (Grey 1984). Clearly, there must be an unambiguous link between stratospheric and tropospheric processes, but these have yet to be physically modeled properly.

A commonly acknowledged solution in incorporating the stratosphere into modeling is to substantially increase the vertical resolution of GCMs; however, clever numerical techniques are also thought to be required for the representation of gravity waves, which are crucial to the "climate" of stratospheric models. A 46-layer (up to 0.1 mbar/~70 km) version of the basic 17-layer NASA/GLA GCM currently is being developed to investigate troposphere-stratosphere interaction (Fox-Rabinovitz et al. 1992). The inclusion of stratospheric processes in climate system GCMs may require a substantial enhancement in both horizontal (1° x 1°) and vertical resolution and more realistic physics.

***Conclusions/Recommendations.*** *The stratosphere is poorly represented in most GCMs. Often, improvements in vertical resolution refer primarily to more model layers in the troposphere. Models of 46 layers or more are required to adequately resolve the stratosphere (up to 0.1 mbar) and stratosphere-troposphere interaction.*

*Properties of the stratosphere and stratospheric transport mechanism can substantially affect the Earth's surface*

*through constituent exchange, influence on vertical wave propagation, and alteration of the radiative budget of the Earth system. For example, uncertainties in the expected ozone changes over most of the Earth are large partly owing to a lack of understanding of transport mechanisms. More research is required on wave-breaking processes, the QBO and its influence on tropospheric weather (e.g., tropical cyclones), the distribution of stratospheric aerosols (from volcanic eruptions), and the modulation of solar flux into tropical oceans.*

*Other issues important to the stratosphere include the cooling of the stratosphere due to greenhouse gases and possible changes in the way in which energy propagates out of the troposphere. Furthermore, the fate of many GHGs depend on how quickly the gases are transported into the stratosphere where they can be removed photochemically.*

*GHGs, aerosols, and radiative aspects are treated in more detail in later sections.*

### 3.3.1.3. The Mesosphere

Recent studies (Roble and Dickinson 1989) suggest that the projected increase in anthropogenic $CO_2$ and $CH_4$, while warming the troposphere, will cool parts of the mesosphere by 10 to 20K in the global mean and the thermosphere by as much as 50K. Figure 10 depicts the global averaged changes in the mesosphere and the thermosphere predicted by global circulation models in response to a doubling or halving of $CO_2$ and $CH_4$ concentrations near the stratosphere. Though long-term observational information is lacking, the analysis of Rayleigh lidar data collected since 1979 in southern France suggests that parts of the mesosphere may indeed be cooling at a remarkably fast rate (see Figure 11), perhaps as much as -0.4K per year at 60 to 70 km in altitude (Hauchecorne et al. 1991). Consequent changes in the thermospheric circulation are expected to alter the electrodynamic structure of the upper atmosphere and, through dynamo action, the magnetosphere-ionosphere coupling processes.

The increasing concentrations of the greenhouse gas $CH_4$, coupled with decreasing temperature, may also be related to the increased formation of noctilucent clouds (NLC) near 82 km (the highest clouds above Earth) over the cold summertime polar caps. Historical records contain no reports of NLC sightings before about 1885, even though skilled observers were monitoring auroral and twilight phenomena at high latitudes for many decades by then (Thomas et al.). Since the discovery of NLCs more than 100 years ago, the brightness and frequency of NLC displays have been increasing. It is believed that $CH_4$ may facilitate NLC formation because of its ability to transport hydrogen through the stratosphere. Once methane reaches the

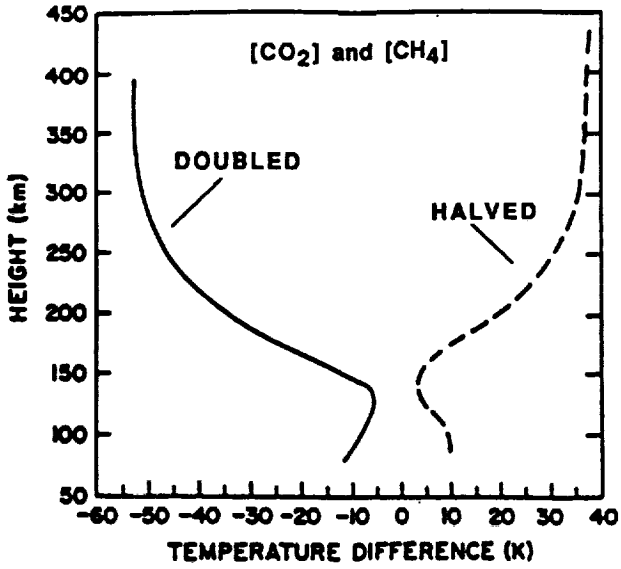


*Figure 10. At the current rates of increase, atmospheric $CO_2$ and $CH_4$ concentrations are predicted to double within the next century. Plotted here are the calculated temperature changes in the mesosphere and stratosphere for the cases in which $CO_2$ and $CH_4$ concentrations at 60 km are doubled (solid curve) and halved (dashed curve). Source: R. Roble and R. Dickinson 1989.*

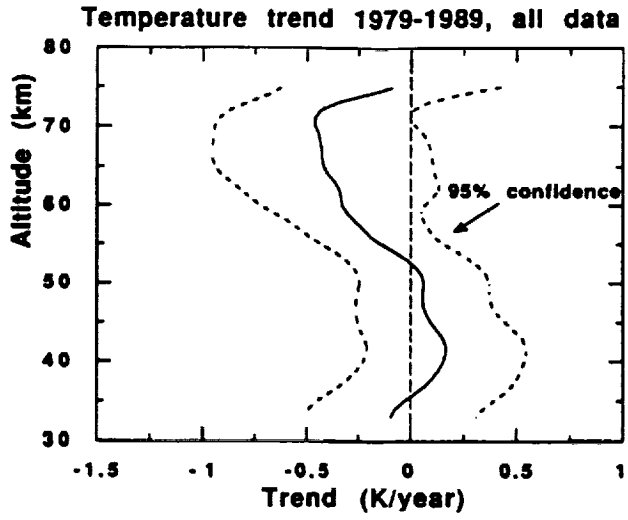


*Figure 11. During the past decade, Rayleigh lidar measurements of stratospheric and mesospheric temperatures above southern France have exhibited cooling trends approaching -0.4K per year at 60–70 km altitude. Source: A. Haucheocorne et al. 1991.*

mesosphere, photochemical reactions in the presence of atomic oxygen produce water vapor that is essential for the formation of noctilucent clouds. The effects of gases of anthropogenic origin on the mesosphere and the thermosphere should also be monitored on a long-term basis for a more comprehensive understanding of change in the global system.

***Conclusions/Recommendations.*** *The upper atmosphere/mesosphere should be monitored in addition to the lower atmosphere. Indeed, the strongest greenhouse effect signal may be in the upper atmosphere. Alterations in the electromagnetic structure of the upper atmosphere, through modifications to the thermospheric circulation, would also affect the shield protecting the Earth from harmful particle fluxes from the Sun.*

### 3.3.2. Convection, Cloud, and Precipitation Processes

The prediction of the distribution of cloudiness and its interactions with other components of the global system (e.g., the radiation budget and the hydrological cycle) is one of the most important goals and, at the same time, one of the more difficult tasks in modeling. Changes in cloudiness critically affect the global energy budget by modifying the planetary albedo and the emitted infrared radiation. For low clouds, the albedo effect dominates (Manabe and Wetherald 1976); that is, other things being equal, increasing the amount of low clouds leads to cooling at the surface. However, if changes in cloud height are associated with changes in cloud amount, the results can be significantly different (Schneider 1972). Empirical studies based on the observed temporal and spatial variability of cloudiness and of radiative fluxes at the top of the atmosphere are inconclusive (Cess 1967; Ohring and Clapp 1980; Hartman and Short 1980; Cess et al. 1982), giving results that vary from a dominance of the albedo effect to a near-perfect balance between long- and shortwave changes. The safest conclusion from these studies is that many details of the cloudiness distribution must be more accurately observed and modeled to conclusively assess the influence of clouds on the variability of the climate of the global system.

Global models typically predict two kinds of clouds: Convective clouds and large-scale clouds. Buoyancy subgrid-scale motions play a dominant role in convective clouds. The parameterization of convective clouds must take into account both the large-scale static stability and the large-scale relative humidity. In all existing convection parameterizations, the intensity of convection depends in some way on the rate at which the column is being destabilized by radiation and by the large-scale circulation. In this way, the inferred fields of convection and the cloudiness depend on both the thermodynamic state (the static stability and the relative humidity) and its large-scale tendency.

The relationship between convective heating and convective cloudiness is not obvious. Although the results of the convection parameterization should imply something about the fractional cloud cover, active deep convection typically accounts for only a few percent of the observed fractional cloudiness. In fact, the smallness of the region of active convection is an explicit assumption in some parameterizations. Inactive cloud debris and cirrus shields account for most of the observed cloudiness. Thus , some memory of the history of convection and some statement about the life cycle of convective clouds seem to be necessary ingredients of a cloud parameterization scheme. Also, since the effects of convection tend to moisten the upper troposphere, cirrus shields and coverage by shallow inactive clouds need to be included in the "large-scale" cloudiness parameterization.

In global models, clouds either are specified as a function of space and time (to take into account seasonal cycles) or are computed. When computed, the precipitation and convective aspects of the model are used to predict where the model clouds exist, depending on whether the atmosphere is near saturation and whether convection is occurring. If the air is saturated but not convective, then a stratiform (layer) of cloud or fog is assumed to exist, occupying all or nearly all of any grid cell. If a cloud is of convective origin, it is usually assumed to occupy a small fraction of a grid cell. Often, relative humidity or some other moisture parameter is used in conjunction with empirical factors to determine cloud amount.

Several models parameterize convective and precipitation processes in terms of the vertical "moist adiabatic" lapse rate of temperature in the atmosphere. This is called "convective adjustment parameterization," first used by Manabe, Smagorinsky, and Strickler (1965). Figure 12 is a schematic of cumulus cloud formation. The lapse rate of temperature could be written in terms of the vertical gradient of potential temperature or equivalent potential temperature. The potential temperature is constant during an adiabatic process (such as if a parcel of air moves along a dry adiabat) and is approximately constant in an air mass as it precipitates (out) excess water vapor. If air is supersaturated but not convective (i.e., stable), then latent heating is computed from the first law of thermodynamics, where the temperature change is the temperature change obtained by the conversion of water vapor to liquid water.

In a stable or nonconvective model, latent heating is computed whenever the atmosphere is supersaturated; usually, the moisture is reset to saturation after precipitation

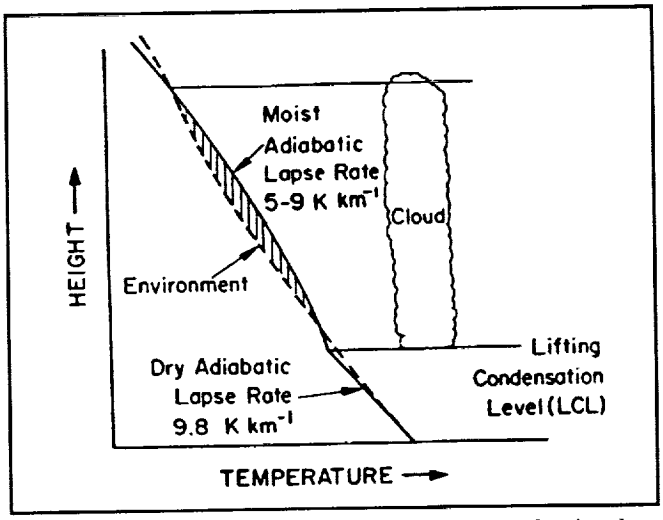


*Figure 12. Schematic of cumulus cloud formation showing the lifting condensation level (LCL), dry and moist adiabatic lapse rates, and lapse rate for the air outside the cloud (labeled "environment"). Source: Washington and Parkinson 1986.*

is assumed to occur. Often, the relative humidity criterion for assuming nonconvective heating is less than 100 percent. Some models use 80 percent. Though somewhat arbitrary, the justification for a criterion of less than 100 percent is that precipitation is known to occur (observationally) on smaller scales than the grid scale of most global models and to take place even if the large-scale environment (i.e., outside individual cloud cells) has a relative humidity of less than 100 percent. The manner in which convective latent heat release is included in atmospheric models is much less uniform, and it is uncertain which of the many methods in use is the best overall.

Physically, the convective cloud process may be described in relatively simple conceptual terms (Washington and Parkinson 1986). If a parcel of air near the Earth's surface (P≅1,000 mbar) starts to rise due to strong heating or kinematic convergence, it will cool at approximately the dry adiabatic lapse rate of 9.8K/km$^{-1}$. Assume that the parcel of air has a relative humidity of 50 percent at the surface and that it does not mix with the environmental air (i.e., there is no entrainment) as it ascends and cools, so that its water vapor content remains the same. As the parcel cools, its relative humidity increases, since cold air is unable to hold as much water as warm air. When the parcel cools sufficiently to have a relative humidity of 100 percent, the parcel is saturated. The level at which this occurs is termed the lifting condensation level (LCL), which typically is at the cloud base (see Figure 12). If the air near the surface is moist, the LCL will be low, perhaps 100 m, whereas if the surface air is dry, the LCL can be quite high. If the parcel does not rise high enough to reach an LCL, a cloud should not form. From the LCL upward, the parcel will cool less rapidly as it continues to rise since the latent heat of condensation or fusion releases heat. This lessened rate of temperature decrease with height is the moist adiabatic lapse rate, which in the lower troposphere is 5 to 6K/km (see Figure 13). When the temperature during a model simulation is greater than 0°C, the latent heat of fusion is used.

In a real cloud, lateral entrainment takes place and this mixing dilutes the temperature and moisture differences between the cloud and the surrounding air. Furthermore, rising motion in a cloud core and compensating sinking motion outside the cloud (sinking causes warming at the dry adiabatic lapse rate) can lead to a large difference in temperature and moisture between cloud and environment.

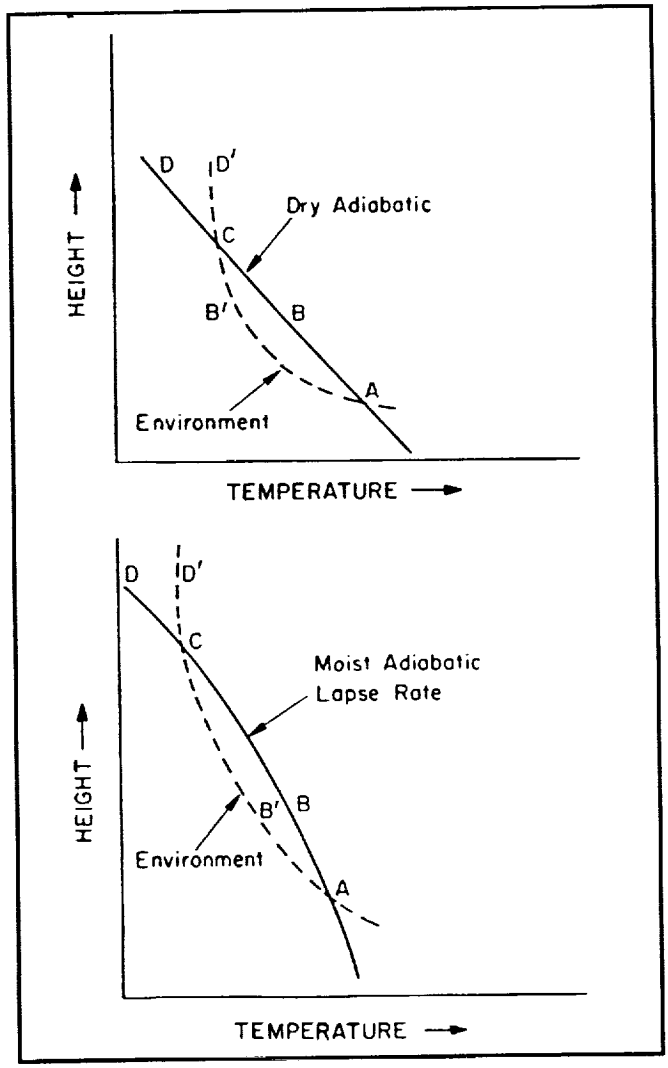


*Figure 13. Diagram of stable and unstable environmental conditions with respect to dry and moist adiabatic lapse rates. In each case the air at point A is unstable, while that at point C is stable. Source: Washington and Parkinson 1986.*

For a stable atmosphere, the lapse rate of potential or equivalent potential temperature must be greater than 0 for dry and moist convection, respectively. In a model, if there is excess moisture, the moisture distribution is adjusted to prevent supersaturation and is allowed to fall out of the column with a resultant addition of latent heat to the atmosphere. If the model atmosphere is unsaturated, the lapse rate is set at the dry adiabatic lapse rate. To start the convective adjustment process, each grid cell of the atmosphere is examined. If no layers are unstable, the lapse rate is not modified. If there are unstable layers, the lapse rate is modified while conserving total (i.e., internal, potential, and latent) static energy.

Convective adjustments to reference lapse rates other than the dry or moist lapse rate have been suggested by Betts and Miller (1986), using empirical studies of deep cumulus convection.

More complex convective cloud parameterization schemes popularly used in global models are modified versions of those of Kuo (1974) and Arakawa-Schubert (1974). The Kuo scheme uses lower level convergence of moisture into a region and low-level lifting as determining conditions of whether cumulus convection is taking place. The scheme is based on experimental studies, especially in the tropics, showing that areas of active precipitation are also areas where the low-level wind pattern shows the convergence of moisture-laden air inflow into a restricted region. In the Kuo scheme, the rate of moisture accession per unit horizontal area is obtained from the convergence of moisture (water vapor) into a vertical column from the top of the troposphere to the Earth's surface and surface evaporation. Kuo assumes that a fraction of the moisture flowing into a column is condensed and precipitated, while the remaining portion is stored in the atmosphere, thereby increasing the relative humidity of the vertical column. The heating due to cumulus convection is a function of the condensation rate, and the vertical and horizontal fluxes of sensible heat within the column. The condensation rate is assumed to be proportional to the large-scale moisture convergence and a vertical density function for condensation (Kuo 1974; Anthes 1977), which is usually made proportional to the temperature difference between in-cloud temperature and the outside environment. Verifying Kuo's scheme is difficult due to limited observations, but models show improved moisture, temperatures, and precipitation forecasts when using the scheme.

The Arakawa-Schubert (1974) scheme shown in Figure 14 considers a coexisting spectrum of idealized model cloud ("subensembles") such as a mixture of shallow and deep clouds, which interact with each other as well as the large-scale environment through the entrainment of drier

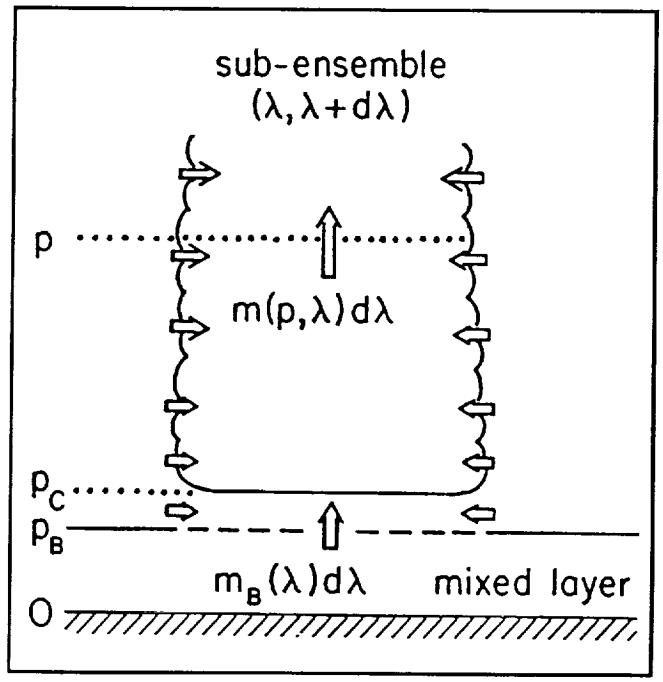


*Figure 14. Schematic diagram showing the sub-ensemble of type λ clouds and the subcloud mixed layer.*
*Source: Garp Publication Series, WMO/ICSU.*

air from outside the cloud core. The scheme also allows strong interaction with the boundary layer. The problem of parameterizing cumulus convection is reduced to the determination of the vertical distributions of the vertical mass flux from the ensemble and the thermodynamic properties of the detraining air. Ensemble cloud type is characterized by the fractional entrainment rate. The budget equations for mass, moist static energy, and total water content can be obtained for each subensemble. For a given thermodynamic vertical structure of the environment, the solution of the budget equations determines for each subensemble the vertical mass flux, normalized at the top of the mixed layer, the thermodynamic properties, and the height of vanishing buoyancy. The large-scale processes involved are horizontal and vertical advections by the large-scale motion, surface heat fluxes, and radiational heating.

Nonpenetrative convective clouds and convection not arising in the planetary boundary layer (PBL) have received special attention in some models. Both are included in a crude way under moist convective adjustment. Ramanathan and Dickinson (1981) proposed an empirical parameterization of nonpenetrative convective clouds, based on the ideas of Lilly (1968), Deardorff (1976), and Randall (1980b). A more detailed parameterization of these clouds is included as part of the planetary boundary layer parameterization in the University of California–Los Angeles (UCLA) model (Suarez et al. 1983).

Large-scale cloudiness parameterization schemes are quite crude. The fractional cloud cover is generally diagnosed using the relative humidity field alone; see, for instance, Smagorinsky (1960). The simplest schemes assume overcast conditions when the model grid box becomes saturated, or make cloudiness some simple function of relative humidity.

A very different approach to modeling large-scale, nonconvective clouds has been proposed by Sundqvist (1978), who introduces a prognostic equation for cloud water and writes source and sink terms by making assumptions for condensation, evaporation, and precipitation over a fraction of the grid area. Fractional cloudiness schemes based on knowledge of the second-order statistics of temperature and total water mixing ratio have also been proposed by Sommeria and Deardorff (1977), Mellor (1977), and Hansen et al. (1983). However, neither prognostic schemes nor statistical condensation methods are widely used in GCMs—the former because of the difficulty in formulating source and sink terms for liquid water with an accuracy that would justify retaining separate storage and advection terms for water vapor and total water, and the latter for a lack of useful diagnostic relations for the higher statistics. Prognostic equations for the higher statistics are beyond current reach both theoretically and computationally.

The parameterizations discussed thus far depend only on thermodynamic quantities and their large-scale tendencies. Situations that depend upon a more direct dependence on large-scale motion are probably common. Examples are deep convection in the presence of vertical wind shear (Moncrieff 1978; Thorpe et al. 1982; Emanuel 1983a,b) and the effects of shear on the maintenance of stratocumulus layers (Brost et al. 1982) and on the organization of cellular shallow cumuli.

The evaluation of cloudiness parameterization in GCMs must deal with two major difficulties: 1) Establishing a proper comparison with observations, and 2) tracing any observed deficiencies to their cause in the model. Global comparisons must rely on satellite observations that give radiances at the top of the atmosphere. These radiances must be inverted to obtain cloud fraction, cloud-top height, emissivity, and albedo. In principle, this inversion process could be bypassed, and modeled and observed radiative fluxes compared directly. However, this would introduce errors because of the GCM's relatively simple radiative transfer calculations, including the assumptions made for the radiative properties of the clouds. On the other hand, if the inverted fields were used, cloudiness is viewed through the radiative transfer calculations used in the inversion whose representation of cloud parameters might be quite different from the GCM's. Thus, care must be taken to understand the relation between the radiative models underlying both GCM output and observational analysis.

A major deficiency in all convective cloud parameterization schemes is that little is known about whether they indeed simulate real clouds well enough for climate prediction purposes, and particularly cloud-radiative processes that are critical in the GHG-surface temperature-cloud-radiation feedback loop. To verify the parameterization of convective cloud and precipitation processes, improved observations are required of the vertical profiles of temperature and moisture, low-level moisture convergence, cloud type and distribution, surface heat fluxes, PBL, and radiational heating.

***Conclusions/Recommendations.*** *Improvements are needed in the treatment of downdrafts in convective cloud clusters, as well as the evaporation of falling rain and evaporative cooling. On the land surface, the apportionment of rainfall into evaporation and surface runoff is also critical for the long-term precipitation climatology, surface fluxes, and surface temperature.*

*Cloud amount and macroscopic cloud optical properties are still poorly understood, as are the effects of clouds on the surface atmosphere energy budgets. The use of prognostic cloud water (and ice) variables will be one of the keys to improved cloudiness simulations in models. Prognostic cloud water provides physical links between phase changes and radiation, memory for cloud fields, and simplification of model design. However, it does not solve the cloud amount problem, does not determine subgrid-scale condensation and evaporation rates, nor does it determine the macroscopic cloud optical properties.*

*Models must also account for the coupling between stratiform clouds and convection, cumulus detrainment (which acts as a source term for liquid and ice), moist convective turbulence inside stratiform clouds, and the links between vertical motion and cloud amount. Space-based and ground truth field experiments are required to improve the modeling of cloud processes.*

*More sophisticated numerical methods are required in global models to properly simulate water vapor transport and precipitation processes. When relative humidity is uniform vertically across a substantial extent of the atmosphere, all models produce similar precipitation distributions. When water vapor is confined to relatively shallow layers, the ability of sigma coordinate models to simulate the location, timing, and amount of precipitation is severely compromised. An experimental 10-layer hybrid isentropic-sigma coordinate model performed better than even a high-resolution sigma model.*

*The ability of a global system model to simulate the hydrological cycle may be considered a litmus test, since it represents the "metabolic rate" of the physical global system. The structure and variability of water vapor and condensate fields are strongly sensitive to parameterized convective processes (deep and shallow), surface energy fluxes, radiation, and large-scale kinematic forcing. Column integrated water vapor from the Special Sensor Microwave/ Imager (SSM/I) as well as a liquid water index from the microwave sounding unit (MSU) are useful for verifying model processes. Better tropospheric wind data are required to document divergent flows associated with diabatic processes.*

*The dynamics of tropical cloud clusters and teleconnections need to be better understood. The accurate modeling of cumulus clusters is also critical to the understanding of water vapor feedback in climate simulations, because cumulus clusters are an important mechanism by which water vapor is distributed in the vertical. The vertical water vapor distribution is linked to the radiation budget at the top of the atmosphere as well as the surface. If different assumptions are made in the changes in the distribution of water vapor, the climate feedback could be quite different. For this research, very high-resolution cloud ensemble models are currently being developed. The Goddard cumulus ensemble (GCE) model has a resolution of 1.5 x 1.5 km in the horizontal, and 30 levels in the vertical; the domain is 200 x 200 km horizontal, and 22 km vertical.*

*The modeling of convection schemes use various assumptions. For example, a new scheme being tried out assumes that one-third of the cloud mass is in the downdraft portion of the cloud. Such assumptions, while they may seem reasonable, need to be verified observationally. Furthermore, even if the various parameterizations of processes result in reproducing present climate, they are not necessarily correct for climate or any other global system change simulation and prediction experiments; thus, models need to be validated for the dynamics of "change" as well.*

*A large fraction of the predicted global warming due to GHGs is caused by cloud and water vapor feedback. To obtain the cloud feedback term, models must be able to predict changes in the cloud fields, including vertically overlapping structure and optical properties.*

*Operational weather forecast models now include elaborate physical parameterizations. To evaluate such models, it is necessary to evaluate the model's physics, including precipitation and surface fluxes. Furthermore, the output of operational models is often used in global research. A question that must be asked is whether the precipitation and surface fluxes are accurate enough to be used in such studies as the Global Energy and Water Cycle Experiment (GEWEX). In this regard, more extensive evaluation of the NMC medium-range forecast (MRF) system's precipitation and surface fluxes is needed, especially time variability, as well as new independent measurements of precipitation and surface fluxes.*

*While the type and distribution of cloud condensation nuclei are important for cloud microphysical processes, it is unclear whether global models need be concerned with this variable.*

*GCM precipitation rates at the grid-square level are quite often incorrect, and 2 x $CO_2$ at this scale are subject to great uncertainty.*

### 3.3.3. Radiation and Radiative Processes

In this review, special emphasis is given to radiative processes on account of their importance in causing potentially rapid climate change. The quantification and/or influence of other elements affecting the radiation budget of the planet are also covered (e.g., GHGs, clouds, water vapor, and aerosols). Some of these are considered direct forcing factors, because they are being anthropogenically injected into the atmosphere and not fluctuating in accord with some other internal instability or quasi-equilibrium process of the global system. For the same reason, aerosols are considered a forcing factor, being injected through industrial activity or by sporadic volcanoes. Clouds and water vapor are considered feedback elements of the global system because they do not "independently control" their destinies; that is, their amount, structure, and distribution depend on temperature and other dynamic processes. However, their interaction with incoming and outgoing radiation can significantly affect and modulate the initial forcing, such as an initial temperature increase or decrease. Some of these distinctions are simply a consequence of the time window of the present conception of the global system in modeling terms. For example, in a more complete Earth system model, and on long time scales, the injection of volcanic aerosols may be considered a natural internal fluctuation of the global system, even if the mathematical treatment of the impact of aerosols on the atmosphere and surface temperature remains the same. Anthropogenic activity is a controversial aspect of the system. Humans have not yet decided whether they are a part of a natural system or not.

The division of this section into subsections is somewhat arbitrary, but serves to highlight various "forcings" and "feedbacks" as a) currently perceived and b) currently modeled. On account of the overlap between the discussions in the following subsections, conclusions and recommendations are contained at the end of the section.

### 3.3.3.1. Orbital and Solar (Forcing)

By far the strongest of all the "forcings" is the Sun, whose energy influx in the form of ultraviolet and visible electromagnetic radiation (0.2 to 4 μm) is the driving force of weather and climate. At the top of the atmosphere, the shortwave energy flux is about 1,368 W/m$^2$. Because of the Earth's spherical shape and rotation, the average radiative flux received over a day-night cycle is one-fourth this value (i.e., ~342 W/m$^2$). Approximately a third is reflected by the atmosphere and the Earth; the rest is absorbed.

As depicted in Figure 15, the absorbed solar energy flux is in approximate equilibrium with the energy emitted by the Earth in the form of longwave terrestrial radiation; otherwise, the Earth would warm up or cool as a result of an imbalance in these quantities. The figure also depicts the warming that would result from an instantaneous doubling of $CO_2$, namely ~4 W/m$^2$. Indeed, small differences persisting over long periods of time would lead to climate change. It is believed that an important cause of recurring glaciation is variation in the seasonal radiation received in the Northern Hemisphere. These variations stem from small changes in the distance of the Earth from the Sun in given seasons, and slow changes in the tilt of the Earth's axis.

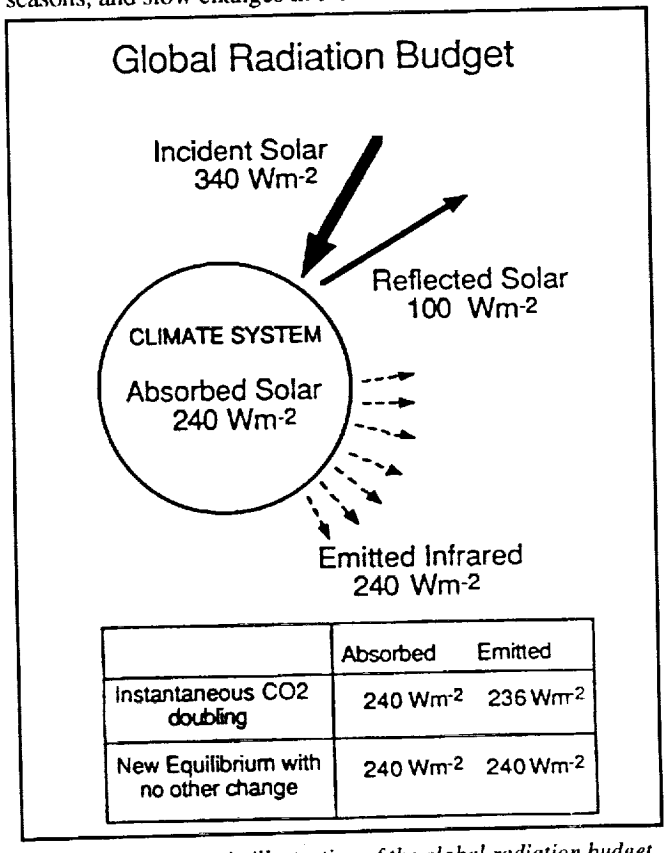


| | Absorbed | Emitted |
|---|---|---|
| Instantaneous CO2 doubling | 240 Wm-2 | 236 Wm-2 |
| New Equilibrium with no other change | 240 Wm-2 | 240 Wm-2 |

*Figure 15. Schematic illustration of the global radiation budget at the top of the atmosphere. Source: IPCC 1990.*

These Milankovitch orbital effects appear to be correlated with the glacial-interglacial cycle, which exhibits temperature variations as great as 10 to 15°C in some mid- and high-latitude regions of the Northern Hemisphere (see Figure 16). On a 100-year time scale, mini-ice ages have been associated with changes in the fluctuation of the envelope of the sunspot cycle.

To provide perspective on the magnitude of solar forcing, it is estimated that in the past 10,000 years the incident solar radiation at 60°N in July has decreased by about 35 W/m$^2$ (Houghton et al., IPCC 1990); the average change in 1 decade is -0.035 W/m$^2$.

Precise measurements from spacecraft show a decline in solar irradiance of 0.1 percent between 1979 and 1986, with a subsequent partial recovery. A 0.1 percent dimming represents a direct heating decrease of about 0.25 W/m$^2$. Fluctuation in reconstructed solar irradiance from 1874 to 1988—derived from the model of Foukal and Lean (1990)—is shown in Figure 17a. The 11-year sunspot cycle is clear. Also evident is the approximately exponential increase in the envelope fitting irradiance maxima. Climatic effects have been attributed to the long-term decadal changes in the envelope of the 22-year sunspot cycle by Eddy, Mitchel, and others, though direct radiational effects are computed to be small. A recent comparison by Friis-Christensen and Lassen (1991) of sunspot cycle length and Northern Hemisphere temperature anomalies is shown in Figure 17b. The correlation is remarkably good, about 0.95. The authors suggest that this parameter based on determinations of cycle length from epochs of maximum and minimum sunspot number may be associated with a physically meaningful index of solar activity. It also removes the apparent lag of the solar activity curve relative to surface temperature as obtained from the smoothed sunspot number. Figure 17c compares the sunspot cycle length with sea ice fluctuations around Iceland. Presently there is considerable discussion about the physics behind such a high correlation with solar activity fluctuations that were previously thought to be rather small from satellite observations. There is, however, some evidence that low-frequency variations could be large and as yet undetected by satellites—for example, a change of solar output of 4 W/m$^2$ between 1968 and 1978 (0.3% of the total output) has been reported by Frohlich (1987).

### 3.3.3.2. GHGs (Forcing)

Figure 18 is a schematic illustration of the greenhouse effect, showing that surface climates are basically a result of the radiational balance between incoming solar radiation and outgoing net (i.e., reflected solar plus infrared) radiation. As implied in Figure 18, the final average land and ocean

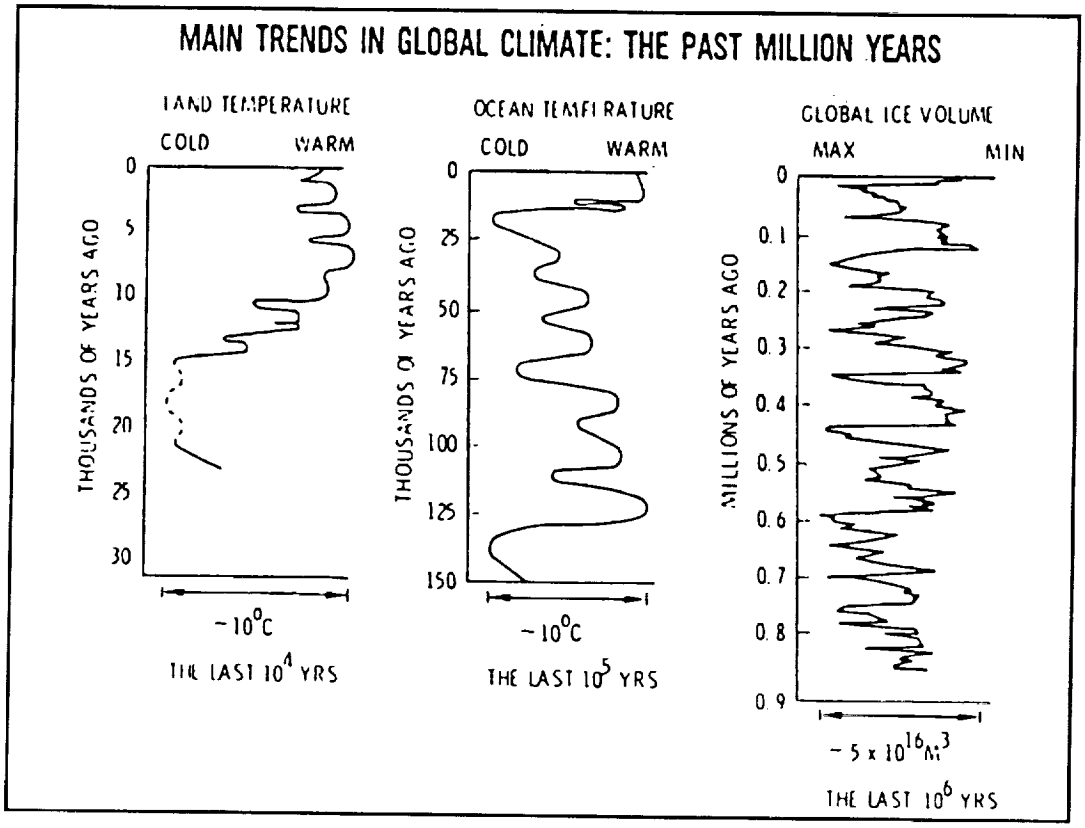


*Figure 16. The main trends in global land temperatures for the last 23,000 years, in global ocean temperatures for the last 150,000 years, and in global ice volume for the last 850,000 years. Source: K.H. Bergman 1983.*

surface temperatures would be modulated by induced or forced changes in the emission, transmission, or reflection of incoming solar radiation or outgoing terrestrial longwave radiation. Thus, changes in solar energy flux, atmospheric aerosols, albedo change due to deforestation or desertification on a large scale, and, of course, infrared-absorbing gases and clouds would affect climate. Internal processes, such as the rate of overturning of the deep ocean circulation, could also cause surface temperature change.

Figure 19 depicts the global annual average fluxes of radiation within the global Earth system. Solar radiation is absorbed by the atmosphere and the Earth's surface, providing the energy required by many terrestrial processes. For the Earth's climate to be in equilibrium, this absorbed solar radiation must be balanced by outgoing thermal radiation. The partial trapping of this thermal radiation by radiatively absorbing molecules helps to increase surface temperature by several tens of degrees compared with what they would be without the atmosphere. This process, called the "greenhouse effect," occurs largely in the first 10 to 15 km of the atmosphere (i.e., the troposphere). Radiatively active constituents both absorb and emit thermal radiation, depending on their effective cross-sections and on temperature. Their emission varies with the local atmospheric temperature, whereas their absorption depends on the temperature of the other atmospheric layers and of the Earth's surface where the radiation was originally emitted. Because tropospheric temperatures decrease with increasing altitude, typically by 5 to 7°C/km, the active atmospheric constituents absorb more upward radiative flux than they emit.

The dominant GHG in the Earth's atmosphere is water vapor. Atmospheric water vapor content is in approximate equilibrium between evaporation and precipitation; this equilibrium is determined by the overall radiational balance of the planet and the dynamic and thermodynamic processes that redistribute the excess solar radiation flux received in the tropics over the middle and polar latitudes. The atmospheric water vapor holding capacity is controlled by the surface temperature, vertical structure, and moisture supply (through evaporation and convective processes). Thus, the water vapor effect is considered to be a "feedback" response to an otherwise introduced temperature change. Likewise, clouds, which are simultaneously very strong infrared warming and shortwave cooling agents, are also dependent on surface temperature, vertical structure, and thermodynamic processes—thus introducing a feedback that could enhance or counter an initial surface warming induced by other forcing agents.

Without the atmosphere's radiatively active constituents, the Earth would lose thermal radiation essentially as a black body at the temperature of its surface (~387 $Wm^2$), neglecting corrections for nonlinearities of the black-body emission, surface emissivities less than 1, and stratospheric effects. The actual radiative flux from the top of the atmosphere is 239 $W/m^2$. Thus the total amount of trapped

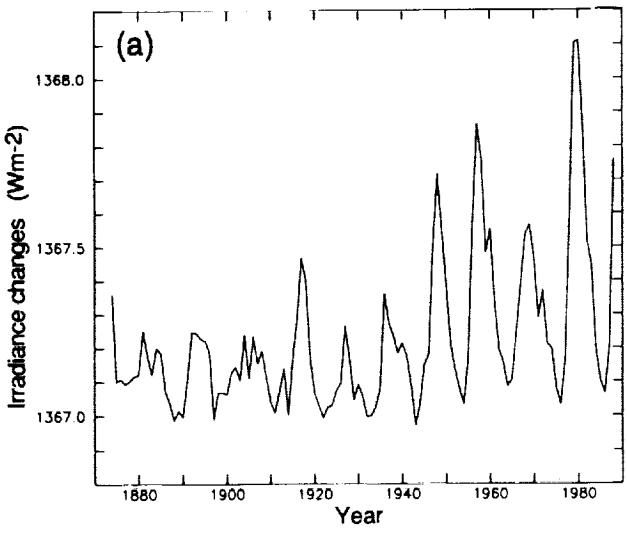


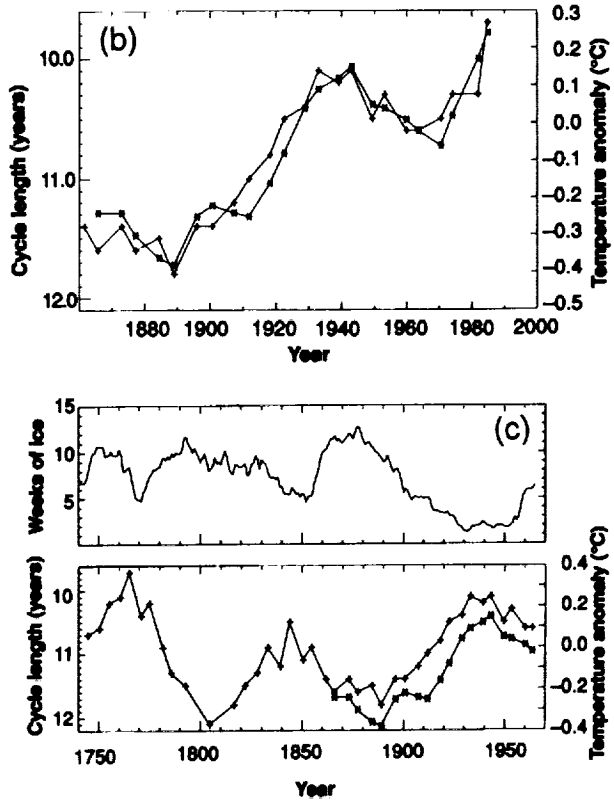


*Figure 17a. Reconstructed solar irradiance ($Wm^{-2}$) from 1874 to 1988 using the model of P. Foukal and J. Lean. Note that solar forcing is only 0.175 times the irradiance due to area and albedo effects. Source: IPCC 1990.*

*Figure 17b. Variation of the sunspot cycle length (lefthand scale) determined as the difference between the actual solar extremum and the previous one. The cycle length is plotted at the central time of the actual cycle (+). The unsmoothed time series have been indicated with a different symbol (*), which represents the Northern Hemisphere anomalies. Source: E. Friis-Christiansen and K. Lassen 1991.*

*Figure 17c. (Top) 22-year running mean of the amount of sea ice around Iceland from 1740 to 1970 during summer (represented by the number of weeks when ice was observed). (Bottom) Smoothed sunspot cycle lengths from 1740 to 1970 (lefthand scale) and Northern Hemisphere mean temperature (righthand scale). Source: E. Friis-Christiansen and K. Lassen 1991.*

radiation is 148 $W/m^2$. Sustained changes to this trapping by as little as 1 $W/m^2$ would change the Earth's radiative balance sufficiently to be of considerable importance for the climate system (Dickinson and Cicerone 1986). Of the radiatively active gases in the current atmosphere, only water vapor ($H_2O$), carbon dioxide ($CO_2$), methane ($CH_4$), nitrous oxide ($N_2O$), and chlorofluorocarbons (CFC-11 and CFC-12) are in sufficient concentrations to be important in the Earth's overall thermal budget. Of these, the strongest absorber by far is water vapor. Indeed, much of the tropospheric radiation can be described with water vapor as the only absorber (Dickinson and Cicerone 1986).

The notion of an "enhanced" GHG effect refers primarily to the incremental global warming caused by increasing concentrations of anthropogenically introduced radiatively active gases, such as $CO_2$, tropospheric $O_3$, $CH_4$, CFCs, and $N_2O$, over and above the greenhouse effect caused by such naturally occurring GHGs as water vapor. Though the word "enhanced" is frequently omitted, the distinction is central to the currently prevalent discussion of greenhouse effects and, indeed, to the way climate models simulate future scenarios of climate change. This central thesis has also been the cause of much of the controversy about predicting future climate change in absolute terms. The controversy arises from uncertainties over the manner in which other forcings and feedbacks compete (with or against) the enhanced GHG effect.

With the exception of ozone, which strongly absorbs solar radiation, primarily in the stratosphere, the other atmospheric

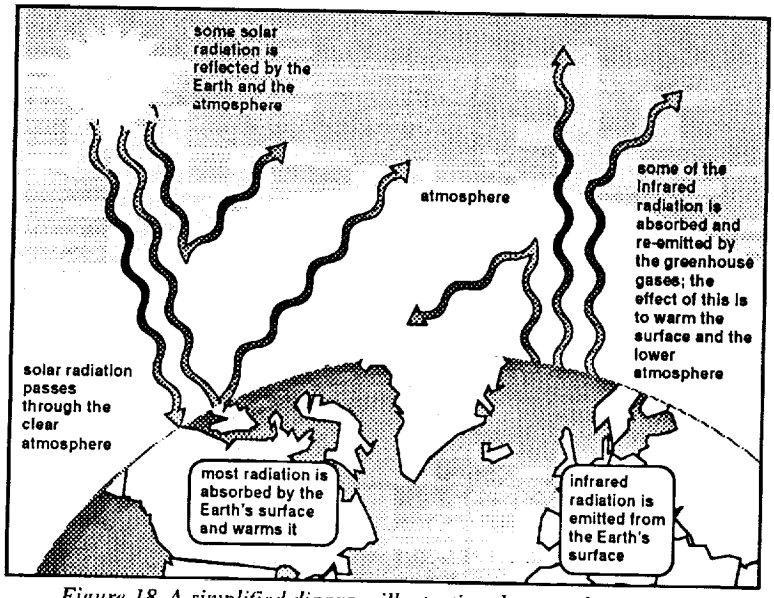


*Figure 18. A simplified diagram illustrating the greenhouse effect. Source: Earth Science Support Office 1992.*

trace gases affect the atmospheric heat budget through their strong absorption and emission of thermal infrared radiation over the wavelength range ~6 to 16 μm. Furthermore, at the wavelengths where water vapor strongly absorbs and emits radiation, the effect of the other gases is minimal. The vibrational-rotational bands of water vapor block radiation at wavelengths less than 8 μm and the rotational bands block wavelengths greater than 18 μm. Carbon dioxide dominates the absorption of radiation between 12 and 18 μm. The remaining spectral region from 8 to 12 μm is known as the "window" because of the atmosphere's relative transparency to radiation over these wavelengths. The intensity of black-body radiation depends on wavelength according to the Planck function; at the temperature of the Earth's surface, this function has its maximum values in the window region. Consequently, ~25% of the thermal emission from the Earth's surface (~100W/$m^2$) is at wavelengths of 8 to 12 μm. A larger fraction of the emission from the top of the atmosphere is in this spectral range. In this wavelength region, emission varies with temperature (T), approximately as exp(-1500/T). A trace gas at a temperature ~33°C less than that of the Earth's emission temperature will thus only reemit about half as much energy as it absorbs. Interestingly, $CH_4$, $O_3$, $N_2O$, CFC-11 ($CCl_3F$), and CFC-12 ($CCl_2F_2$) all have strong absorption bands in the atmospheric window region. These trace gases absorb and emit as functions of wavelength in discrete lines with extended wings. These lines occur in bands and result from the rotational splitting of individual vibrational energy transitions of the molecules. Their strength is determined from the strength of the band transitions, from the concentration of the trace gas, and from the rotational partitioning of the band into individual lines. The emission rate of a line depends on its absorption strength and on local temperature.

The weakest lines absorb radiation significantly only in their line cores, and this absorption increases essentially linearly with concentration of the absorber gas. Somewhat stronger lines absorb radiation mostly in the wings, with only relatively small amounts absorbed by their saturated cores. Increasing absorber concentration pushes the peak absorption farther into the line wings so that wing absorption increases with the square root of the product of atmospheric pressure and absorber concentration. With even stronger line strengths, the peak absorption is pushed so far into line wings that other lines within the band overlap the absorbing wings, and absorption only increases logarithmically with increasing absorber concentration. The absorption of a band varies with absorber concentration according to the variation of its stronger absorbing lines. CFCs and tropospheric $O_3$ are present in such small concentrations and have so many individual lines that their absorption of thermal radiation radiation is nearly proportional to their concentrations; $CH_4$ and $N_2O$, being

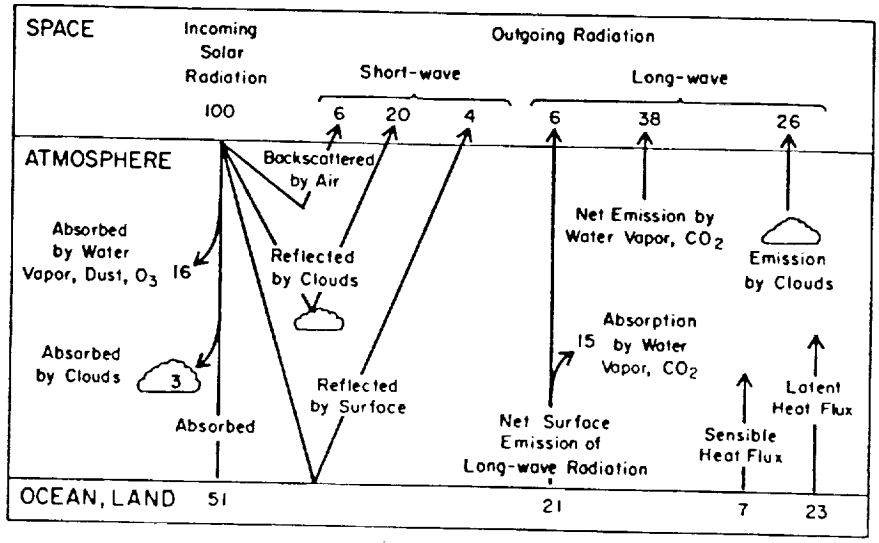


*Figure 19. Schematic of the relative amounts of the various energy inputs and outputs in the Earth/atmosphere system. Source: From NRC data 1975.*

relatively more abundant, increase their absorption essentially according to the square root of their concentrations; $CO_2$ absorption is proportional to the logarithm of its concentration (Dickinson and Cicerone 1986). All the trace gases absorb not in single bands but in multiple bands, and weaker hot and isotopic bands are also present. The above scaling arguments are only approximate and are especially prone to errors if applied to large changes in concentrations where either the stronger bands may change their dependence on absorber amount, or previously unimportant weaker bands of a given gas may become relatively more important.

Figure 20 shows the association of fluctuations in temperature with atmospheric concentrations of $CO_2$ and $CH_4$; the data have been derived from air bubbles trapped in Antarctic ice cores. The correlation is very high, lending credence to the hypothesis that an enhanced GHG effect would cause climate change. The observed global

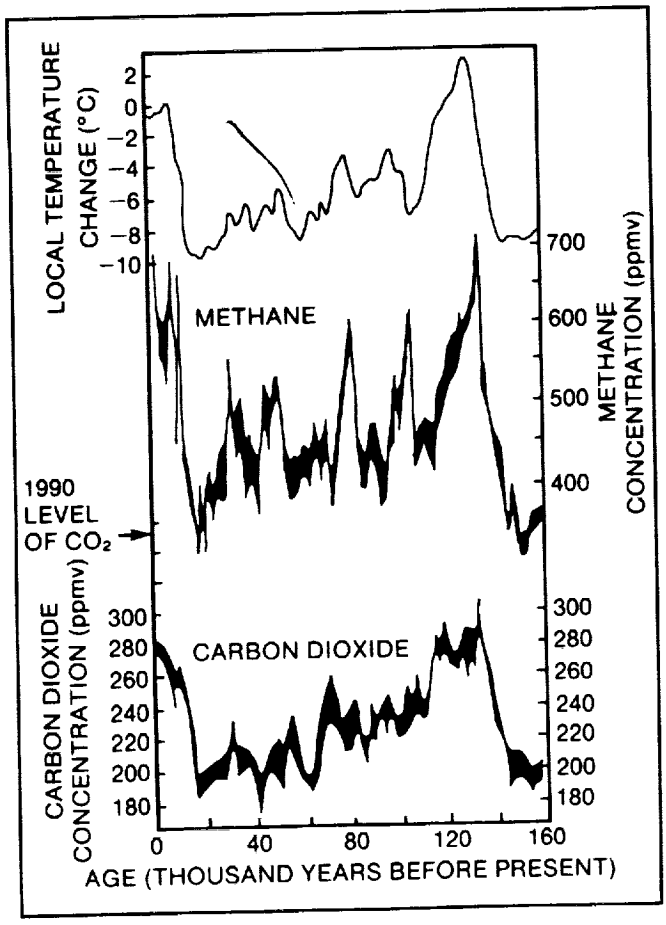


*Figure 20. Analysis of air trapped in Antarctic ice cores showing the correspondence between local temperature and concentrations of methane and carbon dioxide over the last 160,000 years. The 1990 concentration of $CO_2$ is also indicated. Source: Houghton et al., IPCC 1990.*

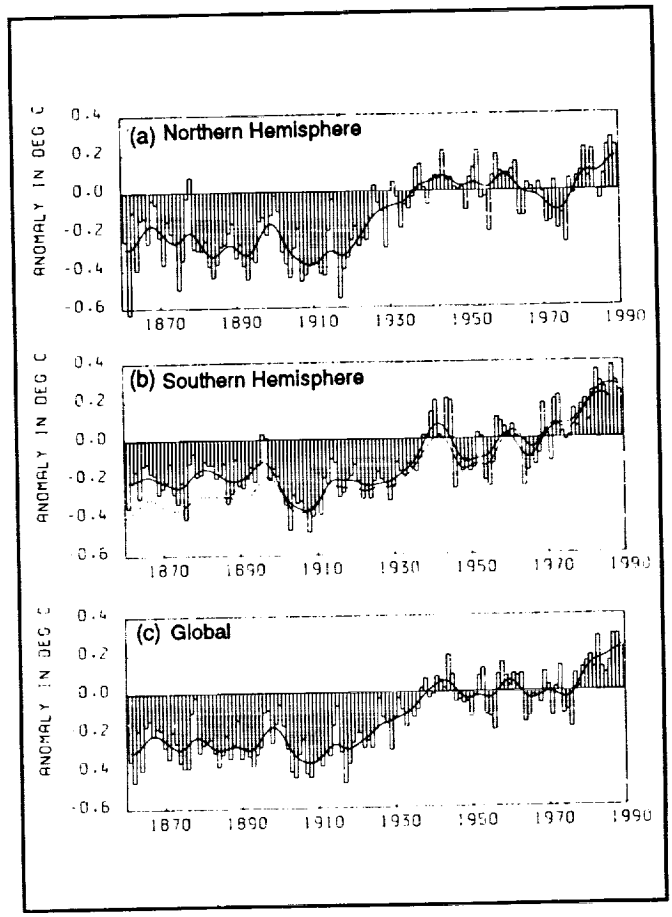


*Figure 21. Combined land air and sea surface temperatures, 1861-1989, relative to 1951-1980. Land air temperatures are from P.D. Jones, and sea surface temperatures are from the U.K. Meteorological Office and Farmer et al. (average of the two data sets). (a) Northern Hemisphere, (b) Southern Hemisphere, (c) globe. Source: Houghton et al., IPCC 1990.*

temperature change is shown in Figure 21, using all available land surface and ocean temperature observations. Since 1979, more accurate and globally consistent observations have been obtained from satellite MSU channel 2R data (see Figure 22), but the subject of global warming is still somewhat controversial because GHG forcing does not operate in isolation. The atmospheric vertical and horizontal distributions of some GHGs (e.g., $O_3$) and greenhouse agents (e.g., clouds), in combination with other elements affecting the radiation balance (e.g., aerosols), would determine the net surface effect (warming or cooling) and magnitude. Also, the surface "climate" change depends on how the physical system responds to an initial change forced by GHGs; thus, feedback processes that may enhance or subdue the initial tendency change need to be taken into account.

The primary reason for concern about increasing concentrations of GHGs is the effect on the planetary

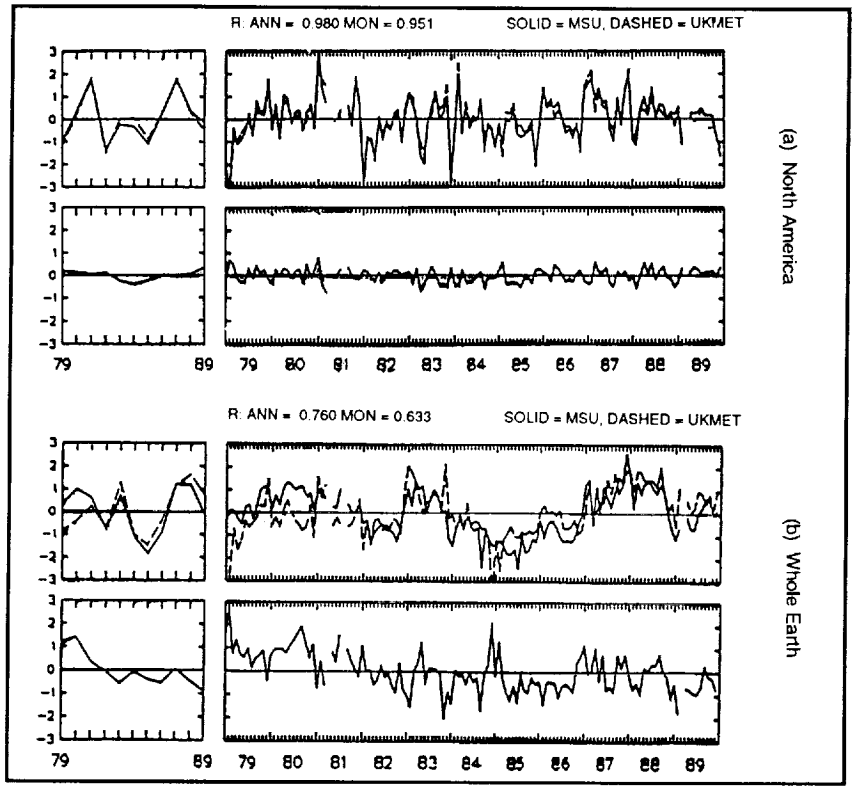


*Figure 22. Comparison between MSU channel 2R and thermometer-derived temperature anomalies for (a) North America and (b) whole Earth. Lower right panels of each set show difference between MSU and thermometer values. Over North America during 1979-1989, there is no trend in the difference, but over the whole Earth the thermometers show a trend +0.18°C warmer than the MSU data. Source: R. Spencer and J.R. Christy 1991.*

*Table 1. Summary of Key Greenhouse Gases Affected by Human Activity*

| Gas | Pre-Industry (1750-1800) | Present (1990) | Rate of Change/yr | Atmospheric Lifetime (yrs) |
|---|---|---|---|---|
| $CO_2$ | 280 ppmv | 360 ppmv | 0.5% | 50-200 |
| $CH_4$ | 800 ppbv | 1720 ppbv | 0.9% | 10 |
| CFC-11 | 0 pptv | 280 pptv | 4% | 65 |
| CFC-12 | 0 pptv | 485 pptv | 4% | 130 |
| $N_2O$ | 300 ppbv | 310 ppbv | 0.25% | 150 |

*Source: Houghton et al. 1990.*

Climate forcing is measured by the change in the heating rate of the Earth in $W/m^2$. For example, the increase in concentrations of the greenhouse gases carbon dioxide, chlorofluorocarbons, methane, and nitrous oxide since the International Geophysical Year in 1958 theoretically caused a heating change of 1.1 $W/m^2$. The accumulated increases in these GHGs since the Industrial Revolution, beginning in 1800, is computed to have caused a heating change of more than 2 $W/m^2$ by decreasing the infrared radiation emitted into space—an amount equivalent to increasing by 1 percent the solar radiation absorbed by the Earth (Hansen 1987). The atmospheric abundance of the above gases has been monitored accurately over long periods, and they are relatively well mixed in the troposphere up to about 10 km. However, ozone in the upper troposphere and stratospheric water vapor—two very important GHGs—are not measured accurately. Both need to be known to assess total GHG climate forcing.

radiation balance, which could alter global surface temperatures. Industrial and agricultural activities over the past century have resulted in an unprecedented rate of increase in the atmospheric concentrations of radiatively active trace GHGs including $CO_2$, $CH_4$, CFCs, and $N_2O$ (see Table 1). Models of the global climate system predict a consequent increase in global average temperature of 1.5 to 4.5°C at equilibrium for a doubling of equivalent $CO_2$. While the regional scale is not accurately resolved by the models, the temperature change is forecast to be even larger in the middle and high latitudes, but smaller in the tropical belt. Attempts to model the existing historical record of global temperature for the past century have not yet provided unambiguous proof that an enhanced GHG effect already exists. Concern about such a warming stems from its potential impact on environmental factors, such as shifting precipitation patterns, weather extremes (e.g., droughts, floods), and sea level rise, and their consequences to agriculture, water supply, the energy and transportation industries, world trade balance, and so forth.

Most global models used to predict climate change use $CO_2$ as a proxy for other GHGs. That is, the models simulate changes in the climate system due to, for example, a doubling of equivalent $CO_2$ concentrations in the atmosphere, and do not explicitly take into account the greenhouse effect of other individual trace gases such as $CH_4$, $N_2O$, and CFCs. The use of an "effective" $CO_2$ concentration to simulate the combined greenhouse effect of $CO_2$ and the trace gases $CH_4$, $N_2O$, CFC-11, and CFC-12 is open to question, because the radiative forcing behavior of $CO_2$ is very different from that of these other gases (Wang et al. 1991, 1992). Atmospheric $CO_2$ is currently increasing at 0.5 percent/year, while $CH_4$, $N_2O$, $CFCl_3$ (CFC-11), and

$CF_2Cl_2$ (CFC-12) are increasing at 0.9, 0.25, 4, and 4 percent/year, respectively. These latter trace gases have strong absorption bands at 8 to 20 μm in the infrared. They are also chemically active and their increase can perturb atmospheric $O_3$ with subsequent climate effects. But the spatial distribution of atmospheric opacity that absorbs and emits the longwave radiation is different for $CO_2$ and for the other trace gases. For example, $CFCl_3$ is optically thin, whereas $CO_2$ is optically thick. This difference can lead to a different distribution of radiative forcing that in turn will affect the dynamics, thereby causing a different climate response.

Table 2 and Figure 23 show the differences in radiative heating and climate from simulations obtained from the NCAR community climate model with and without the other trace gases explicitly treated. Nontrivial differences are apparent. Compared with the response to a doubling of $CO_2$, the addition of other trace gases results in a substantially stronger heating rate in the stratosphere—up to 0.06°C per day at 15 km—and lower tropospheric and near surface cooling over the polar latitudes. In the corresponding equilibrium climate states, the upper troposphere and stratosphere are warmer, as is the surface and the lower troposphere in tropical and subtropical latitudes, when trace gases are increased. Furthermore, in the model, the addition of trace gases yields a more realistic simulation of present climate, correcting the cold bias at the surface and the upper troposphere (especially in the tropics) and the dry bias in the atmosphere. Significant differences are also there in the simulation of regional surface temperature (Wang et al. 1992). The point to be made here is that trace gases and $CO_2$ could have different effects on the Earth's climate and should not be arbitrarily treated as "equivalent" $CO_2$.

Precisely how to handle the entire scientific problem of the detection and prediction of GHG effect and climate change is still the subject of some discussion, even if generalities are commonly assumed to be known. Details on this subject are contained in the report entitled "Greenhouse Effect Detection Experiment-GEDEX" (Schiffer and Unninayar 1992). The global atmospheric temperature record emerges as one of the most analyzed indices of change. Observational analyses generally show that the temperature change over the past 100 years is consistent with climate model simulations, but the change is not large enough to be beyond the range of naturally occurring possibilities. Conceivably, there are other means to detect an enhanced GHG effect, such as a change (increase) in the global average surface downward infrared radiation, but a lack of observational data precludes such an analysis. Multivariable and multivariate fingerprint approaches have been suggested to more convincingly detect the greenhouse effect and to verify the accuracy of predictions from global models (Schiffer and Unninayar 1992), namely by looking for a statistical match between the regional distribution of change in temperature, precipitation, moisture, and sea ice. However, even changes in these parameters may not be the unique result of changes in anthropogenically injected GHGs. Natural biogeochemical processes could alter the moisture and cloud fields, thereby causing a surface temperature change. In order to isolate enhanced GHG effects from changes caused by other processes, all forcings and feedbacks must be quantitatively observed and modeled.

### 3.3.3.3. Ozone (Forcing)

Ozone is the only major greenhouse gas that strongly absorbs solar radiation at the ultraviolet end of the spectrum, primarily in the stratosphere. Stratospheric ozone protects the Earth's surface from harmful solar ultraviolet radiation and plays an important role in controlling the temperature structure of the stratosphere by absorbing both incoming

*Table 2. Radiative Forcing and Climate Statistics*

| | Climate statistics | | | | | | | | Radiative forcing ($Wm^{-2}$) | | | | |
|---|---|---|---|---|---|---|---|---|---|---|---|---|---|
| Case | $T_s$ (K) | $\Delta T_s$ | $P$ (mm per day) | $\Delta P$ | $C$ (%) | $\Delta C$ | $Q$ (mm) | $\Delta Q$ | STS | UTS | LTS | S | TSS |
| A* | 282.8 | — | 3.01 | — | 0.67 | — | 17.4 | — | | | | | |
| B† | 287.0 | 4.2 | 3.26 | 0.26 | 0.65 | −0.019 | 22.6 | 5.18 | −1.06 | 1.09 | 1.47 | 0.950 | 3.51 |
| C‡ | 288.0 | 5.2 | 3.34 | 0.33 | 0.63 | −0.033 | 24.0 | 6.64 | 0.742 | 1.52 | 0.804 | 1.63 | 3.96 |

Annual and global mean values of radiative forcing simulated in the community climate model and the subsequent changes of climate statistics.

The climate statistics are surface air temperatures $T_s$, precipitation $P$, cloud cover $C$ and column water vapour $Q$. The changes of radiative forcing are for the stratosphere (STS; <150 mb), the upper troposphere (UTS; 150–500 mb), the lower troposphere (LTS; 500-mb surface) and on the surface (S) as well as in the troposphere–surface system (TSS).

* 330 p.p.m.v. $CO_2$ without trace gases.

† 660 p.p.m.v. $CO_2$ without trace gases.

‡ 330 p.p.m.v. $CO_2$, 1.7 p.p.m.v. $CH_4$, 0.3 p.p.m.v. $N_2O$, 1 p.p.b.v. (1 part per $10^9$ volume) $CFCl_3$ and 1 p.p.b.v. $CF_2Cl_2$, assumed constant throughout the atmosphere.

*Source: Wang et al. 1991.*

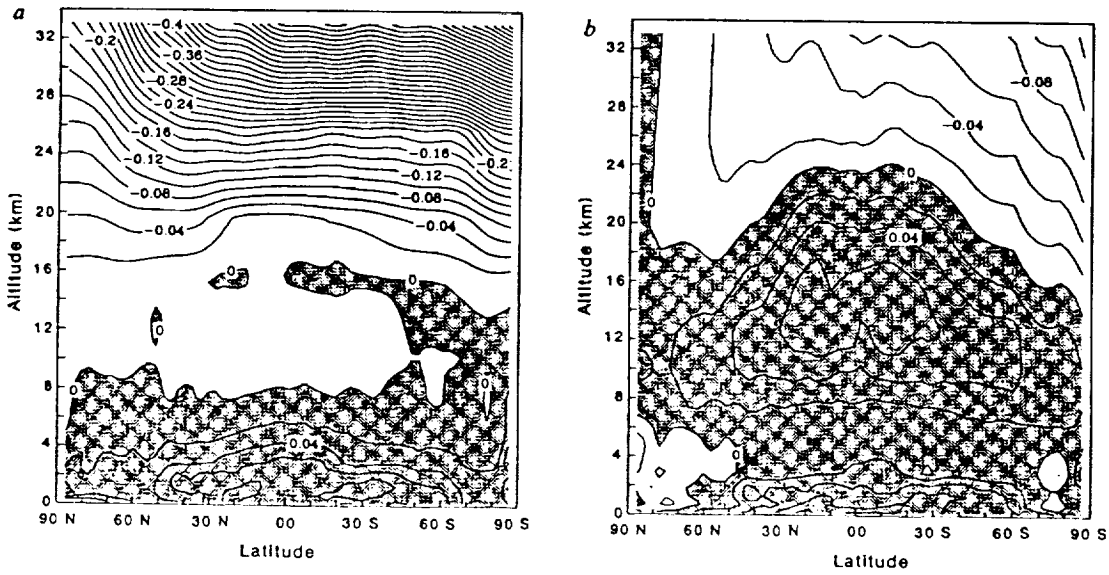


*Figure 23. Latitude-altitude distribution of changes in longwave radiative heating rate (°C per day) caused by a) $CO_2$ doubling and b) the addition of trace gases. The calculations are based on the climatology on January 15, 1991, with an instantaneous increase of the gas concentrations. The shaded areas are warming while others are cooling. The contour intervals are 0.02°C per day. Source: Wang et al. 1991.*

solar ultraviolet radiation and outgoing terrestrial (longwave) radiation. Part of the absorbed outgoing longwave radiation is reradiated to the surface-troposphere system. Reductions in stratospheric $O_3$ can modify the surface temperature through two competing processes: 1) More solar radiation is transmitted to the surface-troposphere system, thereby contributing to a surface warming; and 2) a cooler stratosphere (due to decreased ultraviolet and longwave absorption) emits less to the troposphere, leading to a surface cooling tendency. The solar warming (a function of total column amount of $O_3$) and the longwave cooling (a function of the vertical distribution of $O_3$) are of similar magnitude. Thus the magnitude, as well as the sign of the change in surface temperature, depends critically on the magnitude of the $O_3$ change, which in turn depends strongly on altitude, latitude, and season (IPCC 1990). The reduction of stratospheric ozone is also thought to have potentially serious biological consequences: An increase in the intensity of UV-B at the Earth's surface is expected to increase the incidence of skin cancer and decrease the productivity of marine biota, thus on the biological carbon pump. The latter effect could lead to an increase in the concentration of $CO_2$ in surface waters and, consequently, the atmosphere.

The large seasonal decrease in total ozone (as much as 30 to 40%) over the Antarctic, termed the "ozone hole," has been the cause of considerable investigation and concern in recent years. Stratospheric $O_3$ is photochemically controlled by chemically active species in the oxygen, hydrogen, nitrogen, chlorine, and bromine families. The precursors for the photochemically active species are $O_2$; $H_2O$ and $CH_4$; $N_2O$; CFCs, $CCl_4$, $CH_3CCl_3$, $CH_3Cl$; and halons and $CH_3Br$, respectively. The increasing atmospheric loading of halocarbons, in particular CFCs, is thought to be primarily responsible for the ozone hole—hence the regulatory measures agreed upon under the Montreal Protocol.

An analysis of satellite data measuring aerosol (optical depth), $O_3$, and water vapor (McCormick et al. 1992) indicates a large rate of decrease of about -15 to -20 percent per decade in lower stratospheric ozone for the period 1979-90. This is somewhat larger than the results of Miller et al. (1992) based on balloon ozonesondes (1970-86) of about -6 percent per decade. While the difference in these results is under investigation, they both independently indicate a significant ozone decrease in the lower stratosphere.

Model simulations show that atmospheric temperature is rather sensitive to ozone concentration changes (Hansen). It is hypothesized that some, if not all, the inconsistencies between model results for the 1980s and 1990s, and observational results (Angell), are likely to be due to $O_3$. Because ozone absorbs ultraviolet and infrared thermal radiation, a change in ozone levels can either increase or decrease temperature, depending on the change of the ozone profile.

When $O_3$ is removed in the upper troposphere/lower stratosphere (250 to 20 mbar) in a model, strong cooling of the troposphere (about -1 to 4°C) is produced. When $O_3$ is removed above 10 mbar, a cooling of the stratosphere (up to -80°C) results. Precise measurements of $O_3$, with information on its vertical concentration distribution, are required to accurately quantify the effect of ozone changes. Uncertainties with regard to $O_3$ and tropospheric aerosols are estimated to be 1 $W/m^2$.

### 3.3.3.4. Aerosols and Dust (Forcing)

The impact of aerosol particles (i.e., solid or liquid particles in the range of 0.001 to 10 μm in radius) on the radiation budget of the Earth-atmosphere system is manifold, either directly through scattering and absorption in the solar and thermal infrared spectral ranges, or indirectly through the modification of the microphysical properties of clouds, which affects their radiative properties.

Tropospheric aerosols are important, because they scatter and absorb (primarily solar) radiation, thereby changing the amount of radiation absorbed by the Earth. The composition of the aerosol is important to its radiative effect, because the composition determines whether the aerosol primarily scatters or absorbs solar radiation. A scattering aerosol with an optical depth of 0.125 and with a single scattering albedo of 0.95 could cool the Earth by as much as 1.6°C, whereas the same total abundance of aerosol with a single scattering albedo of 0.75 could warm the Earth by 0.5°C (Charlock and Sellers 1980). The albedo of the aerosol is controlled primarily by the amount of black carbon or soot in the aerosol (although dark soil aerosols can also absorb solar radiation). Quantification of the amount of soot present in the atmospheric aerosol is therefore of importance in order to quantify the overall effect of aerosols on climate. Recent studies have estimated that the amount of radiation scattered as a result of the anthropogenic sulfate in atmospheric aerosols may be a large fraction of the total amount of radiation trapped by increase in GHGs (Charlson et al. 1990). Because emissions of black carbon are associated with sulfur emissions, it is important to quantify the warming effects of soot as well (Penner et al. 1991b).

Aerosols may also affect the Earth's radiation balance through their effects on clouds. Aerosols alter clouds in two ways. First, aerosols act as cloud condensation nuclei (CCN). Changes in the number concentration of aerosols that act as CCN can therefore lead to changes in the number of drops present in clouds. Indeed, clouds that form over continents, where CCN concentrations are high, typically have smaller but more numerous drops than similar clouds that form over the oceans. Other things being equal, these clouds are also more highly reflective of solar radiation (Twomey 1977). Estimates of the effects of anthropogenic and biogenic sulfur aerosols on cloud droplet concentrations have shown that increases in these may be a substantial source of atmospheric cooling (Charlson et al. 1987; Wigley 1990). The effects of aerosols produced in biomass burning can also be substantial (Penner et al. 1991c).

By increasing the number of small drops within a cloud, aerosols may also change cloud lifetime. Warm water clouds with more numerous, but smaller, drops do not form precipitation through the coalescence mechanism as easily as those with large drops. As a result, these clouds may be longer lived and hold more liquid water on average than clouds that form with larger drops (Albrecht 1989; Radke et al. 1989). By increasing the number of CCN, the fractional area covered by clouds may be increased as well as the amount of liquid water present in clouds. Clouds with more liquid water are also more highly reflective of solar radiation. Cold clouds initiate precipitation through ice formation mechanisms; these clouds would not be subject to alteration of their lifetimes through the aerosol mechanism discussed here.

Atmospheric aerosol concentrations and optical depths are highly variable, but, on average, urban concentrations may equal 105 $cm^{-3}$, while pristine ocean areas often have concentrations of less than a few hundred $cm^{-3}$. The corresponding optical depth for these aerosol concentrations varies from a high of about 1.5 to a low of perhaps 0.05. The largest optical depths occur on humid days. This is because above about 80 percent relative humidity aerosols with soluble components deliquesce and form larger haze particles. When particles form a haze they scatter radiation even more efficiently. An ammonium sulfate particle, for example, will increase from 0.1 to 0.2 μm radius when the humidity increases to 95 percent. Its specific scattering cross section then increases by about a factor of 4 (due to its increased cross-sectional area).

The fine particle fraction of the atmospheric aerosol contains most of the aerosol number and is, therefore, the most important to quantify in order to determine the effects of aerosols on clouds. Except in desert dust outbreaks and near the ocean surface where sea salt aerosols are prevalent, the fine particle fraction also contains a large fraction of the aerosol mass as well. Here, the fine particle fraction is defined as those aerosols with diameter less than about 2.0 μm, because emissions have been defined in terms of this component of the aerosol size distribution (Gray 1982; Hildemann et al. 1991a; Hildemann et al.1991b). It is important to quantify the sources of aerosols with a better resolution of size in order to relate aerosol number

concentrations (which often peak at 0.1 to 0.2 μm diameter) to the concentration of particles that act as CCN.

Particles may be composed of sulfate, nitrate, organics, silicates, and other compounds associated with soils and dust, sea salt and compounds associated with the sea salt aerosol, ammonia, soot or black carbon, and trace metals.

The dominant tropospheric aerosols are sulfates, which form from sulfur dioxide ($SO_2$) released by the burning of coal and oil. Their overall impact would be a cooling effect due to the increased reflection of sunlight. About 25 to 50 percent of the aerosols in the atmosphere may be of anthropogenic origin and would correspond to a mean cooling change of between 0.5 and 1.5 $W/m^2$. Thus, the enhanced greenhouse heating caused by the burning of fossil fuels could be offset by cooling due to aerosols produced by the very same anthropogenic activity. Unlike GHGs, however, sulfate aerosols are not well mixed in the atmosphere; therefore, their impact on climate is likely to be different from that of GHGs. The actual tropospheric aerosol loading is very poorly measured.

The stratosphere is relatively clean since the tropopause behaves as a cap over the troposphere, containing most of the atmospheric aerosols, dust, and so on. Stratospheric aerosols are primarily the result of episodic injections of $SO_2$ and dust, among other chemicals thrown high into the atmosphere by large volcanoes. These aerosols can drastically reduce (by up to tens of percent) the direct solar beam, though this is partly compensated for by an increase in diffuse radiation, so that the decreases in total radiation are smaller—typically 5 to 10 percent (Spaenkuch 1978; Coulson 1988). Model results indicate a direct cooling effect of up to 5 years and longer (>10 years) for the relaxation of secondary circulation and feedback processes (Robock). During this period, the aerosol cooling effect would more than offset the enhanced GHG effect. Thus, any change in the frequency of large volcanic eruptions could have a major impact on climate.

Lately, interest has also focused on dimethyl sulfide (DMS) released at the ocean surface to the atmosphere by ocean biological processes. DMS, an efficient condensation nucleus, is thought to be capable of modifying cloud microphysical processes, thereby climate. The atmospheric concentration changes in DMS are relatively unknown. A variety of organic aerosols also exist in the troposphere; however, these are assumed to be in equilibrium and not increasing, as are sulfates.

Large dust clouds originating in the desert regions of the world are likely to have a cooling effect similar to that of aerosols, through the reflection of solar radiation. Satellite pictures also show dust clouds originating in the Sahara region and stretching across the Atlantic to Amazonia (see Figure 24). The causes of fluctuations in this dust cloud are unknown, but they are hypothesized to be linked to fluctuations in the African and Indian monsoon. It is hypothesized that the Amazonian forest is mineralized by the fallout of this Saharan dust, and, on a long-term basis, forest growth cycles fluctuate with the availability of minerals from across the Atlantic. That is, during ages of abundant rainfall over the Sahara, the Amazon rainforest gradually perishes and vice versa. Thus, the desert interacts over the Atlantic to support the living forest.

There are several important questions that require three-dimensional chemistry-climate models (Wuebbles 1991):

- What are the important chemical processes and reaction channels in the gas, aerosol, and aqueous phases that can influence climate, and how do they depend on atmospheric conditions?
- What is the role of sulphur emissions and resulting aerosol chemistry in current climate, and the role of carbonaceous and other aerosols?
- What is the potential impact of changing ozone concentrations on climate and vice versa, and what is the effect of changing climatic (or chemical conditions) on the aerosol-initiated stratospheric ozone depletion in the Arctic and Antarctic?
- What is the impact of the close coupling between tropospheric $CH_4$, CO, OH, $NO_x$, and $O_3$ on projection of climate change, and how might the distribution of these species change?
- How might the exchange of water vapor and other gases between the troposphere and stratosphere be affected by a changing climate, and what is the effect of changes in stratospheric water vapor on stratospheric clouds?

### 3.3.3.5. Clouds (Feedback)

Clouds are simultaneously strong downward infrared radiators and shortwave solar radiation reflectors. How clouds are likely to change with increased greenhouse warming is essentially unknown. Higher surface temperature is expected to cause increased evaporation, which could increase cloud cover, thereby cooling (a negative feedback). But most climate models suggest that increased evaporation would lead to more vigorous moist convection and thunderstorms over a very small portion of the Earth's surface and increased drying by subsidence over the rest of the planet, resulting in reduced overall cloud cover (a positive feedback). Other cloud feedback effects are possible and the signs of their changes currently

unknown (e.g., changes in cloud microphysics such as size and phase of cloud droplets that affect reflection and absorption of solar and terrestrial radiation). Observing and modeling cloud feedback prove crucial to climate change detection and prediction, because the short- and longwave components of cloud-radiative forcing are about 10 times as large as those for a $CO_2$ doubling (Ramanathan et al.). Earth Radiation Budget Experiment (ERBE) data analysis shows that the global shortwave cloud forcing is about -48 $W/m^2$ owing to the enhancement of planetary albedo, while the longwave cloud forcing is about 31 $W/m^2$ as a result of the greenhouse effect of clouds. Therefore the global mean effect of clouds is to cool the climate system by about -17 $W/m^2$. Some studies (Ardanuy) suggest that this could be as much as 27 $W/m^2$.

It must be underscored that even an accurate description of net (i.e., on the average) cloud forcing does not particularly address the issue of forced climate change or cloud-climate feedback. Another quantity—cloud sensitivity, which represents the differential response of Earth radiation budget and other variables of the global system to changes in cloud cover parameters about their mean distribution—proves a critical factor in determining the cloud feedback in simulating or predicting changes in the global system.

### 3.3.3.6. Water Vapor (Feedback)

In warm climate regimes such as the present and that of a 2 x GHG scenario, the thermodynamics of $H_2O$ have a dominant influence in the radiative feedbacks (Ramanathan and Collins). The saturation humidity varies exponentially on temperature; as a result, a 1 percent increase in temperature from 300K would increase saturation humidity by 17 percent. Supporting satellite observations reveal that the total atmospheric water vapor increases by ~17 percent for each 1 percent increase in sea surface temperature. The latent energy of a parcel of air also grows by 17 percent for each 1 percent increment in temperature (T). The surface emission increases at a rate close to 6.1 $W/m^2$ per degree K at around T = 300K, but the emitted energy cannot escape to space; instead, it is trapped in the atmosphere. Further, the trapping increases faster than the surface emission as

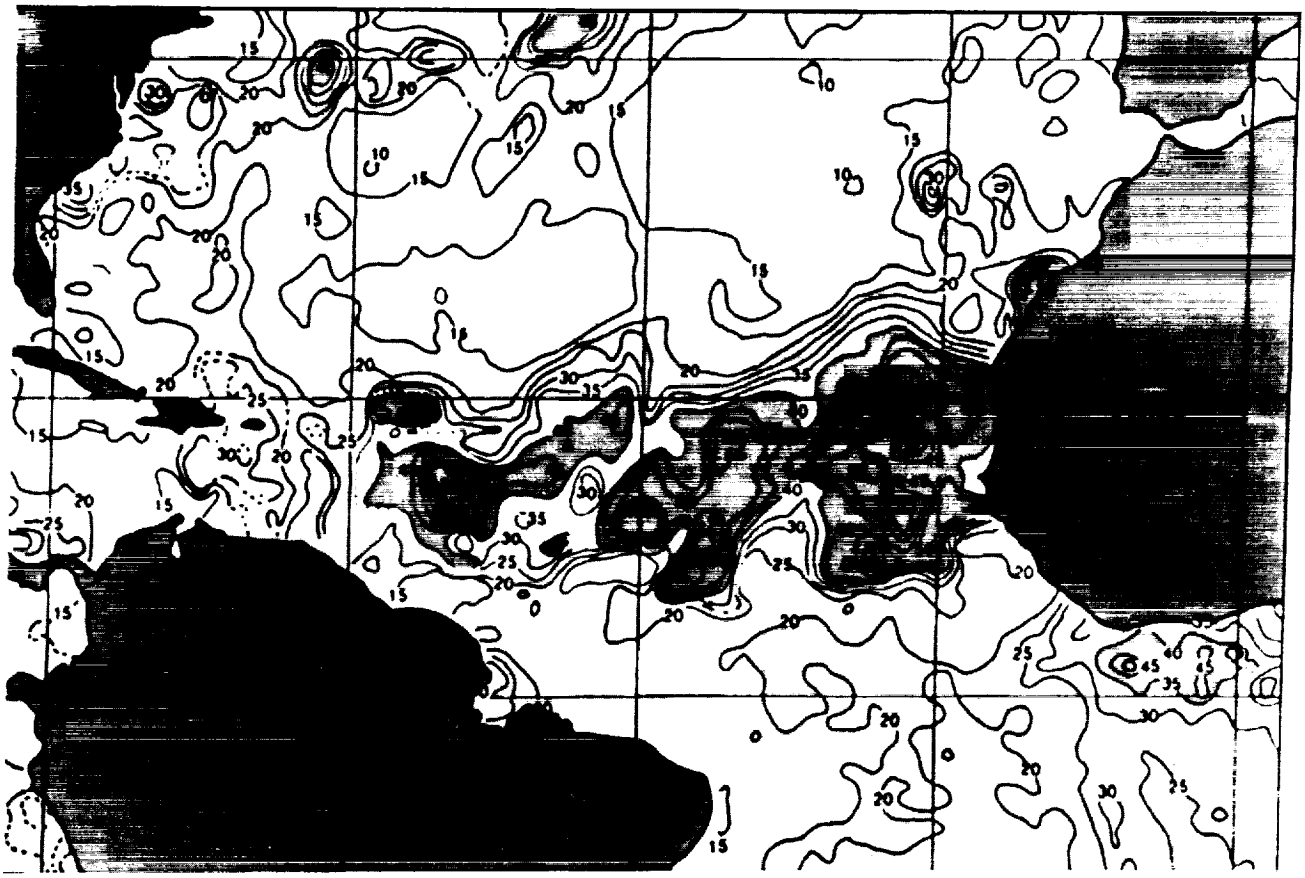

*Figure 24. Aerosol optical depth (x100) on 18-25 June 1987, estimated from the visible channel of AVHRR. Note Sahara dust off Africa and sulfate haze off the U.S. east coast. Source: L. Stowe, NOAA.*

temperatures increase above ~300 K. That is, in the tropics, the warmer tropical ocean/atmosphere system is not governed by the fundamental negative feedback between temperature and infrared emission that expels excess heat by radiating to space.

This tropical "supergreenhouse effect" is caused by a combination of several mutually reinforcing factors, including increases in total column $H_2O$; $H_2O$ continuum absorption that scales quadratically with $H_2O$ partial pressure; higher middle- and upper-troposphere $H_2O$ concentrations; and changes in the lapse rate. When T is greater than 300K, a parcel of moist air near the surface has sufficient latent energy that, if it is forcibly lifted until it reaches saturation, it can overcome the gravitational potential energy and rise to the upper troposphere as a cumulonimbus cloud. The system is potentially unstable unless another negative feedback exists to stabilize it. The warming continues until the clouds become thick enough to shield the ocean from solar radiation and arrest further warming. Most of this shielding is by highly reflective cirrus clouds that act like a thermostat. It is thought that the regulatory effect of these cirrus clouds may limit sea surface temperatures to less than 305K. Wallace and Rossow (1992) dispute the results of the Ramanathan and Collins study in regard to water vapor and cirrus cloud effects.

In the lower atmosphere, water vapor is generally expected to cause a positive climate feedback, because warmer air can hold more water vapor. Models explicitly include such a positive feedback; however, several processes within the large-scale atmospheric circulation and the injection of water by thunderstorms influence the atmospheric humidity profile in different ways. Thus the magnitude of the water vapor feedback is uncertain. Significantly better observations are required, particularly of stratospheric water vapor. Water vapor changes associated with observed climate change must be determined so that the correlation between the two can be quantified.

### 3.3.3.7. Anthropogenically Induced Surface Changes (Forcing)

Changes in the Earth's surface reflectivity (i.e., albedo) due to large-scale deforestation or desertification and urbanization may also produce significant climate forcings. Figure 25 summarizes the relative warming or cooling effect for changes in a range of radiative parameters. Feedback effects are not included. Although they are not accurately known (estimates vary by as much as a factor of 2 or 3), deforestation and desertification rates are increasing with population pressure. Operational meteorological satellites that measure surface reflectivity are not calibrated well enough to provide long-term data, but in several countries major portions of tropical forests have disappeared. Deforestation also continues in the mid-latitude countries.

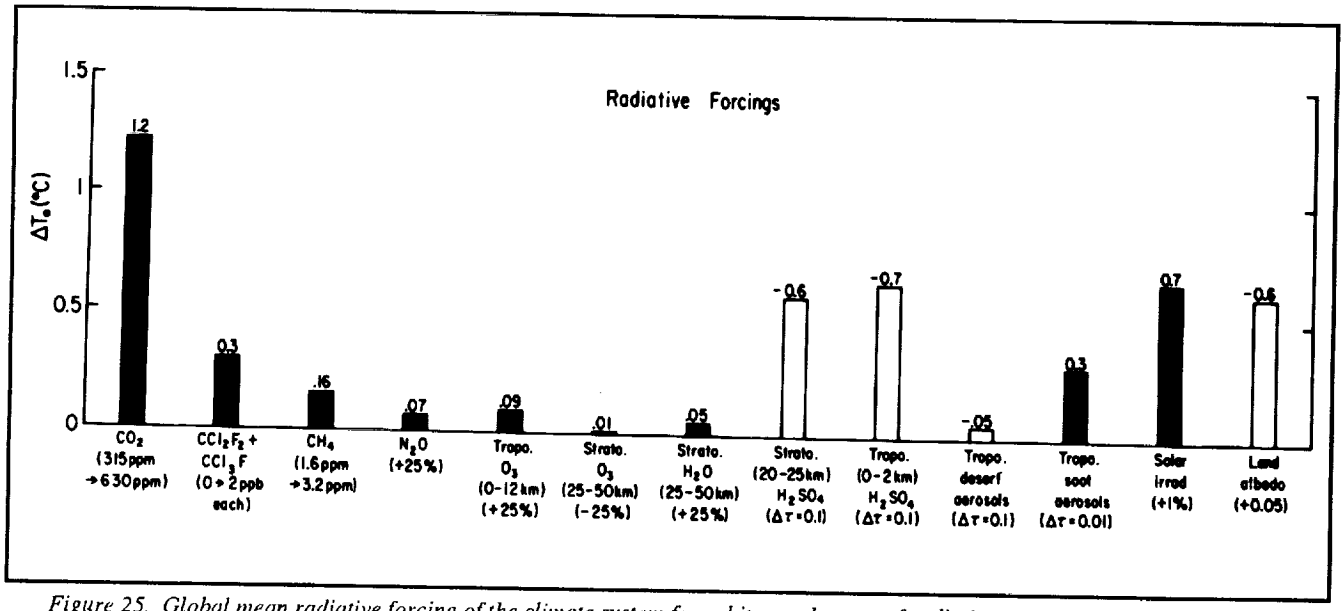


*Figure 25. Global mean radiative forcing of the climate system for arbitrary changes of radiative parameters. Here $\Delta T_0$ is the temperature change at equilibrium ($t \rightarrow \infty$) computed with a one-dimensional RC model for the specified change in radiative forcing parameter, with no climate feedbacks included: $\Delta T_0$ must be multiplied by a feedback factor $f$ to get the equilibrium surface temperature change including feedback effects. Tropospheric aerosols are all placed in the lower 2 km of the atmosphere; the desert aerosols have an effective radius of $r_{eff} \approx 2$ μm and a single scattering albedo $w \approx 0.8$ at wavelength $l = 550$ nm, while the soot aerosols have $r_{eff} \approx 1$ μm and $w \approx 0.5$. The land albedo change of 0.05 is implemented via a change of 0.015 in the surface albedo, corresponding to 30% land cover. Source: J. Hansen et al. 1988.*

***Conclusions/Recommendations (Radiation and Radiative Processes).*** *The conclusions and recommendations below refer to all the subsections covered in Section 3.3.3.*

*More research is required on the relationship between interannual solar fluctuations and stratospheric and tropospheric circulation.*

*More research is required on the influence of decadal and longer term solar fluctuations and the Earth's climate and biological system, including research on physical feedback mechanisms that may be presently unknown.*

*The intriguing and near 100 percent correspondence between sunspot cycle length and global average temperature anomalies during the past 100 years needs to be more fully explored and explained, particularly because it suggests a driving mechanism other than GHG forcing as a possible cause for the observed climate trends. Or, conceivably, solar fluctuations could alter the biosphere (e.g., ocean phytoplankton populations), thereby disturbing the sources and sinks of GHGs which in turn could lead to climate change. Much more complete Earth system models, which include an interactive ocean and land surface biosphere (and not just vegetation), would be required to further research in this area, as well as observations of solar activity and biogeochemical processes.*

*A large number of atmospheric properties contribute to the radiation field. Solar irradiances and heating rates are influenced primarily by the distribution of $H_2O$ at tropospheric levels and $O_3$ in the stratosphere, but a number of other gases (including $CO_2$, $O_2$, $NO_2$, and $CH_4$) also contribute significantly to the heating at some levels. Thermal radiances and cooling rates are sensitive to the distribution of these gases as well as $N_2O$ and CFCs, which absorb strongly in the 8 to 12 μm atmospheric window. A detailed description of the atmospheric and surface temperature distribution is also needed for thermal radiance and cooling rate calculations. Clouds and aerosols at tropospheric and stratospheric levels can also have dramatic influences on the heating and cooling rates. Simplifications and omissions in existing global climate models seriously compromise the accuracies of the net radiative heating rate calculations. Great accuracy is required, particularly in diagnostic models, because the atmosphere is always close to radiative equilibrium. Net heating rates are therefore a small difference (<10%) between the much larger solar and heating components. Small errors in either component can produce much larger heating rate errors. Methods that compute net heating with errors as small as 10 percent are available, but are too computationally expensive for most climate modeling applications. Errors as large as 20 to 80 percent are common in most currently implemented climate modeling applications. More research into efficient radiative transfer models is required. The radiative processes most poorly represented in all climate models are the interaction of absorbing gases and scattering clouds and aerosols at infrared wavelengths. A more accurate treatment of these processes is needed not only for climate models, but also for the analysis of observations to be returned by the EOS system and other remote-sensing instruments.*

*Overall there are two aspects related to the accuracy of GCM radiation calculations. First, given the observed atmospheric and surface parameters, the surface reflectivity and emissivity, atmospheric temperature, and radiatively important constituents (water vapor, $CO_2$, $CH_4$, CFCs, $N_2O$, aerosols, and clouds), how accurately can the GCM radiation codes simulate the observed radiation field? Second, how realistically can the GCM simulate these atmospheric parameters to be used as inputs to the radiation codes? Both aspects are difficult, since the first requires complete and consistent observed data sets, while the second involves the GCM treatment of dynamic and physical processes, as well as chemical and biological processes in the global system.*

*Cloud amount and microscopic optical properties are poorly understood. There is a lot of empiricism involved in getting model simulations to look good—that is, average top-of-the-atmosphere radiation budget. From model output, maps of surface net cloud forcing can also be produced, but nobody knows if the maps are correct. There is a need for new physics regarding physically based cloud fraction, interaction between convection and stability, and more detailed microphysics.*

*Model intercomparisons and observational validations both indicate that cloud-optical depth feedback (CODF) is not well understood or realistically modeled and that it contributes substantially to uncertainties in global warming predictions. Even the global average effect of CODF on surface temperature varies widely from one model to another. Both the sign and magnitude of this effect depend on how CODF is parameterized. Optical depth is proportional to liquid water content; thus, CODF also depends on how cloud water budgets are parameterized. In a 2 x $CO_2$ experiment (UK model) using four different cloud parameterizations, the change in global average surface temperature ranged from 1.9 to 5.4°C.*

*The greenhouse forcing of the climate system is known very accurately for the homogeneously mixed GHGs $CO_2$, $CH_4$,*

*$N_2O$, and CFCs. But the total greenhouse forcing is very uncertain because of likely, but poorly measured, changes in the vertical distribution of ozone. It appears that ozone loss in the lower stratosphere and upper troposphere may be responsible for a temperature decline in the 200-50 mbar region during the past 2 decades. The Goddard Institute for Space Studies (GISS) GCM has been used to make a preliminary estimate of the impact of the Mount Pinatubo volcanic eruption. Assuming an aerosol optical depth of about twice as great as for the 1982 El Chichon eruption, the model forecasts a dramatic but temporary break in the global warming trend. Due to El Niño, the time of minimum global average temperatures could be shifted into 1993. The Pinatubo aerosols should be an acid test of climate models.*

*The effect of volcanic aerosols in the stratosphere (and associated cooling) on surface wind stress and El Niños should be checked.*

*Water vapor is the dominant GHG, and the magnitude of water vapor feedback must be accurately known for climate change prediction. There are large differences between models in water vapor and cloud cover distribution, particularly in the mid-latitudes. The strongest signature for climate change is likely to be in water vapor. Water vapor and temperature lidar sensing is needed for monitoring purposes.*

*Mesoscale simulation experiments show that when temperature increases, water vapor increases in the lower (0 to 1.5 km) and upper (8 to 10 km) troposphere, but decreases in the stratosphere (10 to 22 km).*

*Global chemical transport models are required to obtain the distribution of chemical species in the atmosphere before the heating and cooling effects can be properly determined. Such a model needs to be run interactively with climate models. The climate effects of radiatively active trace gases depend on how well the gas absorbs radiation and the traces' lifetime in the atmosphere. Changes in radiative heating are estimated at 0.54 $W/m^2$ between 1980 and 1990, and 2.45 $W/m^2$ between 1765 and 1990; 55 percent is attributable to $CO_2$ and the rest to CFCs, $CH_4$, $N_2O$, and so on. At present, the actual vertical profile of ozone and ozone depletion is not known accurately. Depending on the level at which it is being depleted, ozone could cause a heating or a cooling. Decreasing ozone concentrations above ~29 km have a warming effect, while decreases below 29 km have a cooling effect. Satellite data show large seasonal and latitudinal changes in ozone. Indirect effects also need to be considered, such as the interaction between CFCs and ozone. CFCs cause heating in regions where ozone causes cooling.*

*In GCM climate experiments, a doubling of equivalent $CO_2$ results in the cooling of the stratosphere and a warming of the troposphere. Reducing $O_3$ by half, for example, leads to a very large cooling of the stratosphere and also the upper troposphere. The stratospheric cooling signal due to 2 x $CO_2$ (or any increase in $CO_2$) needs to be deconvolved from $O_3$ cooling when comparing model results with observations, in order to understand the actual process involved in temperature change. Other issues that need to be resolved more precisely in stratospheric modeling are the fate of the GHGs; radiative impact of aerosol and polar stratospheric clouds; the representation of the tropopause; and the penetration of cyclonic scale disturbances into the stratosphere. For example, one could follow cyclonic disturbances from the 30-mbar level, indicating strong interaction. There is a need to intercompare models with high-resolution campaign data.*

*A distinction needs to be made between stratospheric ozone depletion and tropospheric ozone increases, because their effects on the tropospheric climate are different.*

*Attempts have been made to better parameterize aerosol effects in GCM runs using the results of biomass burning experiments during which detailed measurements were made of droplet concentrations, aerosol concentrations, size distributions, updraft velocities, and so on. Calculations indicate that the effect of biomass burning is in the range of 0.25 to 4 $W/m^2$, but it is not clear whether this is an aerosol effect or a cloud effect.*

*The size of stratospheric aerosols are also important. If the aerosols are very large, they could have a greenhouse effect leading to warming, which could overpower their cooling effect. If ozone is removed from the entire atmosphere, there is a very strong cooling above 10 mbar but very small change at the ground surface; the changes to the heating and cooling effects are canceled out.*

### 3.3.4. The Oceans

This section is relatively short for two reasons: 1) A large part of how a fluid medium is mathematically modeled has already been covered in the Section 3.3.1; and 2) further detail on how the oceans are handled in a global system model are contained in Section 4.6, which deals with simulation and prediction in dynamically coupled models. Had global ocean modeling evolved first (i.e., before global atmospheric models), the situation would have been reversed.

The oceans comprise the saline water of the world. Most solar radiation that reaches the ocean is absorbed, and the high heat capacity of the ocean represents an enormous

energy reservoir. Ocean currents transport large amounts of heat from equatorial regions toward the polar regions [~40% of the total and as high as 74% in the tropics, according to Oort and Haar (1973)], thereby intricately involved in the global energy balance. The upper layers of the ocean interact with the overlying atmosphere or ice on time scales of months to years, while the deeper ocean waters have thermal adjustment times on the order of centuries. The oceans also exchange $CO_2$ with the atmosphere, thus involved in the chemical balance of the climate system. Other interactions involve the hydrological cycle where the freshwater flux into the ocean from precipitating clouds and rivers could alter ocean surface salinity, deep water formation, and ocean circulation. Biochemical feedbacks include the release of DMS by ocean phytoplankton, which being an effective condensation nuclei, could affect cloud formation processes.

The ocean can be both a forcing and a feedback component or element of the global system. The ocean can serve as a forcing element by storing large amounts of heat in subsurface and deep ocean layers, over thousands of years, and releasing this stored heat at a later time. Temperature and salinity distributions and the thermohaline circulation, which determines horizontal and vertical heat transport (and rate), are therefore important ocean features that need to be better understood. On shorter time scales (10 to 100 years), the ocean is treated as a feedback loop in climate models, particularly when addressing the response of the system to a change in climate forcing, such as that caused by GHGs.

Modeling the ocean circulation is similar to modeling the atmosphere in that the mathematical equations used are derived from the same set of fundamental equations that define fluid flow and fluid thermodynamics, together with the specification or calculation of terms defining surface fluxes of radiation momentum, evaporation, and sensible heat. There are, however, significant differences. The time and space scales of relevance are quite different; the radiative flux considerations are more complex for the atmosphere; and water motions are greatly constrained by bottom topography. The oceans are also, by and large, laterally bounded, unlike the atmosphere, which is the reason why the strong boundary currents such as the Gulf Stream and the Kuroshio exist. The dominant time scales in the ocean are very much larger, by orders of magnitude, than those in the atmosphere because of the much greater density and thermal inertia of water. The horizontal length scales are approximately a tenth of those in the atmosphere; thus, ocean models need to use much higher resolution (i.e., smaller grid size) than comparable atmospheric models, but can use much larger integration time steps. Eddy-resolving ocean models use a 0.25° latitude/longitude grid compared with atmospheric climate models that use 2.5° to 5.0° grids. Other differences arise due to salinity. Just as latitudinal differential heating of the atmosphere can cause density differences in the atmosphere, which in large part drive the wind fields, the temperature and salinity differences in the ocean can cause density differences that drive ocean circulations; this effect is seen mainly at high latitudes and in deep waters. Such circulations are termed "thermohaline," "thermo" referring to the temperature influence and "haline" to the salinity influence. The hydrostatic assumption applies even better to the ocean since sea water is nearly incompressible. Thus the equation of continuity is simplified by eliminating the time change of density; however, density variations are included as far as buoyancy effects are concerned. Salinity change is expressed in terms of the horizontal and vertical eddy diffusion of salinity in a manner almost identical to the heat equation. The equation of state is more complicated for the ocean because density is a function of pressure, salinity, and temperature. A modified form of this equation needs to be used at the ocean-ice interface or boundary. That is, a source/sink term needs to be added, which would depend on temperature and whether ice is melting or forming.

Pacanowski and Philander (1981) improved the parameterization of vertical mixing by making the vertical eddy viscosity and diffusion coefficients a function of the local Richardson number. They also found that if the vertical eddy coefficients are too large, the mixing of warmer water in the mixed layer near the surface will be excessive, which results in the thermocline having strong vertical temperature gradients that are possible when local shear is large. If local shear is large and Richardson number small (e.g., less than 0.2), vertical mixing increases dramatically. The revised formulation is based on the evidence that the oceans are, generally, thermally stable except near the polar regions where bottom water may be forming. The instability in these regions is primarily shear-generated. Coarse-resolution models require values for the vertical eddy coefficients different from those used by high-resolution models such as Philander's eddy-resolving model. Other parameters that differ from model to model are the horizontal diffusion coefficients. Coarse-resolution models need to incorporate the effects of subgrid scale eddies.

It is assumed that there is zero stress and no vertical flux of sensible heat or salinity at the ocean bottom. The bottom boundary condition on vertical motion relates vertical motion to horizontal velocity and the local gradient in topography. Thus vertical motions at the bottom are induced by horizontal motions interacting with topography. That is, horizontal flow impinging on an upslope generates upward

motion and vice versa; however, not all topographic effects incorporate slope effects.

At the top of the ocean, fluxes of momentum (wind stress curl), heat, and moisture are either specified from atmospheric data (Bryan and Lewis 1979; Meehl et al. 1982) or calculated using atmospheric models. In either case, flux continuity is assumed across the boundary. Thus the ocean surface wind stress is expressed directly as a function of the local momentum flux in the uppermost ocean water layer, which is a function of surface water density and the vertical gradient of the local ocean currents. The moisture flux from the atmosphere into or out of the ocean is exactly the local precipitation (P) minus evaporation (E). Assuming moisture flux continuity across the surface, this is expressed as a function of the ocean surface water density, salinity, and the local vertical gradient of salinity. On the ocean side of the interface, the atmospheric moisture flux is interpreted or sensed by the ocean as a salinity flux. When P is greater than E, the water becomes less saline; when P is less than E, the water becomes more saline. Ocean salinity is also modulated by the freshwater discharge from rivers. This effect needs to be incorporated, and connects the ocean model to land-surface processes.

The net heat flux into the ocean is obtained from a surface energy balance equation. The net heat flux is equal to the absorbed solar flux at the surface plus the downward infrared flux minus the upward (or outgoing) infrared flux from the ocean surface minus the sensible and latent heat fluxes. The heat flux expression at the ocean surface immediately connects the ocean thermally with several atmospheric processes such as GHG radiative forcing, cloud and convection processes, cloud-radiation feedback, tropospheric and stratospheric aerosol cooling (e.g., via volcanic eruptions), and so forth. Various other boundary conditions and approximations are also used in solving these equations in an ocean model. Very typically for climate system model integration, the deep ocean circulation is held constant or parameterized in terms of its interaction with the upper ocean layers. Details are in Washington and Parkinson (1986).

***Conclusions/Recommendations.*** *Several aspects of the ocean needs more research: Transport of properties by the general circulation; response of the general circulation to wind and thermohaline forcing; the local balance of the oceanic planetary boundary layer and the mixed layer; ventilation and the formation of deep waters; the formation and maintenance of major frontal zones; remote forcing of higher latitudes by the tropics; the response of ocean biota to physical factors; and sea level change.*

*At longer time scales, there is a need to improve the prediction of changes in the deeper layers of the ocean, including the thermohaline circulation and its variability. This requires the accurate prediction of high-latitude freshwater fluxes-evaporation, precipitation, sea-ice processes, and river runoff. That involves all components of the physical global climate system.*

*Several improvements are needed in ocean models. Sea surface temperature is sensitive to both heat flux (e.g., from clouds) and momentum flux (surface winds). These fluxes need to be parameterized accurately. The ocean models used for climate simulations go down to about 3,000 m. Below this, the abyssal circulation is assumed to be quiescent, except at high latitudes. The models are usually not coupled to ice models. When temperatures get too cold, convective adjustment turns on leading to an overturning circulation. When layers become too deep, mass is removed—that is, bottom circulation is implied but not modeled. For stable climatalogical runs, there should be no net heat flux into the ocean from the atmosphere, and no net heat flux into the abyssal bottom ocean.*

*New ocean models need to be developed to run synchronously with the atmosphere so that atmosphere ocean interaction is simulated the way in which it actually takes place in the physical system. The very first such model is currently under development.*

*Most global model experiments use flux corrections (i.e., heat, momentum, salinity, moisture/water) to solve the "climate drift" problem. For the ocean, "climate" would refer to the climate of the ocean. Some groups let the model drift while most use flux corrections to obtain climatologically stable runs. There is a need to investigate exactly what is going on in the model that requires these corrections. Comparing model diagnostics with observations is presently difficult because of the larger errors in the estimates of surface fluxes (~25 W/m$^2$ or more). The Tropical Ocean Global Atmosphere–Coupled Ocean Atmosphere Research Experiment (TOGA-COARE) will get more realistic measurements of surface fluxes. Research on such problems and others should, perhaps, not be overly coordinated, because there is a need for new ideas.*

*The NOAA/NMC medium-range global forecast model (MRF-1989, T80, 18 levels) routinely puts out surface energy budget computations extracted from the 6-hour forecast cycle (the 12- to 36-hour forecast fields are archived at NCAR). Surface heat fluxes follow: Net SW = 200 W/m$^2$; net LW = 70 W/m$^2$; sensible heat flux = 20 W/m$^2$; latent heat flux = 80 W/m$^2$; net heat flux into the ocean = 30 W/m$^2$. The new model (MRF91, T126) produces a net flux into the ocean of about 5 to 10 W/m$^2$. These numbers need to be validated with future observations.*

*The ocean is thought of as a flywheel, but instead it is very active. The atmosphere only sees the surface of the ocean, but with increasing time scales more of the ocean is involved. In regard to running ocean models, there are several questions that need to be answered: How much and to what depth do the oceans need to be initialized, and to what extent does this depend on the time scale of predictions? At what time scale does the ocean lose all memory, and what would be the nature of climate predictions beyond this point (e.g., 1,000 years)? How much more than satellite data is needed for ocean initialization; can we trade off depth of ocean initial data for the time record of wind forcing? Can objective criteria be formulated for the validation of oceanic (or atmospheric) GCMs, and can these criteria be formulated such that atmospheric and oceanic models that individually meet these criteria guarantee a good climatology upon coupling?*

## 3.3.5. The Land Surface and Biosphere

The biosphere includes the plants on the land and in the ocean and the animals of the air, sea, and land, including humans. Although their response characteristics differ widely, these biological elements are sensitive to climate and in turn influence climate. The biosphere plays an important role in the hydrological cycle and in the $CO_2$ budget of the atmosphere, land surface, and the ocean; in the production of aerosols; and in the related chemical balances of other constituents and salts. Natural changes in plants occur over periods ranging from seasonal to thousands of years in response to changes in temperature, radiation, precipitation, and nutrient supply, which consequently has an impact on surface albedo and roughness, evaporation, and ground hydrology. Changes in animal populations also reflect climatic variations through the modified availability of food and habitat. Of particular concern is the erosion of biodiversity and the genetic spectrum of life forms that make the Earth a living planet. The most serious biosphere-climate interaction of concern is human activity leading to increasing concentrations of radiatively active trace gases such as $CO_2$, $CH_4$, $N_2O$, and CFCs; decreasing concentrations of $O_3$; deforestation; and air and water pollution. Some term this aspect of the global system the "technosphere."

Dynamically modeling all aspects of the biosphere is beyond the scope of present-generation models. Substantially more research is required to completely incorporate the biosphere in global Earth system models. As a first step, however, extensive and significant research has been carried out on atmosphere-land surface-vegetation interaction.

### 3.3.5.1. Atmosphere-Land Surface-Vegetation Interaction

Vegetation changes caused by climate would affect the hydrological cycle (through changes in evapotranspiration) and surface boundary layer convergence (through altering surface roughness). Vegetation also interacts directly with atmospheric $CO_2$, and the effect of $CO_2$ enhancement on photosynthetic productivity now appears to be as important as the greenhouse effect due to increasing concentrations of anthropogenically injected atmospheric $CO_2$ (Idso 1991). In a controlled experiment with sour orange trees over a 2-year period, the $CO_2$-enriched trees in an atmosphere of about 680 ppmv contained 2.8 times more above-ground and root-sequestered carbon than did the trees grown in ambient air. The annual cycle of atmospheric $CO_2$ shows sharp changes in response to the vegetation, as would be expected, but the peaks and troughs are becoming more enhanced each year. This is attributed to a more robust global plant life resulting from the aerial "fertilization effect" of the rising $CO_2$ content of the Earth's atmosphere. In a 2 x $CO_2$ atmosphere (i.e., an increase in $CO_2$ of approximately 300 ppmv), mean productivity of the global forests is expected to increase by 182 percent. This number translates into an increase in the rate of carbon sequestering by 2.8 times, leading to a reduction in atmospheric $CO_2$. If all other factors remain the same and deforestation does not decimate planetary biomass, the vegetation-$CO_2$-climate feedback is negative.

Deforestation and desertification processes, urban expansion, and land use changes (e.g., agriculture) alter the character of the land surface, the local hydrological cycle, the *in situ* micro-climate, and sooner or later the socio-economic fabric of the region. When occurring on a large scale, such changes could alter the interaction between the land surface and the atmosphere by affecting the exchange (fluxes) of moisture, heat (sensible and latent), and momentum. Complex interactions between the atmosphere and the biosphere could also affect topsoil erosion (by wind and water), soil nutrient supply, agricultural potential, biodiversity and health, among others. The changes are insidious in that they are not immediately discernible; they are manifest after 10 or more years and sometimes with nearly irreversible consequences. Moreover, micro-climatic changes are usually severely underestimated on account of a lack of research experiments, observations, long-term monitoring, and modeling to provide quantitative information on the nature and cause of the change in question and consequent impact.

At present, there are two vegetation canopy models developed for application in GCMs (and many variants): 1) The biosphere-atmosphere transfer scheme (BATS) (Dickinson et al. 1986), and 2) the simple biosphere model (SiB) (Sellers et al. 1986). Figure 26 shows a schematic of the processes and features relevant to surface hydrology and evapotranspiration. The conceptual construct of both models are somewhat similar, even though several terms in the model are computed differently. Precipitation falls on both the vegetation and ground surface. Some of the precipitation intercepted by the vegetation is reevaporated directly, and the rest moistens the soil. Soil moisture infiltrates the surface, contributes to surface flow, or percolates to deeper layers. In the root zones of plants, moisture is taken up by plant roots, then transpired by leaves. Transpiration rates are defined in terms of the state of the stomata, which generally depends on plant water availability or water stress. The local time rate of change of soil moisture is expressed as precipitation minus evaporation plus snow melt. The snow melt rate is computed from the surface energy balance. The evaporation rate is approximated, albeit crudely, in terms of a critical value of soil moisture and the potential evaporation rate for a saturated surface. Biosphere models interact with atmospheric GCMs through the fluxes of radiation, sensible and latent heat, moisture, and momentum.

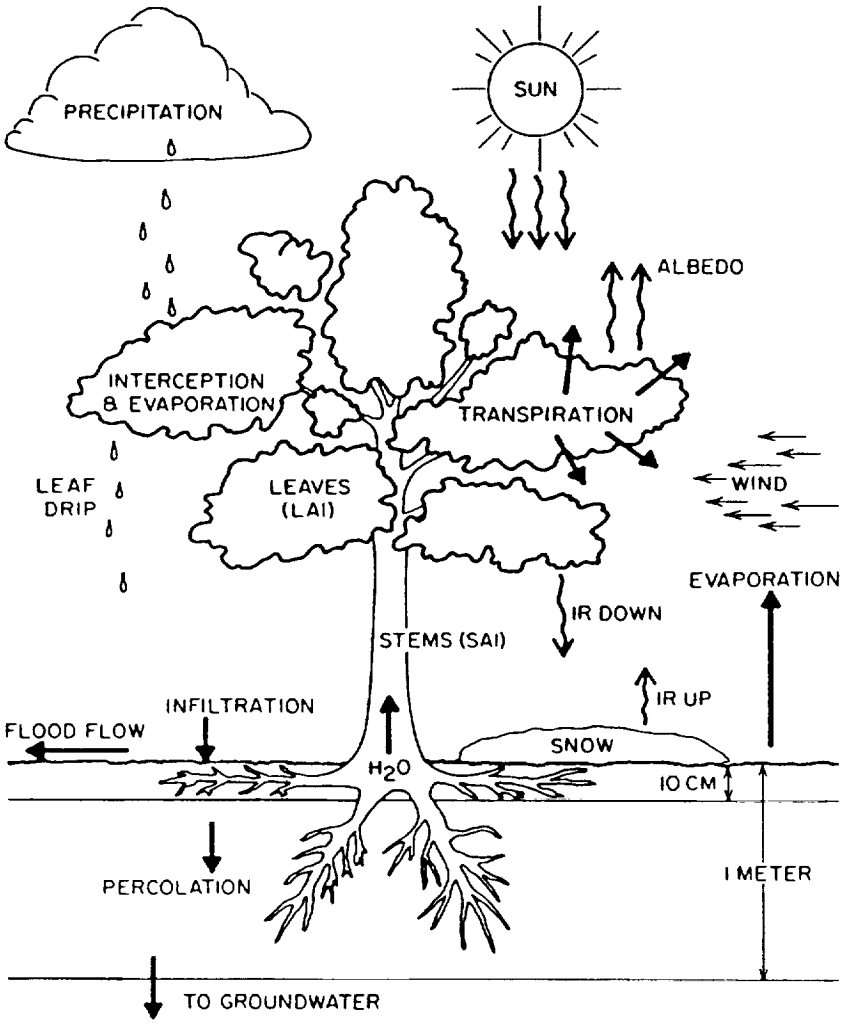


*Figure 26. Schematic of processes and features relevant to surface hydrology and evapotranspiration from Dickinson 1984. Source: Washington and Parkinson.*

Figure 27 depicts the mathematical-physical representation of the SiB model. The model uses or requires the input of approximately 44 parameters. A simplified version of SiB has been developed by Xue et al. (1981), which reportedly performs well but is computationally more efficient. The simplified SiB, called "SSiB," is depicted in Figure 28. Even though simplified, biosphere models can be quite sophisticated. For example, evapotranspiration rate is determined by stomatal resistance, which depends on vegetation type and also on a number of atmospheric and hydrological variables affecting the supply and demand for moisture. Most of the parameters required by SiB are only approximately known for many vegetation types, making model validation difficult.

Figure 29 shows the modeled morphologies of a tropical forest (in this case the Amazon) and degraded pasture scenarios as well as their corresponding SiB parameters. This depiction of the land surface-vegetation was used in an experiment to investigate the effects of deforestation in Amazonia. At present, there are a large number of variants to BATS and SiB, as well as other empirical-mathematical representations of the land surface and biosphere. Serious efforts are being made to intercompare and validate these models (Henderson-Sellers 1992).

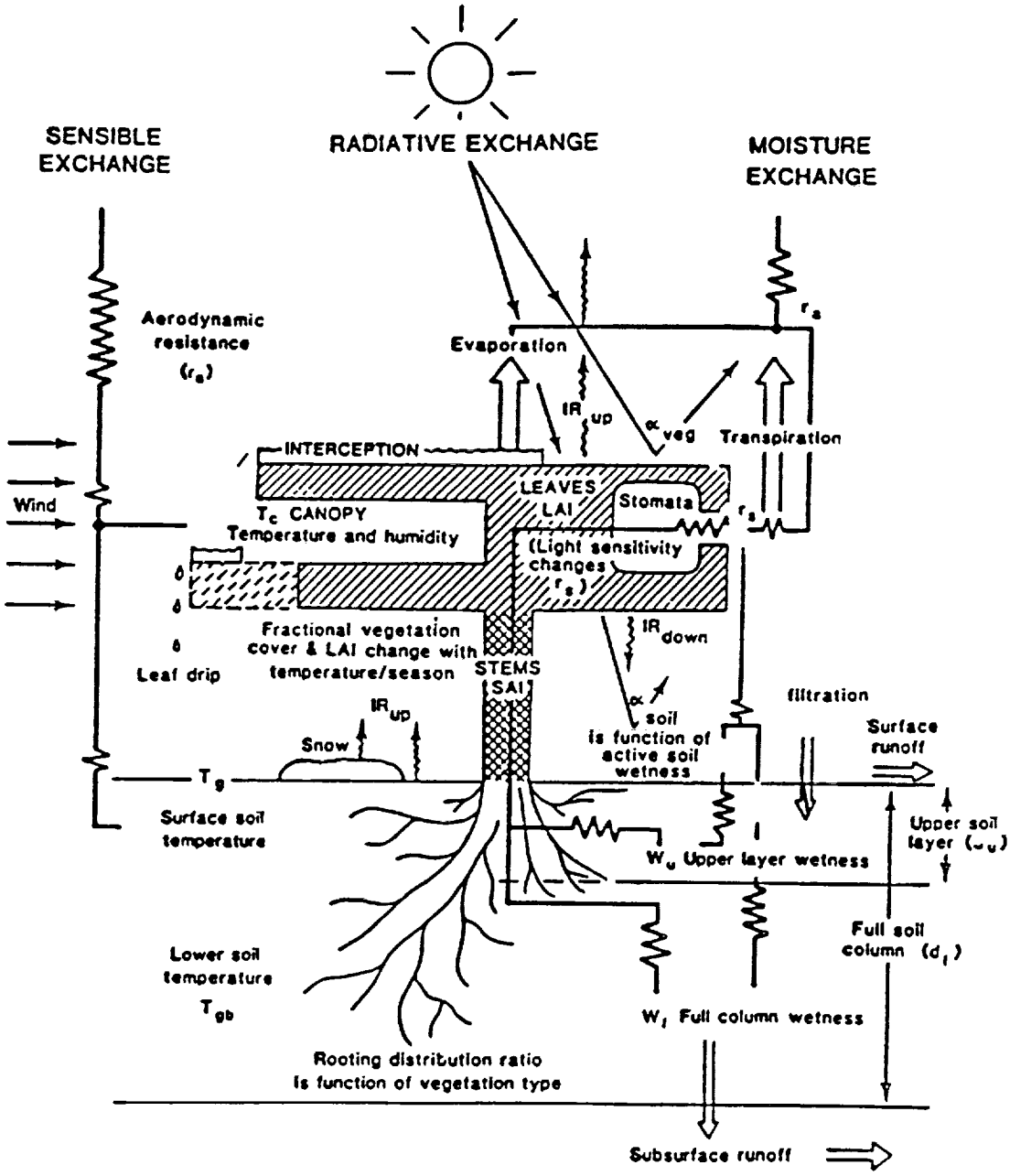


*Figure 27. Schematic representation of the maximum level of complexity so far achieved in land-surface parameterization schemes in GCMs. This scheme controls the radiative, latent, and sensible fluxes occurring at the surface-atmosphere interface. Note especially that the "plant" almost covers one grid element (i.e., ~5° x 5° or approximately 500 km x 500 km).*

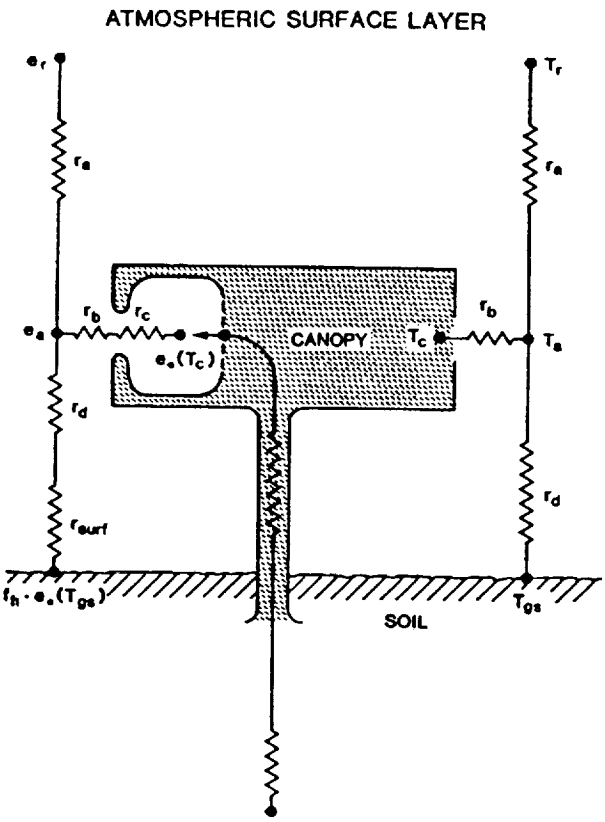


*Figure 28. Schematic diagram of SSiB. $T_r$ is the air temperature at reference height, $T_c$ the canopy temperature, $T_a$ the air temperature within the canopy space, $T_g$ the soil temperature, $r_a$ the aerodynamic resistance between canopy air space and reference height, $r_b$ the bulk boundary layer resistance, $r_c$ the bulk stomatal resistance, and $r_d$ the aerodynamic resistance between canopy air space and ground. Source: Xue et al. 1991.*

***Conclusions/Recommendations.*** *There are several critical issues that need to be addressed: What is the sensitivity of the land system to the most important atmospheric inputs (precipitation, solar and net radiation, surface winds, temperature, and humidity)? How adequate is the formulation of these inputs in models? What is the sensitivity of atmospheric climate to land processes, and how adequate are the current formulations and observations of land processes as measured by this sensitivity (the land processes most affecting climate being albedo, roughness, resistance to evapotranspiration, and water-holding capacity)? In an overall sense, the question is what processes must be modeled to adequately capture the role of land as a component of the climate system? It would be necessary to start with a description of soil and canopies that capture essential processes of energy and water exchange. Some aspects of vegetative properties, such as seasonal variations, should be interactive with atmospheric*

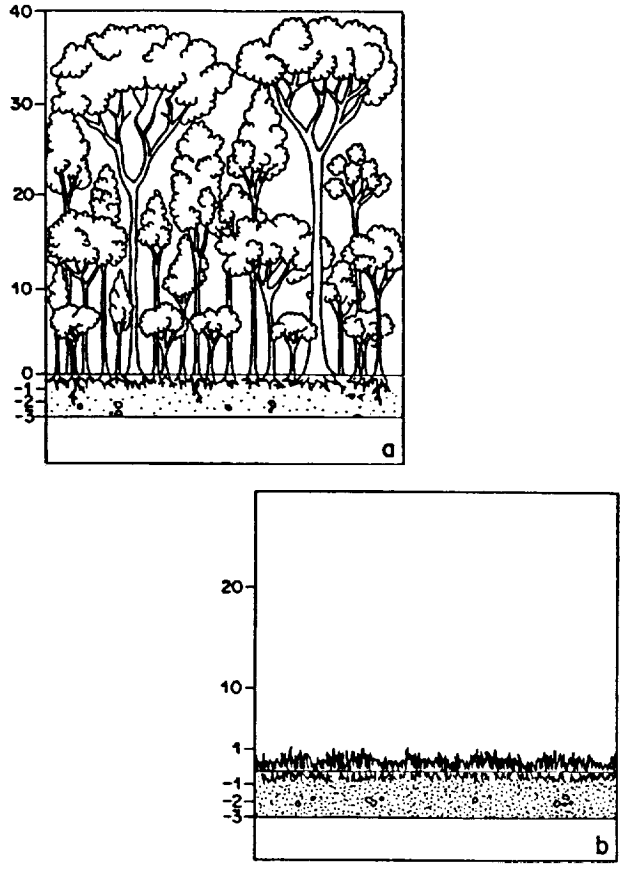


| | Tropical forest | Degraded pasture |
|---|---|---|
| **(a) Vegetation properties** | | |
| Albedo* (%) | 12–14 | 16–24 |
| Roughness length* $z_0$ (m) | 2.65 | 0.08 |
| Displacement height $d$ (m) | 27.4 | 0.25 |
| Minimum canopy resistance* ($sm^{-1}$) | 33.9 | 55.0 |
| Root depth (m) | 2.0 | 0.6 |
| Maximum total root length ($m^{-1}$) | $2 \times 10^4$ | $1 \times 10^4$ |
| Canopy height (m) | 35.0 | 0.6 |
| Maximum total leaf area index | 5.0 | 4–5 |
| Maximum green leaf area index | 4.5 | 2.2 |
| Fractional area covered by vegetation | 1.0 | 0.85 |
| **(b) Soil properties** | | |
| Total soil depth (m) | 3.5 | 3.5 |
| Porosity, $\theta s$ | 0.42 | 0.42 |
| Saturated hydraulic conductivity, $K_s$ (m $s^{-1}$) | $2 \times 10^{-5}$ | $2 \times 10^{-6}$ |
| Soil moisture potential at saturation, $\psi s$ (m) | −0.086 | −0.153 |
| $B$-factor ($B$) relating soil potential, $\psi$, to wetness, $W$ ($\psi = \psi_s W^{-B}$) | 7.12 | 10.4 |

*Figure 29. Schematic diagram depicting the morphologies of a) the forest and b) degraded pasture scenarios used in the study, plus a comparison of SiB parameters for the tropical forest and degraded pasture vegetation types. Source: Nobre and Shukla 1991.*

*models. The coupling of the land surface with the atmosphere should, perhaps, be first approached from a regional perspective. Specific climate change questions follow. What is the role of land surface coupling in projections of global warming (the possibility of a midsummer drought is a serious concern, but surface response to global warming may be highly dependent on atmospheric and surface models)? The adequate treatment of ice and snow may be crucial. How do major natural climate anomalies, especially droughts, depend on land surface coupling? How might anthropogenic land-use changes promote drought and desertification in semiarid regions? How might tropical deforestation, especially in the Amazon, change regional climate (current evidence pointing to major feedbacks in atmospheric precipitation)? Observational field programs and global data sets of relevant parameters and processes are needed to answer these questions.*

*To adequately incorporate land surface-vegetation characteristics into global models, the world should be divided into 10 or 20 ecosystem classes. Surface classification and changes are presently a weak link in global models. For example, surface characteristics (as specified in a model) that determine surface roughness and evapotranspiration would have a strong influence on moisture, heat, and radiative fluxes. The manner in which exchange processes are parameterized has an equally strong influence in the interaction (in a model) between the atmosphere and the land surface. Soil moisture comparisons between the NCAR and the NOAA/GFDL models show vast differences, even though the two models are nearly the same. Such differences are due to varied parameterizations of processes. Amazon deforestation results are model-dependent.*

*Further research is required in incorporating into global models interactive vegetation and an interactive carbon cycle, as well as such impact analysis as climate change-ecosystem interaction.*

*Further details regarding atmosphere/land surface-vegetation coupling are contained in the section dealing with hydrosphere interactions.*

*For a more complete description of the land surface and the biosphere, research is required on the following: Evolution and variability of vegetation and the soils; the uptake and release of water, carbon, and other elements by the soil and biota; atmospheric and soil nutrient cycling; soil moisture storage, runoff, stream flow (surface hydrology), and groundwater flows; the aerodynamic roughness of the land surface, including topographical constraints and vegetative nutritional status; and photosynthetic potential.*

### 3.3.5.2. Land Surface Hydrological Processes

The temporal and spatial scales that characterize surface hydrological processes provide conceptual and practical difficulties to the development of parameterization schemes for incorporation into climate models (Thomas and Henderson-Sellers 1991). In particular, there is a requirement to develop process descriptions that can be applied to large areas but that can model and capture day-to-day, and even hour-to-hour, temporal changes. The forcing of the atmosphere by the heterogeneous character of the land surface is accepted as being an important component of climate variability. Concerning vegetation, global climate system models can now routinely represent both canopy interception and the physiological control of evapotranspiration (Warrilow et al. 1986; Dickinson and Henderson-Sellers 1988) as well as the influence of soil texture on the drainage of moisture through the soil profile (Wilson et al. 1987).

The main problem with modeling land-hydrological processes is the inherent temporal and spatial scales that characterize these processes. This difficulty becomes even more apparent in the context of the spatial grid scales typical of GCMs (i.e., about 200 to 500 km or even more for climate models). The degree to which hydrological processes can be aggregated or disaggregated across space and time while retaining an adequate semblance of hydrologic reality remains unclear. Aggregation is required to incorporate atmosphere-surface-hydrology coupling in a GCM, while disaggregation is required to translate a climate model prediction of, for example, grid-average precipitation (e.g., 500 x 500 km) into values covering 10 to 50 km (maximum) scales of relevance to hydrology. Although the range of space and time scales is formidable at first glance, the problem is not dissimilar to that of modeling convective clouds and subgrid-scale processes in the atmosphere.

Table 3 lists the parameter requirements for models of land surface processes of differing complexity. There is a need to correctly model hydrological processes that involve moisture, water, and energy fluxes between atmosphere-ocean-land surface interfaces and processes within the atmosphere (cloud) and land surface (storage, runoff, soil moisture, and groundwater). This need is demonstrated by the rather dramatic differences in the global distribution of climate in the past. At the peak of the last ice age some 18,000 years ago, 1,500 m of ice covered the land as far south as Kentucky in North America. Increased aridity prevailed in lower latitudes. The Sahara desert advanced nearly 1,000 km southward toward present-day rain forests, virtually burying the river systems of West Africa. The rain forests of Africa,

*Table 3. Parameter Requirements for Models of Land Surface Processes of Differing Complexity*

| Feature | Modeling complexity | | |
|---|---|---|---|
| | Simple | Intermediate | Complex |
| **Vegetation** | albedo [combined value for soil and vegetation] | albedo (single band) | albedo (two band) |
| | | canopy interception fraction<br>fraction of grid cell coverage<br>stomatal resistance (prescribed) | canopy interception fraction<br>fraction of grid cell coverage<br>stomatal resistance (variable) |
| **Soil** | albedo<br>moisture capacity<br>critical moisture deficit | albedo (single band)<br>two-level moisture capacity<br>wilting factor<br>hydraulic conductivity<br>infiltration rate | albedo (two band)<br>*n*-level moisture capacity<br>wilting factor<br>hydraulic conductivity<br>infiltration rate |
| | depth (fixed) | depth (fixed) | depth (subgrid variability) |
| **Landscape** | roughness | roughness | roughness<br>slope<br>aspect<br>drainage network |
| **Snow** | albedo (single band) | albedo (single band)<br>masking by vegetation | albedo (two band)<br>masking by vegetation<br>age |

*Source: Thomas and Henderson-Sellers 1991.*

South America, and (probably) Asia all but disappeared, retreating to a few anomalously humid highland regions. Vast lakes covered the western United States. Millions of tons of glacier ice on land tied up a 100-m layer of the world's oceans, exposing huge areas of continental shelves. Within a few thousand years, the glaciers melted, the sea level rose, and savannas and lakes replaced most of the ice age deserts. About 5,000 years ago, the deserts including the Sahara nearly vanished. The understanding of the processes involved in the transition from glacial to interglacial conditions provide information on the likely range of possible climate conditions (rainfall, flow of rivers, size of lakes, and sea level changes) that could be used for validation purposes.

It is also important to know whether, on a global scale, the partitioning of water among the various reservoirs and the rates of transfer between them (i.e., the fluxes) will change significantly. In other words, is the total global precipitation constant and merely geographically redistributed over time? Or does the efficiency of the hydrological cycle (i.e., the global rates of precipitation and evaporation) change with time? Is the amount of atmospheric water vapor and clouds constant or variable (NRC 1991)?

Serious efforts are being made to improve the parameterization of ground hydrology in global climate system models. According to Rind (1992), the following improvements in the ground hydrological calculations in the NASA/GISS GCM-Model II relative to the old ground hydrology scheme have been proposed:

- Six soil layers instead of two to provide a more realistic representation of soil water dynamics
- Realistic hydraulic and matrix potential, specified as a function of soil texture instead of assigning a constant diffusivity
- The vertical profile of soil properties defined for each grid box (4° x 5° or 8° x 10°) according to soil type instead of vegetation type
- Surface runoff physically modeled instead of prescribed
- Underground runoff included as a physically modeled process
- Gravitational potential included
- Transpiration included in evaporation from land surfaces
- Evaporation of intercepted precipitation and dew on the canopy modeled
- Evaporation from bare soil calculated separately from vegetation covered surface.

Although the above soil-hydrology model parameterization may be coarse when compared with more complex and detailed models—for example, 37 soil depth layers (Nicks)—the latter would be computational timewise prohibitions in a GCM. However, intercomparison runs would need to be carried out to verify and calibrate the GCM.

Other schemes are also being attempted, namely distributed hydrological models. These models attempt to link GCMs to the hydrological scale through nested mesoscale models and PBL parameterization.

***Conclusions/Recommendations.*** *On the land surface, the apportionment of rainfall into evaporation and surface runoff is critical for long-term precipitation climatology, surface fluxes, and surface temperature.*

*GCM simulations should be compared with high-resolution river basin-scale models as well as observations in order to verify the treatment of land surface hydrology in global models. Other issues that need to be addressed include how runoff is computed and the infiltration of precipitation into the ground.*

*Evaporation in the SiB model responds too strongly to changes in specific humidity and changes in ambient temperature profile, leading to an instability that can shut off evaporation under dry conditions.*

*Runoff is computed from atmospheric water flux divergence at the surface—that is, (evaporation - precipitation) = (runoff + infiltration). The biosphere represents a dominant mechanism for the transport of water by transpiration through stomata in vegetation. The dominant process in the flux of moisture from the land surface is evapotranspiration. Big forests release about 100 times more water than bare soil. This important mechanism has only been recently included in GCMs with the use of more realistic parameterization schemes; older models did not have vegetation over the land surface.*

*Applying GCM results to studies of regional hydrology is complicated by the mismatch in the spatial scales of typical hydrological processes compared with the grid resolutions of GCMs. Even if GCMs were accurate at the grid square scale, the grid square results would have to be disaggregated, in some cases arbitrarily, to the hydrological basin scale.*

*GCM precipitation rates at the grid square scale are often quite incorrect, and precipitation rates in a 2 x $CO_2$ simulation are subject to great uncertainty. It is therefore inadvisable to use GCM "global warming" results at the grid square scale to determine the impact of climate change on a region's water resources.*

*Hydrological processes cut across several sections of this report. Numerous other aspects are covered under other sections.*

## 3.3.6. The Cryosphere

The cryosphere, which is composed of the world's ice masses and snow deposits, includes the continental ice sheets, mountain glaciers, sea ice, and surface snow cover. The changes of snow cover and the extent of sea ice show large seasonal variations, whereas glaciers and ice sheets respond much more slowly. Variations in the volume of glaciers and ice sheets are closely linked to variations in sea level. Atmosphere-snow/ice and ocean-ice feedbacks, through altering surface albedo and sensible heat fluxes, could amplify or diminish an initial perturbation in atmospheric temperature. Conclusions and recommendations follow Section 3.3.6.3.

### 3.3.6.1. Sea Ice

Sea ice freezes at approximately -2°C, insulates the atmosphere from the water below, and limits the rate at which the ocean loses energy. However, ice reflects much of the visible radiation that impinges on it, thus limiting the rate at which the ocean gains energy. The area-averaged heat flux from the ocean to the atmosphere is often dominated by the flux through open water "leads" (i.e., a small proportion of the sea ice field). These openings are determined by a combination of surface winds and the underlying ocean circulation.

Generally, increased temperature would tend to melt ice and result in increased absorption of solar energy by the ocean, which is darker than ice (a positive feedback); however, a decrease in sea ice would also lead to larger heat fluxes from the ocean to the atmosphere, which would tend to decrease ocean temperature (a negative feedback). Other effects must also be considered, such as the interaction between the greenhouse effect, the thermohaline circulation, and sea ice. In a warmer climate, there would be a thermal expansion of seawater. But the thermal expansion coefficient of seawater also increases with temperature; hence, smaller meridional temperature gradients do not necessarily mean smaller meridional density gradients. Owing to this effect, the intensity of the thermohaline circulation remains nearly constant over a wide range of warm climates (Manabe and Bryan).

In a cooler climate, the sea surface temperature is likely to be held at the freezing point down to 45° latitude because of the formation of sea ice. The thermohaline circulation will be weak and confined to the region between the ice edge and the equator. The poleward heat transport by the ocean would be significantly lessened as would the upward oceanic heat flux over the region covered by the sea ice. Such a reduction would cause an intense cooling limited to the very stable surface layer of the atmosphere, inducing a further extension of sea ice with high albedo.

Such a positive feedback process between climate, sea ice, and the thermohaline circulation is thought to have induced the cold climates of past ice ages. Thus the interaction among the atmosphere, the ocean, and sea ice; the hydrologic cycle; and the sensitivity of sea ice to climate change need to be observed and quantified.

Modeling and predicting the distribution of sea ice and its interactions with the oceans and atmosphere is crucial for the proper simulation of detailed climatic conditions in the polar regions. Sea ice is both influenced by and influences the oceans and atmosphere. For instance, it serves as a strong insulator by restricting exchanges of heat, mass, and momentum between ocean and atmosphere; it lessens the amount of solar radiation absorbed at the Earth's surface, due to its very high albedo relative to that of open ocean; and its formation often results in a deepening of the oceanic mixed layer, sometimes leading to bottom water formation because of the salt rejection that occurs as the water freezes. Conversely, its motions are significantly influenced by atmospheric winds and ocean currents, and its formation and melt are significantly influenced by atmospheric and oceanic temperatures and oceanic salinity.

Sea ice models typically predict ice thickness and percent areal coverage of ice (i.e., ice "concentration"), with a spatial resolution of ~200 km and a temporal resolution of ~1 day. The calculations include two major parts: 1) Ice thermodynamics based on energy balances, and 2) ice dynamics based on a momentum balance. The major energy fluxes at the top surface of the ice (or the snow if there is a snow layer covering the ice) include the sensible and latent heat fluxes between the ice and atmosphere, incoming solar radiation, incoming longwave radiation from the atmosphere, outgoing longwave radiation from the ice, the conductive flux through the ice, and any flux resulting from surface ice melt. At the bottom of the ice, the three major fluxes are the conductive flux through the ice, the oceanic heat flux, and the flux from bottom ablation or accretion. The calculation of ice movements (or ice "dynamics") is based on Newton's second law of motion, incorporating the major stresses acting on the ice. There appear to be five major stresses: The air stress from above the ice, the water stress from below the ice, the Coriolis force from the rotational motion of the Earth, the dynamic topography from the tilt of the sea surface, and the internal ice stresses from the collisions of ice floes.

Several large-scale sea ice models capable of being used in climate simulations have been developed. The models of Washington et al. (1976) and Semtner (1976) are purely thermodynamic models, simulating large-scale features of the ice cover, though not incorporating any ice dynamics. The model of Parkinson and Washington (1979) extends the thermodynamic model of Washington et al. to include ice dynamics plus a more detailed lead parameterization. The model of Hibler (1979) also includes both ice thermodynamics and ice dynamics, and increases the sophistication of the treatment of internal ice stresses. Even more detailed are the models developed in connection with the Arctic Ice Dynamics Joint Experiment (AIDJEX)—for example, Pritchard et al. (1976), Coon et al. (1976), and Coon (1980)—but these were developed for smaller regions and are generally not considered computationally efficient enough for inclusion in large-scale climate simulations. By contrast, the Washington et al., Parkinson and Washington, and Hibler models have each been used in several large-scale sea ice studies over the past several years. Most notably, the Hibler model has been used in coupled ocean/ice simulations (Hibler and Bryan 1984).

Model simulations have clearly demonstrated the importance in global climate change. The classic example is the prediction of a 20°C warming over the Antarctic Ocean during the austral winter for doubled $CO_2$ experiments run with the GISS GCM. This extreme warming reflects the uninhibited flux of ocean heat to the atmosphere due to a 90 percent reduction in sea ice concentration (Martinson 1991). Recognizing the importance of this boundary layer, most global models today include some form of sea ice formulation such as prescribed sea ice cover or, more commonly, a simple thermodynamic balance with a slab ocean. The adequacy of the ocean-ice coupling is dependent on the time scales of interest as well the region of interest (Arctic versus Antarctic). For short time scales (decadal) in the Arctic, the spatial and temporal distribution of the seasonal sea ice cover (~70 to 80% of the winter ice cover is perennial) represents the largest uncertainty; the ocean heat plays a small role in the Arctic ice budget; and the seasonal distribution depends upon ice dynamics and thermodynamics. In the Antarctic, the marginal stability of the water column and the large contribution of ocean heat (~25 $W/m^2$) require careful treatment (Martinson 1991). Salt rejection during ice growth tends to destabilize, whereas the ocean heat flux acts to limit the ice growth, preventing complete destabilization (i.e., overturning). However, as shown by the Wedell polynya in the mid-1970s, overturn is possible, and the heat flux associated with it will completely eliminate the ice cover. This dramatic response can be triggered by a small perturbation to the air-sea-ice system, and it can be modeled using only an upper ocean model coupled to the ice cover. The ice drift plays a critical role in the stability of the system through its freshwater transport, so it too must be modeled carefully. For long time scales, the ocean stability must be modeled in both Arctic and Antarctic regions, since this controls not only the ability to support ice cover but also the location and the magnitude of deep water

formation and ventilation (tapping the huge deep water reservoir of heat and atmospherically active gases).

Although important work remains in improving sea ice models themselves—such as further consideration of the proper constitutive law and its numerical formulation—an equally important need at the moment is the improved incorporation of sea ice into coupled models. This includes ice/ocean coupling, ice/atmosphere coupling, and ocean/ice/atmosphere coupling. Coupled models should then be used to address such issues as the impact of ice formation on oceanic mixed-layer deepening and bottom water formation, the impact of large polynyas (or open water areas) on atmospheric circulation, and the impact on both the atmosphere and oceans of the ice as an insulator. In addition, there is the need to check model outputs versus observations. This necessitates continued work on compiling sea ice (and other) data sets for comparison, continued efforts to simulate ice conditions in different years, and continued examination of the issue of proper comparison methods.

### 3.3.6.2. Snow Cover

In principle, the snow-albedo-climate feedback may be expected to be a positive one. That is, a warming tendency would tend to decrease snow cover, leading to a decrease in the surface albedo, more absorption of solar radiation, and, consequently, more warming. During a cooling phase, the opposite could be expected to occur. However, even if this process occurs on the long-term average, on shorter time scales change could be more complex. For example, it is not inconceivable that an initial warming trend leading to an acceleration of the hydrological cycle (and Haddley circulation) would transport more moisture from tropical to middle and higher latitudes, thus causing more snow cover. Increased snow cover would, on account of decreased surface albedo, lead to reduced absorption of solar radiation, therefore cooling (a negative feedback) which would counter the magnitude of an initial warming. For a precise understanding of snow feedback, the hydrological cycle needs to be properly understood as well as its linkage with atmospheric, land surface, and oceanic processes.

Even disregarding moisture transport and precipitation processes, recent experiments using the NASA/GISS three-dimensional GCM (Cohen and Rind) indicate that the snow-climate feedback may act counter-intuitively, in that increased snow cover does not necessarily cause reduced surface heating because of the higher albedo of snow.

To fully comprehend the interaction between snow cover and climate and the effects of snow cover on land surface temperature and the energy balance, the influence of snow cover on all the diabatic heating terms must be taken into account. The GISS/GCM experiment suggests that there is a negative feedback built into the interaction between snow cover and climate, through energy balance considerations. The energy terms can be divided into two groups, according to the relationship between the individual energy term and surface temperature. The first group of energy terms is influenced directly by the physical properties of snow cover, its high albedo, and its large latent heat of melting. These properties of snow cover contribute a negative gain of energy to the net heating, which would cause a significant cooling in the surface temperature; they are referred to as the "action" energy terms because they act directly on the surface temperature. The second group of energy terms is indirectly affected by snow cover; they consist of emitted longwave radiation and sensible and latent heat flux. Since they are not altered by the physical properties of snow cover, but rather by the impact of snow cover on the environment, they are referred to as "reaction" terms.

The vertical transfer of energy and mass in the atmosphere is dependent on the vertical temperature profile. The increased stability caused by the cooling quickly suppresses the flux of sensible and latent heat away from the surface. The gain in the net heating is large enough to reverse the negative heating trend at the surface; instead, an overall positive heating term (not including snow melt) is produced for the remainder of the time that an anomalous snow cover remains (a negative feedback). Further modeling, observational, and empirical studies are probably required to confirm the above findings.

### 3.3.6.3. Ice Sheets

The importance of major ice sheets in the global climate is rapidly becoming recognized. No longer are the ice sheets seen solely as a passive reservoir of the Earth's water supply. In either hemisphere, the ice sheets and their connected ice shelves have experienced variations in volume and extent that far exceed the seasonal variations of sea ice. These variations must have affected weather patterns, ocean currents, and, by changing sea level, the entire global climate. However, a major issue yet unresolved is the time scales of these large variations of the ice sheets. Response times for Greenland and Antarctica are usually quoted as thousands to tens of thousands of years, yet data on sea level suggest the possibility of more rapid changes in ice volume (Vail et al. 1978), and fluctuating oxygen isotope values in an ice core from central Greenland have been used to detect a major transition that occurred in less than 100 years (Oeschger 1984).

Ice flow is not easy to model. It is highly nonlinear; the flow rate is very sensitive to the stress applied. Therefore,

small changes in the shape of the ice sheet can cause large changes in flow rates. A further complication is that ice moves not only by deforming the force of gravity but also by sliding over the underlying surface. Modeling of ice sheets controlled by deformational flow has been quite successful. Led by Mahaffey's (1976) model of the Barnes Ice Cap, Budd and Smith (1981) and Oerlemans (1982) have developed similar models that appear to do a good job of simulating the large-scale fluctuations of the Antarctic and Laurentide ice sheets. Birchfield and others' (1981) model of the Northern Hemisphere's ice ages shows the importance of isostatic response of the lithosphere in the initiation of each glacial phase.

However, the results of the Antarctic simulation must remain suspect, because they neglect the primary process of ice sheet discharge—ice streams. Ice streams are akin to rivers of fast-moving ice flowing past much slower ice. A single ice stream in Greenland drains about 5 percent of the entire sheet (Bindschadler 1984). In Antarctica, the majority of the ice is funneled into ice streams, which in turn feed separate or composite ice shelves (i.e., thick slabs of floating ice that eventually generate high tabular icebergs at their seaward margins). The flow of the ice shelves must overcome drag at the sides of the embayment, drag across any isolated bedrock high spots, and the resisting force of the sea. These forces retard the flow of the ice stream. Although a change in snowfall rate or atmospheric temperature will eventually affect the flow rate, therefore the shape, the time scales are of paleoclimatic significance (Whillans 1981). A possible exception to this statement is if the warmed surface of the ice sheet experiences extensive melting, in which case large amounts of water may be released into the oceans. For those broad regions of ice sheet controlled by the ice stream-ice shelf system, the response can be on a time scale perhaps as short as a century.

Recent findings by Blankenship and Bell (Monastersky 1993) indicate an active volcano under the West Antarctic ice sheet, and that the ice sheet lies over a thin, hot crust at least in certain places. Even more than the occasional volcanic erruption, this pervasive geothermal heat melts the base of the ice sheets, providing water for lubricating the ice streams. According to glaciologists, the West Antarctic ice sheet has the potential to collapse because it rests on bedrock well below sea level, unlike the larger stabler East Antarctic ice sheet, which sits atop rock that mostly lies above sea level. Should this frozen mantle melt, world-wide sea levels would rise by roughly 6 m, enough to drown New York City, Los Angeles, New Orleans, Tokyo, Hong Kong, Bangkok, and many other populated spots around the world. Blankenship and Bell believe their volcano discovery reveals an important clue about where ice streams can form and where they cannot. They hypothesize that the onset of streaming is controlled by geology.

***Conclusions/Recommendations.*** *Sea ice processes continue to be a problem in climate global models, as are snow-cloud sensitivity and precipitation. There is a need for dynamic ice models for cryospheric processes that interact with ocean and atmospheric GCMs.*

*There is a strong feedback between sea ice and the atmosphere. If the ice melts (e.g., in a global warming scenario), the cap over the ocean is removed, which substantially increases the heat flux from the ocean to the atmosphere, leading to a further warming (a positive feedback); conversely, if more ice is being formed (cooling scenario), the heat flux from the ocean to the atmosphere is reduced (also a positive feedback). In the Arctic, with about 80 percent perennial sea ice, there is only a 20 percent seasonal variation on the fringe. In contrast, in the Antarctic the seasonal change signal is huge: 20 million $km^2$ in winter compared with 10 million $km^2$ in summer. Sea ice has a large insulating effect and a large albedo effect. In winter, the heat flux from the ocean to the atmosphere is about 30 to 35 $W/m^2$. The flux through the leads is about 100 times greater than thick ice; the 5 percent lead area accounts for about 50 percent of the total heat flux. In the Antarctic, sea ice exists in delicate balance on the surface of an oceanic area with marginal stability. Below the pycnocline, the water temperature is about 2 to 3°C higher than the surface mixed layer waters. The heat flux from below is about 25 $W/m^2$. Ice growth leaves salt in the water, which causes static instability and mixing through the pycnocline. Salt flux generates heat flux by changing the shape of the pycnocline. The consequent downward heat flux through the pycnocline balances the upward heat flux from the lower layers of the ocean, leading to a steady state balance. The pycnocline is a thermal barrier; if a pivotal point is reached the system overturns, setting off deep convection.*

*There is a need for upper ocean models to be coupled to sea ice models, as well as a need for higher resolution. On long time scales, it is important to model the thermohaline circulation properly, especially in the northern Arctic waters where most deep water is formed. During the seasonal transition period, the atmosphere pulls out about 300 to 400 $W/m^2$, which is very large. The balances are very delicate; an error of a few $W/m^2$ can make a large difference.*

*Research and observations are required on the geological and geothermic control of ice sheets. Models need to incorporate such effects when simulating or predicting the dynamics of ice sheets and their interaction with the climate system.*

## 3.3.7. Chemical Processes

Atmospheric, oceanic, and biospheric chemical processes are extremely complex and, by and large, poorly measured and understood. Those chemicals and chemical interactions that directly or indirectly affect the climatic parameters of the Earth atmosphere system, either by modifying the concentrations of radiatively active species or by altering the type and distribution of condensation nucleii that affect cloud processes, are covered in this section.

It has already been established that non-$CO_2$ GHG loading combined equates the effect that $CO_2$ alone has on the greenhouse effect. The atmospheric concentration of such GHGs is determined by biogeochemical processes affecting their emissions, and by the atmospheric and chemical and photochemical processes controlling their destruction (Wuebbles 1991; Penner 1991). For example, there is a strong interaction between $CH_4$, CO, and OH. The hydroxyl radical (OH) is also of particular concern because of its importance in determining the oxidizing capacity of the atmosphere (i.e., its self-cleansing mechanism). Similarly, the effects of $N_2O$ and nitrogen oxides ($NO_x$) on both $O_3$ and OH are also important. Such chemical interactions influence the time-dependent predictability of global climate change. Atmospheric chemistry and constituent transport are important issues that are just beginning to be investigated seriously.

Anthropogenic activity is causing rapid increases not only in the well-known GHGs such as $CO_2$, $CH_4$, $N_2O$, and CFCs but also in, for example, reactive nitrogen ($NO_y$), nonmethane hydrocarbons (NMHCs), reactive sulfur ($SO_x$), and aerosols (Penner 1991). The short lifetime and heterogeneous spatial distributions exhibited by these shorter lived atmospheric components have made it impossible to detect or quantify a trend with any confidence. A major challenge for atmospheric chemists is to quantify the magnitude of the changes in the anthropogenic relative to natural sources, as well as to quantify natural sinks or destructive mechanisms for these constituents. The following subsections summarize existing information on atmospheric chemical constituents, and the interactions and exchange processes affecting their residual quasi-equilibrium concentrations (Wuebbles and Edmonds 1991; Penner 1991; Wuebbles 1992). Conclusions and recommendations follow the subsection discussions.

### 3.3.7.1. Long-Lived Trace Species

Atmospheric carbon dioxide is exchanged with the biosphere on short time scales so that its observed seasonal changes (close to 100 Gt/year) are primarily due to seasonal changes in the abundance of $CO_2$ sequestered by the terrestrial and oceanic biosphere. On larger time scales, $CO_2$ is taken up by the ocean and mixed into deep ocean waters—a net sink for the atmosphere because the time scales for mixing into the deep ocean are long (100 to 1,000 years). The current rate of release of $CO_2$ to the atmosphere from fossil fuel burning and other industrial processes is about 5.7 + 0.5 Gt C/year (Gt = 1,015 g) (Maryland 1989). The release of $CO_2$ from land-clearing practices (including deforestation) ranges from 0.6 to 2.6 Gt C/year (Watson et al. 1990). Accumulation in the atmosphere is about 3.4 + 0.2 Gt C/year, and the uptake by the ocean is estimated at 2.0 + 0.8 Gt C/year. Thus, there is a net global imbalance between present estimates of source and sink mechanism of about 1.6 + 1.4 Gt C/year, representing a missing sink (Penner 1991).

Methane is the most important GHG after $CO_2$. $CH_4$ plays a vital role in atmospheric chemistry through its effect on tropospheric $O_3$ and OH (Logan et al. 1981). Ozone and OH are particularly important because they determine the oxidizing (and cleansing) capacity of the atmosphere. Much of the oxidizing capacity of the troposphere is determined by its odd hydrogen content (the odd hydrogen pool is defined as the sum of OH, $HO_2$, $HNO_2$, $HNO_4$, $H_2O_2$, $H_3O_2$, and other organic radicals) and by the balance of species within the odd hydrogen pool, particularly the OH concentration. Reaction with OH is the single most important scavenger for a variety of species in the troposphere; a second important scavenger whose reactions are particularly important at night is $NO_3$. Methane acts as both a source and sink of odd hydrogen species ($OH_x$) and oxidizing capacity in the troposphere. Thus the oxidation products of $CH_4$ act as a source for $O_3$ and $HO_x$. However, since $CH_4$ also reacts directly with OH, it acts to decrease the tropospheric OH concentration. In the stratosphere, the oxidation of $CH_4$ leads to the production of $H_2O$ and odd hydrogen radicals. Odd hydrogen radicals act to destroy $O_3$ in the upper stratosphere. Reaction sequences involving $CH_4$ can also interfere with the chlorine catalytic cycle, which destroys $O_3$ in the stratosphere. The effect leads to a net increase of lower stratospheric $O_3$ when $CH_4$ increases.

The numerous sources of methane include coal mining and gas drilling practices (80 Tg $CH_4$/year), emissions from landfills (40 Tg), natural wetlands (115 Tg) and rice paddy (110 Tg) emissions, emissions from biomass burning (40 Tg), emissions from enteric fermentation (80 Tg) and termites (40 Tg), ocean (10 Tg) and freshwater (5 Tg)

sources, and $CH_4$ hydrate destabilization (5 Tg) (Cicerone and Oremland 1988). Among these sources, land use by humans is related directly to the source of methane from rice paddies (agriculture), from landfills (urbanization), from biomass burning (forests and grasslands), and from enteric fermentation (pasture or grassland). The present atmospheric loading is about 1.7 ppm, increasing at a rate of 1 percent/year. Accurately estimating the sources of $CH_4$ is made difficult by the large number of small but significant source types.

Chlorofluorocarbons and other halocarbons are of concern to climate change because of their potential for destroying ozone and because they are strong greenhouse gases. The most important halocarbons in the current atmosphere are the chlorofluorocarbons, particularly $CFCl_3$ (CFC-11) and $CF_2Cl_2$ (CFC-12). Additional molecules of these CFCs in the atmosphere are about 12,400 and 15,800 times more effective, respectively, at affecting climate as an additional molecule of $CO_2$.

Nitrous oxide is also a significant greenhouse gas in the atmosphere, serving as a precursor to stratospheric $NO_x$. $N_2O$ has increased from a preindustrial value of about 285 ppb to its current level of 310 ppb. Its increase in the atmosphere explains roughly 4 percent of the increased radiative forcing experienced as a result of GHGs introduced over the last 200 years (Shine et al. 1990). Increases in nitrous oxide can also lead to decreases in stratospheric ozone, since $N_2O$ serves as the major stratospheric source of NO. Thus its tropospheric sources are balanced by removal in the stratosphere by reaction with $O(^1D)$ and through photolysis. The former process is only 10 percent of the total loss rate, but is the important step through which stratospheric NO is produced. Stratospheric $NO_x$ (NO + $NO_2$) destroys $O_3$ through the well-known catalytic cycle wherein NO combines with $O_3$ to form $NO_2$ and $O_2$, and $NO_2$ combines with O to form NO and $O_2$. The net reaction is $O_3$ combining with O (NO being a catalyst) to form $O_2$ plus $O_2$—that is, ozone ($O_3$) is destroyed.

Nitrous oxide is a well-mixed trace constituent with a current global average abundance of about 310 ppb (Watson et al. 1990). The sources of $N_2O$ are very poorly known. Because $N_2O$ has such a long lifetime (about 150 years) even small sources can be important. Stratospheric photolysis was recently estimated to remove close to 13 Tg N/year, though earlier work tended to support a removal rate of close to 10 Tg N/year. The calculated sink from photolysis and the observed increase of $N_2O$ (1 to 2 Tg N/year) must be balanced by the sources of $N_2O$. In addition to the suspected anthropogenic sources mentioned above, $N_2O$ is produced by a wide variety of biological processes in both the ocean and in soils. It also has several different anthropogenic sources. The influence of human activities on fluxes becomes particularly difficult to estimate when factors such as atmospheric deposition of nutrients (supplied by increases in deposition of nitrate from pollution sources, for example) come into play. Additional factors, such as estimation of the importance of nitrogen fertilizer on the flux of $N_2O$, add further complications.

Carbonyl sulfide (COS) is present in the atmosphere at concentrations of about 500 ppt and has a lifetime, based on its reaction with OH in the troposphere, of approximately 10 years. In the stratosphere, it may either react with OH or be photolyzed to form $SO_2$. $SO_2$ reacts with OH and, after a sequence of reactions, forms $SO_{4=}$, the major component of background stratospheric aerosols. Besides direct volcanic input of sulfur compounds (which is episodic in nature), COS is the most important source of the stratospheric sulfate aerosol. Stratospheric aerosols act to scatter solar radiation and can thereby cool the planet, if changes in the sources of COS occur over time. Stratospheric aerosols also act as a site for heterogeneous chemical reactions that may affect the stratospheric ozone layer.

The largest single source of atmospheric COS is emission from the oceans. The oceans emit both COS and $CS_2$. The latter species is converted photochemically to COS in the atmosphere by a rapid reaction with OH. COS is thought to form photochemically in seawater from particulate organic matter (Ferek and Andreae 1984). This source is poorly estimated, because COS concentrations in ocean surface waters vary by over a factor of 10 both spatially and diurnally. $CS_2$ and COS from the ocean are estimated to be 1 to 2 percent of the DMS flux. Given an estimated DMS flux of from 15 to 40 Tg S/year, the estimated flux for COS is roughly 0.2 to 0.6 g S/year. Assuming a similar magnitude source for $CS_2$ and that each $CS_2$ molecule provides one molecule of COS leads to an estimate for the total source of COS from the world's oceans ranging from 0.4 to 1.2 Tg S/year (Penner 1991).

The known anthropogenic sources of COS include the burning of fossil fuels, especially coal, and industrial processes. Industrial processes may also provide a source of $CS_2$. The only other identified anthropogenic source of COS is biomass burning. As pointed out above, this source is associated with land use for agriculture, land use change

during the clearing of forests, and the use of forests for wood fuel. Fossil fuel burning and industrial sources of COS are thought to provide a source of about 0.07 Tg S/year (Khalil and Rasmussen 1984), while industrial sources of $CS_2$ provide a source of COS of 0.2 Tg S/year. Biomass burning may provide a source of between 0.04 to 0.2 Tg S/year (Crutzen and Andreae 1990).

### 3.3.7.2. Reactive Species

Together with $CH_4$, carbon monoxide, nonmethane hydrocarbons, and nitrogen oxide are all involved in the photochemical interactions that determine the concentrations of $O_3$ and OH in the troposphere. Tropospheric $O_3$ is of concern because it is a GHG. It also acts as a respiratory irritant and can damage plants. Through its photolysis to form $O(^1D)$ and through the subsequent reaction of $O(^1D)$ with $H_2O$, it is also the most important source of tropospheric OH.

At present, carbon monoxide levels in the Northern Hemisphere are around 120 to 150 ppb, roughly twice that in the Southern Hemisphere (50 to 60 ppb). Data have also shown that CO exhibits a seasonal cycle with a winter maximum. The seasonal cycle has increasing amplitude at higher latitudes. Recent measurements indicate an increase of about 1 percent/year in the Northern Hemisphere; however, trend data for the Southern Hemisphere are ambiguous (Cicerone 1988).

The dominant sink process for CO is its reaction with the hydroxyl radical (OH). This reaction also serves as a major conversion pathway of OH to other forms of $HO_x$. This latter process is important in controlling the concentration of OH; therefore, it has been postulated that increases in CO contribute to decreases in global tropospheric OH concentrations (Penner et al. 1977). The situation is far more complex because of the projected simultaneous increases in CO, $CH_4$, $NO_x$, and the NMHCs, all of which contribute to determining OH abundances. For example, increasing $NO_x$ concentrations contribute to increases in OH at $NO_x$ levels below a few tenths of ppb, whereas increases in CO, $CH_4$, and NMHCs contribute to decreases in OH. These gases together contribute to $O_3$ formation, which increases OH because $O_3$ photolysis to produce $O(^1D)$ followed by $O(^1D)$ reaction with $H_2O$ is the major source of OH. Because of regional diversity in the sources of these gases and because of uncertainties in their budgets, the relationship between OH and increasing trace species trends is regional in character and demands three-dimensional treatment (Penner 1990). As noted above, changes in atmospheric OH can lead to a suite of changes in other species.

The reaction of CO with OH also initiates a photochemical sequence that, in the presence of sufficient $NO_x$, produces tropospheric $O_3$. The reaction sequence is similar to the sequences of photochemical reactions that produce urban "smog." In regions of low $NO_x$, however, the reaction sequence initiated by the reaction of CO with OH destroys tropospheric $O_3$. An important problem for tropospheric chemistry is to define those regions with sufficient $NO_x$ to produce ozone.

Nonmethane hydrocarbons are often conveniently lumped into the categories of alkanes, alkenes, aromatics, aldehydes, and other oxygenated hydrocarbons, and the biogenically produced compounds isoprene and terpenes. NMHCs participate in the OH and $O_3$ photochemical cycle; they generally react with OH, so that an increase in their concentrations will decrease OH concentrations. However, as these species are oxidized, they also produce odd hydrogen species and organic radicals, so that an increase in the NMHC concentrations contribute to an increase in the concentrations of peroxy radicals and odd hydrogen radicals as a whole. When $HO_2$ and $RO_2$ concentrations are increased, in the presence of sufficient NO, the formation of $NO_2$ is increased. This leads to the production of ozone after photolysis of $NO_2$. The alkenes, isoprene, and terpenes can also react with $O_3$ directly, leading to its removal. Their reaction with $NO_3$ can also be significant.

The lifetimes of the NMHCs vary from a few minutes (for isoprene) to several months for some of the lower molecular weight alkanes. These latter species can be transported a long distance from their sources, while the former can be significant in the formation of ozone and the hydroxyl radical on local scales. The estimated biogenic emissions of isoprene and the terpenes are so large and so widespread, however, that their impact on global photochemistry may also be of importance. In particular, the oxidation of isoprene and the terpenes can lead to the formation of peroxyacetyl nitrate (PAN). This species can be long-lived at lower temperatures and is thought to play a role in the transport of reactive nitrogen from its source regions to the remote troposphere (Singh and Hanst 1981).

Reactive nitrogen ($NO_y$) consists of a suite of nitrogen-containing species—the most important being NO, $NO_2$, $HNO_3$, $NO_3$-, PAN, $NO_3$, $N_2O_5$, and $HNO_4$. The fraction of reactive nitrogen that is present as $NO_x$ (the sum of NO and $NO_2$) is particularly important in both the global troposphere and local urban areas. This is because $NO_x$

plays a major role in the formation of tropospheric $O_3$ and smog. In regions of high $NO_x$, photochemical sequences initiated by the reaction of CO with OH or the reaction of NMHCs with OH lead to $O_3$ formation. In regions of low $NO_x$ (as observed over remote ocean areas), the photochemical sequences lead to $O_3$ destruction. $NO_x$ concentrations also partly control the concentration of OH. Increases in $NO_x$ lead to increases in OH up to $NO_x$ concentrations of a few tenths of a ppb. Increases in $NO_x$ above these levels lead to decreases in OH. At high levels of $NO_x$, such as experienced in some urban areas, the effect of $NO_x$ on hydroxyl concentrations can lead to decreases in $O_3$ as well. This means that a decrease in these emissions would actually increase ozone levels.

A large fraction of $NO_y$ in the troposphere is present as nitric acid ($HNO_3$) and, in the marine boundary layer, as aerosol nitrate ($NO_{3-}$). These two components are important because they are major contributors to acid deposition. Also, their deposition to nitrogen-poor ecosystems and ocean areas can provide an important nutrient for these systems. The long-range transport of reactive nitrogen can be inferred from measurements of $HNO_3$ and particulate nitrate at Mauna Loa (Galasyn et al. 1987). These measurements showed high levels of $HNO_3$ and other pollutants in summer at a time when transport paths could be shown to originate from North America (Moxin 1990). Also, nitrate concentrations in remote regions in the Northern Hemisphere are higher than those measured in the Southern Hemisphere.

There are seven major sources of reactive nitrogen in the troposphere. These include fossil fuel emissions, biomass burning, wood burning, aircraft emissions, lightning discharges, soil microbial activity, and production in the stratosphere from the reaction of $N_2O$ with $O(^1D)$. The biomass and wood burning sources and the source from microbial activity in soils are each associated with land use or land cover. Estimates for the spatial distribution of the global emissions from several of the most important of these sources were developed by Penner et al. (1991a) for a three-dimensional model study of reactive nitrogen. The largest single source of reactive nitrogen and the best determined source appears to be fossil fuel burning. Estimates of the total production in fossil-fuel burning are fairly well-determined and total about 22 Tg N/year (Hameed and Dignon 1988; Dignon 1991).

Reactive sulfur has as its source components the reactive species sulfur dioxide ($SO_2$), dimethylsulfide (DMS), hydrogen sulfide ($H_2S$), and carbon disulfide ($CS_2$). These all undergo chemical reactions leading to their oxidation and the production of sulfuric acid vapor ($H_2SO_4$). Sulfuric acid preferentially condenses to the particulate form, sulfate ($SO_{4=}$), and may either condense on preexisting particles or nucleate to form new particles if the appropriate conditions of humidity, temperature, preexisting particle concentrations, and acid vapor production rates are present. Interest in the reactive sulfur cycle in the atmosphere derives from three concerns. First, $SO_2$ and sulfate contribute to acid rain and acid deposition. Second, the formation of sulfate increases the aerosol burden in the troposphere; sulfate aerosol reflects solar radiation tending to cool the climate (Charlson et al. 1990). Third, the formation of new particles through the homogeneous nucleation of gas phase $H_2SO_4$ can lead to increased CCN concentrations. These particles act as seeds for the condensation of water when cloud droplets form. It has been hypothesized that an increase in CCN concentrations can lead to an increase in cloud droplet number concentrations (Twomey 1977). Clouds with a higher concentration of droplets and the same liquid water content are able to reflect more solar radiation. Increased sulfur emissions may therefore lead to clouds that reflect more solar radiation and cool the climate. Indeed, decreasing temperatures in the Northern Hemisphere during the time period between 1940 and 1970 are possibly associated with an increase in sulfur emissions.

The largest source of reactive sulfur in the atmosphere is fossil fuel burning. This source is estimated to provide approximately 60 Tg S/year (Bates et al. 1991). Industrial processes such as smelting increase the source over that from the burning of fossil fuels by 15 to 20 percent, giving a total anthropogenic source strength of approximately 75 Tg S/year (Bates et al. 1991; Spiro et al. 1991), although estimates as high as 100 Tg S/year have appeared in the literature (Cullis and Hirschler 1980). Fossil fuel and industrial sulfur is released in the form of $SO_2$. Because this source dominates over land areas, its change over time has led to significant increases in the deposition of sulfate to ecosystems and lakes. Ice core evidence from Greenland also indicates that sulfate concentrations over remote areas have increased (Neftel et al. 1985).

The second largest source of sulfur in the atmosphere is the production of DMS by ocean phytoplankton. Because stratus clouds over the ocean are particularly susceptible to alteration of their albedos by changes in CCN, this source has been hypothesized as important for climate change (Charlston et al. 1987). The observation that increased sulfate is associated with ice core data during glacial periods lends support to this theory (Legrand et al. 1988). The

mechanisms involved in the production of DMS by ocean phytoplankton are poorly understood, however, as are the responses of phytoplankton to climate change. Only certain species are involved in the production of DMS, so that correlations of DMS in seawater with total primary productivity or with chlorophyll abundance are poor. Also, the production of DMS may be activated as zooplankton graze on phytoplankton. Thus, the oceanic abundance of DMS depends on ocean ecosystem dynamics as well as primary productivity. Measurements of DMS in seawater together with estimates of flux rates have placed the total source strength of DMS in the ocean at somewhere between 12 and 40 Tg S/year (Bates et al. 1987; Andreae and Raemdonck 1983; Erickson et al. 1990; Spiro et al. 1991). Oceanic emissions of $H_2S$ and $CS_2$ are much smaller than the emissions of DMS.

***Conclusions/Recommendations.*** *Non-$CO_2$ greenhouse gases such as $CH_4$, $N_2O$, and CFCs are adding to the greenhouse effect by an amount comparable to the effect of $CO_2$. Along with their direct radiative effects, they have indirect effects on the climate system through their chemical interactions that affect other important atmospheric constituents. In addition, the atmospheric concentrations of many of the GHGs are determined by biogeochemical processes affecting their emissions and by atmospheric chemical and photochemical processes controlling their destruction. The strong relationship between atmospheric $CH_4$, CO, and OH is also of concern because of the importance of OH in determining the oxidizing capacity of the atmosphere. Similarly, the effects from emissions of nitrogen oxides on both ozone and hydroxyl are also important. Such chemical interactions influence the time-dependent predictability of the global system and climate change on scales extending from the regional to the global.*

*The sources and sinks of most of the radiatively active trace gases need further study to determine the processes responsible for the observed concentration trends. Biogeochemical processes are involved that are poorly understood, as are the changes in these processes with climate change.*

*Anthropogenic activity is causing rapid increases not only in the well-known GHGs, but also in reactive nitrogen, non-methane hydrocarbons, reactive sulfur, and aerosols. The short lifetimes and heterogeneous spatial distribution exhibited by these atmospheric components have made it impossible to detect or quantify a trend with any confidence.*

*A major challenge for atmospheric chemists is to quantify the magnitude of the changes in the anthropogenic sources relative to natural sources, as well as to quantify natural sinks or destructive mechanisms for the chemical constituents of the atmosphere.*

*Because the distributions of non-$CO_2$ green house gases are strongly dependent on atmospheric chemical processes, this implies that understanding of both the current climate and the predictability of future climate depend on the proper consideration of these other greenhouse gases and their chemistry.*

*Global atmospheric chemical transport models are needed to obtain the distribution of chemical species in the atmosphere. Chemical transport models need to be run interactively with climate models—at present there are none. Much better observations are also required of atmospheric chemical constituents.*

### 3.3.8. Atmosphere/Ocean-Geosphere Interaction

Generally, atmosphere/ocean-geosphere interactions are not incorporated in the current generation of global climate system models. However, there is sufficient and significant evidence indicating that this interaction should be accounted for in a predictive scheme for the Earth system. This section describes the observational evidence for the linkage between the atmosphere, the ocean, and the geosphere. Presumably, incorporating this interaction will involve monitoring (of the geosphere), specifying potential changes, and, through momentum balance and hydrological cycle considerations, determining consequent changes to the atmospheric and oceanic general circulation. Thus, just as in the case of atmosphere-biosphere interactions (where the biosphere itself is not modeled, only its interaction), as a first step the geosphere itself need not be modeled. In time, a complete Earth system model would require explicit dynamic subsystem models of both the biosphere and the geosphere, including internal mantle-molten core interaction.

Oort (1985) analyzed in substantial detail the global balance requirements for angular momentum, water, and energy. In particular, he investigates the pathways of these three central and very different physical quantities to elucidate the interrelationships between the various climatic subsystems. The global angular momentum budget and exchange processes that underscore the importance of interactions with the geosphere receive coverage herein. The modeling of these exchange processes could yield potentially useful predictive information for events in the atmosphere-ocean system as well as in the geosphere (e.g., volcanic eruptions and earthquakes).

The absolute angular momentum per unit mass of the atmosphere or the ocean about the Earth's axis is the sum of

the angular momentum of the solid Earth (W—angular momentum) and the angular momentum of the motion of the unit mass relative to the Earth (p—the relative angular momentum). The rate of change of absolute angular momentum moving with the unit volume is balanced by the sum of pressure and friction torques acting on the volume. The friction force can be expressed as the divergence of a stress tensor in which the vertical component near the Earth's surface is of greatest importance. When integrated vertically in the atmosphere throughout a unit area column, the pressure and friction terms on the righthand side reduce to the mountain and friction torque terms, which together link the atmosphere with the underlying surface (Oort and Peixóto 1983). The equations may also be integrated in the zonal direction over a latitudinal belt so that the inflow and outflow of angular momentum through the latitudinal walls are balanced by the surface sources and sinks through the mountain and friction torques, respectively. Since the net mass flow across latitude circles is small to negligible, the main contribution to the inflow and outflow of angular momentum has to be in the form of relative angular momentum—that is, through a correlation between $u$ and $v$.

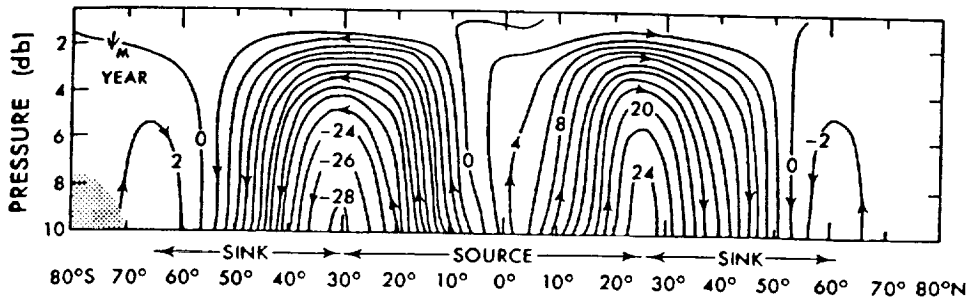


*Figure 31. Zonal-mean cross section of the flow of relative angular momentum in the atmosphere. The streamlines depict, for annual-mean conditions, the atmospheric branch of the cycle with source regions in the tropics between 30°S and 30°N and sink regions in the middle and high latitudes. The units are $10^{18}$ kg $m^2$ $sec^{-2}$. Source: Oort 1985.*

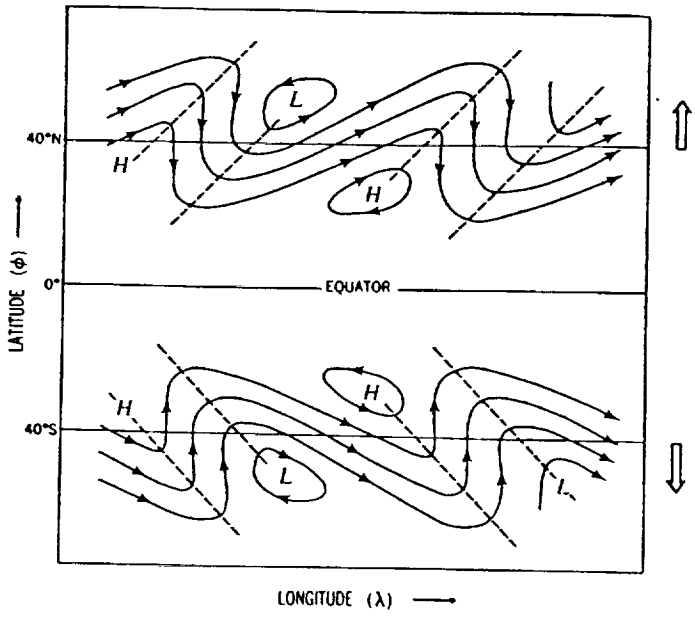


*Figure 30. Schematic diagram of the dominant mechanism of poleward transport of westerly angular momentum by (quasi-horizontal) eddies in the mid-latitudes. Note the preferred SW-NE tilt of the streamlines in the Northern Hemisphere and the SE-NW tilt in the Southern Hemisphere leading to a poleward transport in both hemispheres through the correlation between the v and u components of the wind. Source: Oort 1985.*

The classical dominant transport mechanism is shown schematically in Figure 30 where the NE-SW (NW-SE) tilt of the axis of the wave systems in the Northern (Southern) Hemisphere provides for a poleward transport of relative angular momentum. The observed cycle of relative angular momentum, computed from direct wind observations in the atmosphere is shown in Figure 31 for annual mean conditions. Westerly angular momentum is exported from the Earth's surface (mainly from the oceans) in the tropics, transported upward in the tropical Hadley cells, then transported poleward in the upper troposphere, and finally returned down to the Earth's surface in the middle latitudes.

The atmospheric branch of the cycle of angular momentum as depicted in Figures 30 and 31 is reasonably well-described and understood. Little to nothing is known about the terrestrial branch of the cycle. For global balance, there has to be an equatorward return flow of angular momentum, as shown in Figure 32, within the oceans or the "solid" Earth or both from the middle to low latitudes, which is equal in magnitude but with opposite sign to the transport in the atmosphere. The relative oceanic contribution to this return flow transport is estimated by making a rough comparison between the maximum meridional transports to be expected in the oceans with those measured in the atmosphere at middle latitudes. Typical wind velocities in the atmosphere are of the order of 10 m/sec and the directly observed (and therefore reliable) vertical and zonal mean values of the northward flux of momentum in the atmosphere ($vu$) in the middle latitudes is about 10 $m^2/sec^2$. In the oceans, typical current velocities are much weaker than in the atmosphere, on the order of 0.01 to 0.1 m/sec; therefore, $vu$ values may be expected to be about 0.001 $m^2/sec^2$—that

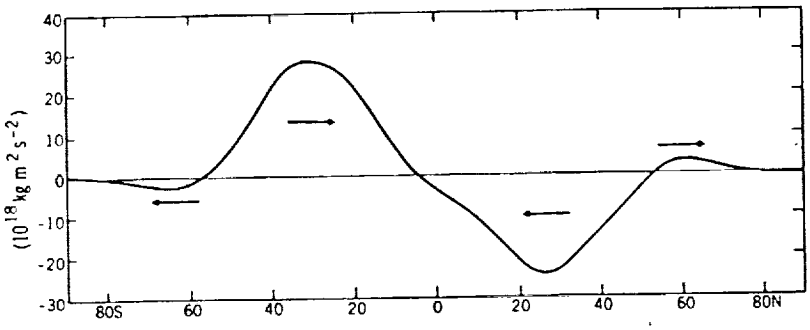


*Figure 32. The annual-mean northward flux of angular momentum in the oceans and/or land (the "terrestrial" branch of the cycle) in units of $10^{18}$ kg $m^2$ $sec^{-2}$ required to close the angular momentum cycle. Source: Oort 1985.*

is, values a factor of 10,000 smaller than in the atmosphere. Taking into account the much greater mass of the oceans (i.e., ~1,000 m of water in the oceans versus 10 m of equivalent water mass in the atmosphere), the oceanic transport would be too weak by about a factor of 100. Thus, a different mechanism for the equatorward transport of angular momentum must be found.

It is hypothesized that the oceans must transport angular momentum only laterally within each latitude belt and not across the latitude circles (Oort 1985). In fact, the oceans must transfer the angular momentum to the continents in the same belt, thereby acting as an intermediary or handover agent between the atmosphere and the continents. It is speculated that this takes place through continental torques exerted by the oceans through raised or lowered sea levels along the continental margins in a fashion comparable to the pressure torques across mountains in the atmosphere. The concept is depicted in Figure 33. The main contribution to the pressure torque is probably due to the difference in sea level across each continent. Differences in sea level of 50 cm are found between the west and east coasts, leading to a westward torque on the low-latitude continents (see Figure 34). Similarly, an eastward torque would be exerted in the middle latitudes where the westerly winds dominate. See Figure 35 for quantitative estimates of the continental torques using more recent data of dynamic topography (Levitus 1985). The figure also shows the total required surface torque derived using atmospheric data only. The agreement between the two curves, despite the

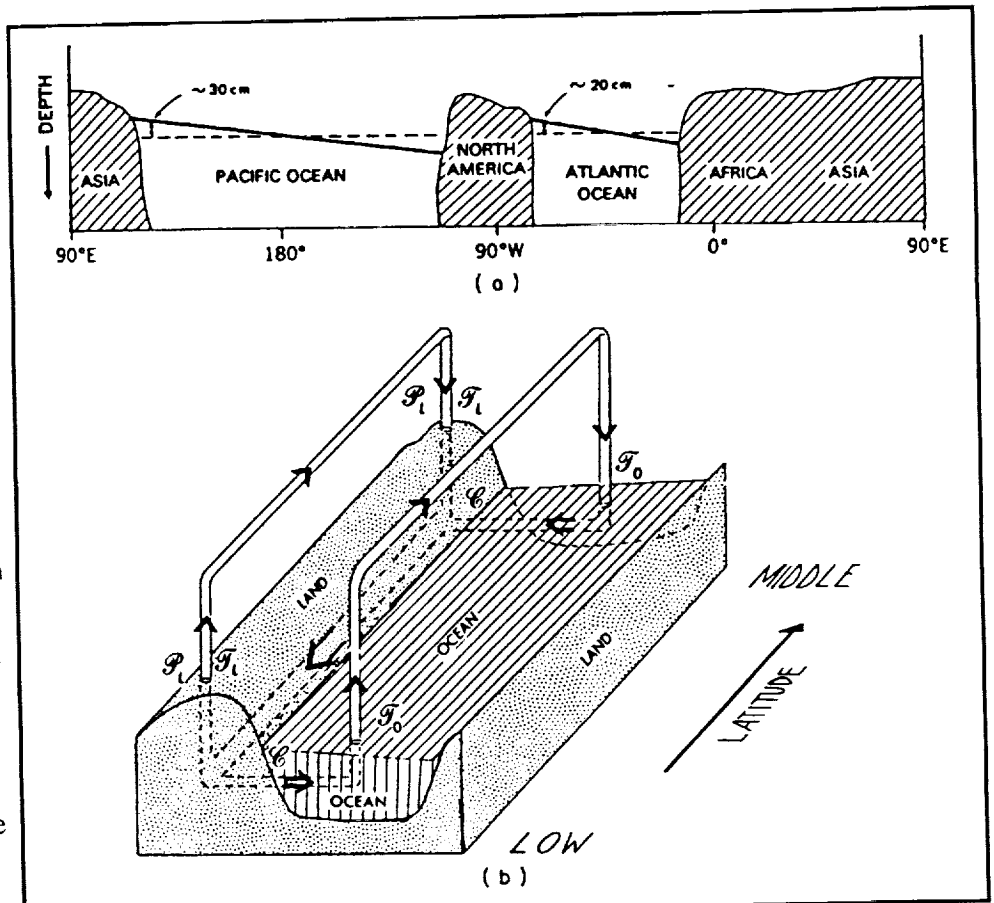


*Figure 33. (a) Schematic diagram of the observed east-west sloping of sea level along the 25°N latitude circle. The resulting pressure differences across the low-latitude continents together with similar differences (but of opposite sign) across the mid-latitude continents are suggested to lead to continental torques needed to satisfy global angular momentum constraints. (b) Schematic diagram of the cycle of angular momentum in the atmosphere-ocean-solid Earth system. In the atmosphere, there is a continuous poleward flow of westerly angular momentum with sources in low latitudes through the mountain and friction torques over land $P_L$ and $T_L$ and through the friction torque over the oceans $T_O$. The corresponding sinks of westerly angular momentum are found in the middle and high latitudes. When considering the atmosphere plus the oceans as the total fluid envelope of the Earth, the low-latitude sources and mid-latitude sinks are given by the three terms $P_L$, $T_L$, and the continental torque $\oint$. The return equatorward flow of angular momentum must occur entirely in the solid Earth (land). Source: Oort 1985.*

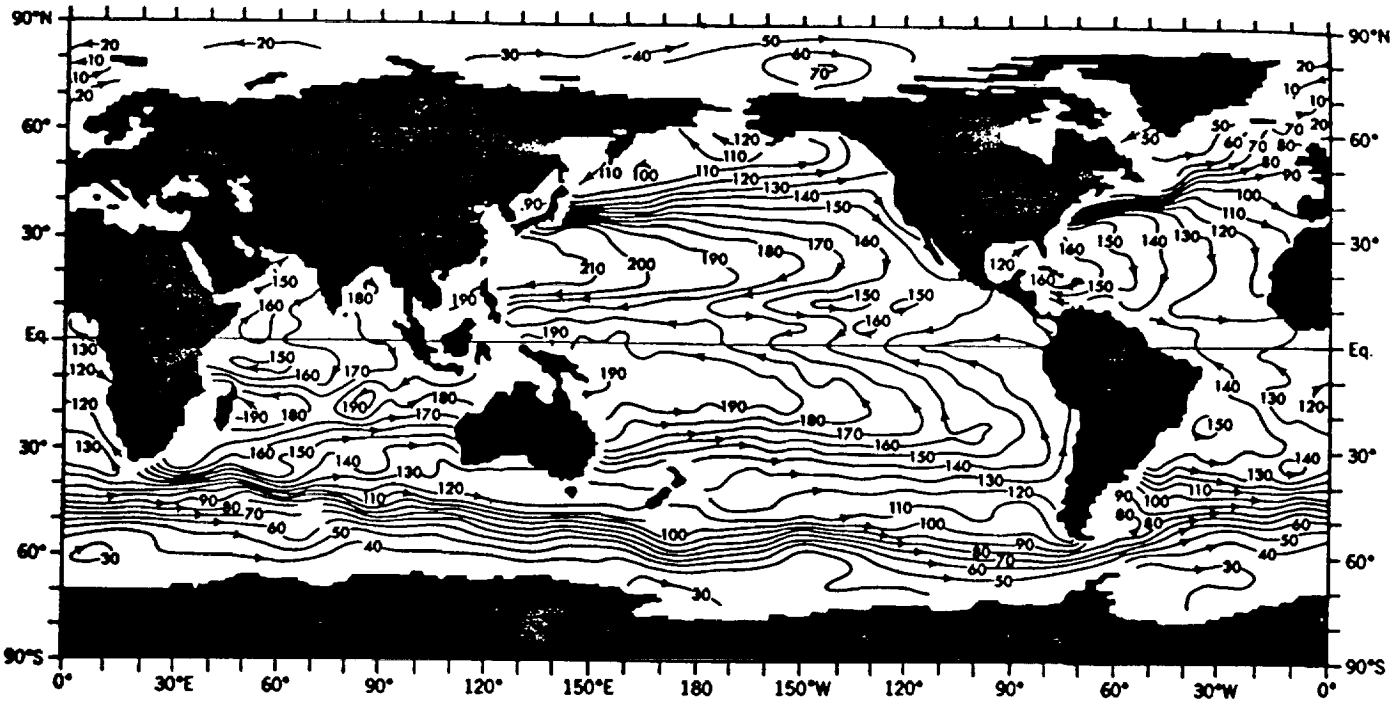


*Figure 34. The relative height of sea level (in cm) for annual mean conditions as computed from global density data (derived from the basic temperature and salinity observations) in the oceans, assuming a level of no motion at 1,000 m depth, from Levitus and Oort (1977). Reproduced with permission from Bulletin of the American Meteorological Society.*

drastic simplifications made in computing the oceanic curve and the neglect of the land pressure torques, is remarkably good, lending credence to the hypothesis of a dominant lateral exchange of angular momentum between the oceans and the continents.

What remains is the postulation of a viable mechanism for the required return flow of angular momentum from middle to low latitudes: The required return flow has to occur almost completely within the "solid" Earth. A possible mechanism that suggests itself is by the preferred tilt of the motions along faults in continents—that is, through the SE-NW-oriented displacements in the crust in the Northern Hemisphere middle latitudes and through the preferred SW-NE displacements along faults in the Southern Hemisphere middle latitudes. Examples are shown in Figure 36 for the San Andreas fault and the New Zealand fault system. These preferred orientations would lead to a correlation comparable to that in the atmospheric waves shown earlier in Figure 30. Processes in the Earth's crust would be much more localized and intermittent. The implications of the pathways suggested for angular momentum could be profound—namely, that continental torques link in a clear manner the motions in the atmosphere and the oceans with some of the motions in the "solid" Earth's crust. Their future study might lead to a

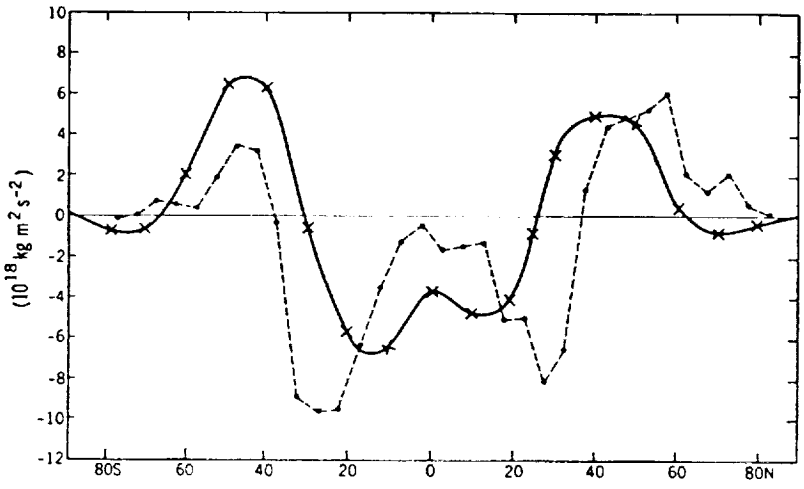


*Figure 35. Meridional profiles of the surface torque exerted by the atmosphere on the oceans and land (solid line), $P_L + T_L + T_O$, and the torque exerted by the oceans (due to sloping sea level) on the continents (dashed line) $\wp$. If there were no net surface torques over land ($P_L + T_L = 0$), and if observational inaccuracies are disregarded, the two curves should almost overlap ($\wp \approx T_O$). The values represent integrals over 5° latitude belts in units of $10^{18}$ kg m$^2$ sec$^{-2}$. Source: Oort 1985.*

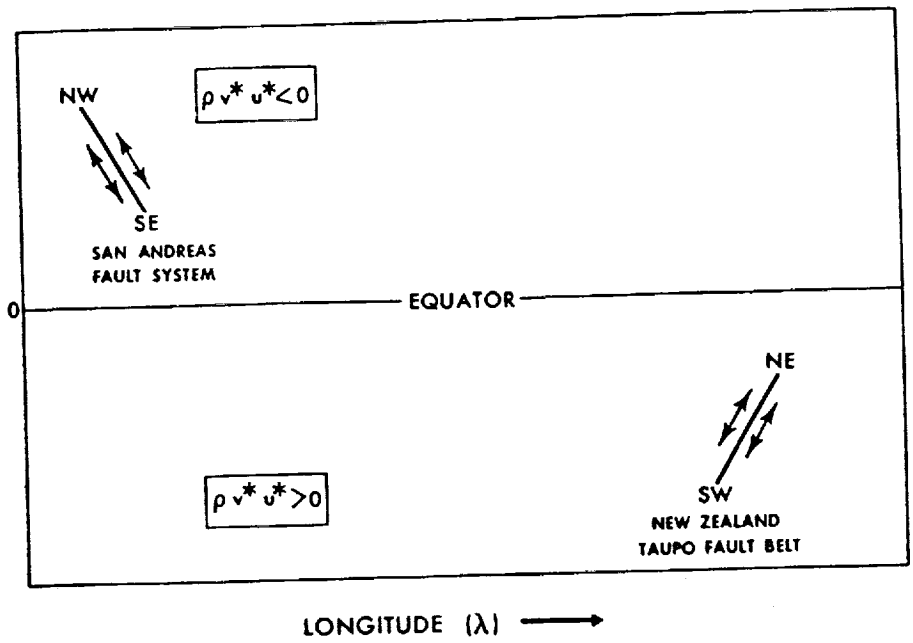


*Figure 36. Two examples of typical fault systems in the continental land masses that could lead to SE-NW mass shifts in the Northern Hemisphere and SW-NE shifts in the Southern Hemisphere required to (occasionally) relieve the angular momentum (atmosphere-ocean) torques imposed on the continents. Source: Oort 1985.*

better understanding, and perhaps also prediction, of how certain stress patterns may build up in the Earth's crust and how these stresses may eventually be released, conceivably leading to the intermittent occurrence of earthquakes along fault zones.

The angular momentum pathways identified by Oort (1985) provide mechanisms for the accumulation or storage of stresses in the continental Earth's crust through angular momentum transfers between the atmosphere and ocean, and the ocean and the solid Earth. Could a sporadic release of these stresses be associated with the occurrence of major ENSO events? Figure 37 shows that there is a strong association between ENSO events (as captured by the Southern Oscillation Index), the Earth's rotation, and earthquakes. Although volcanic eruptions may not directly participate in angular momentum transport, they presumably occur in conjunction with the release of stress accumulations in the Earth's crust combined with the dynamics of molten core-mantle interactions. The injection of volcanic aerosols into the upper atmospheres alters climate for years, as well as the global general circulation of the atmosphere, and possibly the ocean. Shifts in the positions of atmospheric jet streams, ocean currents, and sea level would alter the angular momentum budget of the atmosphere-ocean system, which would be reflected in the rotation speed of the Earth. In fact, on the monthly-to-interannual time scale, there is a near-total correspondence between changes in atmospheric angular momentum and the rotation speed of the Earth.

Figure 38 shows the correspondence between observed changes in length-of day (LOD) and changes estimated from calculations of atmospheric angular momentum. Atmospheric angular momentum computations are based on global observations of the wind field and computer analysis techniques that transform irregular point measurements into regular three-dimensional global grids. The first observations of nonconstant LOD were made in the 1930s, when fluctuations of LOD on a decadal time scale were detected astronomically from star position data. In recent years, variations in Earth rotation during periods of less than 1 year have been discovered using atomic clocks and a number of sophisticated techniques. Among these techniques that supplement the classical method of star observations are 1) Very Long Baseline Interferometry (VLBI), in which different antennas receive radio wave emissions from the same source outside the galaxy; and 2) laser ranging, which uses accurate measurements of the round trip it takes a laser light pulse to travel between the Earth and a remote reflector. Reflectors have been placed on the moon and on the Laser Geodynamics Satellite (LAGEOS) series. The information acquired with this combination of techniques has provided for unprecedented accuracy in Earth rotation speed estimates.

Associated with the 1982-83 ENSO sea surface warming and shift in tropical circulation systems, the strong westerly jet stream winds over the North Pacific and the rest of the globe were altered; generally, the upper tropospheric westerly winds were more zonal in character and positioned approximately 5° equatorward of their normal latitudinal position (Oort 1985). These and other changes in the atmospheric and ocean circulation were sufficient to slow the Earth down. Figure 39 shows a schematic of the relationship between the atmospheric wind field and Earth rotation.

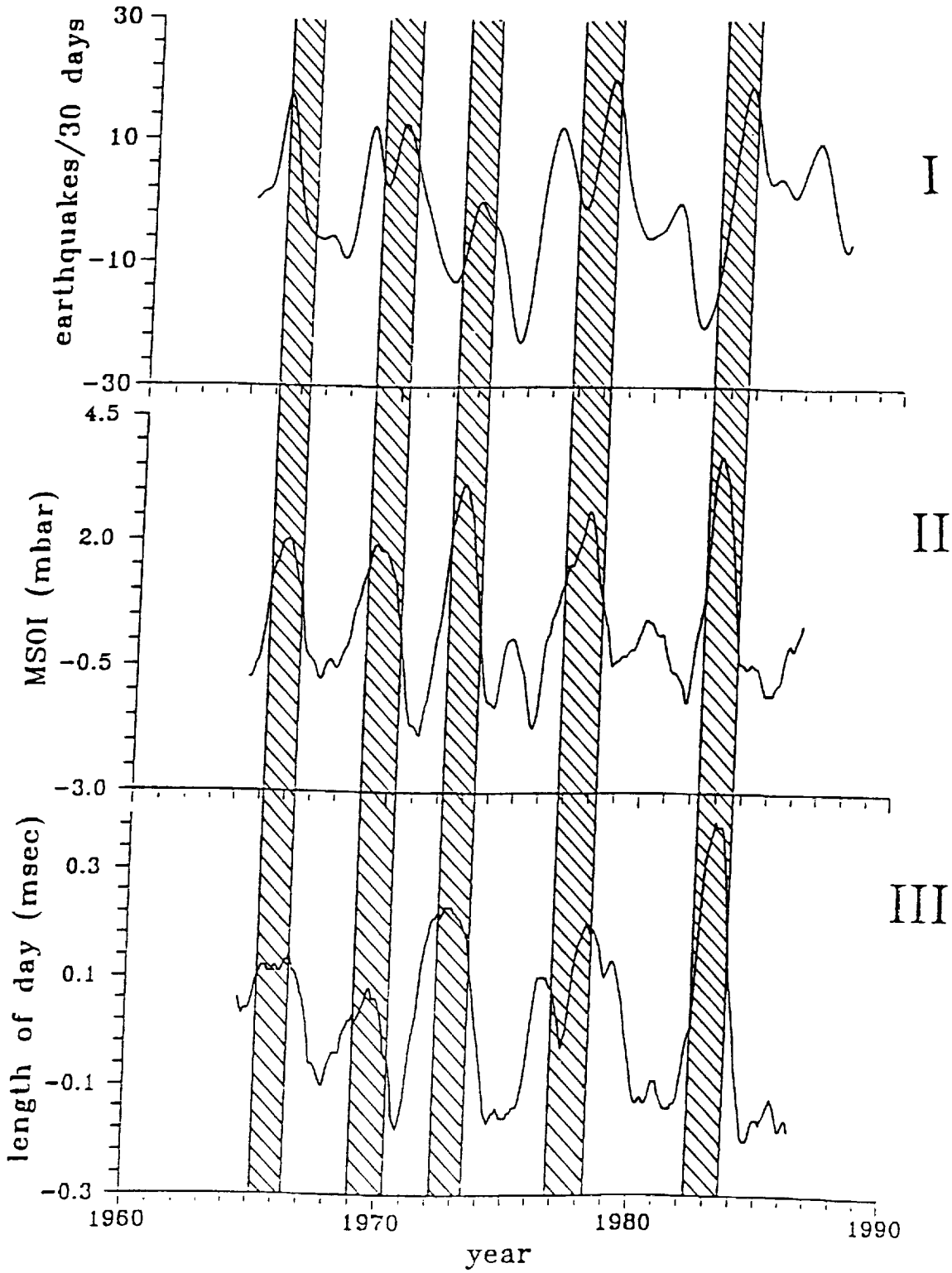


*Figure 37. (Curve I) 30-day counts of all shallow earthquakes (depth 0-100 km) with magnitude greater than or equal to 5.0 in the Earthquake Catalog of the International Seismological Center. A linear trend has been removed from the data set, and a low pass filter (3 db point at 500 days) applied. (Curve II) A Modified Southern Oscillation Index (MSOI) defined as the negative of the 1-year moving average of the Southern Oscillation Index. (Curve III) The interannual variation in LOD. (Vertical Bands) ENSO events. Source: Chinnery 1992 (NOAA/NGDC, personal communication).*

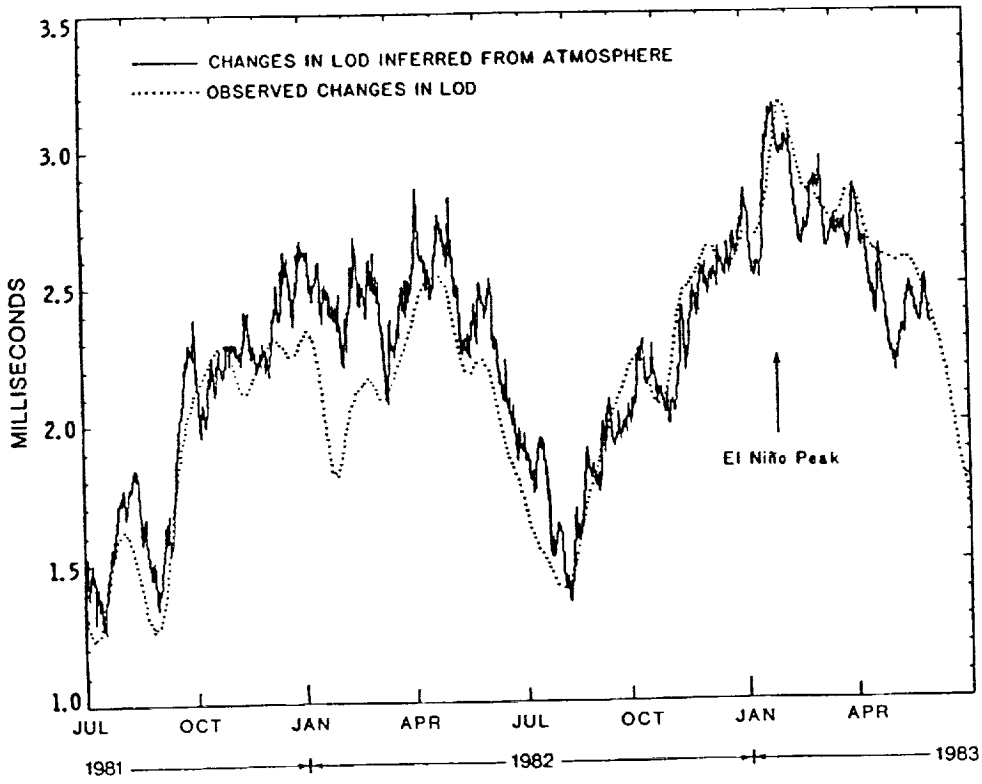


*Figure 38. Changes in LOD as inferred from the angular momentum of the atmosphere (solid line) and observed changes in LOD (dotted line). Tides have been removed from the LOD changes.*
*Source: Rosen et al. 1984.*

***Conclusions/Recommendations.*** *There are several aspects of atmosphere-geosphere interaction that are presently not considered or incorporated in the current generation of global Earth system models. This is an area that requires substantially more research, particularly when decadal time scales are an integral part of the climate and global change problem. Cross- and multidisciplinary research, as well as perspective, is required.*

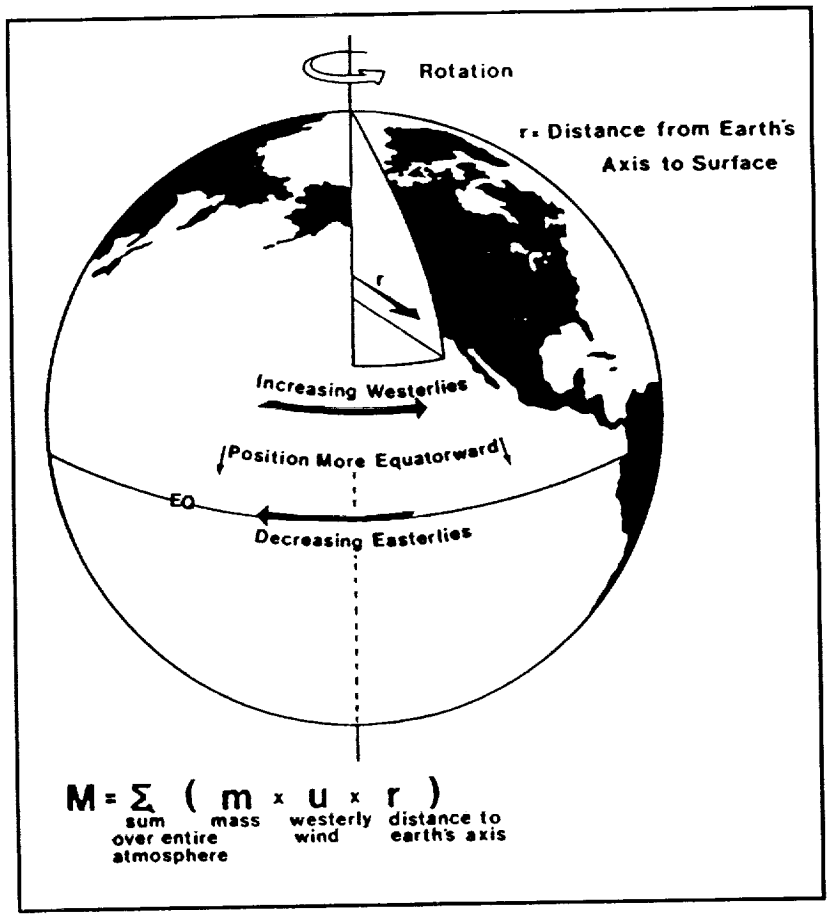


*Figure 39. Wind changes during the ENSO of 1982-83, and their relation to Earth rotation. The atmospheric angular momentum (M) is computed by the equation given below the figure. The angular momentum of a parcel of air increases if it moves equatorward (larger r) or if there is an increase in density or speed (u component).*
*Source: Rosen 1984.*

# 4. Simulation and Prediction of the Global Earth System

## 4.1. The Forecast/Predictability Problem

Lorenz (1969) defined the "range" of predictability as "the time interval within which the errors in prediction do not exceed some pre-chosen magnitude, which for practical purposes should be considered greater than the magnitude of typical errors of observation but less than the magnitude of the difference between randomly chosen states of the system."

This concept still applies and also raises profound questions regarding the predictability of the global Earth system and/or any of its subsystems. It has been customary to evaluate numerical prediction "skill scores" based on comparing a prediction with "persistence" or, in the case of meteorology, climatology. The persistence forecast assumes that the state of the system during the next (forecast) time period is exactly the same as that of the present (initial state), whatever the chosen time period is. The "climatalogical" forecast relies on the historically observed statistics of the fluctuations of the system to extrapolate in time into the future. The basic concepts apply to any system. In terms of weather systems, the climatological forecast would refer primarily to the average seasonal cycle, together with information (as available) on interannual variability that would introduce a probabilistic element into the system feature being forecast. If analyzing the global Earth system, a knowledge of possible states could require 10,000 to 100,000 years of observations. This suggests that the extent to which the global system is predictable is as yet unresolved.

## 4.2. Simulation/Prediction Time Ranges

This section briefly describes the various time scales of variability, as well as the components and processes of the global system involved in each of these time scales. The distinction is mathematically and numerically expedient and in some cases necessary because of limitations imposed by speeds of the present generation of computers. From a practical standpoint, the separation by time scale is not unreasonable. For example, the atmosphere interacts with the ocean primarily through the exchange of heat (sensible and latent), moisture, and momentum fluxes. The momentum transfer is particularly important to the ocean near-surface circulation. In fact, most ocean models use the surface wind stress obtained from an atmospheric model as the primary driving mechanism that generates the ocean currents. Radiative and moisture (water) fluxes are important for long-term integrations. Similarly, the atmosphere responds primarily to ocean sea surface temperature (SST). Thus, if SST is prescribed as a boundary condition, the model simulates atmospheric circulation changes rather well. This is in fact the basis for most ENSO simulation/prediction experiments. The fact that the two are thermodynamically coupled to form one interactive system may be ignored (on very short time scales) through continually reinitializing the atmospheric GCM with observed SST. This need be done only about once a month, because the SST changes somewhat slowly. For a 1- to 10-day weather forecast, SST is assumed to be constant. Older GCMs simply used monthly mean climatological SST values with reasonably good results. Present models use SST observed from satellite, ship, and buoys.

The point to be noted in the above example is that a continuing cycle of global predictions can be made in an engineering sense with an incomplete model of the total system, if those components and processes of the system that are not (or cannot be) explicitly modeled and that change relatively slowly are continually monitored. That is, the observed fields are specified as either internal or external boundary conditions to the global model for a particular forecasting/prediction objective (e.g., a specified time scale such as 1 month, 1 year, 10 years, or 100 years). Conversely, all assumptions used in a model, including implied assumptions (e.g., a static deep ocean circulation, vegetation distribution, cloud distribution, or aerosol concentration and distribution) will constrain the potential predictability limits of the model. Otherwise, these assumed "static" fields must be continually monitored globally, and the global system prediction regularly updated. Currently, the long-term prediction of the global system is considered to be more a research exercise than an operational activity.

In this section, no serious distinction is made between simulation and prediction as far as the mathematics and structure of the global system model used for the exercise are concerned. This is because all prediction models require 1) observations for initialization even for a single prediction experiment, 2) observations for validation, and 3) runs in a simulation mode [i.e., a model must first be able to simulate (reproduce) those aspects of the global system the model is attempting to predict].

Simulation is a necessary, but not sufficient, condition a model must satisfy before it can be credibly applied for prediction purposes. It should also be noted that specifying a boundary condition such as SST immediately implies that the thermal adjustment time of the ocean is infinity and the heat capacity of the surface ocean is infinite—namely, SST will not change even if there is interaction with the atmosphere, and the ocean receives or releases sensible and

latent heat. It is for this reason that the specification of a boundary condition is termed "boundary forcing." Many simulation experiments are conducted in this manner (e.g., ENSO, deforestation, paleoclimatic reconstruction). The surface boundary condition is imposed from observations or from estimates of boundary-forcing fields. For example, a typical SST anomaly field may be specified representing ENSO conditions in order to obtain the equilibrium response of the atmosphere; the observed surface atmospheric wind stress on the ocean may be specified to obtain the equilibrium response of the surface ocean circulation; or an altered surface vegetation layer may be specified together with corresponding changes in albedo and roughness for a deforestation experiment. The technique permits studying the interaction between components of the global system during specific states of one or more components of the system and helps the understanding of processes. For prediction experiments, the boundary conditions must themselves be predicted.

Currently, most global simulation and prediction experiments with global models deal with weather and climate issues. In accordance with the World Climate Research Program's delineation of climate research objectives into Streams I, II, and III, climate system prediction requirements may be correspondingly divided into three ranges: 1) Short range [weeks to a few months (intraseasonal)]; 2) medium range [seasons to several years (interseasonal and interannual)]; and 3) long range [years to several decades (decadal)]. This should not be confused with the terminology used in weather forecasting, wherein short is equivalent to 1 to 3 days, medium up to 10 days, and long greater than 10 days. Basically, climate prediction assumes the time scales where weather forecasting stops—usually around 2 weeks, the deterministic predictability limit for the atmosphere. A further and important difference is that a weather forecast must predict specific weather events at any given location and the absolute values of state variables such as temperature, wind, precipitation, and so on. Climate forecasts are more concerned with changes in the statistical character of weather. Thus, a climate prediction would not typically refer to when and where a particular snowstorm might occur sometime during the next year or 10 years from now, but rather the prediction would refer to the possibilities of a colder or warmer than normal winter, or a more active or less active monsoon circulation, or, of course, the familiar example of global warming in 30 to 50 years owing to increasing concentrations of GHGs. An Earth system model would also need to predict changes in the land surface (e.g., soil) and the biosphere (e.g., vegetation cover and type), as well as ocean biomass production, changes in species diversity, population movements, and impacts on socio-economic activity.

## *4.3. Short Range (Intraseasonal)*

This time range overlaps substantially with the "medium" and "extended" range of weather forecasting. While weather forecasts primarily cover a few days (e.g., 1 to 3) in order to provide warnings about impending severe weather, a variety of user industries (e.g., agriculture, energy, water supply) require longer term guidance. The time range of operational weather forecasts now routinely extends to 10 days. There is strong pressure to extend operational forecasting to 1 month. As described in Section 2, extending the time scale involves incorporating explicitly more components and interactive processes of the global system. For short time scale predictions, a global GCM relies in principle on the memory built into the initialization field or the initial conditions at a particular point in time. It is typical to run a global GCM at a certain spatial resolution (e.g., a 2.5° to 5° grid) and run nested grid-limited area models at much higher resolution to provide "local" weather detail. An example of a nested grid scheme is shown in Figure 40. Generally the GCMs used for this time range of prediction utilize a variety of prescribed boundary conditions to simulate coupling with the land surface and the ocean, sea ice, and so on. Often climatological (i.e., mean) values/fields are used.

Fixed boundary conditions, even if varying with the season, have been found to limit the range of extended range predictability. Current operational GCMs utilize observed monthly mean SST. Some also include highly simplified interaction with the very upper ocean layers. Most have already incorporated fairly sophisticated "physics" packages that represent, in parameterized form, cloud/convective processes, some radiative processes, and the planetary boundary layer. Although sophisticated, all parameterized "physics" packages need to be verified, validated, and improved. While the general character of the large-scale wave systems are predicted by all models rather well, there are significant regional differences between models in second and higher order parameters such as precipitation, soil moisture, and fluxes of heat, moisture, and momentum, which point to deficiencies in the current representation of these processes.

An examination of the "skill scores" of current generation short-range prediction models (e.g., NOAA/NMC, ECMWF) shows that beyond a few weeks there is a definite degradation of the forecasts. With the availability of more powerful computers, most forecast centers have increased the resolution of their models in order to obtain more accurate regional and *in situ* predictions. Results have been mixed. Performance has improved in some cases, but not in others.

Research is also under way to understand, model, and predict intraseasonal oscillations in the tropical atmosphere

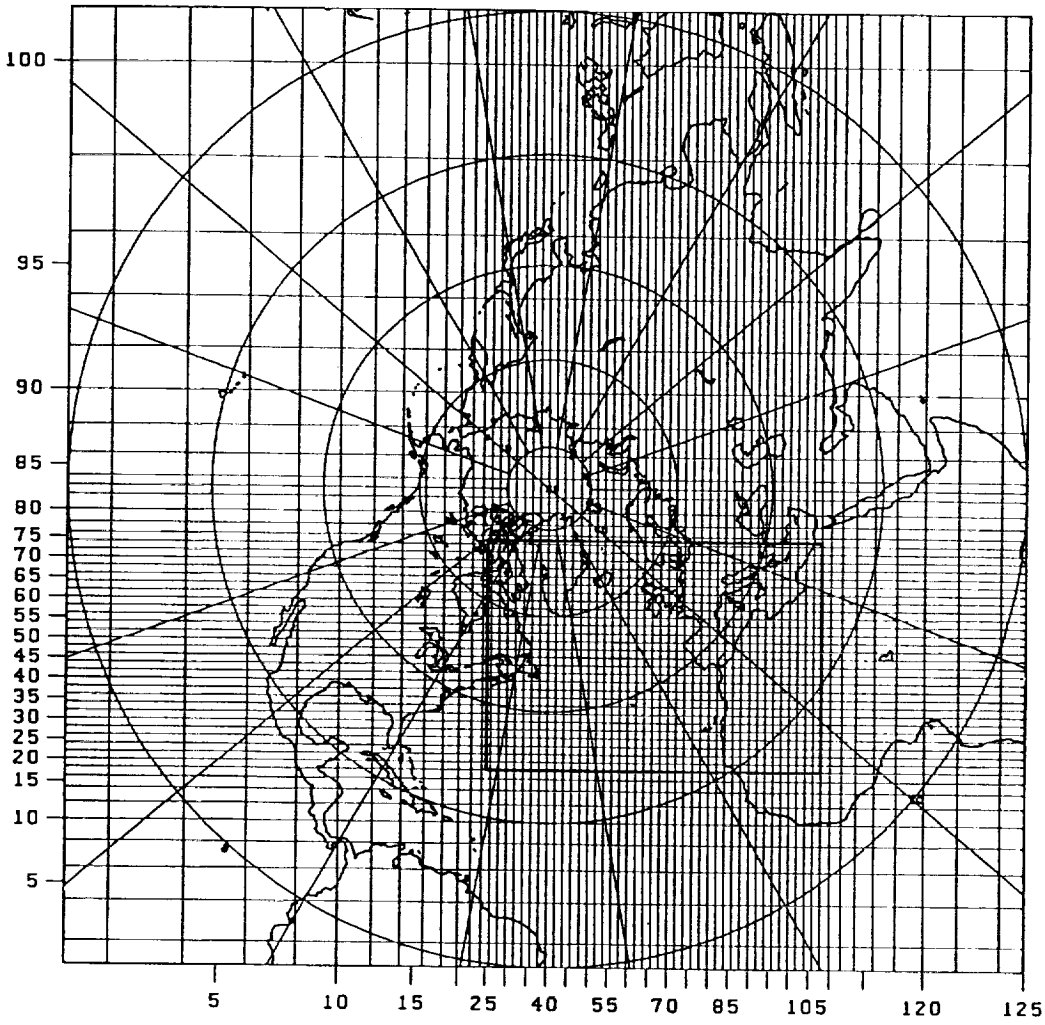


*Figure 40. Grid system of the regional meteorological model. Source: Pudykiewicz et al. 1992.*

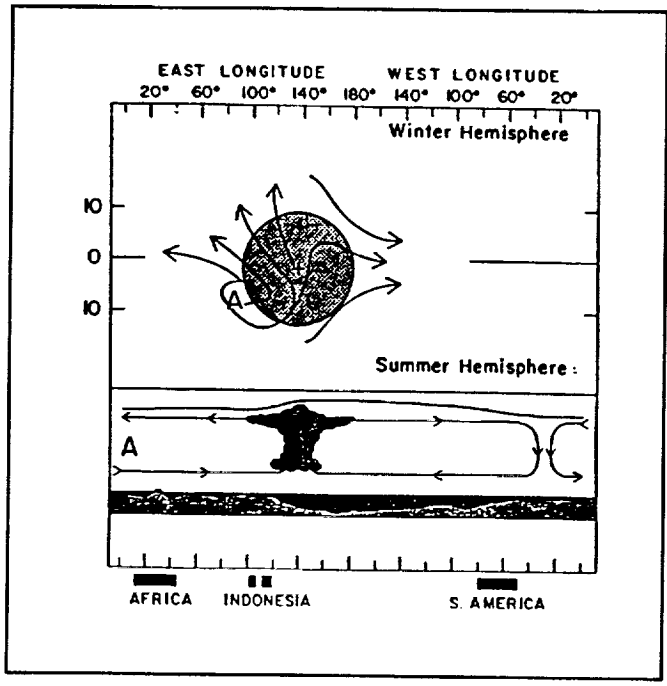


(Lau and Chang 1991). Intraseasonal oscillations (ISO) in the form of 30- to 60-day oscillations were first detected by Madden and Julian (1971). Based on extensive data analysis and theoretical and modeling studies, Madden (1986) constructed a schematic of the 30- to 60-day disturbance (see Figure 41). The whole complex is strongest during the northern winter, increasing in intensity as it propagates from the Indian Ocean to the central Pacific where it weakens. The relationship between cloudiness is derived from outgoing longwave radiation and the 250 mb circulation as shown in Figure 42. The inverse pattern becomes established as cloudiness pushes to the dateline. Lau and Chang investigated the forecast capabilities of the operational NMC model from December 14, 1986, to March 3, 1987 [Phase II of the Dynamical Extended Range Forecast (DERF)]. Their results suggest that the model's ability to forecast tropical intraseasonal oscillations and low-frequency extratropical modes of the atmosphere was considerably enhanced during special periods when ISO was strong. The increase in extratropical forecast skill is conjectured to be due to the following: 1) The model's ability to better capture the ISO signals in the tropics, and 2) the increased coupling between the tropics and the extratropics during periods of strong ISO. Tropical ISO may therefore be a physical basis for extended-range forecasts in both the tropics and the extratropics, but

*Figure 41. Schematic depiction of the structure of the 40- to 50-day oscillation at a time of large amplitude. The lower panel represents the structure in the equatorial plane. Shading at the bottom represents the negative pressure anomalies. The line at the top of the lower panel represents the tropopause. The upper panel is a plan view of the disturbance in the upper troposphere. The shaded area there corresponds to a positive anomaly in convection with a center displaced into the summer hemisphere. Source: Madden 1986.*

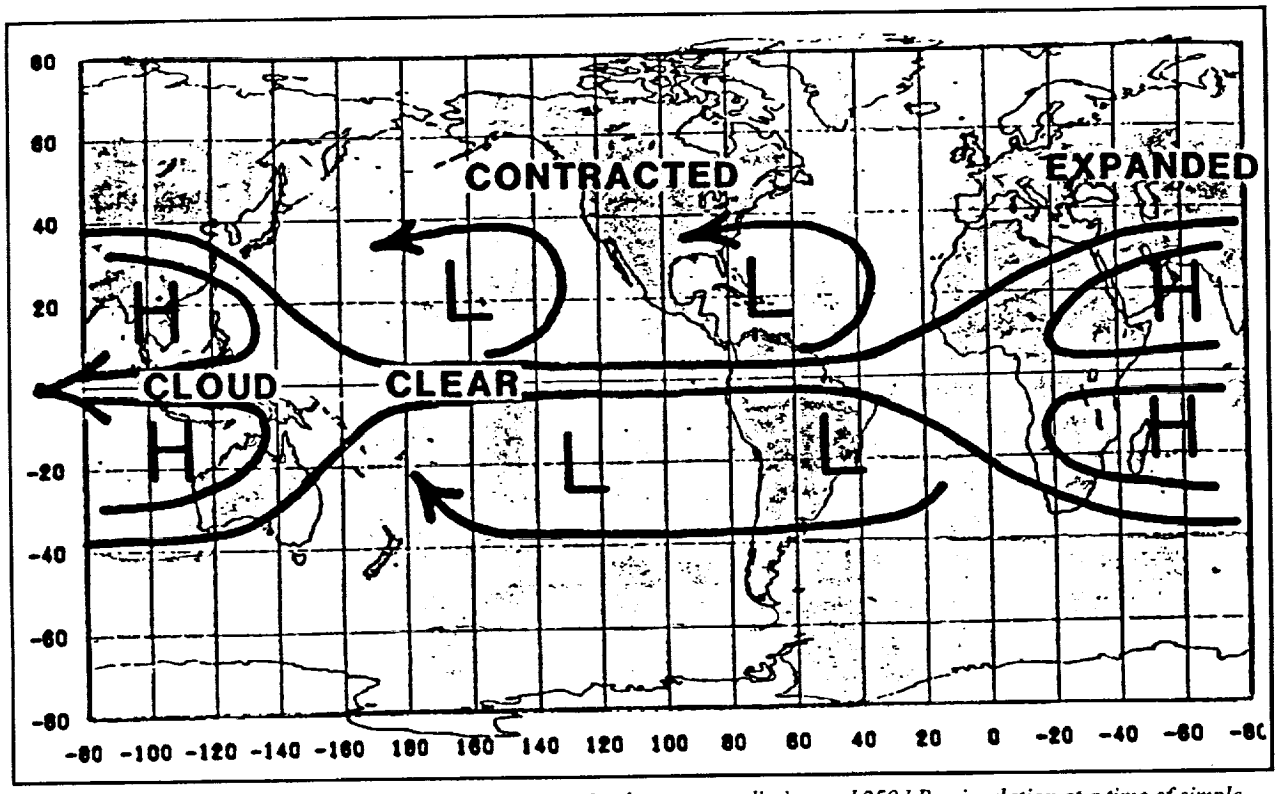


*Figure 42. Schematic of the relationship between outgoing longwave radiation and 250 hPa circulation at a time of simple structure in the 30- to 60-day life cycle of the intraseasonal oscillation. Source: Weickmann, Lussky, and Kutzbach 1985.*

improvements vary from case to case, depending on the strength of ISO.

## 4.4. *Medium Range (Interseasonal and Interannual)*

The most notable and pronounced example of year-to-year variability of the climate system is the ENSO phenomenon (WMO 1984, 1986). The El Niño originally referred to the winter (December through February) warming of ocean waters off the coast of Peru. Every 2 to 7 years, this warming appeared to spread to the central and eastern Pacific. The Southern Oscillation is a global-scale ice saw of surface pressure with centers of action around Indonesia/North Australia and the southeastern Pacific region. The two phenomena were discovered and studied for decades as separate entities. Only in recent years have they been recognized as linked parts of the atmosphere-ocean climate system, hence the term "El Niño/Southern Oscillation."

Major ENSO episodes such as that during 1982-83 led to massive displacements of the rainfall regions of the tropics, bringing drought to vast areas and torrential rains to otherwise arid areas. The related atmospheric circulation anomalies extend deep into the extratropics, where they are associated with unusual conditions over regions as far apart as the United States and New Zealand. Because ENSO is a global event, near-simultaneous and large climatic anomalies appear over many regions of the world. Owing to the enormous socio-economic environmental and ecological impact of ENSOs, major efforts are being made to observe ENSO and improve predictive models of the coupled atmosphere-ocean climate system. The WCRP's Tropical Ocean Global Atmosphere (TOGA) Program (1985-95) and, in particular, the TOGA–Coupled Ocean Atmosphere Research Experiment (COARE) are specifically targeted at improving the predictive capability of the coupled ocean-atmosphere system. This is also one of the priority objectives of the Global Change Research Program (GCRP).

Figure 43 shows the global tropical (20°N-20°S) Intergovernmental Panel on Climate Change (IPCC) temperature anomaly time series and the correspondence of this global signal with ENSO (marked by wedges). During ENSO years, the Southern Oscillation index (Tahiti-Darwin pressure) is negative. The temperature anomaly is dominant on account of the SST warming in the central and eastern Pacific, which is associated with a large shift in the tropical convective zone from the western Pacific to the central Pacific near the date line. Figure 43a shows the areas and times of year with a consistent ENSO precipitation signal.

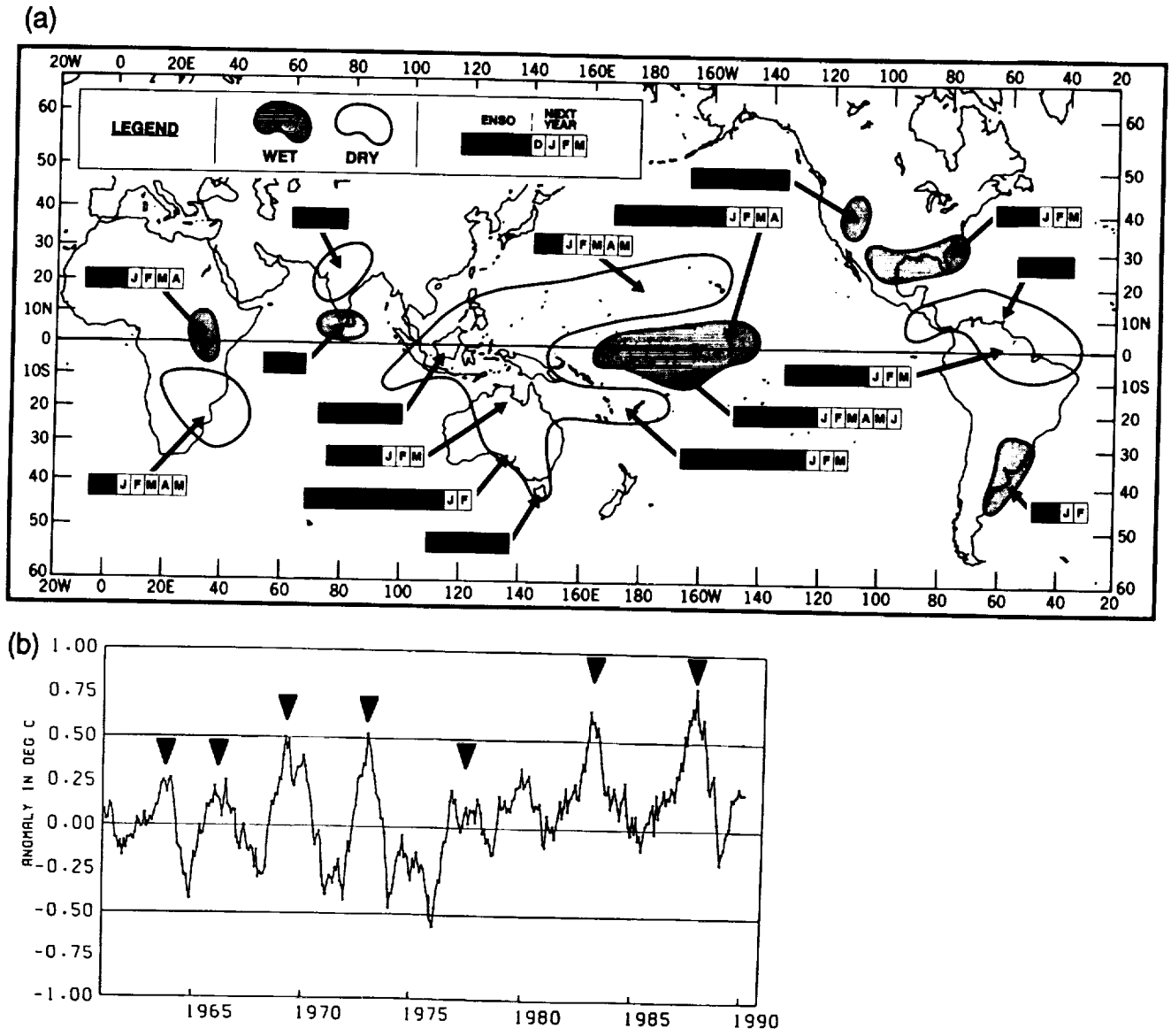


*Figure 43. (a) Schematic diagram of areas and times of the year with a consistent ENSO precipitation signal (adapted from Ropelewski and Halpert, 1989). (b) Monthly tropical (20°N-20°S) sea surface and land air temperature anomalies, 1961-1989; land data from P.D. Jones and sea surface temperature data from UKMO; arrows mark maximum ENSO warmth in the tropics. Source: Houghton et al., IPCC 1990.*

The physical reasoning behind ENSO events is not completely known, but a sequential process has been postulated by Klaus Wyrtki and others, and depicted in Figures 44 and 45—namely, 1) above-normal trade winds build up over warm equatorial waters in the western Pacific; 2) once in approximately 2 to 7 years the trade winds slacken, followed by a relaxation of the surface ocean system, which triggers a Kelvin-wave upper oceanic response to this slackening of surface wind stress; 3) accompanying this "sloshing" of the ocean, sea surface temperatures rise in the eastern and central Pacific; 4) elevated SST causes increased low-level moisture convergence as well as somewhat increased sensible heat flux; 5) a large-scale connection shifts from its predominant position in the western Pacific toward the international dateline; and 6) the shift in convection shifts the tropical diabatic heating pattern as a result of the release of latent heat in the mid-troposphere, which results in changes in the tropical and extratropical atmospheric general circulation. As a part of this altered state of the climate system, there is a shift in the ascending branches of large-scale east-west overturning circulations, causing either increased or phase-shifted subsidence in tropical locations

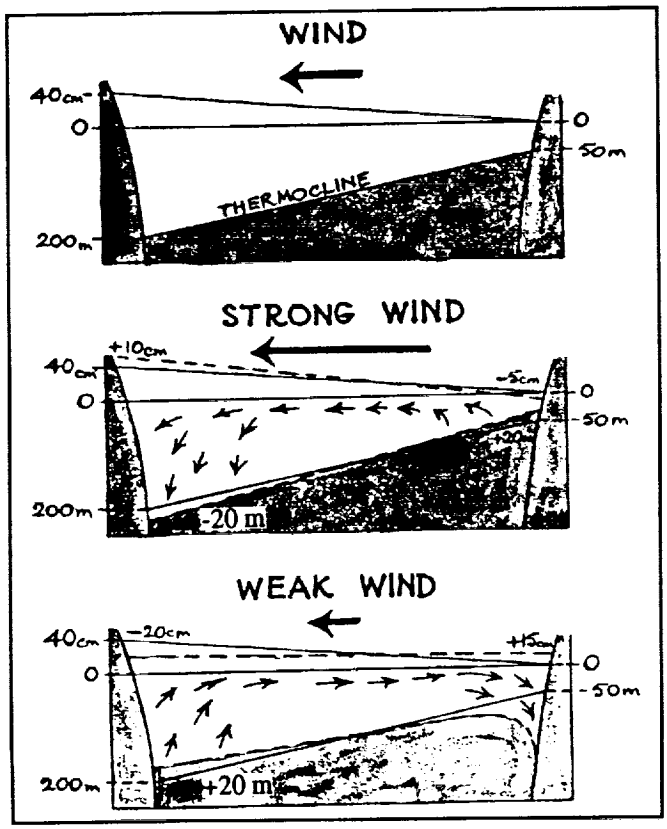


*Figure 44. The response of the thermal structure of the equatorial Pacific to changing winds. (Top) Under normal easterly trade wind conditions, sea level rises to the west and the thermocline deepens. (Center) This situation is amplified during strong trade winds. (Bottom) When the winds relax, water sloshes east, which leads to a rise in sea level and a deepening of the thermocline along South America. In the western Pacific, sea level drops and the thermocline rises. Source: WMO 1984.*

far removed from the location of the initial SST anomaly (WMO 1984).

Although it has been convenient to identify the ENSO cycle by the SST and Southern Oscillation indices (covering the Pacific basin region) because it is here that the "signal" is first detected (SST by satellites and ship observations), clearly the ENSO is a result of coupled atmosphere-ocean interaction. The ability to simulate and predict ENSO events is an important test of the mechanics and physics of a climate system model—in this case, atmosphere-ocean coupling. Generally, it is found that the atmospheric response is reasonably well-simulated by prescribing the observed (during an ENSO) SST anomaly, and the ocean response is reasonably well-simulated by specifying as a boundary condition the observed surface wind stress. The "observed" surface wind stress is obtained using observations, an atmospheric GCM, and special algorithms to convert model winds at the lowest model layer to surface wind stress vectors.

Significant success has been achieved in ENSO prediction by Cane and Zebiak's (1987) model, which uses a highly simplified ocean model emphasizing the upper ocean layers. Figure 46 shows the results of prediction runs with lead times ranging from 0 to 15 months. Curiously, the 9-month forecasts are reported to statistically verify better with observations than forecasts made with shorter lead times. This could, in principle, be on account of "spin-up" problems associated with initialization shock. Initialization shock and spin-up problems are a common occurrence with all modeling or prediction exercises where the initialization data fields (i.e., observed) are not consistent with the dynamics and physics of the resolved scales and processes of

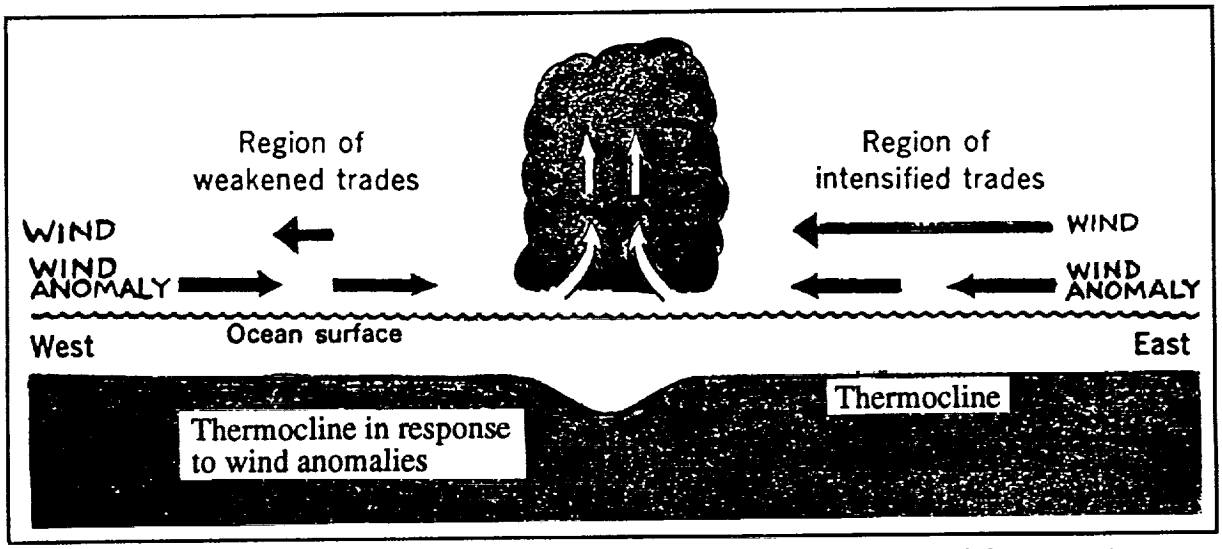


*Figure 45. Schematic of a simplified model atmosphere's response to a prescribed surface oceanic heat source (warm sea surface temperature anomaly and depressed thermocline). Source: WMO 1984.*

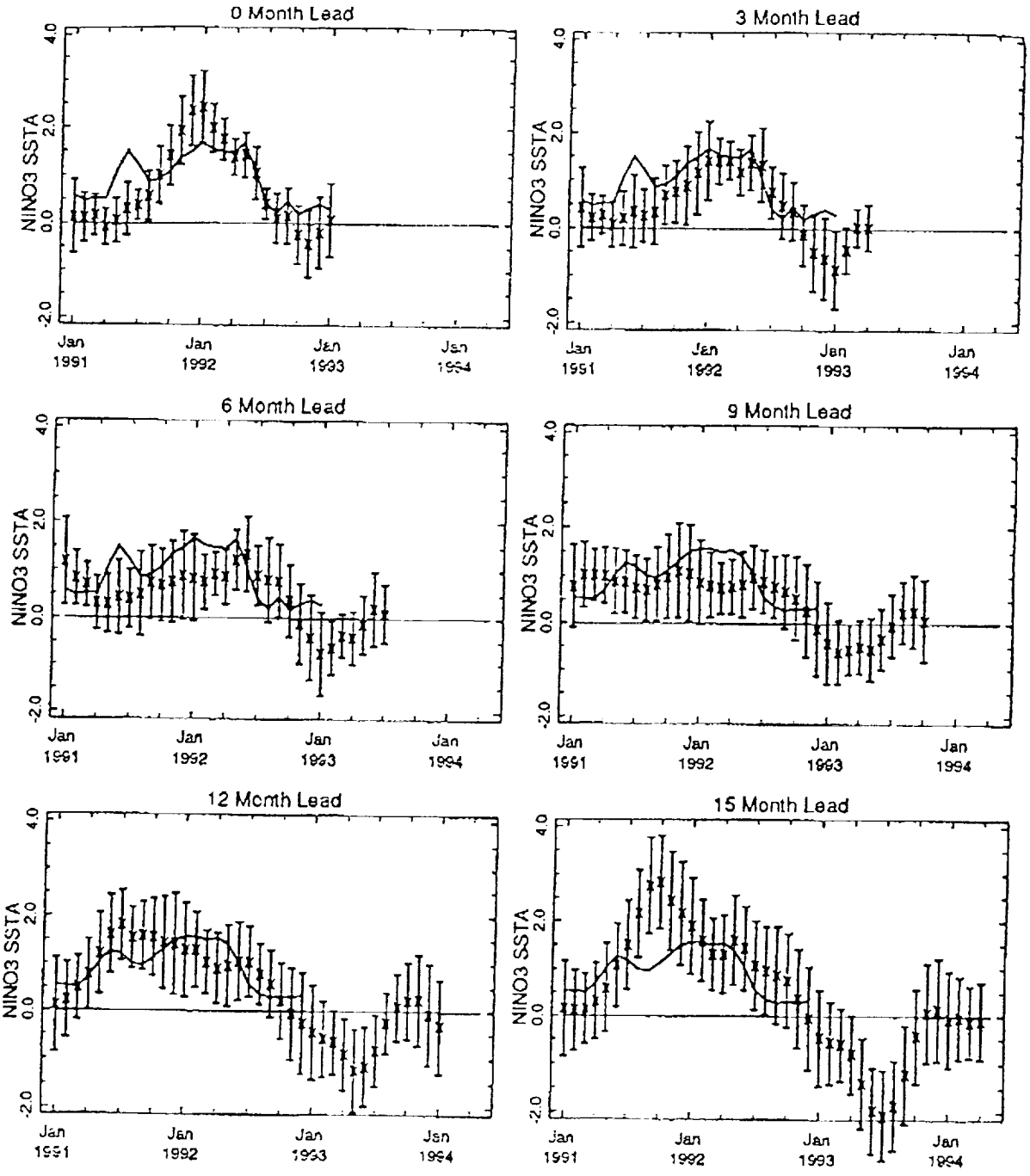


*Figure 46. Forecasts are made using the model and procedures outlined in Cane, Zebiak, and Dolan 1986 and Barnett et al. 1988. Results are presented for six different lead times ranging from 0 to 15 months. Each forecast is actually the mean of forecasts from 6 consecutive months, adjusted to have the same mean and standard deviation as the observed. Note that 0-month lead can differ from the observed, because SST data are not used in initialization. For each lead time, forecast values are indicated by 'x's and observed values by a solid line (for 9-, 12-, and 15-month lead times, observed values are 3-month averages; otherwise they are monthly averages). Error bars represent ± 1 root-mean-square error, based on the years 1972-1987. The latest forecast (from January initial conditions) is provisional. All but the longest lead indices show near zero or weak negative anomalies throughout the first half of 1993. None of the indices show significant positive anomalies developing during the year. Source: Ropelewski 1993.*

a model. Cane et al. attribute the inconsistencies between the 0-month lead time forecast and observations to the fact that the ocean model is not initialized with the observed SST values. The reason for the 6- to 9-month spin-up required for the Cane et al. coupled model is at present unknown.

In the case of atmospheric GCMs, spin-up problems very clearly show up in precipitation, evaporation, and soil moisture estimates (from model calculations). For example, soil moisture in a previous version of the ECMWF model verified better with observations with a ~3-day time lag. ENSO-type simulations with modified convective parameterization schemes have been conducted to test improvements to global climate models (Meehl and Albrecht 1991).

Studies of ENSO and interannual variability are particularly important for improving the physics of global models, because the ENSO represents a strong "climate system change" signal. In this case, the change is driven by the geographical distribution of solar radiation forcing owing to the tilt in the Earth's axis from the orbital plane. Because the two hemispheres interact through the atmospheric and ocean circulation, the effects of change is redistributed over the entire global surface. Thus it is not the same as a change in solar forcing itself. Ramanathan and others have used this feature to investigate changes in the radiation budget, cloud-radiation feedback, and the sensitivity of the global climate system to change in surface temperature.

## 4.5. *Long Range (Decadal)*

The approach used for long-range global simulation and prediction is somewhat different from that applied to shorter time scale predictions, even though the respective models used are becoming rather similar. On interannual and shorter time scales, the prediction must refer to specific events to be useful; examples include the occurrence of an ENSO or a drought. Of current concern is the issue of climate change caused by enhanced GHG effects—that is, the change likely to be caused to the climate system due to the increasing anthropogenic injection of GHGs into the atmosphere. The approach here is first to determine the direct radiative effects of GHGs (e.g., $CO_2$, $CH_4$, $N_2O$, CFCs) either individually or combined as an ensemble through some simplifying assumptions such as using equivalent $CO_2$ concentrations. A variety of global models, from very simple to very complex, have been used to probe the problem. All involve various assumptions that at the very least include projections on the rate of increase of GHGs over 30 to 50 years. In the global system model, an initial heating causes changes to atmospheric water vapor content, cloud cover and type, sea ice, and so forth through feedback processes. These feedbacks generally add to the initial change in surface temperature (i.e., they constitute a positive feedback). The final predicted change is thus a result of both direct and indirect effects and, consequently, dependent on how a global model handles various feedback processes.

The general consensus on climate change (IPCC 1990) is that for a doubling of equivalent $CO_2$ concentrations, from present concentrations, the equilibrium global mean temperature change is likely to be in the range of 1.5 to 4.5°C. In general, the change is forecast (by models) to be smaller in the tropics and larger in the middle and higher latitudes. Key and somewhat controversial issues follow: 1) climate sensitivity, 2) climate system response time, and 3) the regional distribution of temperature and precipitation. Other impacts of a global warming such as sea level rise and the melting of sea ice and ice sheets also need to be accurately known. The models used are generally atmosphere-ocean coupled models, and computationally expensive if the oceans are incorporated properly. The use of simplified oceans are customary; yet, this introduces uncertainties in the magnitude and timing of the projected or predicted climate change. The models also contain in one form or another interaction with the land surface, vegetation, and the cryosphere—often in highly simplified form.

Large uncertainties also arise because of the unknown representatives of the parameterization of several subgrid-scale processes and other interactive and feedback processes. Other sources of uncertainty are introduced by those aspects of the climate system that are not modeled explicitly—for example, volcanic eruptions and the injection of aerosols into the stratosphere. The present approach is to incorporate such "forcings" *post facto* into the model, and simulate and/or predict the impact of the change on the evolution of the model's climate.

Figure 47 from Hansen (1991) shows the predicted climate change over the next 20 to 40 years for different scenarios for the rate of change of GHGs. Figure 48 depicts the Mount Pinatubo volcanic eruption using the same model—namely, through a cooling effect spread over about 5 to 10 years, superimposed over "natural variability" and the warming trend due to GHGs. At the time when the model was run, two estimates were used for the strength of the Mount Pinatubo eruption: 1)Equivalent to the El Chichon eruption, and 2) twice that of El Chichon. As in Figure 47, the model runs A and B refer to GHG growth rate scenarios.

It should be noted here that decadal scale (and longer) natural system variability (i.e., inherent variability) is a complex problem, since it could and probably would bring

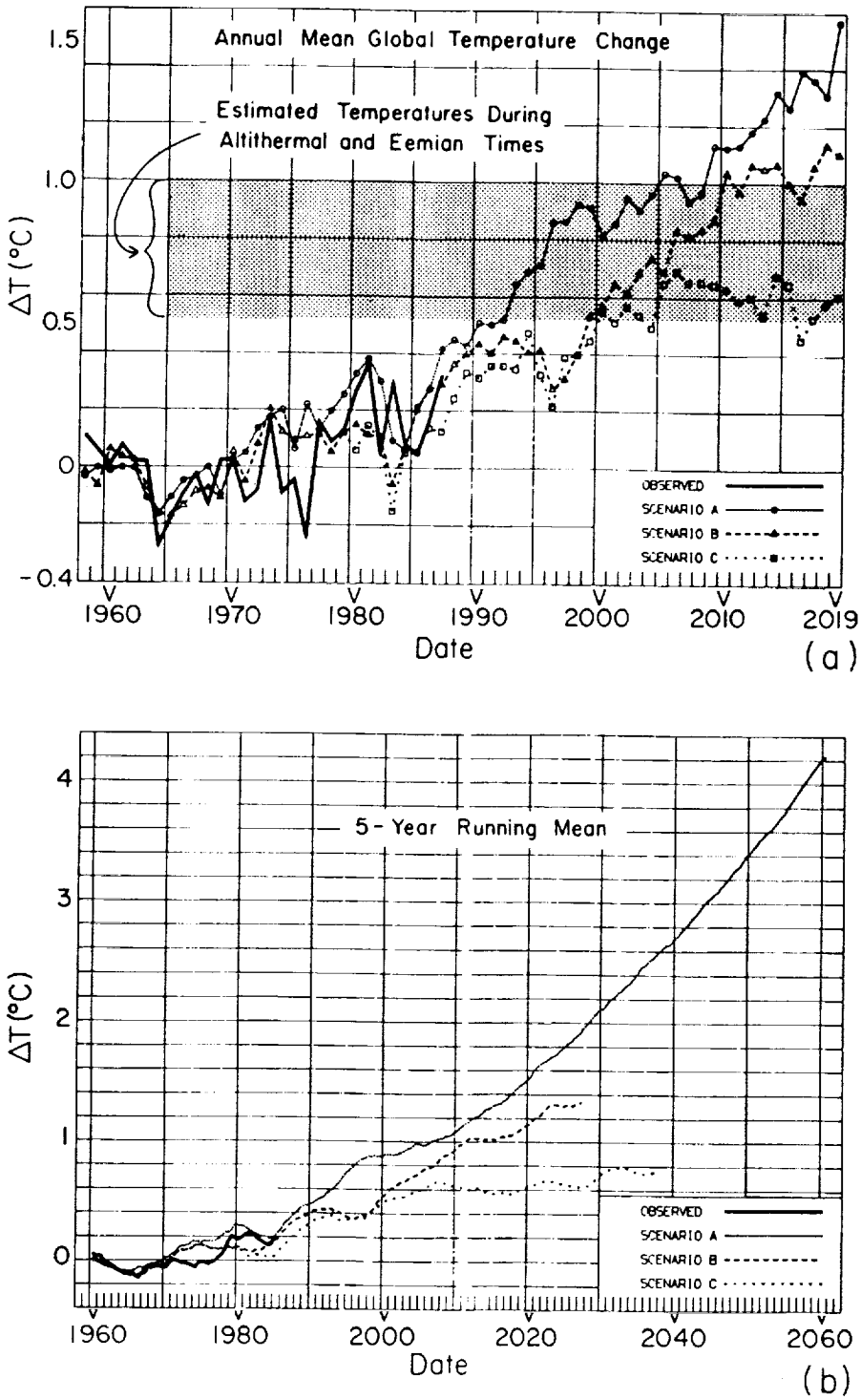


*Figure 47. Annual mean global surface air temperature computed for scenarios A, B, and C. (a) Annual mean global temperature change, 1958-2019; and (b) 5-year running mean, 1960-2060. Observed data are from Hansen and Lebedeff (1987, 1988). The shaded region in part (a) is an estimate of global temperature during the peak of the current and previous interglacial periods—about 6,000 and 120,000 before the present, respectively. The zero point for observations is the 1951-1980 mean (Hansen and Lebedeff 1987); the zero point for the model is the control run mean. Scenario A: Growth rate of trace gas emissions increasing at present level of about 1.5% per year. Scenario B: Decreasing trace gas growth rate such that annual increase in GHG climate forcing remains constant at present level. Scenario C: Drastically reduced trace gas growth between 1990 and 2000 such that GHG climate forcing ceases to increase after 2000. Source: J. Hansen et al. 1988.*

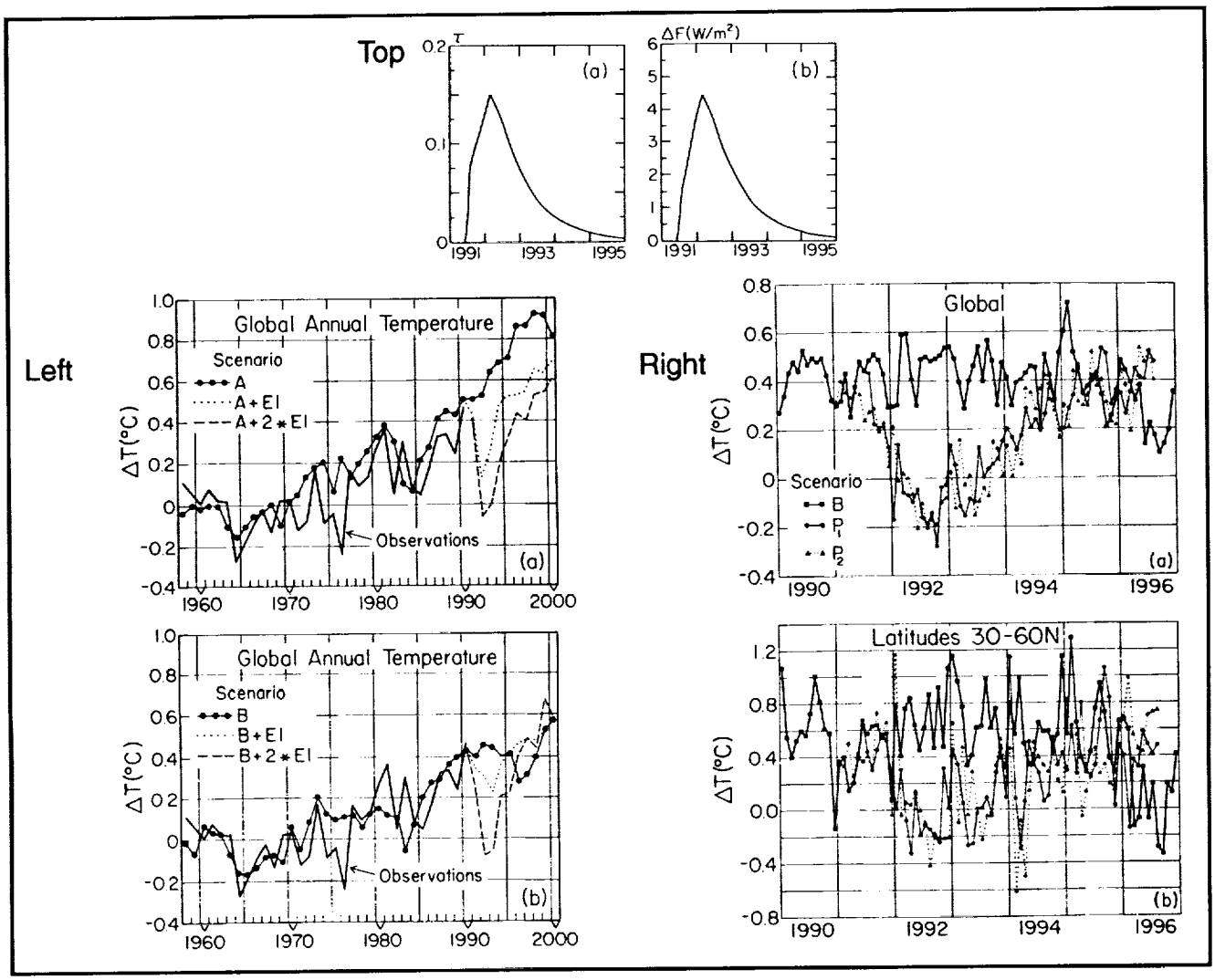


*Figure 48. (Top) Global mean aerosol optical depth and radiative forcing at tropopause for Mt. Pinatubo ($P_n$) simulations. (Left) Annual mean global surface air temperature computed for scenarios A, A+El, and A+2*El (a) and B, B+El, and B+2*El (b). Observational data are an update of Hansen and Lebedeff (1987). Zero point for observations is 1951-1980 mean; model zero point is 100-year control run mean. (Right) Monthly mean global (a) and northern latitude (b) surface air temperature for Scenarios B, $P_1$, and $P_2$. Source: Hansen 1992.*

into play various parts of the climate system that are not yet explicitly included in the model (e.g., deep ocean).

Decadal and longer term fluctuations have also been noted in precipitation in the Sudano-Sahel and the drought cycles in the United States, for example. Figure 49 shows that there is a decadal time scale correlation between sea surface temperature anomalies and rainfall over the Sahel. Changes in global sea surface temperature are hypothesized to alter low-level moisture convergence and the global hydrological cycle. By specifying observed SST changes in their global forecast model, the United Kingdom Meteorological Office (UKMO) routinely makes seasonal, extended-range predictions of Sahelian rainfall.

Some decadal time scale global system changes have been attributed to anthropogenic causes as well. In the case of the Sahel, Charney hypothesized that changes in precipitation could also be caused by the impact of human activity on land surface and vegetation. Investigating such problems are currently carried out using coupled climate system models. For example, Shukla et al.(1991) investigated the effect of deforestation in the Amazon region of South America; they used a coupled model of the atmosphere and biosphere. Figure 50 shows the area covered by tropical forests in the control simulation. The forested area was replaced by degraded grass (pasture) in the deforestation experiment. In model terms (refer back to Figure 29), this replacement translates into a changed surface albedo, roughness, and

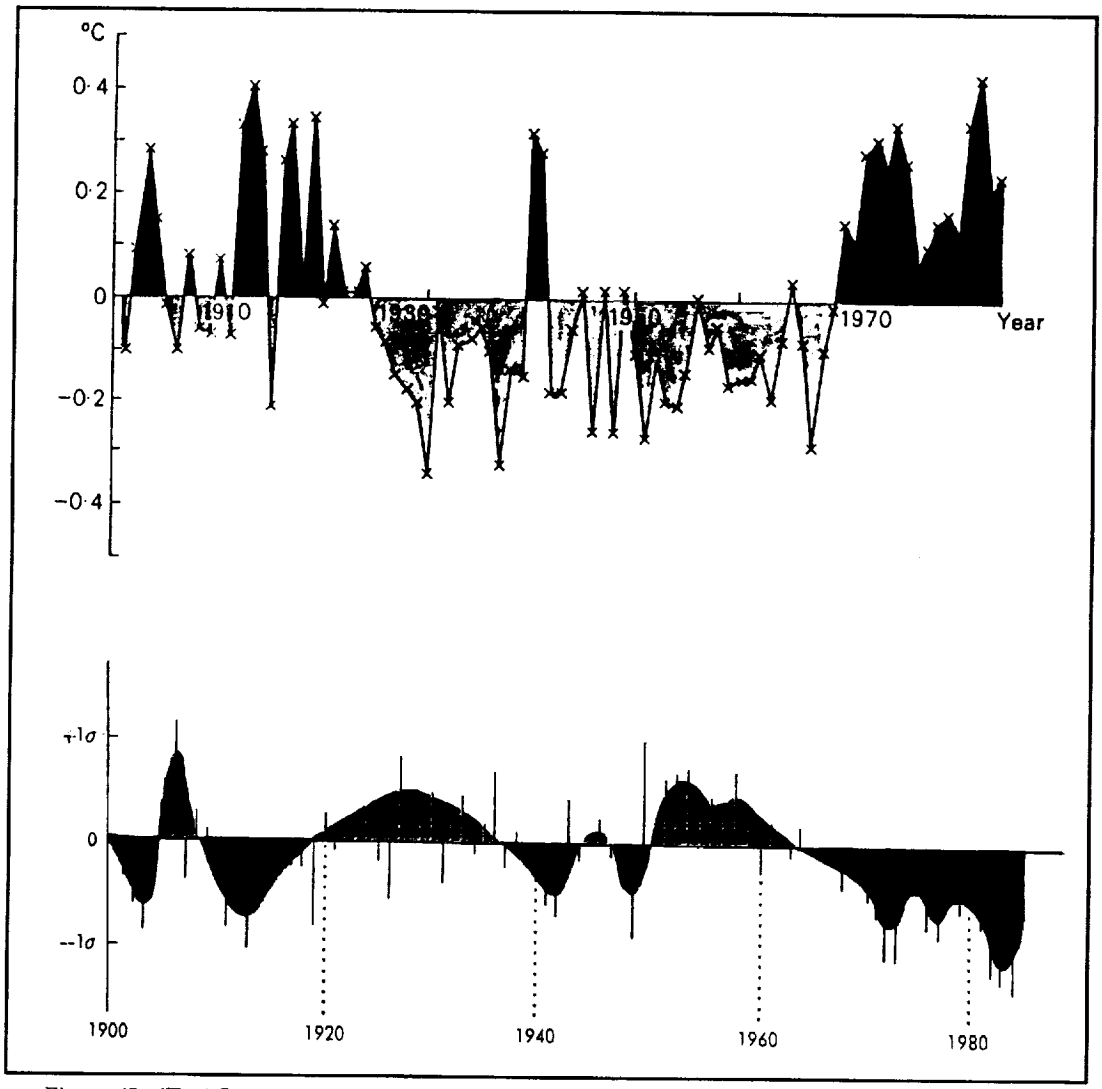


*Figure 49. (Top) Sea surface temperature anomaly differences—Southern Hemisphere minus Northern Hemisphere. The Southern Hemisphere included and the Northern Hemisphere excluded the Indian Ocean in this analysis. Anomalies were computed relative to the 1951-1980 period, for July to September 1901-1985. (Bottom) Standardized annual rainfall anomalies for the Sahel, 1901-85. Source: Folland 1985.*

various parameterizations (e.g., stomatal resistance or depth of root zone in the biosphere model). The consequence of these changes is altered momentum, moisture, and heat fluxes between the atmosphere and the land/vegetation surface.

Figures 51 and 52 show the model-predicted change in surface temperature, deep soil temperature, precipitation, and evapotranspiration. The first two increase, while the latter two decrease substantially. In the simulation, the length of the dry season also increased, which could render the reestablishment of the tropical forest difficult.

Changing the convective-diabatic heating of the troposphere over Amazonia is speculated to have effects in the general global atmospheric circulation and, possibly, through atmosphere-ocean interaction. These feedback effects have not yet been quantified and can get quite complicated.

It needs to be noted that the reliability of such predictions (i.e., climate change due to Amazonian deforestation) depends clearly on all other assumptions and parameterization in the model, such as the parameterization of cloud and convective processors, the planetary boundary layer, the choice of vertical coordinate system, and how the model handles mountains—hence the reason why such predictions are frequently termed "climate scenarios." Much more detailed observational and modeling studies, as well as diagnostic and monitoring experiments, are needed for model verification and validation.

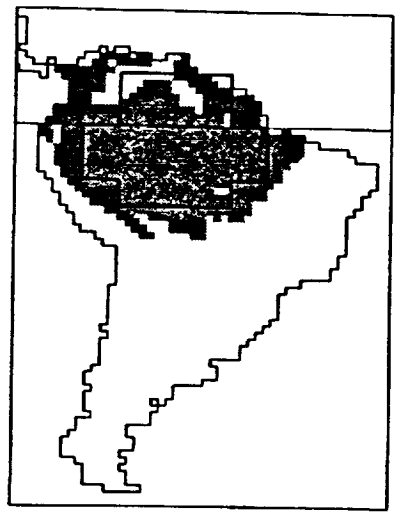

*Figure 50. The South American region. Stippling depicts the area covered by the tropical forest in the control simulation.*

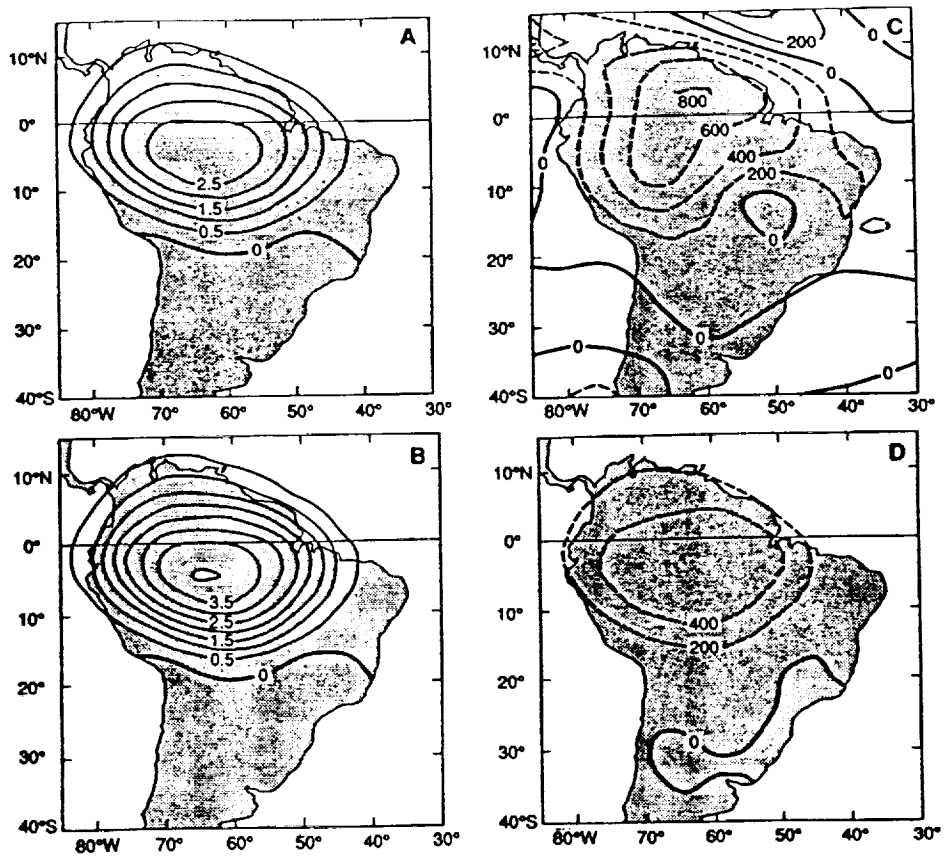


*Figure 51. Differences between 12-month means (1 January to 31 December) of deforestation and control cases (deforested—control) for the South American sector: (A) Surface temperature increase (°C); (B) deep soil temperature increase (°C); (C) total precipitation changes (dashed lines indicate a decrease) in millimeters; and (D) evapotranspiration decrease in millimeters. Model results were smoothed before plotting.*

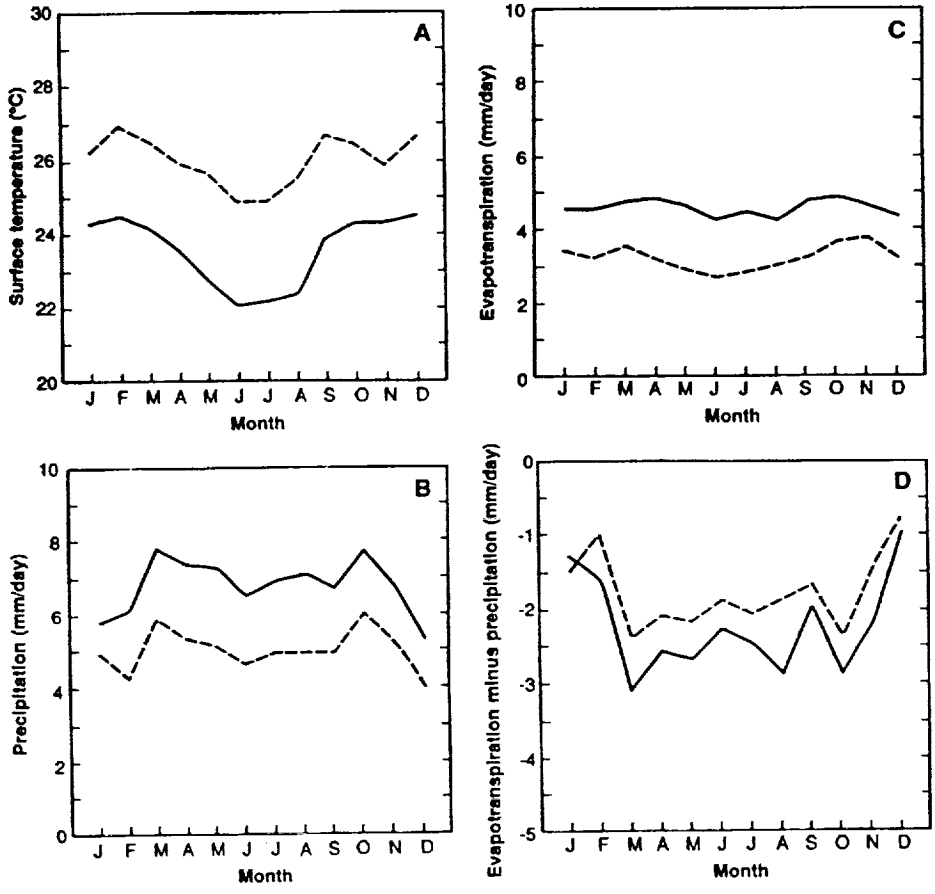


*Figure 52. Monthly distribution (1 January to 31 December) of the areal average of (A) surface temperature, (B) total precipitation, (C) evapotranspiration, and (D) evapotranspiration minus total precipitation. The solid line is for the control case, and the dashed line is for the deforestation case.*

## 4.6. *Simulation/Prediction with Dynamically Coupled Models*

Given the complexity of the physical climate system, time-integrating, coupled models are computationally very expensive. They also have special difficulties on account of the increased degrees of freedom introduced by the dynamic interaction at interfaces of the coupled system. For example, prescribing and maintaining a fixed sea surface temperature and surface snow/ice distribution as a boundary condition to an atmospheric GCM implies an ocean with infinite heat capacity and, *de facto*, sets the surface albedo. Thus, coupling an atmospheric and ocean GCM can allow imbalances in the interface flux of heat and moisture to develop, thereby introducing a gradual artificial drift in one or both components of the coupled system. Such imbalances could be due to a variety of causes, among which are deficiencies in the parameterization of some of the subgrid-scale processes (in the model) or the overestimate or underestimate of various transports. In a climate simulation (i.e., all forcings are held constant or cyclical for the annual cycle), such imbalances need to be compensated on some sensible, physically realistic basis before the model can be used for climate prediction experiments. Choosing or prescribing the right compensation, usually in the form of flux corrections, involves a best guess about the cause of the imbalance.

With advances in climate system modeling, more and more interaction between the components of the climate system are included. But this does not necessarily imply that such coupling is dynamic. For example, interaction takes place with the biosphere; yet, the surface and lithosphere do not have dynamic models as input to a climate model. For the decadal time scale of present interest, this may be sufficient, even though this may constrain the model. However, in this time scale, dynamic coupling with the ocean and cryosphere does prove essential for climate prediction purposes, because they are subject to significant changes in interannual to decadal fluctuations.

Most atmosphere-ocean coupled models do not include a full dynamic ocean. They usually consist of an atmospheric GCM interacting with a simplified mixed-layer ocean model that is an approximately 50-m slab of vertically well-mixed water. The rate of heat exchange between the mixed layer and the deep ocean layers is prescribed such that the seasonal and geographical distributions of sea surface temperature and sea ice are realistic. However, they do (usually) contain idealized schemes for sea ice prediction (change). Most 2 x $CO_2$ equilibrium experiments are carried out with such (albeit simplified) atmosphere-ocean coupled models. Such a configuration of the modeled climate system is conceivably adequate for prediction on time scales less than that associated with the deep ocean circulation (namely 100 to 1,000 years)—even if it does in the process introduce some errors. Predictions will need to be updated periodically. Double $CO_2$ equilibrium experiments do not provide information on the rate of change of global and regional temperature, or information on the time lags that may be introduced by the deeper layers of the ocean. The lag introduced when the ocean spreads the heat trapped by downward GHGs reduces the rate of warming of the oceanic surface.

It is therefore important to develop comprehensive ocean models and to conduct experiments with dynamically coupled models. Indeed, there have been several notable experiments. One such example is detailed below for illustrative purposes, besides providing important insights into $CO_2$-induced warming. The example is from a transient response experiment using a coupled ocean-atmosphere model (Manabe et al. 1991). In this experiment, $CO_2$ is increased gradually at the rate of 1percent per year. The estimated rate of increase was chosen because the total $CO_2$-equivalent radiative forcing of various GHGs other than water vapor is estimated to be currently increasing at ~1 percent per year (Hansen et al. 1988). A parallel experiment was conducted with equivalent $CO_2$ concentrations decreasing at 1 percent per year to investigate whether the climate system response was symmetric. Significant deviations from symmetry would indicate that the coupled model responds nonlinearly to thermal forcings of opposite sign.

In the atmospheric component of the model, the dynamic computation is performed using a spectral transform method in which the horizontal distribution of a predicted variable is represented by a truncated series of spherical harmonies and grid point values. The resolution is limited by a cutoff beyond zonal wave number 15. The same number of degrees of freedom is used in representing the latitudinal distribution of each final wave component. The effects of clouds, water vapor, $CO_2$, and $O_3$ are included in the calculations of solar and terrestrial radiation. The distribution of water vapor is predicted in the model, but the mixing ratio of $CO_2$ is assumed to be constant throughout the model atmosphere. Ozone is specified as a function of latitude and height from observations. Overcast cloud is assumed whenever the relative humidity of air exceeds a critical value (99 percent). Otherwise, clear sky is predicted. The insolation imposed at the top of the atmosphere has seasonal variation; however, its diurnal variation is removed for the sake of simplicity and economy of computation. The solar constant is assumed to be 1,353 W/m$^2$.

Precipitation is simulated whenever supersaturation is indicated by the prognostic equations for water vapor. The precipitation is identified as snowfall when the air temperature near the surface falls below freezing; otherwise, it is identified as rain. Moist convective processes are parameterized by a moist convective adjustment scheme as described by Manabe et al. (1965).

The computation of land surface temperature satisfies the constraint of no surface heat storage. That is, the contributions from net fluxes of solar and terrestrial radiation and turbulent fluxes of sensible latent heat must balance locally and continually. The albedo of snow-free surfaces is determined according to Posey and Clapp (1964). When the surface is covered by snow, the albedo is replaced by a higher value, depending on surface temperature and snow depth. For deep snow (water equivalent of at least 2 cm), the surface albedo is set to 60 percent if the surface temperature is below -10°C and 45 percent at 0°C with a linear interpolation in between. When the water equivalent of the snow depth is less than 2 cm, it is assumed that the albedo decreases from the deep snow values to the albedo of the underlying surface as a square root function of snow depth is computed. The change in snow depth is computed as the contribution of snowfall, sublimation, and snowmelt, which is determined from the requirement of surface heat balance. See Manabe (1969) for further details.

The budget of soil moisture is computed by the so-called bucket method (Manabe 1969). Within the model, soil is assumed to have the ability to contain 15 cm of liquid water. When soil is not saturated with water, the change of soil moisture is predicted as the net contribution of rain fall, evaporation, and snowmelt. If the soil moisture value reaches the field capacity of 15 cm, the excess water is regarded as runoff. The rate of evaporation from the soil surface is determined as a function of the water content of the "bucket" and potential evaporation (i.e., the hypothetical evaporation rate from a completely wet surface).

The basic structure of the oceanic component of the model is similar to the model described by Bryan and Lewis (1979). The primitive equations of motion are constructed by use of Boussinesq, rigid-lid, and hydrostatic approximations. Subgrid-scale motion is included as turbulent viscosity or turbulent diffusion. Whenever the vertical stratification in the model oceans is unstable, it is assumed that the coefficient of vertical diffusion becomes infinitely large, and the vertical gradients of both temperature and salinity are removed. This process of convective adjustment, together with the large-scale sinking of dense water, contributes to the formation of deep water in the model oceans.

The finite difference mesh of the oceanic component of the model has a spacing between grid points of 4.5° latitude and 3.75° longitude. It has 12 levels for the finite differencing in the vertical direction. The computational resolution specified above is marginally adequate for representing coastal currents, but cannot describe mesoscale eddies.

Because of the coarse horizontal resolution of the model, many features of bottom topography are only crudely resolved. For example, the Mid-Atlantic Ridge of the model is not as high above the sea floor as observed; also, Iceland is eliminated. To computationally resolve the ocean currents passing through the narrow Drake Passage, the meridional span of the passage in the upper oceanic layers is expanded to four grid intervals (i.e., 2,000 km). No attempt is made to resolve the flow through the Strait of Gibraltar. Instead, the water at the westernmost Mediterranean grid point is mixed horizontally and completely with the water at the adjacent Atlantic grid point to a depth of 1,350 m. No net flow is permitted through the Bering Strait.

The prognostic system of sea ice is similar to the very simple free drift model developed by Bryan (1969). The sea ice moves freely with the surface ocean currents, provided that its thickness is less than 4 m, but is stationary for higher values. Following Broccoli and Manabe (1987), the albedo of sea ice depends on surface temperature and ice thickness. For thick sea ice (at least 1-m thick), the surface albedo is 80 percent if the surface temperature is below -10°C and 55 percent at 0°C, with a linear interpolation between these values for intermediate temperatures. If the ice thickness is less than 1 m, the albedo decreases with a square root function of ice thickness from the thick ice values to the albedo of the underlying water surface.

The atmospheric and oceanic components interact with each other through exchanges of heat, water, and momentum. The heat exchange is accomplished by the net radiative flux and turbulent fluxes of sensible and latent heat. The water (or ice) exchange consists of evaporation (or sublimation), rainfall (or snowfall), and runoff from the continents. The runoff flows in the direction of steepest descent based on the specified topography. Glacier flow is computed in a similar manner. To prevent indefinite growth of an ice sheet through snow accumulation, it is assumed that the water equivalent depth of snow does not exceed 20 cm, and the excess snow also runs off by glacial flow in the direction of the steepest descent and instantly reaches the oceans. The ocean surface temperature and sea ice predicted in the ocean are used as lower boundary conditions for the atmosphere. Details of the heat, moisture, and momentum exchange processes are also given by Manabe (1969).

The preceding paragraphs serve as an illustration of the large number of assumptions and approximations that are made to make the equations mathematically tractable, to represent the large number of detailed processes in the climate system, and to enable the numerical integration of the coupled model within the constraints of present-generation supercomputers. The model does not have an interactive biosphere, other than the rough parameterization of soil moisture.

The atmosphere-ocean coupled model is not integrated from scratch in coupled mode, because the ocean takes a very long time to reach equilibrium. Thus, prior to coupling, the atmospheric and ocean GCMs are independently initialized and integrated to reach an equilibrium approximating present climate conditions.

Starting from the initial condition of an isothermal and dry atmosphere at rest, the atmospheric component of the model is time-integrated over a period of 12 years, with the seasonally and geographically varying observed sea surface temperature and sea ice as a lower boundary condition. The seasonally varying geographical distribution of sea ice thickness is obtained from satellite observations of sea ice concentration (Parkinson et al. 1987; Zwally et al. 1983). During the last 10 years, the model attains a quasi-steady state in which its seasonal variation nearly repeats itself. The atmosphere reached at the end of this integration is used as the atmospheric part of the initial condition for the integration of the coupled ocean-atmospheric model. The average (last 10 annual cycles) distribution of surface momentum flux is used as an upper boundary condition for the oceanic leg of the preliminary initializing integration.

The oceanic component of the model is time-integrated over 2,400 years. The surface temperature and salinity are relaxed toward the observed values, which vary seasonally and geographically. The relaxation time is chosen to be 50 days, which is short enough to prevent significant deviations of the surface condition from the observed. The distribution of surface flux of momentum from the atmospheric leg of the integration is also imposed. In this time integration, the approach of the deeper layers of the model ocean toward the state of equilibrium is accelerated as described by Bryan et al. (1975) and Bryan (1984), thereby extending the effective length of time integration to 34,000 years. Toward the end of this integration, there is little systematic trend in the temporal variation of the oceanic state. The oceanic state reached at the end of the integration is used as the oceanic part of the initial condition for the time integration of the coupled ocean-atmosphere model.

The next step in the process is to couple the atmosphere and oceanic GCMs. This coupling is not necessarily a trivial step because, even though both the model atmosphere and ocean have reached equilibrium climate states for the prescribed boundary conditions, the two models are not necessarily in equilibrium with one another in terms of the exchange of fluxes of heat, momentum, and moisture. Due to model imperfections, the distribution of the surface fluxes of heat and water obtained from the atmospheric GCM integration with realistic sea surface temperature and sea ice differ from the annual cycles of these fluxes, which are needed to maintain the realistic condition in the ocean GCM integrations. Flux adjustments are necessary to induce an equilibrium between the two models. For the required flux adjustments, the seasonal and geographical distributions of net downward atmospheric fluxes of heat and moisture at the oceanic surface are obtained by averaging over the last 10 annual cycles of the atmospheric leg of the initial integration. Correspondingly, the seasonal and geographical distributions of the surface fluxes of water and heat needed to maintain the realistic distributions of imposed sea surface temperature, surface salinity, and sea ice are computed from the last 500 annual cycles of the ocean model integration. These fluxes are used for the determination of flux adjustments in the time integration of the ocean-atmosphere coupled model.

To prevent a systematic drift of climate in the coupled model and an unrealistic equilibrium state of the ocean (i.e., without flux corrections), the surface fluxes of water and heat (but not of momentum) from the atmospheric component of the model are modified by amounts equal to the difference between the two sets of fluxes derived in the preliminary integrations before they are imposed on the oceanic component in coupled mode. Recall that even when coupled, the primary manner in which the atmosphere interacts with the ocean or the land surface is through the computed or assumed flux terms at each integration time step. The net ocean-surface flux before and after the adjustment averaged over 100 years of the standard(S) integration is shown in Figure 53. Averaged over the surface, heat flux into the ocean is negative; it is near zero after the adjustment. Thus without the correction, the climate of the ocean would have been too cold. This cold bias is attributed to the tendency of the cloud prediction scheme to overestimate low cloud and underestimate high cloud. The magnitude of the adjustment is particularly larger ($\sim$40 W/m$^2$) in the Northern Hemisphere subtropics, where the cloudiness is overestimated over the the oceans and, accordingly, the surface absorption of solar radiation is underestimated by the model. Although the flux adjustment depends upon season and geographical location, it is changed from one year to the next. The fact that the state of the coupled model remains near quasi-equilibrium conditions underscores its stability and, to some immeasurable degree, its representativeness.

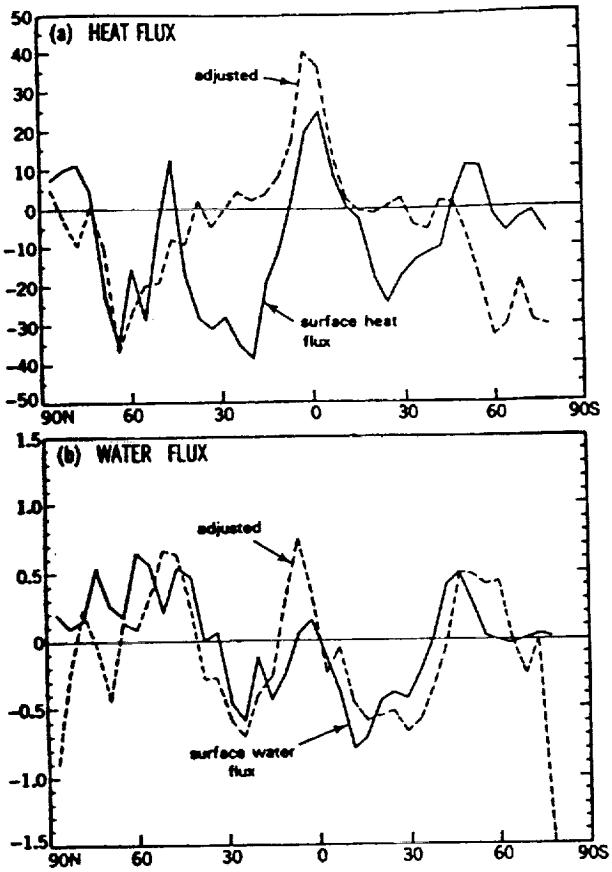


*Figure 53. The latitudinal profiles of net ocean-surface flux before and after the adjustment in the S integration of the coupled model. (a) Heat flux ($W m^{-2}$), and (b) Water flux ($m yr^{-1}$). The fluxes are zonal means over the ocean, averaged over the 100-year period of the integration. Source: Manabe et al. 1991.*

The ocean-atmosphere coupled model integrations were done in this particular experiment under three $CO_2$ scenarios, as depicted in Figure 54. Each integration was for a 100-year period with "S" denoting the integration with constant (or stable) $CO_2$, "G" denoting growth or increasing $CO_2$, and "D" denoting decreasing $CO_2$. The "S" integration of the coupled model should, on the average, represent present climate. Figures 55, 56, and 57 of the constant $CO_2$ S integration shows that the geographical distribution of annual, mean sea surface temperature, sea surface salinity, and surface air temperature averaged over the 100 model years reproduces the observed climate rather well, providing credence to the coupled model.

Figure 58 shows a time series of deviations of annual mean air temperature from the 100-year mean. This also is a measure of the variability of climate in the coupled model. Note that there are long-period fluctuations of above and below "normal" temperature over periods from 10 to 15 years (e.g., Northern Hemisphere) to 30 to 40 years (Southern Hemisphere). Shorter time scale fluctuations in climate variability are also seen in other model experiments and is observed in nature. The temperature anomalies are on the order of ±0.2°C and rates of change of up to 0.4°C per 20 or 25 years. The experiment demonstrates that there is an inherent variability of the coupled climate system on relatively long time scales (i.e., 10 to 50 years). Interannual variability is on the order of 0.2 to 0.4°C per 5 years. There is no long-term climate trend in this integration.

The coupled model integrations (again for 100 years each) for the increasing and decreasing scenarios of $CO_2$ concentration are shown in Figure 59. At first glance, the response of the model is symmetric, implying internal consistency. Figure 60 compares the response of the coupled ocean-atmosphere model to a 1 percent per year increase in $CO_2$ averaged over the 60th to the 80th year (shown as a difference from the equilibrium integration) and the corresponding equilibrium response to a doubling of $CO_2$. The equilibrium response refers to the following:

- Starting from the state reached at the end of the preliminary integration, the atmospheric GCM (only) is integrated for another 40 years, allowing both the temperature and ice thickness of the simplified mixed layer ocean to change thermodynamically. The heat flux, determined from the preliminary integration, is prescribed at

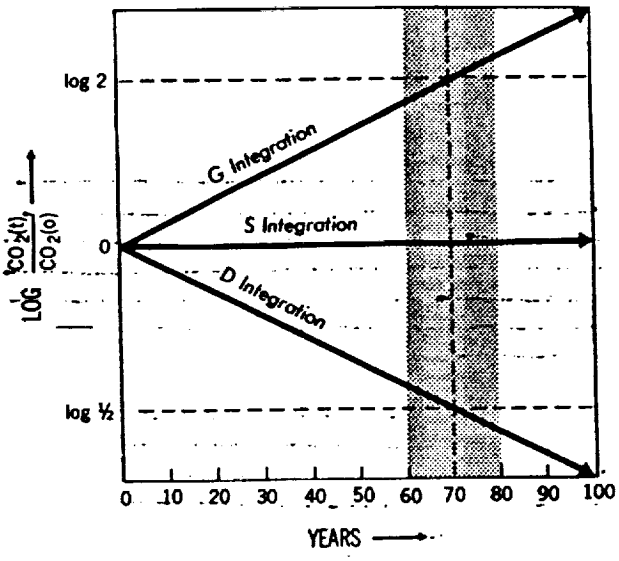


*Figure 54. Schematic diagram of the G, S, and D integrations. The abscissa denotes time in years and the ordinate is the logarithm of the ratio of atmospheric carbon dioxide at time t to its initial value. The period chosen for detailed analysis is indicated by shading. Source: Manabe et al. 1991.*

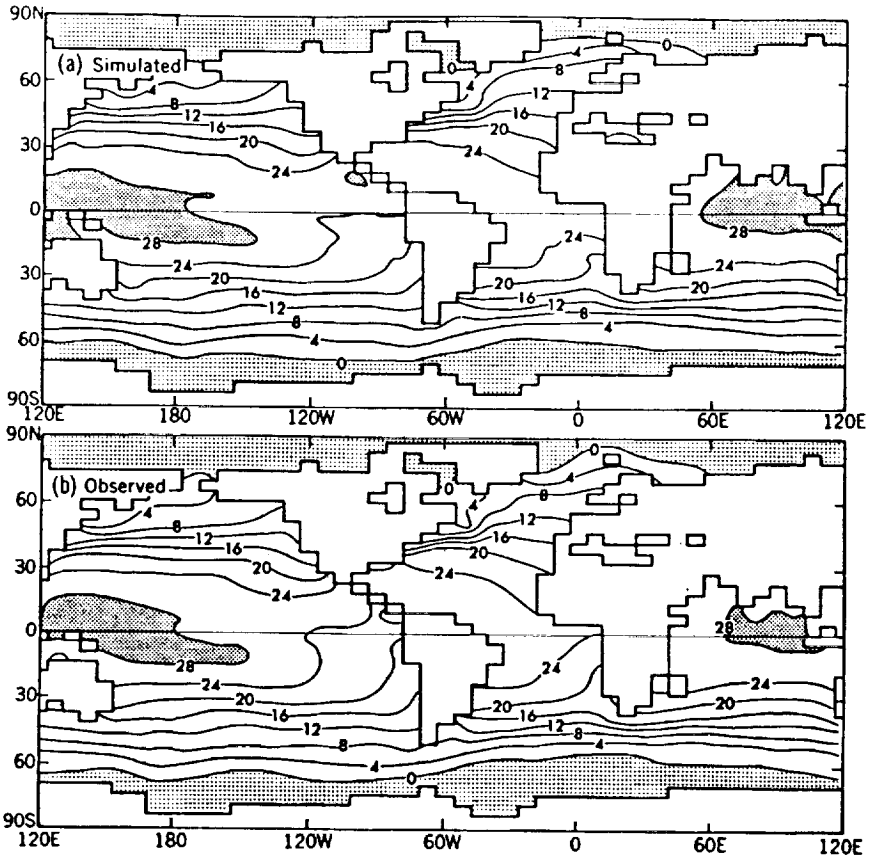


*Figure 55. Geographical distribution of annual-mean sea surface temperature (°C). (a) The simulated distribution of the temperature averaged over the 100-year period of the S integration of the coupled model, and (b) the observed distribution from Levitus (1982).*
*Source: Manabe et al. 1991.*

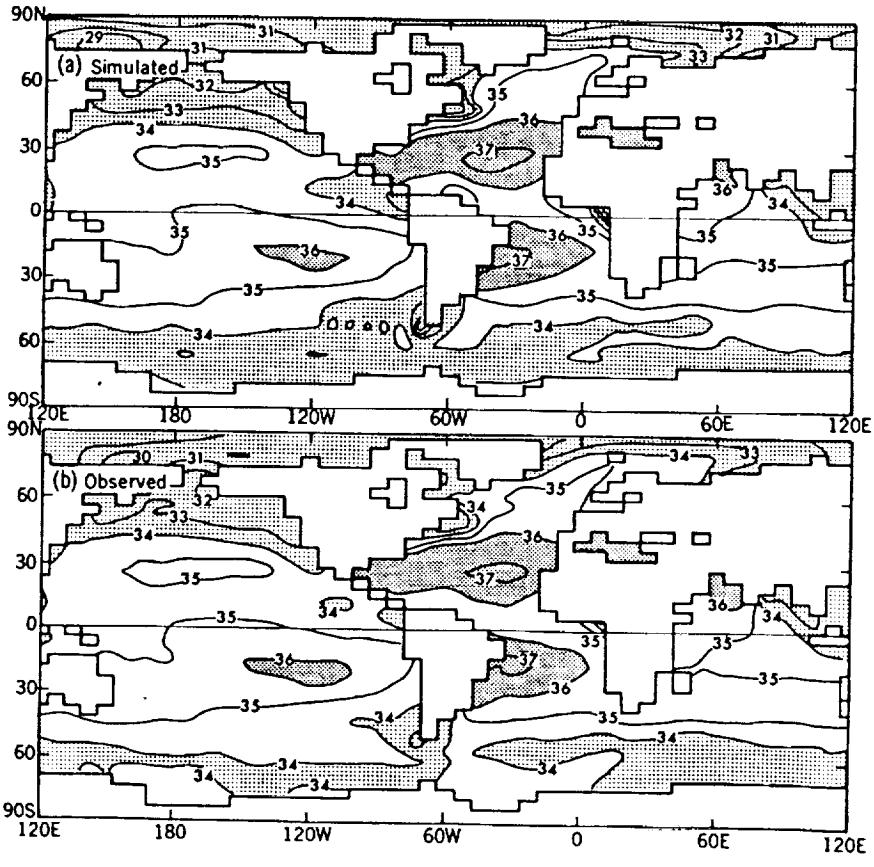


*Figure 56. Geographical distribution of annual-mean sea surface salinity (psu). (a) The simulated distribution of the salinity averaged over the 100-year period of the S integration, and (b) the observed distribution from Levitus (1982).*
*Source: Manabe et al. 1991.*

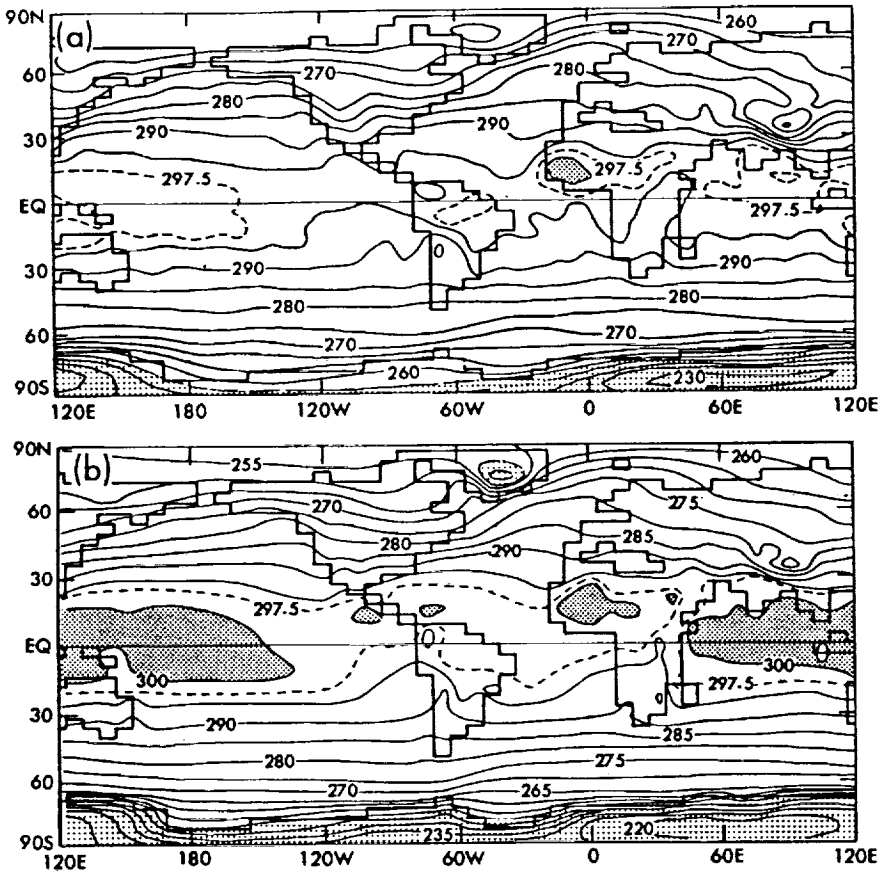


*Figure 57. Geographical distribution of annual-mean surface air temperature (K). (a) The simulated distribution of the temperature averaged over the 100-year period of the S integration of the coupled model, and (b) the observed distribution from Crutcher and Meserve (1970) and Taljaard et al. (1969). The surface air temperature of the model is the temperature at the lowest finite difference level located at ~70 m above the surface. Source: Manabe et al. 1991.*

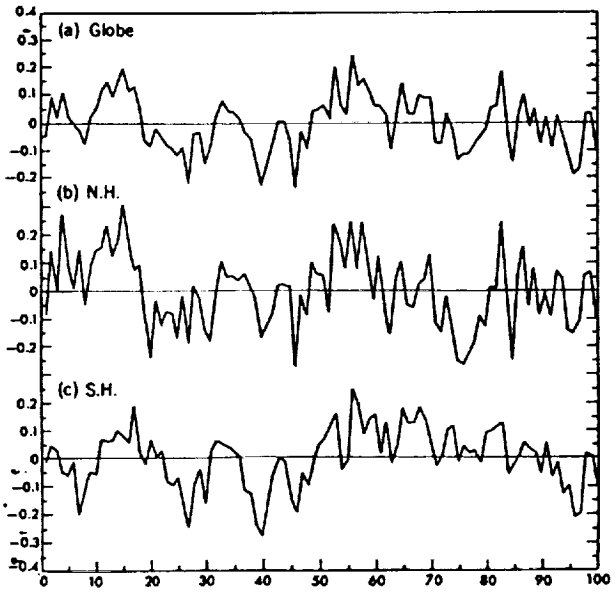


*Figure 58. The temporal variations of area-averaged deviation of annual-mean surface air temperature (°C) from the 100-year mean temperature produced by the S integration of the coupled model for (a) globe, (b) Northern Hemisphere, and (c) Southern Hemisphere. Source: Manabe et al. 1991.*

*Figure 59. The temporal variation of the differences in area-averaged, decadal-mean surface air temperature (°C) between the integrations (a) G and S, and (b) D and S. Solid, dashed, and dotted lines indicate the differences over the globe, and Northern and Southern Hemispheres, respectively. Source: Manabe et al. 1991.*

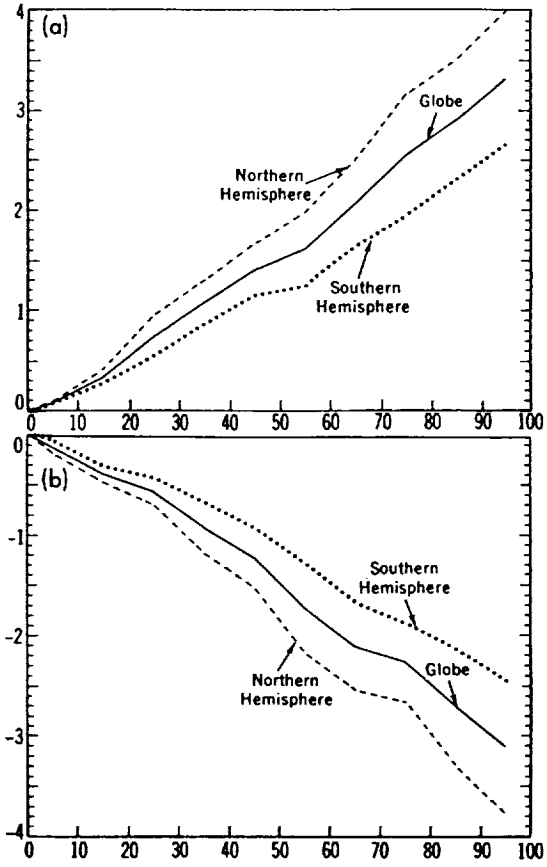

the bottom of the mixed layer and a function of season as geography. This heat flux prescription prevented any systematic (spurious) drift in the model, and the sea surface temperature and sea ice thickness did not deviate from the observed climatology. This integration with constant $CO_2$ is termed the "ES integration."

- Equilibrium integrations were conducted with the same partially coupled model (i.e., with only a simplified mixed layer ocean model) with an artificially imposed 2 x $CO_2$ and 0.5 x $CO_2$ concentration. The very same "heat flux" prescribed at the bottom of the mixed layer in the standard (climatology simulation) integration was prescribed in these integrations also. These integrations are termed "E2X" and "EX/2," respectively.

From Figure 60, it is clear that there are significant differences between the transient (fully coupled model) response and the equilibrium 2 x $CO_2$ (E2X)

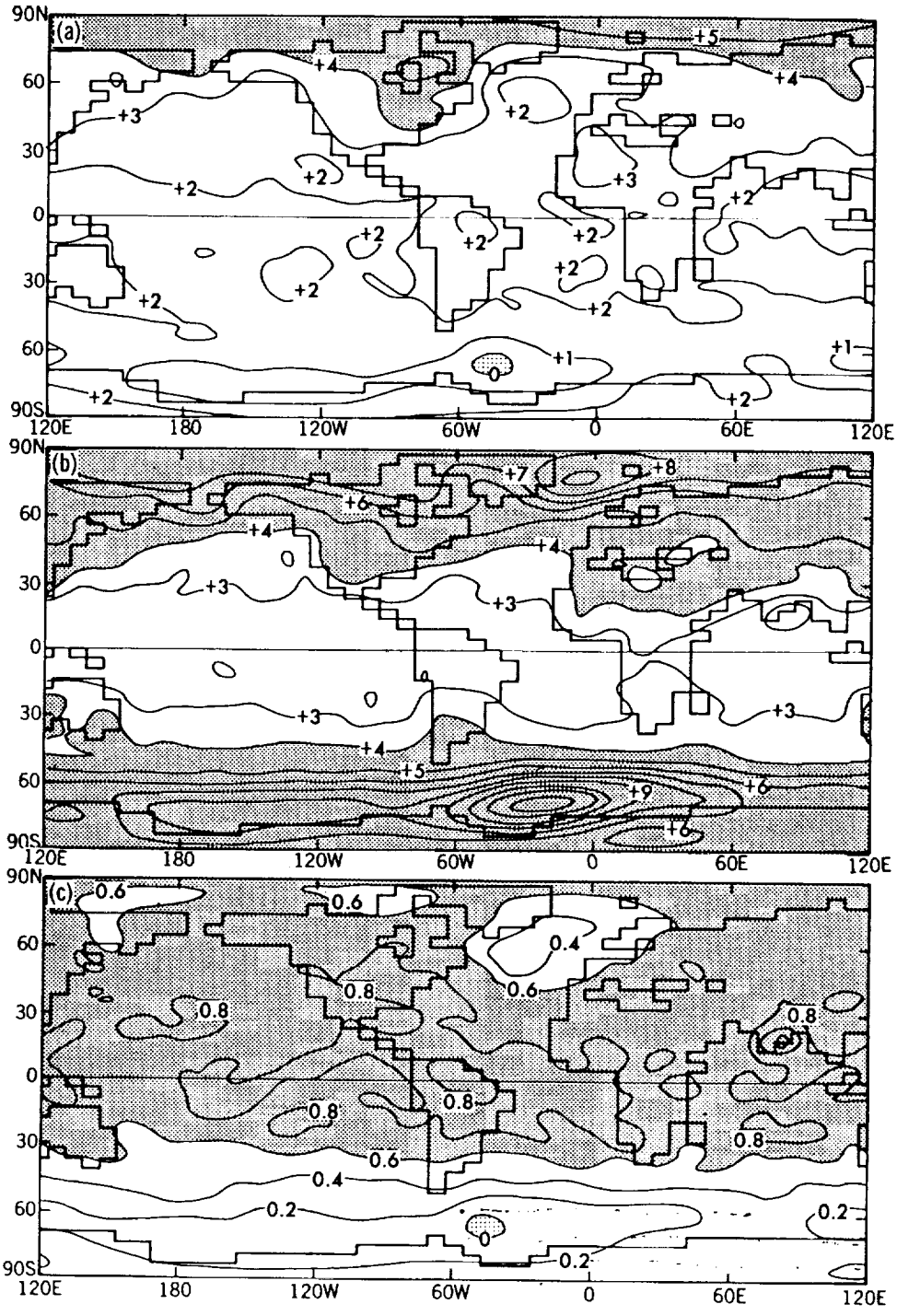


*Figure 60. (a) The transient response of the surface air temperature of the coupled ocean-atmosphere model to the 1percent per year increase of atmospheric carbon dioxide. The response (°C) is the difference between the 20-year (60th to 80th year) mean surface air temperature from the G integration and 100-year mean temperature from the S integration. (b) The equilibrium response of surface air temperature to the doubling of atmospheric carbon dioxide. The response is the difference between the two 10-year mean states of the E2X and ES integrations. (c) The ratio of the transient to equilibrium responses. Source: Manabe et al. 1991.*

model response. Particularly obvious are the much larger warming temperature anomalies in the mid- and high-latitude responses in the 2 x $CO_2$ equilibrium climate compared with the transient (fully coupled model) response. The differences are particularly dramatic over the Antarctic region. The ratios in Figure 60 would have been much more startling had they been inversed by the authors. The smaller warming over both oceanic and land areas is speculated to be on account of the time delay caused by the large effective thermal inertia of the oceans.

Figure 61 compares the penetration depths (in the ocean) of temperature anomalies between the $CO_2$ growth experiment and the $CO_2$ decrease experiments. The vertical spreading of positive and negative anomalies of oceanic temperature are reflected in the computation of the effective penetration depth of the positive and negative anomalies (Manabe et al. 1991). From Figure 60, there is a substantial difference in the penetration depth of the positive and negative anomalies corresponding to the $CO_2$ increasing and decreasing experiments. The latter is usually larger in high latitudes. The difference in penetration depth is attributable to opposing changes in the static stability of the upper layer of the model ocean. Because of the difference in the penetration depth of the thermal anomaly, the effective thermal inertia of the ocean is much larger in the $CO_2$ reduction than the $CO_2$ growth experiment. Thus, the coupled system response to thermal forcing anomalies is nonlinear and nonsymmetric.

Also note that without the flux adjustments the climate of the model system would have been too cold. This cold bias is attributable to the tendency of the cloud prediction scheme in the model toward overestimating low cloud and underestimating high cloud. The magnitude of the adjustment is particularly large even in the subtropics (refer back to Figure 53); when the total cloudiness is overestimated over the oceans, the surface absorption of solar energy is underestimated by the model. Concerning water flux, a disturbingly high adjustment is required in high regions of the Northern Hemisphere. Such a large adjustment is needed partly because the present atmospheric model with relatively low computational resolution tends to overestimate the poleward atmospheric transport of moisture and, accordingly, the excess of precipitation over evaporation in high latitudes. It may also be attributable to the inability of a low-resolution ocean model with high subgrid-scale diffusions to bring sufficiently saline water to the northern North Atlantic where the sinking branch of the thermohaline circulation is located.

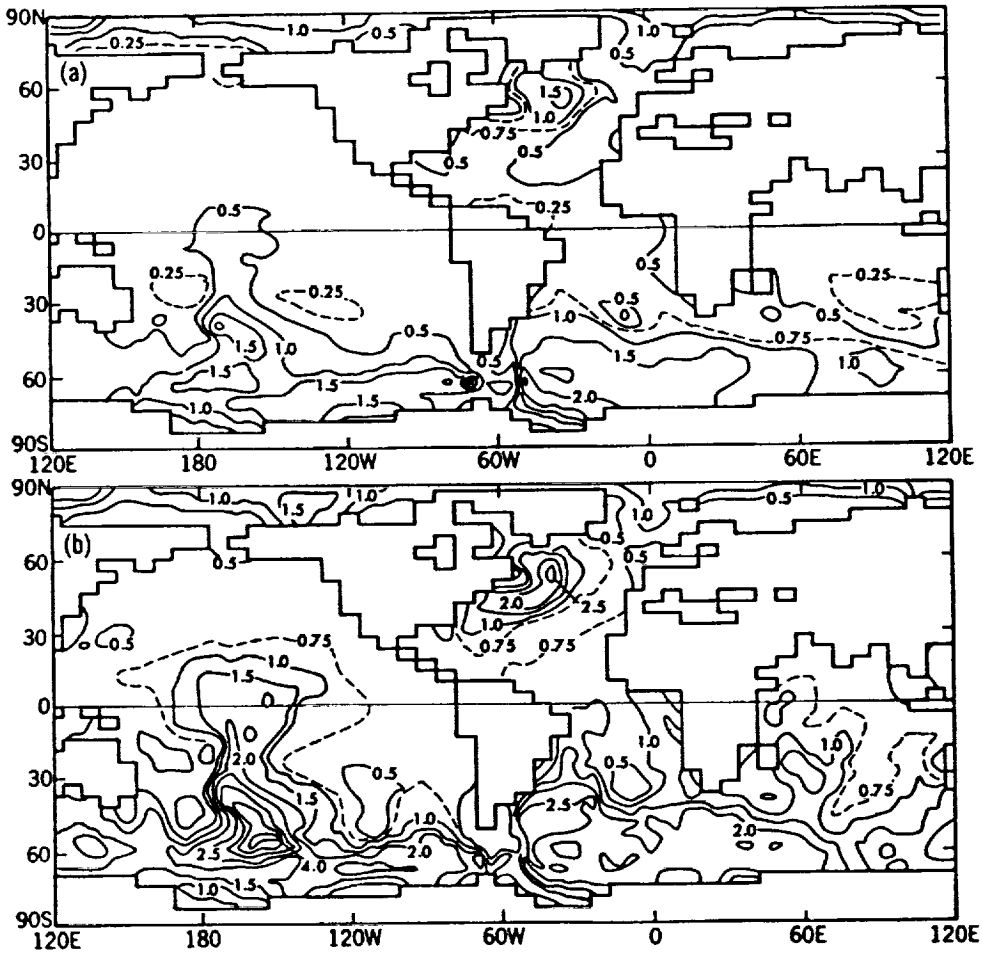


*Figure 61. The geographical distributions of penetration depth of (a) the positive anomaly of oceanic temperature in the $CO_2$ growth experiment, and (b) the negative anomaly of temperature in the $CO_2$ reduction experiment. Source: Manabe et al. 1991.*

***Conclusions/Recommendations (for all of Section 4).*** *The NMC model loses much of its skill in predicting low-frequency modes in the tropics at lead times longer than 10 days; however, during periods of strong tropical ISOs, error growth for the tropical as well as extratropical low-frequency modes are considerably reduced.*

*For the prediction of day-to-day weather, the growth of initial error is an important consideration. For seasonal mean prediction, the initial error growth rate is not important, but the saturation value of the error is. For seasonal and interannual predictability, the distinction between the tropics and the extratropics becomes very important. The tropical mean atmospheric circulation is strongly linked with the lower boundary condition, especially sea surface temperature and soil moisture. The predictability of seasonal and interannual variability resides in the initial conditions of the ocean. Observations show a large correlation between global SST and atmospheric circulation, and classical predictability studies show potential for extended-range predictability. What is not known is how much of the potential is actually realizable.*

*High-quality global data sets are essential for the evaluation of the performance of global models. Although global models capture many of the gross features of the Earth system, they often lack detailed depictions or fail to predict the observed variability. Such problems contribute to speculation about the model's ability to predict climate change due to human-induced or natural causes. At NASA's Marshall Space Flight Center, the strategy is to employ a hierarchy of physical models (from complex numerical models to simple laboratory models) on a variety of temporal and spatial scales in conjunction with global data sets generated from space-based measurements. Model runs will be compared with the data sets to identify model weaknesses and to develop requirements for new observations.*

*During the past decade, with low-resolution models and simplified ocean, sea ice, hydrology, and biospheric effects, scientists began to explore the myriad interactions of the climate system, albeit with limited success. In spite of difficulties, climate models have simulated the annual cycles of basic temperature, moisture, wind, and precipitation distributions. Although significant differences still exist between models and observations, several international comparison studies are now underway to understand these differences. Additional observational data will ultimately be required to decrease reliance on partially artificial methods of parameterization of complex processes.*

*Coupled models (e.g., atmosphere-ocean) are not simply the sum of component parts; they are distinct and separate entities. There are serious and unresolved questions about how coupled models should be initialized. The nature and ultimate limit of climate predictability is also unknown and needs to be addressed.*

*As we consider more and more complex coupled models to simulate the Earth system, we must remain aware of several key elements of coupled modeling: 1) Feedbacks that are not present in uncoupled models may act to destabilize the system when coupling is included; 2) wholly new modes of variability may arise that can only exist in coupled systems (e.g., ENSO); 3) model errors couple (and may be unstable) as well as model physics; and 4) details often matter, and measures of "success" in uncoupled simulations may not be appropriate predictors of success in coupled models. As the time scales of interest extend beyond the interannual, it becomes necessary to improve the prediction of changes in the deeper layers of the ocean, including the thermohaline circulation and its variability. This requires the prediction of high-latitude, freshwater fluxes (i.e., evaporation, precipitation, sea ice processes, and river runoff), which involves all components of the physical system.*

*Making seasonal and longer forecasts depends on the ability to accurately predict the evolution of the SST fields. This requires that the fluxes of heat and momentum produced by the atmospheric model be tuned to eliminate climate drift and climate "crash." The latter occurs when stresses produced by the coupled model, especially in the equatorial zone, cannot balance the pressure gradients present in the ocean initial fields. The results are ubiquitous El Niños. To date, most atmospheric models produce stresses that are too weak in the equatorial zone—hence a serious obstacle to seasonal forecasting. The strength of the atmospheric stresses in the tropics depends strongly on properly representing the interactions between the SST field and the thermally driven atmospheric circulations. Improvements are required for accurately modeling atmospheric deep convection and boundary layer processes, including radiation, clouds, and the vertical transfers of heat and moisture away from the convective zone. For such tunings, ground truth on tropical rainfall is vital.*

*Northern hemispheric data records show two types of low-frequency variability. One is concentrated in low latitudes and penetrates very high in the atmosphere, namely the El Niño with a period of 3 to 5 years. The other variability is polar-amplified, has its greatest amplitude near the Earth's surface, and has a period of 20 to 60 years. Familiar climate events associated with this are the warming of the entire Northern Hemisphere during the 1930s and the abrupt return to much cooler conditions in the 1960s. An abrupt cooling episode also seems to have taken place around 1910. The type of model needed to study very low-frequency air-sea*

*interaction (amplified at high latitudes) is very different from the type of models required for El Niño. The SST anomaly pattern [i.e., the difference between the average for the cold of 1965 to 1986 and the warmth of 1951 to 1962 (Kushnir 1991] has a maximum amplitude in a region of deep wintertime convection in the Labrador Sea, south of Greenland. Insignificant amplitudes exist in the tropics. A very simple model would allow only a local response of the ocean. Much deeper penetration would be allowed in polar and subpolar ocean regions where deep overturning normally takes place. Heat storage in the upper ocean allows for very great amplification of low-frequency forcing by the atmosphere, conforming to Hasselmann's (1974) climate model. Another type of model is required, if nonlocal response takes place associated with changes in ocean circulation. The GFDL control run has been extended for 200 years, showing variability of the coupled system with an average period of about 40 years with maximum SST anomalies in the northwestern Atlantic. Simulated variations in the intensity of the North Atlantic thermoclinal conveyor belt are only ~5 percent.*

*There are several key questions that may be raised with regard to Earth system modeling and prediction: Is climate prediction on decadal time scales possible? Is ocean modeling a more crucial problem for the future than atmospheric modeling? To what extent can we improve climate simulations simply by increasing resolution, and how much resolution is enough? Do spectral models have a future in climate modeling?*

*It would be necessary to improve models so that in climatological runs there is no net heat flux into the ocean from the atmosphere and no net heat flux into the abyss in ocean models.*

*There is as yet no established theoretical basis for climate system or Earth system predictions. Models work with primitive equations, making forecasts with various numerical techniques. The deterministic limit for weather forecasting is a couple of weeks. The reason that the limit exists is not because of the complicated physical processes that are inadequately modeled, but rather the nonlinear nature of the equations. Even though we know that detailed weather cannot be predicted, we go ahead and use these models to predict climate. This has not been proven valid. Even if the current state-of-the-art models were to give climate statistics that resemble the atmosphere (and even this is arguable), since the models are tuned to the present climate, how can we justify their use in predicting climate change? The question is whether climate itself (not just weather) could be chaotic and inherently unpredictable. More research is needed in comparing numerical predictions of highly nonlinear fluid systems with the behavior of actual physical analog laboratory models.*

*One-dimensional radiative-convective equilibrium (RCE) models include only vertical transport by radiation and small-scale convection, and neglect (vertical and horizontal) heat transport by large-scale dynamics. Because of this, they are valid for global climate simulations but not appropriate for regional simulations.*

*Obviously, climate system sensitivity is a major issue. The sensitivity of climate (both modeled and the real world) needs to be gauged—for example, by temperature change in response to changes in forcings and feedbacks. Model intercomparisons show that the major differences between model simulations of 2 x $CO_2$ climates are primarily due to differences in the parameterizations and treatment of cloud and convection processes.*

*The next steps in the further development of coupled models would entail the following: 1) An interactive biosphere (vegetation), 2) an eddy-resolving ocean model, 3) more complex treatment of radiative physics and chemistry, 4) improved cloud parameterization and cloud radiation physics, and 5) the inclusion of aerosols and their effect in the climate model.*

# 5. *The Validation and Intercomparison of Models*

Even if a model simulates the present global system and compares well with other models, there is no absolute guarantee that a prediction using the same model is reliable. Predictions will need to be validated separately with observational data before one may feel confident about a model's ability to handle the physics and interactions of global change. Generally, validation should refer exclusively to comparisons with observational evidence; however, model-to-model intercomparisons are also being used as indirect validation, because the reliability of current observational data is in itself somewhat questionable.

The validation of climate system models is an immense task, partly because several components and processes of the total Earth system are not explicitly modeled. There are four basic methods of validation:

- Compare model(s)/simulations of present climate with observed climatology
- Compare the simulation of climate obtained from different climate models, highlighting areas of uncertainty in model physics and parameterization
- Compare model(s)-produced climate with altered boundary or other (e.g., solar) forcing with observational evidence (e.g., paleoclimatic information)
- Compare the climate sensitivity of various models to an imposed altered forcing or boundary state such as 2 x GHG, +2°C ($\Delta$T), and so on; the response of a model to such an imposed change would depend on how various processes are parameterized as well as how various feedbacks are handled by the model (e.g., water vapor or cloud).

All of the above require that comparisons be made using not only basic state variables such as temperature, wind, and precipitation, but also more complex parameters such as radiation fluxes, soil moisture, momentum fluxes, and sensible and latent heat fluxes. These variables indicate how well the model handles, among others, the hydrological cycle and radiation balance and the interactions between such components of the climate system as atmosphere-land surface/vegetation, atmosphere-ocean, and ocean-sea ice.

Several investigations have attempted to compare the simulation of present climate by different models and with observed climatology. Even comparisons with observed climate presents some difficulty since global climate statistics are not well-known for a number of basic climatological parameters such as soil moisture and cloud amount and distribution, precipitation and evaporation, sea-ice thickness, and especially fluxes and stresses that connect the atmosphere to the ocean and the land. Techniques of verification are not particularly well-developed and must include appropriate statistical measures that take into account the natural variability of the climate system and the uncertainities in the "observation-based" climate statistics (G.J. Boer et al. 1991).

A first-order comparison frequently applied is to compare mean (i.e., long-term) zonally averaged values of a selection of parameters (e.g., pressure, temperature, and precipitation) with that observed for summer (June, July, August) and winter (December, January, February). Comparisons are usually made of the geographical distribution of the same variables in order to identify regional differences. Figures 62 through 66 show the zonally averaged climate simulated by a selection of global general circulation models, with the parameters being pressure, temperature, precipitation, upper level winds, and soil moisture, respectively. The models used for this comparison are identified in Table 4. Most models depict the latitudinal distribution of these variables reasonably well, possibly with the exception of soil moisture. Figure 66 shows model weaknesses for soil moisture—a more complex variable that involves temperature, evaporation, precipitation (therefore clouds), and the parameterization of soil water/moisture budget. This also points to deficiencies in the hydrological cycle in models. Regional differences in this parameter (as with precipitation) are substantial between models.

G.J. Boer et al. (1991) reached the following conclusions when comparing 14 atmospheric general circulation models (AGCMs). (a) The simulated temperature of the atmosphere is too cold on average, especially in the polar upper troposphere and tropical lower troposphere. This deficiency is found in all models despite differences in numerics, resolution, and physics; such common model deficiencies are termed "systematic," "tenacious," "insensitive," "universal," or "essential." It is conjectured that all models are misrepresenting or even omitting some mechanism which results in this deficiency. (b) Zonal wind structures are closely connected to temperature structures but represent additional information concerning gradients. Deficiencies in zonal winds are those that would be expected from temperature deficiencies; zonal wind maxima that are shifted or that extend upward are notable common features. There is some evidence of increasing zonal winds with increasing resolution. (c) The distribution of mean sea-level pressure is

a sensitive indicator of the dynamical and thermodynamical behavior of the model. There has been a clear improvement in the simulation of this field in more recent models, most of which have higher horizontal resolution. The nature and explanation for this improvement—including the parameterization of a previously omitted physical process (i.e., gravity-wave drag)—indicates how difficult it is to understand the intertwined effects of model formulation on simulated climate. (d) Characteristic deficiencies remain in the simulations of precipitation—an important variable linking the moisture, thermodynamic, and dynamic equations.

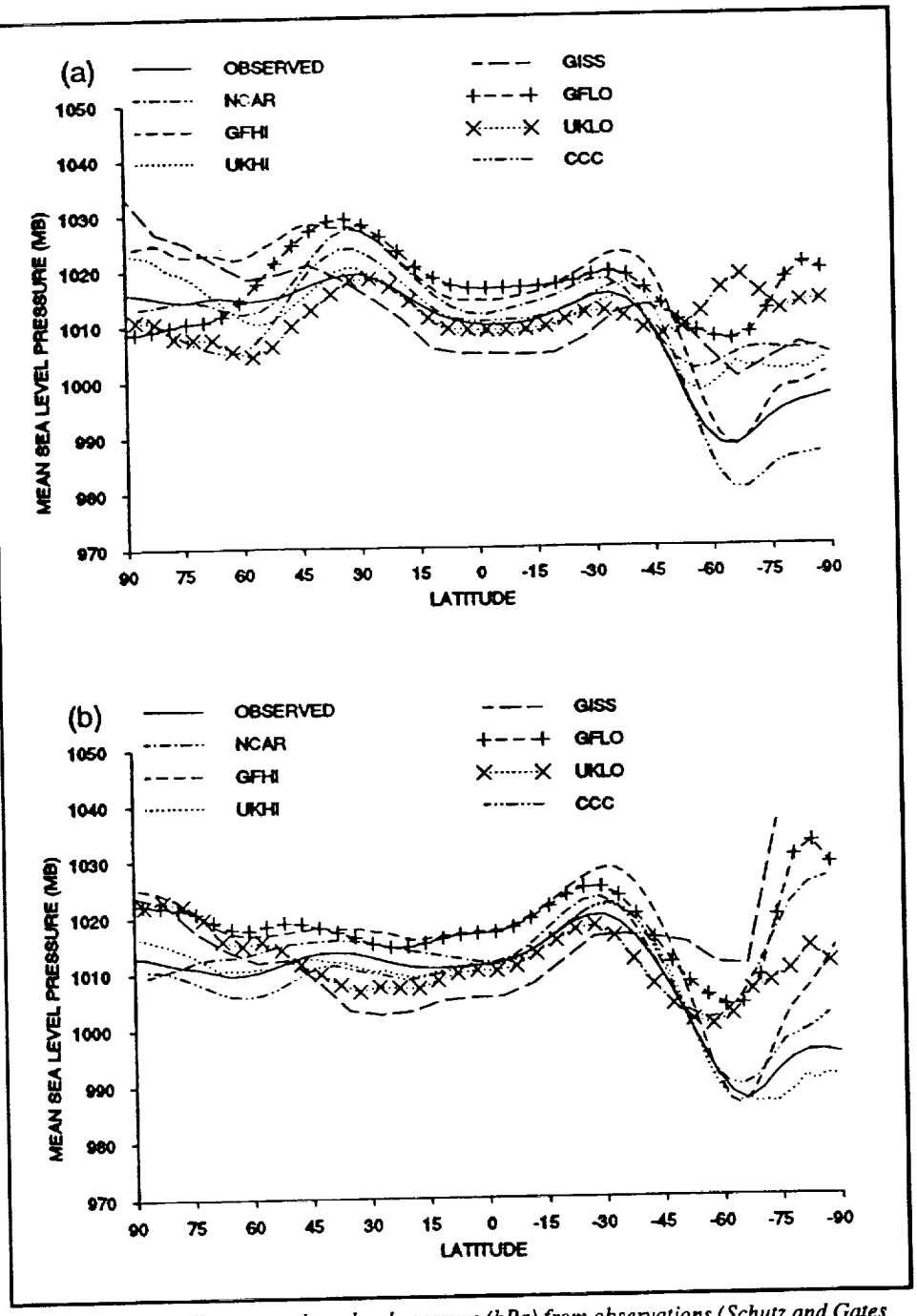


*Figure 62. Zonally averaged sea-level pressure (hPa) from observations (Schutz and Gates 1971 and 1972) and models: (a) December-January-February, and (b) June-July-August. Source: IPCC 1990.*

Validating the predictive skills of global models is not easy. For the sake of simplicity, emphasis has been placed (in model experiments and intercomparisons) in global-mean quantities, and the interpretation of climate change as a two-stage process—forcing and response. This has proved useful in interpreting climate feedback mechanisms in general circulation models. The most extensive intercomparison studies carried out recently have been of model climate responses to a doubling of equivalent $CO_2$ or the responses to an imposed change in surface temperature. Table 4 summarizes the results from 22 mixed-layer ocean-atmosphere models used in equilibrium 2 x $CO_2$ experiments (Houghton et al. 1990). The change in global average surface temperature varies from 1.9 to 5.2°C, which reflects the different climate sensitivities of the models. The corresponding change in global average precipitation varies from 3 to 15 percent. Cess et al. (1989) defined climate sensitivity as the ratio of the change in surface temperature to the change in the net radiative forcing change at the top of the atmosphere (TOA).

The definition of radiative forcing requires some interpretation. Strictly speaking, it is defined as the change in net downward radiative flux at the tropopause so that, for an instantaneous doubling of $CO_2$, an ~4 W/m$^2$ constitutes the radiative heating of the surface-troposphere system (IPCC 1990). If the stratosphere is allowed to respond to this forcing,

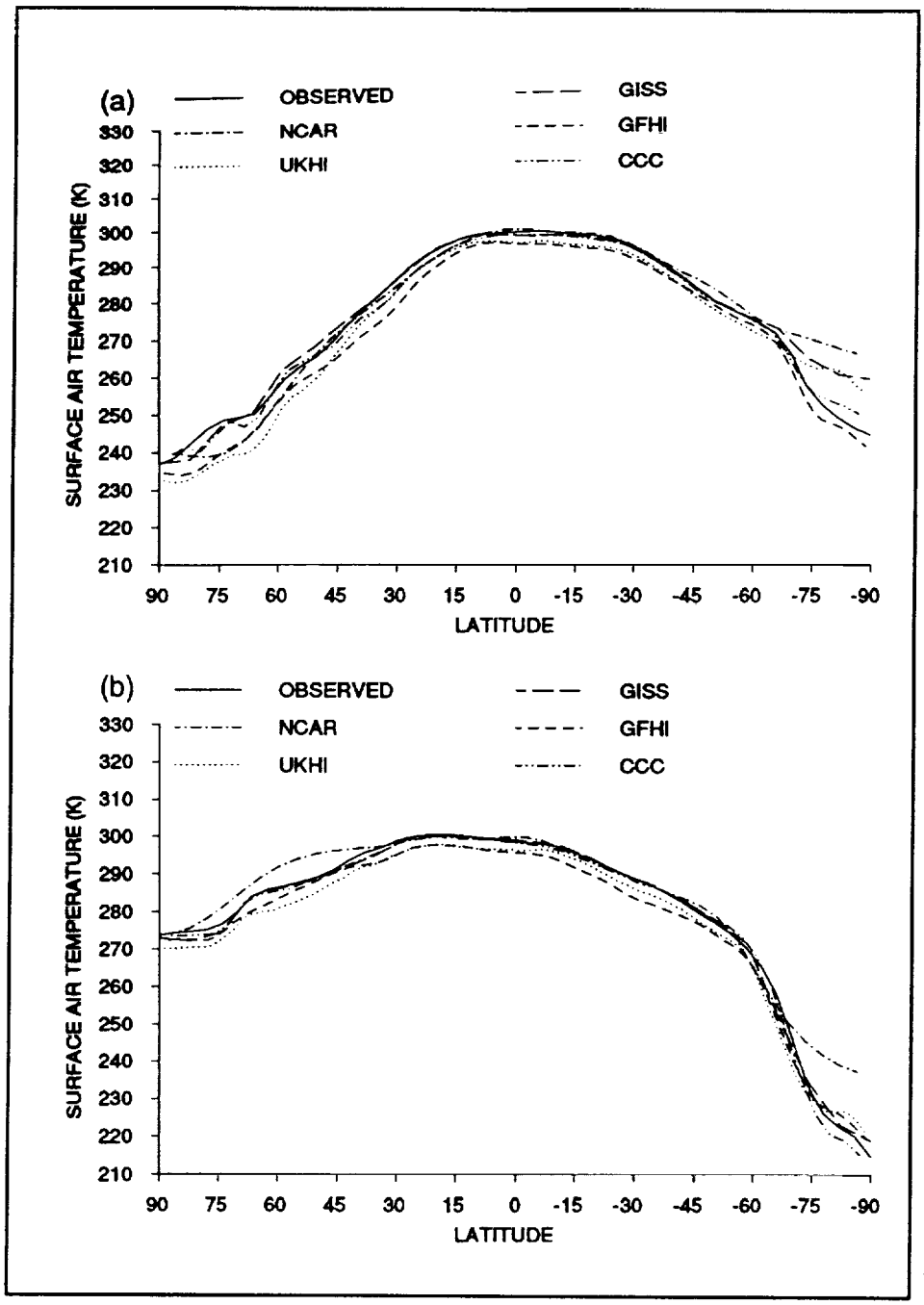


*Figure 63. Zonally averaged surface air temperatures (K) for various models and as observed (Schutz and Gates 1971 and 1972): (a) December-January-February, and (b) June-July-August. Source: IPCC 1990.*

while the climate parameters are fixed for the surface-troposphere system, then this 4 $W/m^2$ flux change also applies at TOA. A doubling of atmospheric $CO_2$ serves to illustrate the use of $\lambda$ to evaluate feedback mechanisms. Averaged over the year and over the globe there are 340 $W/m^2$ of incident solar radiation at the TOA. Of this, roughly 30 percent (~100 $W/m^2$) is reflected by the surface-atmosphere system. Thus, the climate system absorbs ~240 $W/m^2$ of solar radiation, so that under equilibrium conditions it must emit 240 $W/m^2$ of infrared radiation. The $CO_2$ radiative forcing constitutes a reduction in the emitted infrared radiation, since this 4 $W/m^2$ forcing represents a heating of the climate system. The $CO_2$ doubling results in the climate system absorbing 4 $W/m^2$ more energy than it emits, and global warming occurs so as to increase the emitted radiation in order to reestablish the Earth's radiation balance. In the absence of climate feedback mechanisms $\Delta F/\Delta Ts = 3.3\ W/m^{-2}k^{-1}$ while $\Delta S/\Delta Ts = 0$ so that $\lambda = 0.3K\ m^2W^{-1}$ (Cess et al. 1989). In turn, it follows that $\Delta Ts = \lambda \times SQ = 1.2°C$. If it were not for the numerous interactive feedback mechanisms, $\Delta Ts = 1.2°C$ would be quite a robust global mean quantity.

Cess et al. (1989 and 1990) also investigated the response of a large fraction of the world's atmospheric GCMs to prescribed changes in sea surface temperature distribution. Two runs were made with each model—one with SSTs reduced by an arbitrary and geographically uniform 2K from the observed climatological July SSTs, and a second with SSTs arbitrarily increased by 2K from their climatological values. Other input data used in both of the runs conformed with observed July conditions.

Results were analyzed to determine the "global sensitivity" of the various models, defined as the ratio of the change of the globally averaged surface air temperature to that of the globally averaged net radiation at TOA. Global sensitivities

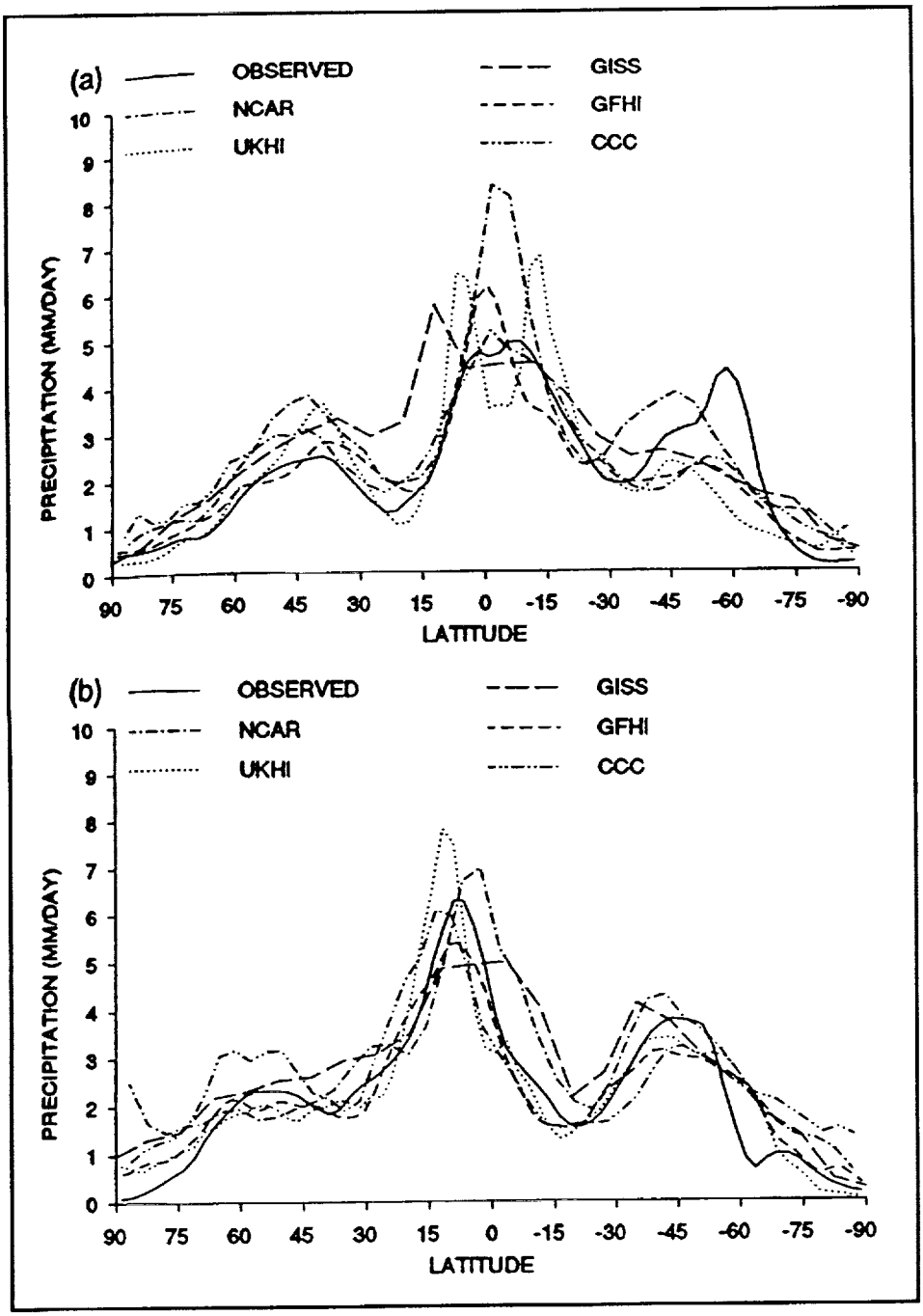


*Figure 64. Zonally averaged precipitation (mm day$^{-1}$) for various models and as observed (Jaeger 1976) for (a) December-January-February and (b) June-July-August. Source: IPCC 1990.*

ranged over a factor of 3. Further analysis showed that nearly all of this variation among models could be accounted for by differences in their simulated cloud feedback.

Table 5 compares a sensitivity parameter ($\lambda$) defined by 1 ($\Delta F \Delta Ts - \Delta Q/\Delta Ts$) for five classes of models. The overall $\lambda$ for the models shows a variation between 0.39 and 1.11. When $\lambda$ is computed for clear-sky regions only, the range is much less (between 0.42 to 0.49). Table 5 indicates that most of the differences between models are due to cloud processes.

***Conclusions/Recommendations.*** *Several global climate models appear to simulate present climatology reasonably, but they seem to have the wrong sensitivity to climate change. The parameterization of physical processes can be made to reproduce present climates with appropriate tuning, but they are not necessarily correct for climate change.*

*Paleoclimatic experiments are needed to validate climate models, especially climate sensitivity. For example, the analysis of paleo data shows that the low-latitude temperature change between the last ice age (18,000 years ago) and the present was not very much; a 1-km ice and pollen lines descent represents a change of about 5°C. Models do not reproduce such observed data. Solar insulation variations have produced 4°C cooling at high latitudes. During previous warmer climates (e.g., Mesozoic and Tertiary periods), there was very strong warming at high latitudes, with very little at the tropics. 2 x $CO_2$ cannot produce the temperature gradients needed to increase oceanic heat transport. No climate model can produce the strong heating at high latitudes with $CO_2$ heating alone.*

*Presently available high-quality global data sets (MSU and others from GOES, Nimbus, radar, lidar, etc.) and the output of high-resolution mesoscale models should be used to validate the accuracy of global models, including variability.*

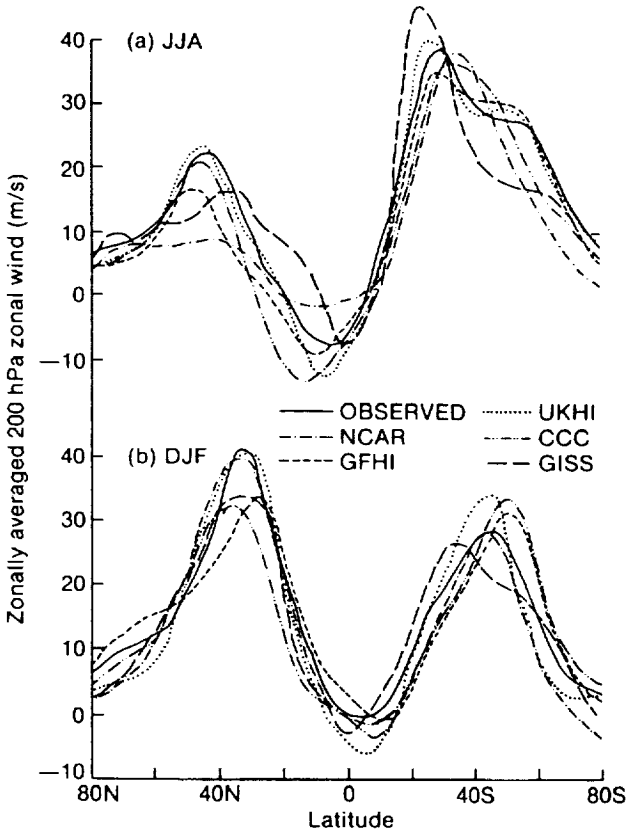


*Figure 65. Zonally averaged 200 hPa zonal wind ($ms^{-1}$) for various models and as observed (Trenberth, personal communication) for (a) June-July-August, (b) December-January-February. Source: IPCC 1990.*

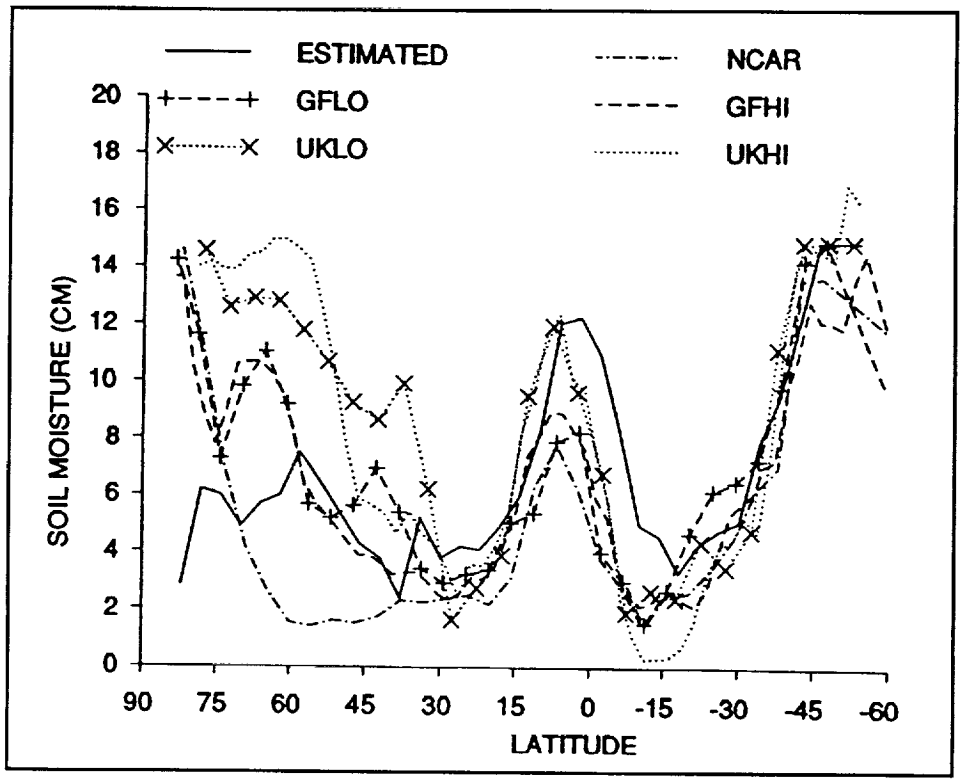


*Figure 66. Zonally averaged soil moisture (cm) for land points as estimated by Mintz and Serafini (1989) for July and as modeled for June-July-August. Source: IPCC 1990.*

*Table 4. Summary of Results from Global Mixed Layer Ocean-Atmosphere Models Used in Equilibrium 2 x $CO_2$ Experiments. Source: IPCC 1990.*

| ENTRY | Group | Investigators | Year | RESOLUTION No. of waves, or °lat. x °long. | RESOLUTION No. of Vertical Layers | Diurnal Cycle | Convection | Ocean Heat Transport | Cloud | Cloud Properties | ΔT (°C) | ΔP (%) | COMMENTS |
|---|---|---|---|---|---|---|---|---|---|---|---|---|---|
| **A.** | **Fixed, zonally averaged cloud; no ocean heat transport** | | | | | | | | | | | | |
| 1. | GFDL | Manabe & Stouffer | 1980 | R15 | 9 | N | MCA | N | FC | F | 2.0 | 3.5 | Based on 4 x $CO_2$ simulation |
| 2. | | Wetherald & Manabe | 1986, 8 | R15 | 9 | N | MCA | N | FC | F | 3.2 | n/a | |
| **B.** | **Variable cloud; no ocean heat transport** | | | | | | | | | | | | |
| 3. | OSU | Schlesinger & Zhao | 1989 | 4° x 5° | 2 | N | PC | N | RH | F | 2.8 | 8 | |
| 4. | | | 1989 | 4° x 5° | 2 | N | PC | N | RH | F | 4.4 | 11 | As (3), but with revised clouds. |
| 5. | MRI | Noda & Tokioka | 1989 | 4° x 5° | 5 | Y | PC | N | RH | F | 4.3 * | 7 * | * Equilibrium not reached . |
| 6. | NCAR | Washington & Meehl | 1984 | R15 | 9 | N | MCA | N | RH | F | 3.5 * | 7 * | * Excessive ice. Estimate ΔT = 4°C at equilibrium. |
| 7. | | | 1989 | R15 | 9 | N | MCA | N | RH | F | 4.0 | 8 | As (6), but with revised albedos for sea-ice, snow. |
| 8. | GFDL | Wetherald & Manabe | 1986, 8 | R15 | 9 | N | MCA | N | RH | F | 4.0 | 9 | As (2), but with variable cloud. |
| **C.** | **Variable cloud; prescribed oceanic heat transport** | | | | | | | | | | | | |
| 9. | AUS | Gordon & Hunt | 1989 | R21 | 4 | Y | MCA | Y | RH | F | 4.0 | 7 | |
| 10. | GISS | Hansen et al. | 1981 | 8° x 10° | 7 | Y | PC | Y | RH | F | 3.9 | n/a | |
| 11. | | Hansen et al. | 1984 | 8° x 10° | 9 | Y | PC | Y | RH | F | 4.2 | 11 | |
| 12. | | Hansen et al. | 1984 | 8° x 10° | 9 | Y | PC | Y | RH | F | 4.8 | 13 | As (11), but with more sea-ice control. |
| 13. | GFDL | Wetherald & Manabe | 1989 † | R15 | 9 | N | MCA | Y | RH | F | 4.0 | 8 | |
| 14. | MGO | Meleshko et al. | 1990 | T21 | 9 | N | PC | Y | RH | F | n/a | n/a | Simulation in progress. |
| 15. | UKMO | Wilson & Mitchell | 1987 | 5° x 7.5° | 11 | Y | PC | Y | RH | F | 5.2 | 15 | |
| 16. | | Mitchell & Warrilow | 1987 | 5° x 7.5° | 11 | Y | PC | Y | RH | F | 5.2 | 15 | As (15), but with four revised surface schemes. |
| 17. | | Mitchell et al. | 1989 | 5° x 7.5° | 11 | Y | PC | Y | CW | F | 2.7 | 6 | As (16), but with cloud water scheme. |
| 18. | | | 1989 | 5° x 7.5° | 11 | Y | PC | Y | CW | F | 3.2 | 8 | As (17), but with alternative ice formulation. |
| 19. | | | 1989 | 5° x 7.5° | 11 | Y | PC | Y | CW | V | 1.9 | 3 | As (17), but with variable cloud radiative properties. |
| **D.** | **High Resolution** | | | | | | | | | | | | |
| 20. | CCC | Boer et al. | 1989 | T32 | 10 | Y | MCA | Y | RH | V | 3.5 | 4 | * "Soft" convective adjustment. |
| 21. | GFDL | Wetherald & Manabe | 1989 † | R30 | 9 | N | MCA | * | RH | F | 4.0 | 8 | * SSTs prescribed, changes prescribed from (13). |
| 22. | UKMO | Mitchell et al. | 1989 | 2.5°x3.75° | 11 | Y | PC | Y | CW | F | 3.5 | 9 | As (18), but with gravity wave drag. |

All models are global, with realistic geography, a mixed-layer ocean, and a seasonal cycle of insolation. Except where stated, results are the equilibrium response to doubling $CO_2$.

R, T = Rhomboidal/Triangular truncation in spectral space;
N = Not included;
PC = Penetrative convection;
FC = Fixed cloud;
F = Fixed cloud radiative properties;
GFDL = Geophysical Fluid Dynamics Laboratory,Princeton, USA;
MGO = Main Geophysical Observatory, Leningrad, USSR;
AUS = CSIRO, Australia;
ΔT = Equilibrium surface temperature change on doubling $CO_2$;
Y = Included;
CA = Convective adjustment;
RH = Condensation or relative humidity based cloud;
† = Personal communication.
NCAR = National Center for Atmospheric Research, Boulder, CO, USA;
CCC = Canadian Climate Center;
ΔP = Percentage change in precipitation;
MCA = Moist convective adjustment;
CW = Cloud water;
V = Variable cloud radiative properties;
n/a = Not available
MRI = Meteorological Research Institute, Japan;
UKMO = Meteorological Office, United Kingdom;

*Table 5. Sensitivity Parameter Intercomparison Atmospheric Feedback Processes*

| Model | λ Clear Sky | λ Global |
|---|---|---|
| I | 0.42 | 0.39 |
| II | 0.46 | 0.50 |
| III | 0.48 | 0.52 |
| IV | 0.49 | 0.76 |
| V | 0.47 | 1.11 |

$$\lambda = 1 \div (\Delta F/\Delta T_s - \Delta Q/\Delta T_s)$$

Note: $\lambda \approx 0.3$ in the absence of water vapor and lapse rate feedbacks

*Long-term continuity in observing systems is important for global system monitoring and, more importantly, model validation. There are serious questions about whether the present global observing system can be maintained into the 1990s. International data may be at risk due to commercialization.*

*Model intercomparisons and comparisons with observations show that cloud sensitivity varies widely in models in response to 2 x $CO_2$. Also, most model studies use flux corrections to keep climatologically stable runs. Studies are needed to investigate what is going on in the models; model diagnostics as well as data diagnostics are needed. A strong emphasis on satellite data analysis should be continued.*

*Comparisons with the SiB model parameterization of land surface and vegetation processes, with observations in the Amazon, show substantial differences in the surface energy budget and fluxes. This points to the need for better tuning process models, and improving parameterizations with actual observations. It is insufficient to tune parameterizations in terms of their impact on the overall performance of a global model. Process-by-process verification is required to improve the physical basis of parameterizations.*

*International Satellite Cloud Climatology Project (ISCCP), Earth Radiation Budget Experiment (ERBE), and Earth Observing System (EOS) data are good for model evaluation, but not necessarily for model formulation. More ground truth experiments such as the First ISCCP Regional Experiment (FIRE) and First ISLSCP Field Experiment (FIFE) are required to understand processes better.*

*Models show substantial differences in cloud sensitivity and cloud forcing in response to 2 x $CO_2$ (e.g., the UK model).*

*Plug-compatible software designs are required to effectively carry out model intercomparisons and the sensitivity of global models to different parameterization schemes. It is important to know how the same global model performs with different physics packages to isolate specific processes.*

*Experiments such as those studying Amazon deforestation are model-dependent. Surface classification and change is a weak link in atmosphere-land surface models.*

*Atmosphere-ocean interaction heat fluxes are essentially unobservable and not known to better than about 40 to 50 $W/m^2$. It is better to concentrate on SST and surface winds.*

# 6. *The Use of Global System Models (and Predictions) in Impact Assessments and Policy Guidance*

Making policy decisions is an extremely complicated process, integrating both qualitative and quantitative information from a variety of sources and concerning a broad range of natural, social, technological, and economic phenomena. Modeling such a process is impossible if taken in its totality, and predicting the future (especially in the long term) absolute state of the system is equally impossible. However, a large number of tools are currently available from which policy guidance information can be derived. These tools include models of the physical components of the total physical, biological, social-economic global system and various empirical and analytical methods to monitor and quantify social and economic processes.

Throughout the history of civilization, climate and climate change have often been among the predominant factors determining the success or failure of species (be it plant or animal) and human social and economic structures. Currently, a major point of concern is the potential for rather rapid global climate change on account of human activity (e.g., GHG emissions, land use changes, deforestation, emissions of tropospheric aerosols and toxic chemicals). Until more complete global Earth system models are developed, it is convenient to begin with the climate system and use models of this system to provide guidance to policymakers. Of course, a variety of assumptions would need to be made: 1) Several processes are not or cannot yet be modeled; 2) several changes are perhaps inherently unpredictable (e.g., political turbulence); and 3) there could be significant uncertainties and inaccuracies regarding the specification of boundary conditions to both the physical system and to social and economic processes. Thus, even assuming a perfect physical system model, the best that can be done pragmatically is to obtain a set of future scenarios and policy options. This set of predictors would need to be updated periodically to "steer" the system along some chosen equilibrium path. The desired equilibrium path for country A may not, and usually is not, the same as that which may be chosen by country B. The details of international interactions are beyond the scope of this report.

The interaction between global models, effect/impact assessments, and policy options has been simplified in Figure 67 (Unninayar 1992). The process depicted is not

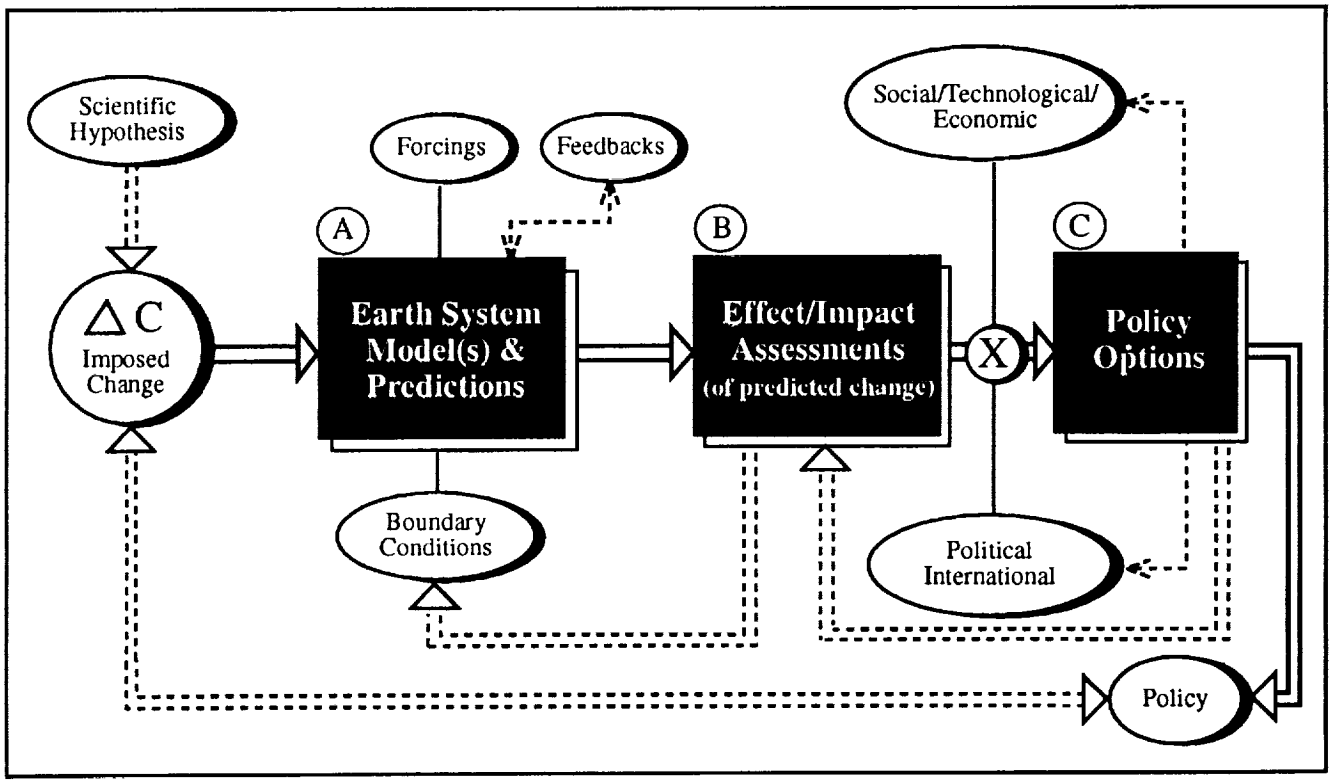


*Figure 67. The interaction between global models, impact assessments, and policy options. Source: Unninayar 1992.*

linear, in that there are feedback loops (represented by dashed lines) that render the system interactive and, conceivably, interactive in possibly unknown ways. Currently, it is customary to ignore some of the feedbacks involved, in order to simplify the problem. From all sections in this report, it should be clear that even simplified systems are enormously complex. For example, while climate system models are getting increasingly sophisticated with parameterized interactions between the atmosphere and the land surface and biosphere, the biosphere is not a dynamically changing entity. That is, if the climate change prediction resulting from enhanced GHGs suggests that region X would dry out and receive zero rainfall, the existing vegetation (biosphere) does not change automatically in the model. The land surface, vegetation cover and type, and so on—even in the best available (and most complicated) models—are specified as boundary conditions. At best, present parameterizations approximate the interaction and exchanges of moisture, heat, and momentum with the atmosphere. Similarly, soil would be fixed, thus no erosion or sediment transport would take place. These "dynamic" interactions are required to obtain more complete Earth system models, and that certainly is the ultimate objective of the Global Change Research Program. But for the present, these long time-scale processes could be handled through clever engineering approximations that breakdown processes, as follows:

1) Use the best available global system model(s) to provide a prediction or a set of future global change scenarios, time-integrated within specified constraints on forcings and boundary conditions. The model would essentially determine the response of the system to a chosen and imposed change ($\Delta C$). These predictions would generally be of large-scale features at horizontal resolutions of 200 to 300 km, even though 50-km resolutions are conceivable in the near future.
2) Make a series of "effect" assessments quantitatively (e.g., sea level and any other parameter not explicitly computed within the model). Assumptions would have to be made on, for example, the subgrid-scale distribution of temperature and precipitation and other system state variables, including fluxes of radiation, heat, moisture, and momentum. In principle, very high-resolution nested grid models could be run at a selection of representative subregions around the globe, using boundary conditions obtained from the global system model.
3) Derive a series of "impact" assessments (quantitatively) on, for example, vegetation productivity, crop-by-crop productivity, coastal zone loss, soil erosion, nutrient loss, and loss of habitat. Empirical or empirical-dynamical subcomponent models will need to be used for these calculations.
4) Translate the impacts obtained in approximation #3 into social and economic terms, using input information from existing technological and economic systems. International considerations such as the impact on import and export of food and energy should also be computed.
5) Deduce a first-guess policy action plan tentatively based on the cost and existing technological practice. This should then be refined to obtain a set of policy options that would make $\Delta C = 0$ or acceptably small (i.e., $\Delta C < E$) through several iterations that juggle possible changes to technology, social practice, land use, energy consumption efficiency, and the cost of doing so simultaneously or gradually over an assumed time period in which costs may also be "discounted."
6) Check to ascertain whether there are policy options that affect "impact" parameters or the boundary conditions specified in the model used (see Figure 67). If so, the climate model would need to run again to ascertain if the policy decision leads to a stable equilibrium and desirable result.
7) Reintegrate the global model after the determination of effect and impact parameters that alter initial conditions, boundary conditions, forcing functions, or feedbacks applicable to the global system model. Go through steps #1 through #7 repeatedly until a convergent solution is obtained.

In theory, the feedback loop connecting "A" and "B" functional modules in Figure 67 needs to be exercised until equilibrium is attained. This could be very time-consuming and costly in terms of computer resources, since each global prediction experiment (particularly with an interactive ocean) may require a model integration of 100 or more years for the system to attain a stable state. Although this may not be practical, at the very least sensitivity studies would need to be carried out to ascertain the validity of a strictly linear single pass through the schematic in Figure 67.

As global system models advance, various components of "B" would get incorporated into "A"—that is, into the primary global model. This is likely, particularly with increasing GCM spatial resolution. However, the drastic increase in resolution that is required to do this would require a major reexamination of most, if not all, subgrid-scale parameterization schemes and equations. It cannot be assumed arbitrarily that the same parameterizations are physically relevant or, indeed, valid at all at substantially increased horizontal and vertical resolutions.



C-2

It should be noted that whenever there are changes due to natural (e.g., forcings) or anthropogenic causes, the changes' effect on the model climate system must be reevaluated. In other words, changes in forcings, feedbacks, and prescribed boundary conditions could all be similar to the effect of the imposition of a particular $\Delta C$ initial condition prescription.

This section does not, by design, deal with the actual policy option scenarios that are currently being considered for the adaptation, mitigation, or prevention of climate change that could occur as a result of increasing emissions of GHGs (e.g., the options considered at the Intergovernmental Panel on Climate Change in 1990, and the United Nations Earth Summit in Rio de Janeiro in 1992). The IPCC exercise represents, perhaps for the first time, the exercise of the schematic in Figure 67—a simple, linear, forward sequence, with no feedbacks considered. Thus, it should be clear that the entire operation must be repeated; however, the next time it would be easier. The objective of course should be for each country (and the world) to systematically and operationally implement the "A, B, C" process so that policy is made with due consideration of all relevant and science guidance.

A country or government may opt to disregard the guidance received from the system for one reason or another, but such a decision should be made with the full cognizance of potential impact, be it good or bad. The day-to-day running of political systems is not necessarily affected by the process suggested here on account of the short time scales involved and their erratic nature (even the 4- to 6-year election cycle is relatively short). But in the long term, strategic global system management should be based on something substantive.

***Conclusions/Recommendations.*** *Until complete global Earth system models are available with interactive subsystems and components, some caution should be exercised in the interpretation and application of long-term predictions obtained from global models. Even "complete" global system model predictions would contain inherent uncertainties and errors caused by the approximations used in handling nonlinearities, the parameterization of physical processes, and the specification of initial and boundary conditions. Nevertheless, global models are valuable research and experimental tools to quantify the response of the system to natural or anthropogenically induced change. Quantifying the uncertainties in predictions can be done through a combination of model intercomparisons and model experiments; however, an absolute evaluation would require long-term global observations in order to validate the results of the models.*

*Until perfect global models and perfect global observations are available, global models can be used effectively to provide medium-term policy guidance, if a systematic sequential process is followed based on a full understanding of the limitations of the global model being used. Such a process has been suggested in this section. That is, the predictions obtained from global system models could be used to obtain assessments of impact on subcomponents that are not explicitly and interactively included in the model as a first step. Typically, the prediction would consist of the response of the model to prescribed "forced" changes, such as those anticipated from GHG concentrations, deforestation, solar radiation, and so on. The next step would be to evaluate the cost of such impact and the policy actions necessary to stop, adapt to, or stretch over time the projected change, if it is deemed significant.*

*To use global models as a guidance tool for predictions of the natural system and for policy-planning purposes, it would be crucial to run, in parallel, global observing systems to regularly update information on the state of the global system. This is particularly true of parameters specified as initial or boundary conditions in the model, as well as physical constituents such as atmospheric trace gas and aerosol type, concentration, and global three-dimensional distribution.*

# 7. Data Analysis and Assimilation Requirements

Comprehensive model-based data assimilation systems are developed to prepare consistent four-dimensional descriptions of the global system in terms of gridded or spectral fields of all the variables and parameters required for diagnostic analysis, research, process studies, the initialization of models, and the validation of global prediction experiments. These data sets need to be generated for the atmosphere, the oceans and land surface/biosphere, the cryosphere, and the geosphere. A more advanced use for such data sets involves the visual depiction of four-dimensional global system processes, using animation techniques developed on supercomputers (e.g., at the Illinois Supercomputer Center). Some are of the opinion that, until all modeled global processes are visually depicted (using animation techniques) and compared with observations of the actual physical global system, research into improved parameterization schemes would progress slowly. That is, until such visualization methods are available, it would be very difficult to grasp the details of what the models are doing correctly or incorrectly.

At present, model-based data sets of atmospheric circulation are a byproduct of the daily requirements of producing initial conditions for numerical weather prediction (NWP) models. These data sets have been widely used for studying fundamental dynamic and physical processes, and for describing the general nature of the circulation of the atmosphere. However, due to limitations in early data assimilation systems and inconsistencies caused by numerous model changes, the available model-based global data sets may not be suitable for studying global climate change (Bengtsson and Shukla 1988). Evolutionary changes are essential to improve model performance, but they also cause problems with continuity of data time series. Time continuity issues are not crucial for operational atmospheric or oceanic short-term models, but they pose special problems for climate research. The same applies for satellite data retrieval algorithms that transform the satellite sensor-measured spectral radiance into the required geophysical parameters. Data assimilation models also incorporate satellite measurements into the data initialization/model forecast cycle.

A good example of how a comprehensive model can be used to obtain continuous global fields when the actual observations are sparse is depicted in Figures 68 and 69 (Bengtsson and Shukla 1988), which illustrate a region in tropical Africa. The model used a first-guess field from the forecast cycle before ingesting new observations. The first-guess field is shown in Figure 69. Without such a first guess, there would have been no means by which the central and western parts of Africa could have been analyzed. Of course, climatology could have been used for a first-guess field, but on any one specific day it is unlikely that climatology would have provided as good an analysis.

As models for data assimilation analysis and prediction improve, they could introduce spurious interannual variability that may be difficult to distinguish from natural variability (Sardeshunnkh and Haikine 1978). This may be a continuing problem, but at the moment it is felt that present GCMs are sufficiently comprehensive to be used in assimilation mode for a substantive data reanalysis of the past 20 or 30 years, in order to produce a consistent,

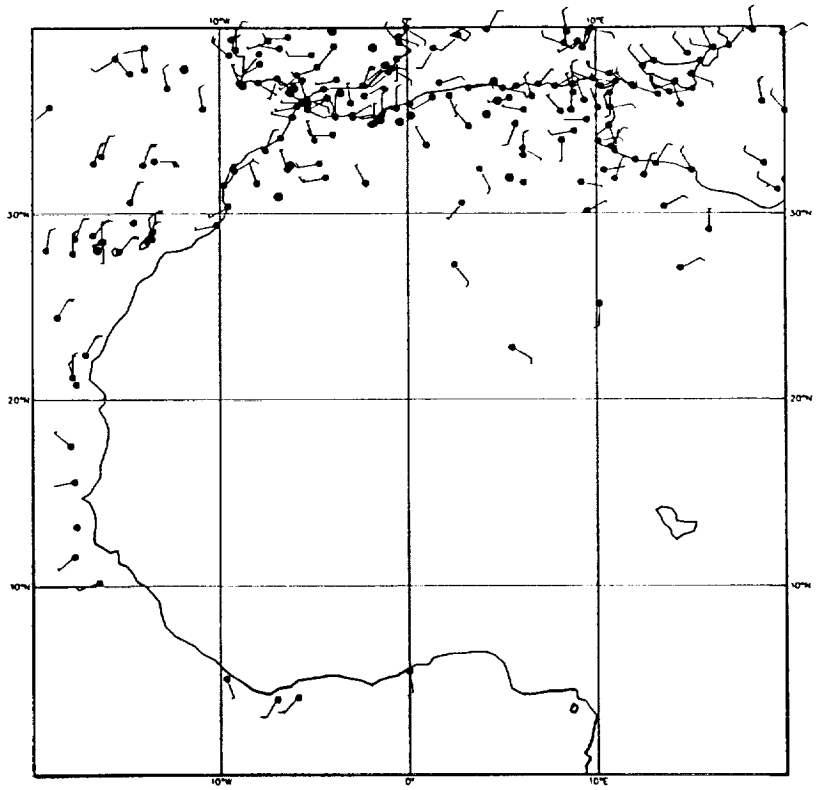

*Figure 68. Surface observations for 12 UTC, 29 August 1985. Source: Bulletin of the American Meteorological Society 1988.*

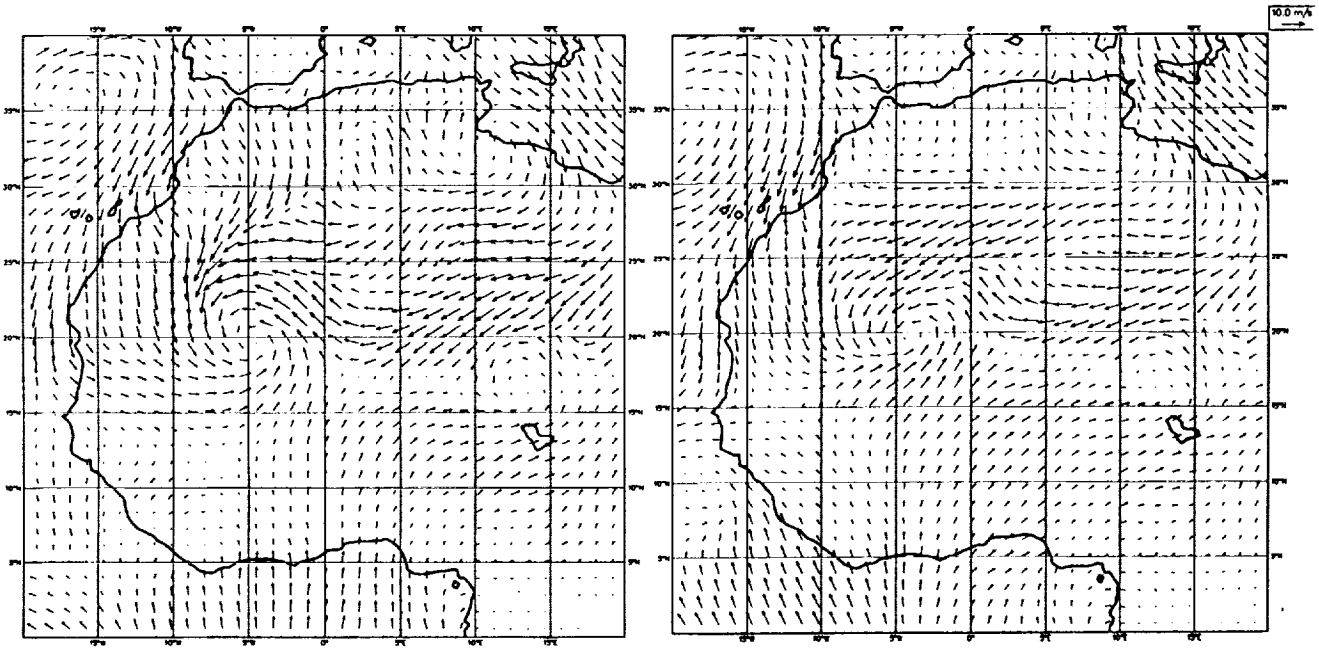

*Figure 69. (Left) ECMWF analysis for 12 UTC, 29 August 1985, and (Right) 24-hour forecast from initial condition of same date. Source: Bulletin of the American Meteorological Society 1988.*

temporally and spatially homogeneous data set for research. There may be a need to carry out such reanalysis projects every 10 to 15 years as models improve. The above concepts, which draw from atmospheric science, apply even more to oceanography. The oceanic observing network of ships, buoys, and so forth are sparse, and the problem is compounded by the relatively small space scales of the energetic ocean eddies. A high-resolution ocean data assimilation model is essential to produce the necessary multi-layer circulation, temperature, salinity, and flux fields for the ocean.

Section 3 highlighted the manner in which various components were modeled and processes parameterized. Section 4 covered the basic strategies involved in short-, medium-, and long-range climate system prediction. Most prediction models require, in parallel, data of various types to specify either initialization or boundary conditions—the latter because present models of the climate system are not complete, thus all quantities that are not explicitly computed need to be specified through observing systems. Section 8 highlights the large number of parameters that are or could be measured by existing and planned observing systems. Most, if not all, space-based platforms make very high-volume measurements and have relatively high resolution (i.e., ~1 km). This level of resolution or better is required for many subgrid-scale processes. In any event, this data stream must be assimilated by a comprehensive model before the data are of any use for research, diagnostics, and climate system modeling. The EOS Data and Information System (EOSDIS) plans to look after data management, data access, and distribution functions; however, a significant research effort will be required to develop the next generation of data assimilation and data analysis models. To make better use of computer time, there have been recent developments in multi-level atmospheric models using vector semi-Lagrangian finite difference schemes for data assimilation (Bates et al. 1991). An advantage of the semi-Lagrangian approach is that the integration time step can be relaxed from 10 or 15 minutes to 1 hour or more without significant degradation in analysis error.

A further reason for requiring data analysis and assimilation models is to obtain a large number of parameters and fields that must be computed from measured variables—that is, sensible and latent heat flux, momentum flux, moisture/water flux, and so on. These fluxes are required to integrate coupled Earth system models. Verification will need to be done through dedicated field experiments. The output of data assimilation systems should be archived and available for monitoring purposes. Until the next-generation satellite platforms are launched, models will

be the only source of data for such fields as surface wind stress.

In the near future, the observational data volume will become even more immense, and will require conversion through retrieval algorithm and dynamic interpolation/ extrapolation methods to produce fields suitable for the initialization of global system models. For surface features, there is considerable research being done (and more is required) on the spatial extrapolation of surface features such as soil and vegetation. This is a complex subject. For practical application purposes, global satellite observations need to be calibrated to measure or estimate the required quantities.

For the foreseeable future, observation of the nonlinear and complex global system will be irregularly distributed in space and time. In addition, observations are frequently too sparsely distributed to resolve adequately the spectrum of scales and processes involved (NRC 1991). Data assimilation schemes and models are required to absorb the global data obtained from satellite observations and to improve the analysis of state parameters required for research and climate model initialization.

***Conclusions/Recommendations.*** *Four-dimensional assimilation of data is a powerful technique to combine data from different instruments taken at different times in different places. In current meteorological applications, data assimilation represents the art of combining statistical objective analysis and general circulation models. At its best, data assimilation techniques create a value-added product with both sophisticated error control and the physical consistency provided by a GCM. Problems in data assimilation include the possible corruption of good data with bad; also, an assimilation scheme assumes that the model used (i.e., knowledge) is complete, though in reality it is not and could introduce artifacts in data sets. Yet, assimilation is essential for combining different types of data and generating data sets. At present, there are sometimes major differences between observed data and assimilated fields. Resolution problems are related to differences in the scales needed to represent physical systems as compared to existing model grid scales. For example, assimilation will usually sample the smallest scales badly.*

*Observing systems simulation experiments are presently being conducted for EOS. There is a need to assess the impact of satellite observations on model-assimilated data sets. The basic procedure involves using the results of a long-period integration of an independent model called the "nature" run. From this run, a set of simulated observations may be derived of the various parameters measured by present or future observing systems; these observations are assumed to represent truth. Next, the simulated observations with assumed errors are passed through a data assimilation model, the output of which is compared with truth. The assimilated data are fed into the model to produce a forecast that is then compared with the "nature" run time series to quantify the errors involved in the scheme. The advantage in using such a system is that truth is exactly known. The disadvantage is that truth is itself dependent on a formulating model. Thus, the "nature" run itself needs to be validated. The technique has been used to analyze the impact of data from the Laser Atmospheric Wind Sounder (LAWS) and several other existing or planned satellite-based observing systems.*

*For research and climate monitoring purposes, there is a need to reanalyze past data with the best assimilation system available so that the same internally consistent assimilation system applies over the time duration of the data set. In this manner, errors associated with changes in assimilation schemes are eliminated. This would also partly compensate for changes in the type and distribution of observing systems. In particular, as in past years when the number of upper air station and ship reports were sparse, it would be impossible to obtain reasonable global fields without a model-driven assimilation system.*

*Data assimilation has the potential of making major contributions to climate research, as follows:*

1) *To help detect climate change and quantitatively bound the uncertainties in estimates of parameters defining the current climate, specifically on regional scales. Included here is the need to reanalyze multi-year historical periods with assimilation systems that have been extended and optimized to produce verifiable time- and space-dependent error estimates for the primary fields of temperature, winds, and moisture. The use of assimilation background fields as a standard for the comparison of observations from various observing systems will also be of increasing importance.*
2) *To aid in unraveling the relative importance of the various physical processes that combine to produce the observed change. The diagnostics computed by models during the assimilation process will help explain the underlying causes of observed change. Conversely, systematic errors exhibited by the model when it is constrained by observations can be detected and the model corrected accordingly. True four-dimensional assimilation, as well as a solution of spin-up problems for model physical parameterizations, will be needed before the assimilation model can be fully utilized in this manner.*

3) *To provide global scale fields of temperature, wind, and moisture for use in diagnostic and chemical transport studies and to provide boundary conditions for the interpretation of results from regional-scale measurement campaigns and process studies.*

*Moisture, tropical divergence, troposphere-stratosphere exchange, and the optimal use of such nonconventional data sources as cloud and precipitation observations in assimilation techniques are among the areas needing increased attention. There is also a need to develop methods for coupled (e.g., atmosphere-ocean) data assimilation to support the initialization and integration of coupled models.*

# 8. *Future Monitoring and Data Requirements*

It should be apparent that a large number of observations are necessary to comprehensively monitor the climate system. Each set of observations would compose a three-dimensional snapshot of each component of the system. Repeated observations would provide information about the time evolution and change of the system. The space and time resolution required of the observing system would depend on the dominant spatial features that need to be described quantitatively, and on how fast these features change. In principle, however, it is not sufficient to monitor only the "dominant" scales of motion or action, because a large number of interactive processes occur on rather small space and time scales—even down to 1 sec and 1 m, or less. At present, it is impractical (if not impossible) to construct an observing system to continually monitor the entire global system at this resolution. Nor is there sufficient computer and data handling capacity available for data transmission and exchange, processing, and storage. Nor are there global models that can use data of such high resolution. It is customary to obtain very high-resolution data sets during special observing experiments of limited time duration in order to understand and model processes, while operating global observing systems at much lower time and space resolution. These global observations need to remain accurate over time to meet monitoring and modeling needs.

The accuracy, precision, and absolute calibration over time of the observations required for climate change and global change purposes are considerably more stringent than those for operational real-time or near-real-time applications. At present, with the exception of perhaps Microwave Sounding Unit (MSU) data, few observing systems are capable of maintaining accuracy and calibration over time, particularly in terms of derived geophysical variables. This is partly because most observing systems have been established for operational applications dominated by the annual seasonal solar cycle, where temperatures can vary between a monthly average of -60 to 40°C, vegetation cover (green leaf area) from 0 to 100 percent, rainfall from 0 to 500 mm (or more), and so forth. When interest is focused on these large differences, there is little incentive to deploy highly accurate (particularly over time) observing instruments. The introduction of errors in the measurement of absolute values of change on a global basis arise on account of several reasons, not all of which are electronic sensor related. For surface or near-surface measurement, the station network's resolution is usually insufficient.

Major problems exist in modeling oceanic areas (i.e., ~70 percent of the Earth's surface); thus, measuring precipitation globally and observing/quantifying the global hydrological cycle are almost impossible until the next generation of satellites is launched. Problems are encountered even over land surface areas, on account of changes (often undocumented) in instrument calibration, instrument relocation, and observing practices. Several satellite measurements suffer from uncertain vertical resolution and/or precision and uncertain or unknown calibration and accuracy between years, rendering the detection of interannual and decadal change difficult. Reprocessing of older data also may be required before long-term accuracy and time continuity can be ensured.

An additional difficulty arises in that all the required monitoring variables cannot be directly measured (e.g., the various heat, energy, momentum, radiation interaction, and other flux terms). Thus, they need to be derived using a combination of measurements and models that compute the required quantities. The final research data set is often as much observing system-dependent as model-dependent. Changes in data assimilation and analysis systems introduce as many subtle discontinuities as do changes in observing systems' sensors and satellite data retrieval algorithms.

Given that data are prone to various errors, the detection and modeling of global change should not rely on any one particular field, such as temperature. Multi-variable observations and analyses are necessary to provide credence to the diagnostic analysis of the climate system. Initializing a climate model needs the specification of several variables, and validating the performance of models requires the simultaneous observation of the entire range of parameters of the global system.

Defining or specifying observational requirements may be performed in one of several ways. It is perhaps convenient to begin with parameters that, by and large, define the surface environment and climate, then specify all other variables and parameters that describe components or processes of the global system that interact to result in surface climate as conventionally understood. The following attempts do just that:

1) **Surface Environment and Climate**—Temperature, precipitation, wind, pressure, humidity, solar radiation, infrared radiation, evaporation, evapotranspiration, soil and vegetation type/distribution, topography, sea level, pollutants, chemical constituents, albedo, snow cover and glaciers, roughness, and water storage and flow are all components. Ocean surface and near-surface measurements also are required to provide global coverage.

2) **Near Surface and Subsurface**—The surface is linked to the subsurface (land and ocean) and near-surface atmospheric boundary layers. Interaction involves the transfer of momentum, sensible and latent heat, and energy and mass (i.e., chemical and water substances). To obtain these parameters, which have to be computed from other variables, measurements are required of vertical gradients (hence profiles) of wind, temperature, moisture, and pressure in the atmosphere; temperature and moisture profiles in soil layers, at least up to the root zone, and soil type, porosity, and conductivity; temperature, salinity, and currents in the upper layers of the ocean; and sea level, sea state, and sea ice. It is also important to monitor biogeochemical processes that determine the exchange of chemicals between the atmosphere, land surface, and the ocean. Some of these chemicals are GHGs, and others affect radiation or cloud formation mechanisms.

3) **Free Atmosphere, Deep Ocean, and Land**—In order to model, simulate, and predict changes in surface climate, all forcings, feedbacks, and radiative and circulation features that affect or determine surface climate must also be observed. For example, the vertical profiles and lapse rates of temperature and moisture are needed in atmosphere measurements. Note that several convective parameterization schemes are based on lapse-rate changes. Precipitation depends on clouds; thus, clouds must be monitored, including their water droplet and ice particle concentrations (also needed for cloud-radiation interaction). The vertical temperature profiles also depend on the concentrations and distribution of radiatively active gases; thus, $H_2O$, $CO_2$, CFCs, $CH_4$, $N_2O$, and $O_3$ (and their precursor chemical compounds) need to be monitored, as well as cloud distributions and optical depth. Radiation reaching the Earth's surface is altered by tropospheric and stratospheric aerosols and dust, which need to be monitored, as well as their sources and sinks. External forcing such as the solar radiation reaching the Earth is a fundamental driving force that needs to be monitored at the top of the atmosphere, as well as the net infrared emission of the planetary system. The equator-to-pole gradient in net heating needs to be derived from radiation-budget measurements, since this gradient basically drives the atmospheric and oceanic circulation.

4) **Subgrid-Scale Processes and Parameterization**—A large number of processes occurs in the subgrid-scale domain. Even land surface hydrological processes that are modeled at a 1- to 10-km resolution and are subgrid scale to an atmospheric or climate model (200- to 500-km scale) have subgrid-scale processes of their own. Thus, the parameterization problem is universal, and compounded for lower grid resolutions. Special observing experiments are required for subgrid-scale process studies with such high-frequency, fast-response sensors as those needed for turbulent momentum and heat fluxes measurements, for example. Such experiments would provide the necessary data for determining or improving the physics behind parameterization schemes.

For many of the climate system basic state parameters, present operational observation systems need to be continued indefinitely into the future with enhancements as needed in terms of spatial resolution, global coverage, and data exchange. The current operational system providing global data for climate system studies consists of approximately 3,000 land surface stations; 700 upper-air stations; geostationary and polar orbiting satellites; ship and commercial aircraft track/flight level measurements; and ocean fixed and drifting buoys with surface and subsurface measurements of current (drifters) temperature and/or salinity. These data are exchanged regularly through the Global Telecommunications System (GTS) of the World Meteorological Organization (WMO). Other systems measure land surface characteristics (e.g., Landsat, SPOT), selected GHGs at land stations, and $O_3$ from satellites (e.g., TOMS, SAGE).

The basic international operational data exchange system was set up for atmospheric and, more recently, oceanic data exchange in support of short- to medium-term forecasting. During the past few years, normalized vegetation index fields (a proxy for the "greenness" of vegetation and crops) have been derived from satellite data and are available through data distribution centers, but their operational exchange and utilization is limited. Their application or use has also been limited on account of a lack of discrimination (i.e., between vegetation types) and the lack of supporting surface ground truth classification information. Landsat and SPOT data have been used for case studies, but their global utilization has been restricted by high cost and perhaps lack of processing capacity in many countries. This past experience points to the need for an improved international system for the exchange of data and information, and an agreed-upon policy for the unrestricted and mutually beneficial exchange of complementary data to support global

change research and applications. Unlike the data exchange required for day-to-day weather forecasting, the exchange needed for climate system and Earth system models (particularly as they become more and more used operationally but at longer time scales, namely seasonal to interannual to decadal) does not necessarily have to take place in real-time. That is, a delayed-mode exchange system would suffice, be it via satellite communications or mail. Yet, a regular operational exchange system is necessary to meet the needs of monitoring the Earth system, for the validation and verification of global model-generated predictions and projections, and for understanding the mechanisms behind change. Such an international exchange system should also deliver to the end user (both in research and applications) appropriately analyzed sets or subsets of the output from global models and global observing systems. To achieve the above, an internationally coordinated data and information exchange and delivery system must be established with cooperative agreements and protocols guiding its functional operation.

It should be noted that the distinctions between raw observations (i.e., direct instrument measurements), monitoring (a combination of selected raw observations and computed or derived results over time), and data (a combination of observations, monitoring information, model-assimilated information, and model prediction information, together with a host of supporting metadata, estimates, and guesstimates) are generally transparent to the broader multidisciplinary research community. This is because it is impossible for any one individual to be simultaneously a specialist in engineering, electronic instrumentation, remote sensing, computer programming, and all of the component disciplines involved in the global Earth system. Consequently, there is widespread use of multidisciplinary data of which rather few people have detailed knowledge in the intricacies and associated uncertainties of the actual measurements. It is therefore important for instrument system operators to calibrate and validate the observations being taken. Various suggestions referring to the need for analysis and studies to quantify errors are provided below.

***Conclusions/Recommendations.*** *There is a need to look at the errors involved in sampling frequency and the sampling by present and future observing systems (e.g., EOS) of atmospheric chemistry constituents. Such an analysis also should look at the errors involved in data assimilation.*

*Observations need to be better coupled to models—for example, satellite observations of ocean color to physical oceanographic models, observations of land surface vegetation and clouds to atmospheric models, and so on.*

*Paleoclimatic data are required for climate model verification and quantifying climate system sensitivity.*

*Well-calibrated data sets are needed for long-term studies and modeling. International data are at risk due to possible commercialization. There are concerns about whether present observing systems can be maintained into the 1990s.*

*There is a need for detailed observations of cloud and optical properties, as well as radiation climatology—that is, a detailed description of spectrally and spatially dependent radiation at the surface and at the top of the atmosphere.*

*ISCCP, ERBE, EOS, and so on are or will be good for model evaluation, but not necessarily for the formulation of models; as such, in situ experiments to investigate detailed processes are also needed.*

*There is a need for space-based observations to obtain surface radiation budget parameters, with lidar data to give the three-dimensional distribution of clouds; lidar should be flown on EOS. At the same time, ground truth experiments such as FIRE and FIFE should be continued.*

*Better observations are needed of water vapor (the dominant GHG) as well as of water vapor feedback (i.e., changes with temperature). Atmospheric heating fields can be obtained from ERBE over the oceans with an accuracy of about 20 $W/m^2$. Land areas are a problem, with estimated accuracies of only about 50 $W/m^2$. As such, it would be very useful to have lidar to sense water vapor and temperature profiles over land.*

*Biogeochemical source and sink terms need to be measured, as well as the fluctuations associated with changing climate. Better data are needed in the stratosphere (e.g., from UARS).*

*Model results need to compared with campaign-type observational data, in addition to data from UARS, EOS, TOMS, ATLAS, and so on.*

*The most important atmospheric inputs in land surface processes are solar radiation, net radiation, and precipitation. The biosphere moves water through stomata; the dominant process is evapotranspiration. Depending on the type of vegetation, evapotranspiration can vary by a factor of 100. Better surface classifications are required as are observations of change. The land surface needs to be divided into 10 or 20 basic types of ecosystems.*

*Ocean models require the specification of surface fluxes of momentum and heat. Oceanic heat flux at the surface is not*

*observable to better than 40 to 50 W/m$^2$. Thus, it is best to concentrate on wind and sea surface temperature observations.*

*Wind stress along the equatorial wave guide is very critical. Also, on account of the long-term memory of the ocean, good data sets are required to initialize ocean models.*

*The Comprehensive Ocean-Air Data Set (COADS) is spotty and contains poorly sampled data from monthly mean ship distributions. The HIRS2/MSU data set is global but not tested for accuracy. The simulations obtained by running the UCLA model forced with SST from the above two data sets were quite different, pointing to the importance of getting accurate observed fields. In addition to SST, good wind and altimeter data are required.*

*Tropical rainfall needs to be measured accurately in order to compute heat release in the atmosphere. The systematic temperature bias in GCMs could be due to poorly simulated convective heating patterns in the tropics. Major improvements are required in the observations of wind and rainfall in the tropics.*

*For most parameters, global coverage can be provided only by satellites. However, the remote sensing of surface parameters is subject to error. For example, the Mount Pinatubo volcanic eruption caused a satellite-derived SST anomaly of -1 to -2°C, requiring a correction in the satellite SST fields. Thus, it would be impossible to use satellites alone for climate research. Satellite bias corrections are determined using in situ information; data from voluntary observing ship reports contain the worst errors for SST, yet are essential. Other data required are from drifting buoys, expendable bathythermographs, and tropical atmosphere-ocean moorings in arrays.*

*There is a strong linkage between convection, low-level circulation, and evaporation fluxes; therefore, there is a need for observations of precipitation, moisture, and winds.*

*Just as SST is used for initializing ocean models, soil moisture is required for predictions over land; thus, there is a need to obtain observationally estimates of soil moisture.*

*Overturning in the North Atlantic basin is very important for 10- to 100-year time scale climate change. Deep sinking of surface waters is in precarious balance, and changes could affect ocean and global climate. A task force should be set up jointly between agencies to study ocean monitoring and high-latitude air-sea interaction.*

*Aerosol size distribution is important. Large aerosols may have a greenhouse heating effect, which may overpower the cooling effect of aerosols through the scattering of solar radiation. It is very hard to measure single scattering albedo remotely. Water vapor from radiosonde data is a problem due to calibration difficulties. SAGE provides water vapor in the stratosphere and the upper troposphere, and data are available for the past 4 to 5 years.*

*Observational systems are either planned or in place to provide useful information on SST, topography, sea ice, polar ice sheets, ocean surface properties, ocean color, primary ocean productivity, atmospheric temperature and moisture profiles, precipitation rates, and tropospheric winds. Radiation budget, clouds, and solar irradiance are also being observed. These observing systems must be maintained.*

# 9. Mission to Planet Earth

## 9.1. Introduction

As models of the global Earth system become sophisticated, they include more and more components and interactive processes in order to simulate and predict changes to the state of the system, particularly with an increase of the prediction time range (see Section 4). The existing global data sets prepared on the basis of operationally exchanged surface- and even space-based measurements do not adequately satisfy the requirements of the next-generation Earth system models, nor the requirements for comprehensively (and globally) monitoring the total Earth system and diagnosing the causative forces behind change.

Mission to Planet Earth (MTPE) is a NASA-initiated concept that uses space- and ground-based measurement systems to provide the scientific basis for understanding global change. NASA's contribution to MTPE includes ongoing and near-term satellite missions, new missions under development, planned future missions, management and analysis of satellite and *in situ* data, and a continuing basic research program focused on process studies and modeling. The space-based components of Mission to Planet Earth will provide a constellation of satellites to monitor the Earth from space. Sustained observations are planned to allow researchers to monitor Earth system variables over time to determine trends; however, space-based monitoring alone is not sufficient. A comprehensive data and information system, a community of scientists performing research with the data acquired, and extensive ground campaigns are all important components.

Tables 6 and 7 summarize the ongoing and near-term satellite programs contributing to Mission to Planet Earth. Satellites stationed in a variety of orbits form the space component of MTPE. No single orbit permits the gathering of complete information of Earth processes; for example, the medium-inclination orbit of UARS was chosen specifically because of its focus on the processes influencing ozone depletion. High-inclination, polar-orbiting satellites are needed to observe phenomena that require relatively detailed observations on a routine basis, often from a constant solar illumination angle. Geostationary satellites are needed to provide continuous monitoring of high temporal resolution processes. An international array of these platforms now provides coverage on a near-global basis. The scope and extent of this coverage will be improved substantially in the next century by geostationary satellite systems planned by NASA and its international partners.

The centerpiece of Mission to Planet Earth—the Earth Observing System (EOS)—involves a series of polar-orbiting and low-inclination satellites for long-term global observations of the land surface, biosphere, solid Earth, atmosphere, and oceans (see Table 8). EOS science objectives address the fundamental physical, chemical, and biological phenomena that govern and integrate the Earth

*Table 6. MTPE Phase I: NASA Contributions*

| NASA Satellites (Launch Status) | Mission Objectives |
|---|---|
| **ERBS** (Operating)<br>Earth Radiation Budget Satellite | Radiation budget, aerosols, and ozone |
| **TOMS/Meteor-3** (Operating)<br>Total Ozone Mapping Spectrometer | Ozone mapping and monitoring (joint with Russia) |
| **UARS** (Operating)<br>Upper Atmosphere Research Satellite | Stratospheric and mesospheric chemistry |
| **TOPEX/Poseidon** (Operating)<br>Ocean Topography Experiment | Ocean circulation (joint with France) |
| **LAGEOS-2** (Operating)<br>Laser Geodynamics Satellite | Crustal motion and Earth rotation (joint with Italy) |
| **NASA Spacelab Series** (1992 on)<br>Shuttle-based experiments | Atmospheric and solar dynamics (ATLAS), atmospheric aerosols (LITE), and surface radar backscatter, polarization, and phase function [SIR-C and X-SAR (joint with Germany)] |
| **SeaWIFS** (March 1994)<br>Sea-Viewing Wide Field Sensor | Ocean primary production (data purchase) |
| **TOMS/Earth Probe** (July 1994)<br>Total Ozone Mapping Spectrometer | Ozone mapping and monitoring |
| **NSCAT/ADEOS** (February 1996)<br>NASA Scatterometer | Ocean surface wind speed and direction (joint with Japan) |
| **TOMS/ADEOS** (February 1996)<br>Total Ozone Mapping Spectrometer | Ozone mapping and monitoring (joint with Japan) |
| **TRMM** (August 1997)<br>Tropical Rainfall Measuring Mission | Precipitation, clouds, and radiation in low latitudes (joint with Japan) |
| **Landsat-7** (January 1998)<br>Land Remote-Sensing Satellite | Land surface features at high spatial resolution (joint with DoD) |

*Table 7. MTPE Phase I: Non-NASA Contributions*

| Non-NASA Satellites (Launch Status) | Mission Objectives |
|---|---|
| **NOAA-9 through -J** (U.S.—Operational) | Visible and infrared radiance/reflectance, infrared atmospheric sounding, and ozone measurements |
| **Landsat-4/5/6** (U.S.—Operational) Land Remote-Sensing Satellite | High spatial resolution visible and infrared radiance/reflectance |
| **DMSP** (U.S.—Operational) Defense Meteorological Satellite Program | Visible, infrared, and passive microwave atmospheric and surface measurements |
| **ERS-1** (ESA—Pre-Operational) European Remote-Sensing Satellite | C-band SAR, microwave altimeter, scatterometer, and sea surface temperature |
| **JERS-1** (Japan—Pre-Operational) Japan's Earth Resources Satellite | L-band SAR backscatter and high spatial resolution visible and infrared radiance/reflectance |
| **ERS-2** (ESA—1994) European Remote-Sensing Satellite | Same as ERS-1, plus ozone mapping and monitoring |
| **Radarsat** (Canada—1995) Radar Satellite | C-band SAR measurements of Earth's surface (joint U.S./Canadian mission) |
| **NOAA-K through -N** (U.S.—1994 on) | Visible, infrared, and microwave radiance/reflectance; infrared atmospheric sounding; and ozone measurements |
| **ADEOS** (Japan—February 1996) Advanced Earth Observing Satellite | Visible and near-infrared radiance/reflectance, scatterometry, and tropospheric and stratospheric chemistry (joint with U.S. and France) |

system. EOS observations will permit the assessment of various Earth system processes, including:

- Hydrological processes, which govern the interactions of land and ocean surfaces with the atmosphere through the transport of heat, mass, and momentum
- Biogeochemical processes, which contribute to the formation, dissipation, and transport of trace gases and aerosols, and their global distribution
- Climatological processes, which control the formation and dissipation of clouds and their interactions with solar radiation
- Ecological processes, which are affected by and/or will affect global change and their response to such through adaptation
- Geophysical processes, which have shaped or continue to modify the surface of the Earth through tectonics, volcanism, and the melting of glaciers and sea ice.

EOS mission objectives include support of the overall U.S. Global Change Research Program (USGCRP) by acquiring and assembling a global database. Priorities for acquiring these data will conform to the seven issues identified by USGCRP and the Intergovernmental Panel on Climate Change (IPCC) as key to understanding global climate change, namely:

- The role of clouds, radiation, water vapor, and precipitation
- The productivity of the oceans, their circulation, and air-sea exchange
- The sources and sinks of greenhouse gases and their atmospheric transformations
- Changes in land use, land cover, primary productivity, and the water cycle
- The role of polar ice sheets and sea level
- The coupling of ozone chemistry with climate and the biosphere
- The role of volcanoes in climate change.

## 9.2. *The Rescoped EOS Program*

The original EOS Program covered a broad range of global change issues. The baseline EOS Program included a total of 30 selected instruments, which were chosen to address the seven IPCC priority areas identified above. By focusing on climate change, the required instruments were reduced to 23 that need to fly before 2002. The remaining instruments were to be deployed as follows: Three intermediate spacecraft series to be launched on intermediate expendable launch vehicles (ELVs), one smaller spacecraft series to be launched on medium ELVs, and two small spacecraft series to be launched on small ELVs. The spacecraft series, initial launch date, launch vehicle class, and disciplinary focus follow:

- EOS-AM (June 1998, IELV)—Characterization of the terrestrial and oceanic surfaces; clouds, radiation and aerosols; and radiative balance
- EOS-COLOR (1998, SELV)—Ocean color and productivity
- EOS-AERO (2000, SELV)—Atmospheric aerosols and ozone
- EOS-PM (2000, IELV)—Clouds, precipitation, and radiative balance; terrestrial snow and sea ice; sea surface temperature; terrestrial and oceanic productivity; and atmospheric temperature
- EOS-ALT (2002, MELV)—Ocean circulation, ice sheet mass balance, and land-surface topography
- EOS-CHEM (2002, IELV)—Atmospheric chemical species and their transformations, ocean surface stress.

*Table 8. EOS-Era Remote-Sensing Satellites*

| Satellites (Launch Status) | Mission Objectives |
|---|---|
| **EOS-AM Series** (1998)<br>Earth Observing System<br>Morning Crossing (Descending) | Clouds, aerosols and radiation balance, characterization of the terrestrial ecosystem; land use, soils, terrestrial energy/moisture, tropospheric chemical composition; contribution of volcanoes to climate, and ocean primary productivity (includes Canadian and Japanese instruments) |
| **EOS-COLOR** (1998)<br>EOS Ocean Color Mission | Ocean primary productivity |
| **POEM-ENVISAT Series** (ESA—1998)<br>Polar-Orbit Earth Observation Mission<br>Environmental Satellite | Environmental studies in atmospheric chemistry and marine biology and continuation of ERS mission objectives |
| **ADEOS IIa and IIb** (Japan—1999)<br>Advanced Earth Observing Satellite IIa and IIb | Visible and near-infrared microwave radiance/reflectance, scatterometry, infrared and laser atmospheric sounding, tropospheric and stratospheric chemistry, and altimetry (may include French and U.S. instruments) |
| **EOS-PM Series** (2000)<br>Earth Observing System<br>Afternoon Crossing (Ascending) | Cloud formation, precipitation, and radiative properties; air-sea fluxes of energy and moisture; and sea-ice extent (includes European instruments) |
| **EOS-AERO Series** (2000)<br>EOS Aerosol Mission | Distribution of aerosols and greenhouse gases in the lower stratosphere (spacecraft to be provided through international cooperation) |
| **POEM-METOP Series** (ESA—2000)<br>Polar-Orbit Earth Observation Mission<br>Meteorological Operational Satellite | Operational meteorology and climate monitoring, with the future objective of operational climatology (joint with EUMETSAT and NOAA) |
| **TRMM-2** (Japan and NASA—Proposed for 2000)<br>Tropical Rainfall Measuring Mission | Precipitation and related variables and Earth radiation budget in tropics and higher latitudes |
| **EOS-ALT Series** (2002)<br>EOS Altimetry Mission | Ocean circulation and ice sheet mass balance (may include French instruments) |
| **EOS-CHEM Series** (2002)<br>EOS Chemistry Mission | Atmospheric chemical composition; chemistry-climate interactions; air-sea exchange of chemicals and energy (to include an as yet to be determined Japanese instrument) |

The following subsections briefly address the instrument complements slated for each platform, with more indepth coverage provided in the "1993 EOS Reference Handbook" (Asrar and Dokken 1993).

## 9.2.1. EOS-AM

- Advanced Spaceborne Emission and Reflection Radiometer (ASTER)—Imaging radiometer with 14 multispectral bands from visible through infrared, providing high spatial resolution (15- to 30-m) images of the land surface, water, ice, and clouds; same orbit stereo capability; to be accommodated on EOS-AM1.
- Clouds and Earth's Radiant Energy System (CERES)—Two broad band scanning radiometers (one cross-track mode, one rotating plane), with three channels in each radiometer [total radiance (0.3 to >50 μm), shortwave (0.3 to 5 μm), longwave (8 to 12 μm); measures the Earth's radiation budget and atmospheric radiation from the top of the atmosphere to the surface; to be accommodated on EOS-AM and -PM series.
- Earth Observing Scanning Polarimeter (EOSP)—Cross-track scanning polarimeter that globally maps radiance and linear polarization of reflected and scattered sunlight for 12 spectral bands from 0.41 to 2.25 μm; provides global aerosol distribution, cloud properties (such as optical thickness and phase) at 40- to 100-km resolution depending on the product; to be accommodated on EOS-AM2 and -AM3.
- Multi-Angle Imaging SpectroRadiometer (MISR)—Provides top-of-the atmosphere cloud and surface angular reflectance functions, and global maps of planetary/surface albedo and aerosols and vegetation properties; employs nine separate charge coupled device-based pushbroom cameras to observe the Earth at nine discrete view angles; images at each angle will be obtained in four spectral bands centered at 0.443, 0.555, 0.67, and 0.865 μm; each of the 36 instrument data channels is commandable to provide ground sampling of 240 m, 480 m, 960 m, or 1.92 km; to be accommodated on EOS-AM series.
- Moderate-Resolution Imaging Spectroradiometer (MODIS)—Medium-resolution, cross-track multispectral scanning radiometer measuring biological and physical processes such as cloud cover and associated properties, ocean sea surface temperature and chlorophyll, land cover changes, land surface temperature, and vegetation properties; optical arrangements will provide imagery in 36 discrete bands between 0.4 and 15 μm, at a spatial resolution of 250 m, 500 m, or 1 km at nadir; to be accommodated on EOS-AM and -PM series.
- Measurements of Pollution in the Troposphere (MOPITT)—Four channel correlation spectrometer

with cross-track scanning; measures upwelling radiances at 2.3, 2.4, and 4.7 μm; uses pressure modulation and length modulation cells to obtain CO concentrations in 3-km layers and $CH_4$ column; spatial resolution 22 km; to be accommodated on EOS-AM1 and possibly on -AM2.

- Tropospheric Emission Spectrometer (TES)—High spectral resolution infrared imaging Fourier transform spectrometer generating three-dimensional profiles on a global scale of virtually all infrared active species from the Earth's surface to the lower stratosphere; spectral coverage of 2.3 to 15.4 μm at a spectral resolution of 0.025 $cm^{-1}$, thus offering line-width limited discrimination of essentially all radiatively active molecular species in the Earth's lower atmosphere; limb mode height resolution of 2.3 km with coverage from 0 to 32 km; down-looking mode resolution of 50 x 5 km (global) and 5 x 0.5 km (local), with a swath of 50 x 180 km (global) and 5 x 18 km (local); to be accommodated on EOS-AM2 and -AM3.

### 9.2.2. EOS-COLOR

This second-generation sensor—based on the Coastal Zone Color Scanner (CZCS) on Nimbus-7 and the Sea-Viewing Wide Field Sensor (SeaWiFS) on the SeaStar satellite (planned for launch in 1994)—will be launched in 1998. The instrument is an advanced visible and near-infrared ocean color imager with eight spectral bands in the range 402 to 885 nm, to monitor and provide daily global coverage of primary production by marine phytoplankton. EOS-COLOR will have spatial resolutions of 1.1 km (local) and 4.5 km (global), with a swath width of 2,800 km.

### 9.2.3. EOS-AERO

At present, only one instrument is slated for the EOS-AERO series—the Stratospheric Aerosol and Gas Experiment III (SAGE III). This Earth limb-scanning grating spectrometer will be a natural and improved extension of the successful Stratospheric Aerosol Measurement II (SAM II), SAGE I, and SAGE II experiments. SAGE III will obtain global profiles of aerosols, $O_3$, $H_2O$, $NO_2$, $NO_3$, OClO, clouds, temperature, and pressure in the mesosphere, stratosphere, and troposphere, with a resolution of 1 to 2 km in the vertical. SAGE III takes advantage of both solar and lunar occultation to measure aerosol and gaseous constituents of the atmosphere. Most of its science objectives rely on the solar occultation technique, which involves measuring the extinction of solar energy by aerosol and gaseous constituents in the spectral region from 0.29 to 1.55 μm, during spacecraft sunrise and sunset. The moon will be used as another source of light for occultation.

### 9.2.4. EOS-PM

- Atmospheric Infrared Sounder, Advanced Microwave Sounding Unit, and Microwave Humidity Sounder (AIRS, AMSU, and MHS)—AIRS is a high-resolution sounder designed to cover the spectral range 0.4 to 15.4 μm, measuring simultaneously in over 2,300 spectral channels. The high spectral resolution enables the removal of unwanted spectral emissions and, in particular, provides spectrally clean "super windows" that are ideal for surface observations. AIRS will have a resolution of 1 km in the vertical and 13.5 km in the horizontal at nadir. AMSU is a passive microwave radiometer designed primarily to obtain profiles of stratospheric temperature and to provide cloud-filtering capability for tropospheric observations. AMSU will have a resolution of 40 km in the horizontal at nadir. MHS is a passive microwave radiometer for humidity profiling via five channels: One at 89 GHz, one at 166 GHz, and three at 183.3 GHz. The instrument is also designed to detect precipitation under clouds. MHS will have a resolution of 13.5 km at nadir. AIRS, AMSU, and MHS measurements will be analyzed jointly to filter out the effects of clouds from the infrared data in order to derive clear-column air temperature profiles and surface temperatures with high vertical resolution and accuracy. Together they constitute a single facility instrument program. Standard products will include atmospheric temperature and humidity profiles, total precipitable water, fractional cloud cover, cloud-top height and temperature, land skin surface temperature plus day-night surface temperature difference, outgoing day/night longwave surface flux, ocean skin surface temperature, and day/night longwave surface flux. Research products will include precipitation estimates, tropopause and stratopause heights, outgoing spectral radiation and cloud optical thickness, cloud thermodynamic phase (ice/water) and cloud water content, land surface spectral emmissivity, surface albedo and net shortwave flux, ocean surface net shortwave flux, sea ice cover (old/new), and ocean surface scalar wind speed.
- Clouds and Earth's Radiant Energy System (CERES)—See Section 9.2.1.
- Multifrequency Imaging Microwave Radiometer (MIMR)—MIMR is a high-resolution microwave spectrometer (frequencies between 6.8 and 90 GHz) that will measure precipitation rate, cloud water, water vapor, sea surface roughness, sea

surface temperature, ice, snow, and soil moisture. It will have a spatial resolution of 4.86 km (at 90 GHz) to 60.3 km (at 6.8 GHz). The instrument will operate at six frequencies each with horizontal and vertical polarization (6.8, 10.65, 18.7, 23.8, 36.5, and 90 GHz), and employs nine feedhorns to yield 20 available channels.

- Moderate-Resolution Imaging Spectroradiometer (MODIS)—See Section 9.2.1.

### 9.2.5. EOS-ALT

EOS-ALT is a collaborative effort between NASA and the French Centre National d'Etudes Spatiales (CNES), with the details of the partnership currently being negotiated. The payload consists of Doppler Orbitography and Radiopositioning Integrated by Satellite (DORIS), Geoscience Laser Altimeter System (GLAS), Solid-State Altimeter (SSALT), and TOPEX Microwave Radiometer (TMR). In addition to precise orbit tracking (DORIS, TMR) and altimeter calibration and orbit determination (SSALT), the EOS-ALT series will provide measurements of sea-ice and glacier surface topography, and cloud heights (GLAS), as described below:

- DORIS is a precision orbit determining system using a dual doppler receiver tracking system operated by CNES. The DORIS receiver listens at two frequencies for signals from a world-wide (50 at present) network of orbit-determining beacons. The instrument determines the satellite velocity by measuring the doppler shifts of two ultra-stable microwave frequencies (401.25 and 2036.25 MHz) transmitted by the beacons. The instrument provides orbital positioning information and ionospheric correction for SSALT.
- GLAS is a laser altimeter designed to measure ice-sheet topography and associated temporal changes, as well as cloud and atmospheric properties. In addition, operation of GLAS over land and water will provide along-track topography. For ice-sheet applications, the laser altimeter will measure height from the spacecraft to the ice sheet, with an intrinsic precision of better than 10 cm with a 70-m surface spot size. The height measurement, coupled with knowledge of the radial orbit position, will determine topography. Characteristics of the return pulse will be used to determine surface roughness. Along-track cloud and aerosol height distributions will be determined with a vertical resolution of 75 to 200 m and a horizontal resolution from 150 m for dense cloud to 50 km for aerosol structure and planetary boundary layer height. The GLAS laser is a frequency-doubled, cavity-pumped, solid-state Nd:YAG laser with energy levels of 120 mJ (1.064 μm) and 60 mJ (0.532 μm). The infrared pulse will be used for surface altimetry, and the green pulse for atmosphere measurements.
- SSALT is a single-frequency radar altimeter developed by Alcatel Espace Systems under contract from CNES. SSALT uses the same type of antenna as the NASA Altimeter (ALT) aboard the U.S./French Ocean Topography Experiment (TOPEX)/Poseidon, but operates at a single frequency of 13.6 GHz. The ionospheric-electron correction is provided by a model that makes use of the simultaneous dual-frequency measurements of the DORIS tracking system. SSALT will provide measurements of ocean height and wind speed, and information on ocean surface current velocity. It also will map the topography of the sea surface and polar ice sheets.
- TMR will measure the radiometric brightness temperature related to water vapor and liquid water in the same field-of-view as the altimeter. In turn these brightness temperatures are converted to path-delay information required by SSALT for precise topographic measurements. The TMR instrument utilizes modified hardware from the Nimbus-7 Scanning Multichannel Microwave Radiometer (SMMR); however, the data chassis (i.e., the digital programmer, analog multiplexer, and satellite interface circuitry) is new. Developed by the Jet Propulsion Laboratory (JPL), TMR operates at frequencies of 18, 21, and 37 GHz.

### 9.2.6. EOS-CHEM

Ultimately, the EOS-CHEM series will have a payload that consists of six instruments; however, only five have been selected as of this writing (see below). An as yet to be determined Japanese instrument will be accommodated on the EOS-CHEM platforms as reciprocation for flight of the NASA Scatterometer II (NSCAT II) on the Advanced Earth Observing System II (ADEOS) scheduled for launch in 1999.

- Active Cavity Radiometer Irradiance Monitor (ACRIM)—Consists of three total irradiance detectors (one to monitor solar irradiance, two to calibrate optical degradation of the first). The instrument will monitor the variability of total solar irradiance, and will sustain and extend the high-precision database compiled by NASA since 1980. ACRIM data products will consist of the average solar irradiance at one Astronomical Unit (in $W/m^2$) for each ACRIM shutter-open cycle. Results will be corrected for variations in satellite-sun

distance and the relativistic effects of the platform's orbital velocity toward and away from the sun. Measurements of the total (bolometric) solar irradiance above the atmosphere will have an absolute accuracy of 0.1 percent and a long-term precision of 0.0005 percent per year.

- High-Resolution Dynamics Limb Sounder (HIRDLS)—Observes global distribution of temperature and concentrations of $O_3$, $H_2O$, $CH_4$, $N_2O$, $NO_2$, $HNO_3$, $CFC_{11}$, $CFC_{12}$, $ClONO_2$, and aerosols in the upper troposphere, stratosphere, and mesosphere. HIRDLS will perform limb scans in the vertical at multiple azimuth angles, measuring infrared emissions in 21 channels ranging from 6.12 to 17.76 μm. Four channels measure the emission by $CO_2$. Taking advantage of the known mixing ratio of $CO_2$, the transmittance can be calculated, and the equation of radiative transfer is inverted to determine the vertical distribution of the Plank black body function from which the temperature is derived as a function of pressure. Once the temperature profile has been established, it is used to determine the Plank function profile for the trace gas channels. The measured radiance and the Plank function profiles are then used to determine the transmittance of each trace species and its mixing ratio distribution.
- Microwave Limb Sounder (MLS)—Passive radiationally cooled microwave limb-sounding radiometer/spectrometer to measure thermal emission from the atmospheric limb. The EOS version of this instrument will continue the successful international effort started on UARS. MLS will measures lower stratospheric temperature and concentrations of $H_2O$, $O_3$, ClO, HCl, OH, $HNO_3$, NO, $N_2O$, HF, and CO for their affects on (and diagnosis of) transformations of greenhouse gases, radiative forcing of climate change, ozone depletion, and so on. MLS will have bands centered at 215, 440, and 640 GHz, and 2.5 THz, with a spectral resolution of 1 MHz; its spatial resolution will be 3 x 300 km diameter horizontal and 1.2 km vertical.
- Stratospheric Aerosol and Gas Experiment III (SAGE III)—See Section 9.2.3.
- Solar Stellar Irradiance Comparison Experiment II (SOLSTICE II)—Four-channel ultraviolet spectrometer (two-axis solar track) composed of an ultrahigh-resolution spectrometer, low-resolution spectrometers, and an extreme ultraviolet photometer; provides daily measurements of full-disk solar ultraviolet irradiance with calibration maintained by comparison to bright, early-type stars. SOLSTICE II will have a spectral range of 115 to 440 nm; three channels have a spectral resolution of 0.2 nm, and the fourth a resolution of 0.0015 nm.

## 9.3. *Summary*

The above instrument descriptions refer only to NASA's EOS Program in order to provide the reader with a feel for the next-generation satellite platforms being designed, built, or planned. From Tables 6, 7, and 8, it should be clear that there are a large number of instruments already operating and/or planned for the pre-EOS era. Several of these missions are being or will be undertaken jointly with or by other countries and agencies. Besides NASA's contribution, the satellite missions that fall under the International Earth Observing System (IEOS) rubric include the POEM-ENVISAT series (ESA), ADEOS IIa and IIb (Japan), the POEM-METOP series (ESA), TRMM (Japan and NASA), and the POES series (NOAA). For brevity, the instruments onboard these platforms are not described here; details are contained in the "1993 EOS Reference Handbook" (Asrar and Dokken 1993).

In tandem, these space observatories will provide a large number of the parameters and variables involved in the monitoring, understanding, modeling, and prediction of Earth system processes, which either define the state of the system at any moment in time or are factors involved in bringing about changes to the system. As stated earlier, space-based measurements alone are not sufficient to completely address observational and monitoring requirements. Ground truth is required to calibrate most remotely sensed measurements, and many sub-surface (land and ocean) parameters will need direct surveys and the development of models that can use space-based observations to compute sub-surface characteristics. Ecological and biological systems require indepth observations of how the dynamics of such systems work, and how they respond to, interact with, and possibly drive or modulate the physical environment; on a large scale, changes in the biosphere could alter the state of the global Earth climate system through complex physical, chemical and radiative interaction. For a comprehensive grasp of the biosphere and its internal and external dynamics, substantially more research and observational experiments (over sufficiently long periods of time) are required. Fragmentary but nevertheless clues to these types of interactive processes have been and are being pieced together from paleo- and proxy-data and information. To date, such investigations have only scratched at the surface despite the best efforts of the scientific community. The dynamics of human socio-economic systems is yet another dimension that is fundamentally unknown despite detailed historical accounts (and retrospective analysis) of the past performance of these systems. Very recent global changes are marked pointers to the depth of the cumulative ignorance surrounding (and possibly driving) the dynamics of the human dimensions of global change. Such issues are beyond the scope of this report, but must be addressed by the Global Change Research Program if it is to fulfill its mandate.

# 10. Concluding Remarks

## Global Change

A fundamental objective of the U.S. Global Change Research Program (USGCRP) and parallel international programs (i.e., IGBP and WCRP) is to improve the predictive understanding of the Earth system to support national and international policymaking activities that cover a broad spectrum of global and regional environmental issues (CEES 1991). To fulfill this goal, the USGCRP addresses three parallel, but interconnected, streams of activity (see Figure 70):

- Document global change through the establishment of an integrated, comprehensive, long-term program of observing and monitoring Earth system changes on a global scale
- Enhance the understanding of key processes through a program of focused studies to improve the knowledge of physical, geological, chemical, biological, and social processes that influence and govern the behavior of the Earth system
- Predict global and regional environmental change through the development and application of integrated conceptual and numerical predictive Earth system models.

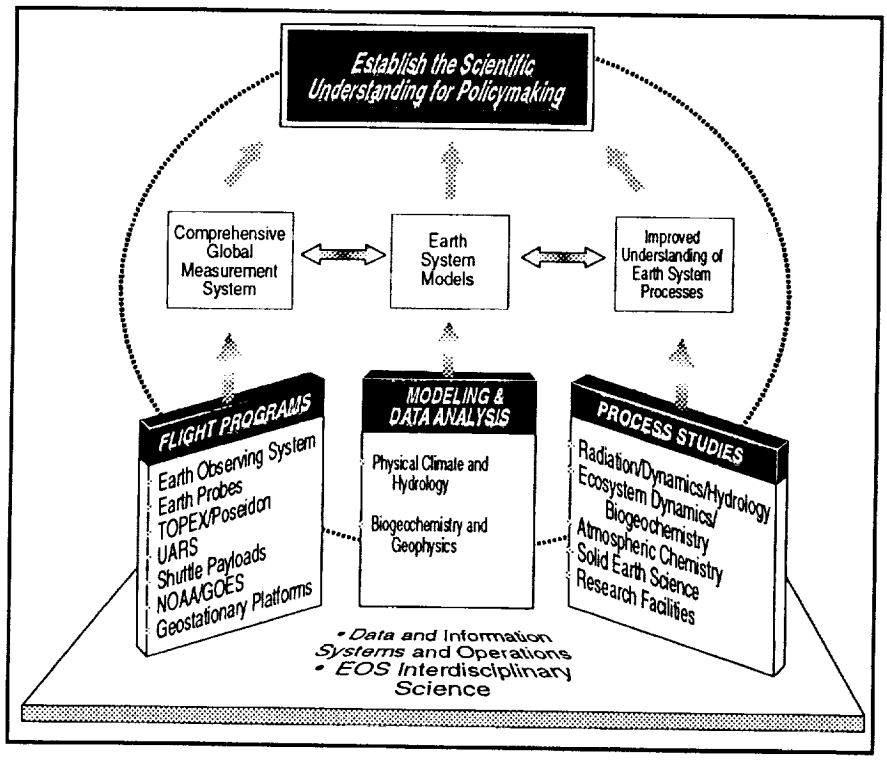


*Figure 70. U.S. Global Change Research Program—Science to Policy*

## Modeling and Data

Central to the above strategy is a close interaction between observations and modeling. Modeling begins with observations of natural systems or processes [i.e., the measurement of all variables likely to affect the system(s) or process(es)]. Next, the processes' behavior is described according to basic laws of physics, chemistry, and mathematics. The fundamental laws are actually known independent of climate observations; many have been derived from painstaking laboratory experiments and developments in mathematics and physics over centuries. However, the application of these fundamental laws to the global system requires approximations (averaging to time steps and grid sizes characteristic of models) and simplifications (parameterizations). Because of the complex nature of natural processes, a large number of variables are needed to describe these processes, requiring the use of very large supercomputers to manipulate the mathematical equations. The resulting physical-numerical model first needs to be verified against observational evidence for accuracy. This is usually done process by process. Each subsystem and/or process model is then integrated with other models of other processes to form a system of processes that interact with each other in a manner simulating the global environment. The validation of these large models requires observational evidence and, more often than not, leads to modifications and improvement in the model itself, as well as its subcomponents. Inevitably, this is an interactive sequence wherein data influences the modeling effort, and, in turn, the models put new demands on data.

## Space- and Ground-Based Research

Both ground- and space-based research are required. *In situ* and theoretical studies of physical, chemical, biological, and geological processes must be complemented by comprehensive space-based observations to provide global coverage of key environmental parameters. Long-term monitoring is essential to describe the dynamic and changing nature of the global system. As the integration time scales increase to address global climate system change issues, models need to comprehensively and explicitly incorporate interactions between the relatively fast components of the system (i.e., the atmosphere) with the slow (i.e.,

ocean, biospheres, land surface). Detailed subgrid-scale process studies require special experiments, usually unlimited in space and time, which deploy high-resolution, research-oriented instrumentation systems. Such observations elucidate such processes as air-sea interaction, atmosphere-biosphere interaction, convective and precipitation processes, and cloud-radiation feedback, and enable improvements in their parameterization in global models. Other processes require global observations—for instance, planetary radiation budget, cloud-climate feedback, climate-water vapor-radiation feedback, and climate-vegetation feedback—for obtaining basic statistics on state variables, which are needed to verify and validate model climate simulations.

To preclude the possibility that climate system models accidentally simulate the present climate, observations or descriptions are required of past climate system states—hence the need for historical instrumental observations and prehistoric proxy data (e.g., paleoclimatic data from tree rings, ice cores, ocean sediment, fossils, etc.). Predicting the response of the climate system to an imposed change (a forcing on the system) such as that due to a doubling of equivalent $CO_2$ requires the monitoring of all other forcings (e.g., solar, aerosol) that may add to or subtract from the results of $CO_2$ forcing alone. Being a complex, nonlinear, physical system, a change in one or more forcings would cause a series of feedbacks that could enhance or diminish the initial direct change (e.g., cloud and water vapor feedback, ocean feedback). Thus, feedbacks also must be observed and modeled before a climate system model could be applied to forecasting future system states. Present and planned observing systems should be operated for indefinitely long time periods to provide monitoring and model validation information.

## *Data Assimilation*

Obtaining usable information from complex observing systems requires the development and application of model-based data assimilation systems that blend information from a variety of sources to produce uniform global fields for real-time monitoring, diagnostic studies, and initializing and validating predictive models of the global system. Such model-assimilated data sets will incorporate model dynamics and physics to get the best possible and most consistent fit of variable fields to the observed data. They will represent value added to the set of original observations, and are expected to form the database for most modeling development and applications. Recent developments in semi-Lagrangian, semi-implicit numerical methods for models show considerable promise (and computational efficiency) for application in four-dimensional data assimilation.

There is also a need to reprocess historical data to obtain global fields of system state variables that are internally consistent over time with the analysis technique used. Moreover, the latest generation of data assimilation systems is better able to fill the inevitable data voids in the past, when the observational coverage was poorer than at present.

## *Parameterization and Scaling*

A major component of research required is in the improved parameterization of subgrid-scale processes—that is, processes that take place in a space-time scale domain smaller than that which the models can handle. For a global atmospheric model, the smallest grid box is approximately 250 x 250 km; the better ocean models use grids of about 50 x 50 km. A large number of dynamic, thermodynamic, chemical, and biochemical interactions take place at substantially smaller space scales (i.e., down to the molecular scale). All these processes need to be parameterized and expressed in terms of measurable grid-scale model variables. This is in addition to the proper representation of large-scale interactions and processes. Due to a lack of data, and other mathematical problems, this leads to a large number of best guess assumptions and/or empirical coefficients. The total number of tunable parameters in a complex, interactive, global climate system model is large, estimated at between 100 and 300, if all interactive component systems are included. The expression "tunable" refers to the fact that the values of a variety of coefficients and parameters are specified and may be adjusted by using observational, empirical, or model performance evidence. However, they cannot and should not be arbitrarily tuned; the parameters must be chosen very carefully to obtain the right interaction and behavior of the system being modeled. As model resolution is increased, some parameterizations can be replaced with explicit formulations, and others can be made more physically realistic and less dependent on tunable parameters.

For the proper linkage of atmospheric and land surface hydrology, as an example, a different form of parameterization (of the interaction of space scales) is required. Ground hydrological model computations usually refer to the 1- to 10-km space scale. Thus computational results of surface evaporation, water runoff, soil moisture, percolation, and so on need to be aggregated up to the 250-km grid scale used by climate models. In the near future, 50-km grids for global models are highly possible, and this would help make the atmospheric and hydrological models more compatible. It is presently not completely clear how the inverse problem is to be handled—that is, how the results of a climate prediction are to be used to derive subgrid-scale effects such as precipitation, evaporation, runoff, and so forth. Being

considered is the use of variable grid and nested grid models in conjunction with climate models.

## *Computers*

The increasing complexity of models and, indeed, observational information places significant demands on the computer resources required. Time and space scale resolutions are restricted by available supercomputer computational speeds and cost. The availability of greatly increased computer resources, with speeds and capacities up to 1000 times those of present-generation systems, will be essential for further significant progress in global climate/Earth system modeling. Attempts are currently being made to utilize massive parallel processing to enhance speeds, but this effort requires very careful and complex software code adjustments. The government-wide High Performance Computing and Communications (HPCC) Program is directed toward maximizing efficient use of state-of-the-art computational architectures. Even with substantially increased three-dimensional space and time resolutions, the issue of parameterizing subgrid-scale processes will remain a problem that will need to be revisited at each quantum improvement in resolution.

## *Total Earth System Modeling/Observing*

The ultimate goal of modeling is to develop comprehensive dynamically, thermally, and chemically interactive modes of the physical-biological Earth system. This is, of course, a rather daunting task. A complete model would include component models of the biosphere (i.e., plant, animal, and human) on account of their being dominant mechanisms for chemical transport and exchange. Even fossil fuel burning and the consequent release into the atmosphere of $CO_2$, and nitrous and sulfur oxides may be considered a highly accelerated (via anthropogenic agents) natural process. This is because fossil fuels trapped in the Earth which took ten or hundreds of millions of years to form would eventually be recycled through natural geological processes such as tectonic plate movement, volcanism, earthquakes, and fires. The 10 to 100 million-year time scale is, however, well beyond the attention span and, perhaps, even the life span of the human species.

A total Earth system model would have only two external forces to deal with, namely solar and gravitational, although anthropogenic influences such as atmospheric and oceanic pollutants and changes in the land surface could be treated as variable "scenarios" that would have the effect of externally prescribed forcings for all practical purposes. External electromagnetic forces may also play a role in influencing the molten core, but this is thought to be small except under unusual circumstances. With the prescription of these forces, the system's climate would in theory be totally deterministic (i.e., predictable) if every single component subsystem were modeled exactly and perfectly, including internal interactions and feedback processes. In practice, observational limitations along with remaining model approximations embedded in parameterizations and the model numerics would limit the accuracy of model predictions.

As described in Section 3.3, the total Earth system needs to be first sectioned into the components (illustrated in Figure 67) where social, economic, technological, and policy components are removed from the basic system to be modeled. At present, even interactions with these components are basically nonexistent; they are handled in a somewhat *ad hoc* manner to provide interim answers to immediate policy questions. Second, various biospheric and biological (e.g., ecosystems) models are also externalized, even though interactions in terms of the exchange of heat, moisture, momentum, and, to some extent, gaseous chemicals are retained. This is one of the areas that requires substantial improvements in terms of observations, long-term monitoring, and the modeling of interaction and feedback processes. Long-term observations are required to understand the dynamics of change of, for example, a biological system to fluctuations in climate, habitat, and environment. Until observed for sufficiently long periods of time, they cannot be fully modeled. Models developed on the basis of short observations are likely to be deficient or speculative. In order to improve the modeling of interactive processes, a series of specific and highly focused field experiments would need to be conducted. Indeed there are many such special observational experiments carried out in just about all disciplines of science. However, interdisciplinary research on large-scale interactions are of relatively recent origin, partly due to a lack of appropriate technology (in the past) and partly on account of the cost and logistics involved in conducting such experiments. Examples of such experiments include TOGA-COARE (to investigate large-scale atmosphere-ocean interaction) and FIRE (to study atmosphere-biosphere processes).

To link specialized *in situ* observation with global monitoring, all such experiments need to relate locally observed parameters with measurements from global space-based observing systems. Though the next generation of observing systems are experimental and meant for research purposes, they may be considered operational owing to the need for the long-term (10 to 15 years and more) monitoring required for global change research.

The increasing reliance on space-based systems to obtain global coverage places special demands on electronic sensor development deployment and data processing. Remote sensing precludes the direct measurement of many of the

required physical, geophysical, or biophysical parameters. An example would be soil moisture, which could be inferred from the moisture stress on plants that is made manifest in the wilting of leaves (and browning if prolonged), which can be sensed by satellites observing reflected (visible) or emitted (infrared, microwave) radiation, in particular wavelengths of the electromagnetic spectrum. There are, of course, exceptions to this rule. For example, active radar altimeters onboard a space platform sense the reflected beam signal transmission and reception, and obtain the distance from the reflecting surface to the satellite exactly. In theory, this would enable the direct measurement of sea level if the precise shape of the geoid and the orbit of the satellite are known.

Similarly, scatterometers observing the state of the ocean surface (capillary waves) are used to obtain a measure of wind stress forcing on the ocean. Improving the spectral resolution of space-based sensors in both the shortwave and longwave ranges of the electromagnetic spectrum would be required to measure, simultaneously, the atmospheric distribution of chemical species as well as aerosols and particulates.

Mission to Planet Earth will use a combination of space- and ground-based measurement systems to provide the scientific basis for understanding and predicting global change. The centerpiece of MTPE—the Earth Observing System—will utilize a series of polar-orbiting and low-inclination satellites for long-term global observations of the land surface, biosphere, solid Earth, atmosphere, and oceans with unprecedented spectral, spatial, and time resolution. For many of the parameters required for global Earth system monitoring and modeling, such as radiation balance, atmospheric chemical composition, ocean surface state and wind stress, ocean and land bio-production, cloud and optical properties, aerosols, etc., there would be no other means to make adequate global measurements. These measurements from space need to be complemented by an array of regular surface observations, as well as detailed *in situ* expeditions to capture microphysical processes. Such campaigns are planned under the Global Change Research Program.

## *Future Research Framework for Earth System Modeling*

Although substantial progress has been made over the past 10 years in modeling and monitoring, each incremental improvement has led to expanded requirements for observational data, theoretical studies, process studies through field experiments, and global modeling research. This is not an unexpected sequence, given the complexities of the coupled, interactive global Earth system. In fact, progress has been justifiably remarkable. Many other disciplines have demonstrated much less success with what on the surface appears to be much simpler systems (e.g., the real estate or stock market). However, the present state of the science is not considered to be complete enough for unambiguous and absolute predictions of the future state of the global system, given the lack of observational information on key processes (e.g., cloud-radiation feedback) and uncertainties associated with the parameterization of a variety of other processes. Nevertheless, it is generally felt that sufficient progress has been made to feel confident that over the next 10 or 15 years significantly more realistic models and predictions are indeed achievable. These future models are expected to substantively reduce the uncertainties of present prediction models, thereby providing much clearer (though not absolute) guidance for policymaking regarding environmental global change. In conjunction with improved monitoring capability provided by EOS, Earth Probes, and other observing systems, and improved computational power, it is also envisioned that near-future models would provide a much more precise basis for determining the impact of potential or real environmental change on socio-economic activities the world over.

# *Acronyms*

| | |
|---|---|
| ACRIM | Active Cavity Radiometer Irradiance Monitor |
| ADEOS | Advanced Earth Observing System |
| AGCM | Atmospheric General Circulation Model |
| AIDJEX | Arctic Ice Dymanics Joint Experiment |
| AIRS | Atmospheric Infrared Sounder |
| ALT | Altimeter |
| AMSU | Advanced Microwave Sounding Unit |
| ASTER | Advanced Spaceborne Thermal Emission and Reflection Radiometer |
| ATLAS | Atmospheric Laboratory for Applications and Science |
| BATS | Biosphere-Atmosphere Transfer Scheme |
| CCN | Cloud Condensation Nuclei |
| CDAS | Climate Data Assimilation System |
| CEES | Committee on Earth and Environmental Sciences |
| CERES | Clouds and Earth's Radiant Energy System |
| CFC | Chlorofluorocarbon |
| CNES | Centre National d'Etudes Spatiales |
| COADS | Comprehensive Ocean-Air Data Set |
| COARE | Coupled Ocean-Atmosphere Response Experiment |
| CODF | Cloud-Optical Depth Feedback |
| CTD | Conductive Temperature Depth |
| CZCS | Coastal Zone Color Scanner |
| DERF | Dynamical Extended Range Forecast |
| DMSP | Defense Meteorological Satellite Program |
| DoD | Department of Defense |
| DORIS | Doppler Orbitography and Radiopositioning Integrated by Satellite |
| EBM | Energy Balance Model |
| ECMWF | European Centre for Medium Range Weather Forecasting |
| ELV | Expendable Launch Vehicle |
| ENSO | El Niño/Southern Oscillation |
| ENVISAT | Environmental Satellite |
| EOS | Earth Observing System |
| EOSDIS | EOS Data and Information System |
| EOSP | Earth Observing Scanning Polarimeter |
| ERBE | Earth Radiation Budget Experiment |
| ERBS | Earth Radiation Budget Satellite |
| ERS | European Remote-Sensing Satellite |
| ESA | European Space Agency |
| EUMETSAT | European Organisation for the Exploitation of Meteorological Satellites |
| GCE | Goddard Cumulus Ensemble |
| GCM | General Circulation Model |
| GCRP | Global Change Research Program |
| GEM | Global Earth System Model |
| GEWEX | Global Energy and Water Cycle Experiment |
| GHG | Greenhouse Gas |
| GISS | Goddard Institute for Space Studies |
| GLAS | Geoscience Laser Altimeter System |
| GOES | Geostationary Operational Environmental Satellite |
| GTS | Global Telecommunications System |
| HIRDLS | High-Resolution Dynamics Limb Sounder |
| HIRS | High-Resolution Infrared Sounder |
| HPCC | High Performance Computing and Communications |
| ICSU | International Council of Scientific Unions |
| IEOS | International Earth Observing System |
| IGBP | International Geosphere-Biosphere Program |
| IPCC | Intergovernmental Panel on Climate Change |
| ISCCP | International Satellite Cloud Climatology Project |
| ISLSCP | International Satellite Land Surface Climatology Project |
| ISO | Intraseasonal Oscillations |
| ITCZ | Inter-Tropical Convergence Zone |
| JERS | Japan's Earth Resources Satellite |
| JPL | Jet Propulsion Laboratory |
| LAGEOS | Laser Geodynamics Satellite |
| Landsat | Land Remote-Sensing Satellite |
| LAWS | Laser Atmospheric Wind Sounder |
| LCL | Lifting Condensation Level |
| LITE | Lidar In-Space Technology Experiment |
| LOD | Length-of-Day |
| METOP | Meteorological Operational Satellite |
| MHS | Microwave Humidity Sounder |
| MIMR | Multifrequency Imaging Microwave Radiometer |
| MISR | Multi-Angle Imaging SpectroRadiometer |
| MLS | Microwave Limb Sounder |
| MODIS | Moderate-Resolution Imaging Spectroradiometer |
| MOPITT | Measurements of Pollution in the Troposphere |
| MRF | Medium-Range Forecast |
| MSU | Microwave Sounding Unit |
| MTPE | Mission to Planet Earth |
| NASA | National Aeronautics and Space Administration |
| NCAR | National Center for Atmospheric Research |
| NLC | Noctilucent Cloud |
| NMC | National Meteorological Center |
| NMHC | Nonmethane Hydrocarbons |
| NOAA | National Oceanic and Atmospheric Administration |
| NRC | National Research Council |
| NSCAT | NASA Scatterometer |
| NWP | Numerical Weather Prediction |
| OGCM | Ocean General Circulation Model |
| PBL | Planetary Boundary Layer |

| | |
|---|---|
| POEM | Polar-Orbit Earth Observation Mission |
| POES | Polar-Orbiting Operational Environmental Satellite |
| PPM | Piecewise Parabolic Method |
| QBO | Quasi-Biennial Oscillation |
| Radarsat | Radar Satellite |
| RCE | Radiative-Convective Equilibrium |
| RCM | Radiative-Convective Models |
| RE | Radiative Equilibrium |
| SAGE | Stratospheric Aerosol and Gas Experiment |
| SAR | Synthetic Aperture Radar |
| SBUV | Solar Backscatter Ultraviolet |
| SeaWiFS | Sea-Viewing Wide Field Sensor |
| SiB | Simplified Biosphere |
| SIR-C | Shuttle Imaging Radar-C |
| SMMR | Scanning Multispectral Microwave Radiometer |
| SPOT | Systeme pour l'Observation de la Terre |
| SSALT | Solid-State Altimeter |
| SSM/I | Special Sensor Microwave/Imager |
| SST | Sea Surface Temperature |
| TES | Tropospheric Emission Spectrometer |
| TMR | TOPEX Microwave Radiometer |
| TOA | Top of the Atmosphere |
| TOGA | Tropical Ocean Global Atmosphere |
| TOMS | Total Ozone Mapping Spectrometer |
| TOPEX | Ocean Topography Experiment |
| TRMM | Tropical Rainfall Measuring Mission |
| UARS | Upper Atmosphere Research Satellite |
| UKMO | United Kingdom Meteorological Office |
| USGCRP | U.S. Global Change Research Program |
| VLBI | Very Long Baseline Interferometry |
| WCRP | World Climate Research Program |
| WMO | World Meteorological Organization |
| X-SAR | X-Band Synthetic Aperture Radar |

# References


Albrecht, B.A., 1989: Aerosols, cloud microphysics, and fractional cloudiness. *Science*, 242, pp. 1227-1330.

Alldredge, L.R., 1984: Geomagnetic secular variation and varying dipoles in the core. *Journal of Geomagnetics and Geoelectricity*, 36, pp. 621-633.

Anderson, J.R. and R.D. Rosen, 1983: The latitude-height structure of 40-50 day variations in atmospheric angular momentum. *Journal of the Atmospheric Sciences*, 40, pp. 1585-1590.

Angell, J.K., 1990: Variations in global tropospheric temperature after adjustment for El Niño influence. *Geophysical Research Letters*, 17, pp. 1093-1096.

Angell, J.K., 1988: Impact of El Niño on the delineation of tropospheric cooling due to volcanic eruptions. *Journal of Geophysical Research*, 93, pp. 3697-3704.

Anthes, R.A., 1977: A cumulus parameterization scheme utilizing a one-dimensional cloud model. *Monthly Weather Review*, 105, pp. 270-286.

Arakawa, A. and W.H. Schubert, 1974: Interaction of a cumulus cloud ensemble with the large-scale environment, part I. *Journal of the Atmospheric Sciences*, 31, pp. 674-701.

Arkin, P.A. and P.E. Ardanuy, 1989: Estimating climatic-scale precipitation from space: A review. *Journal of Climate*, 2, pp. 1229-1238.

Arking, A., 1991: The radiative effects of clouds and their impact on climate. *Bulletin of the American Meteorological Society*, 71, pp. 795-813.

Arrhenius, S., 1896: On the influence of carbonic acid in the air upon the temperature of the ground. *Philosophical Magazine*, 41, pp. 237-271.

Asrar, G. and D. Dokken, 1993: *1993 EOS Reference Handbook*. NASA Headquarters, NP-202, 145 pp.

Ballish, B., X. Cao, E. Kalnay, and M. Kanamitsu, 1992: Incremental nonlinear normal-mode initialization. *Monthly Weather Review*, 120, pp. 1723-1734.

Barnett, T.P., R. Haskins, and M. Chahine, 1991: Detection of the greenhouse gas signal from space: A progress report. *Advances in Space Research*, 11, pp. 3(37)-3(44).

Barnett, T., N. Graham, M. Cane, S. Zebiak, S. Dolan, J. O'Brien, and D. Legler, 1988: On the prediction of the El Niño of 1986-1987. *Science*, 241, pp. 192-196.

Barnett, T.P. and M.E. Schlesinger, 1987: Detecting changes in global climate induced by greenhouse gases. *Journal of Geophysical Research*, 92, pp. 14,772-14,780.

Barnett, T.P., 1985: Three-dimensional structure of low-frequency pressure variations in the tropical atmosphere. *Journal of the Atmospheric Sciences*, 42, pp. 2798-2803.

Barry, R.G., A. Henderson-Sellers, and K.P. Shine, 1984: *Climate sensitivity and the marginal cryosphere*. Climate Processes and Climate Sensitivity, Geophysical Monograph, 29, pp. 221-237.

Bates, J.R., F.H.M. Semazzi, R.W. Higgins, and S.R.M. Barros, 1990: Integration of the shallow water equations on the sphere using a vector semi-Lagrangian scheme with a multigrid solver. *Monthly Weather Review*, 118, pp. 1615-1627.

Bengtsson, L. and J. Shukla, 1988: Integration of space and *in situ* observations to study global climate change. *Bulletin American Meteorological Society*, 69, pp. 1130-1143.

Bengtsson, L., 1985: Medium-range forecasting at the ECMWF. *Advances in Geophysics*, 28, pp. 3-54.

Berger, A., 1980: The Milankovitch astronomical theory of paleoclimates: A modern review. *Vistas in Astronomy*, 24, pp. 103-122.

Bergman, K.H., 1983: Climate change. *International Journal of Environmental Studies*, 20, pp. 91-101.

Bergman, K.H., A. Hecht, and S.H. Schneider, 1981: Climate models. *Physics Today*, October 1981, pp. 44-51.

Björkström, A., 1979: A model for $CO_2$ interaction between atmosphere, oceans, and land biota. In *The Global Carbon Cycle*. Edited by B. Bolin, E.T. Degens, S. Kempe, and P. Ketner. SCOPE 13, John Wiley and Sons, Chichester, pp. 403-458.

Boer, G.J., et al., 1991: An intercomparison of the climates simulated by 14 atmospheric general circulation models. CAS/JSC Working Group on Numerical Experimentation. WMO/ICSU WCRP-58, 37 pp.

Bolin, B., 1986: How much $CO_2$ will remain in the atmosphere? In *The Greenhouse Effect, Climate Change, and Ecosystems (SCOPE 29)*. Edited by B. Bolin, B.R. Doos, J. Jager, and R.A. Warrick. John Wiley and Sons, Chichester, pp. 93-155.

Bourke, W., 1974: A multi-level spectral model, part I: Formulation and hemispheric integrations. *Monthly Weather Review*, 102, pp. 687-701.

Bourke, W., 1972: An efficient, one-level, primitive-equation spectral model. *Monthly Weather Review*, 100, pp. 683-689.

Bowen, R.I., 1986: Unusual seabird activity in the Galapagos Islands. *WMO/CSM Bulletin*, 1986-5.

Boyle, E.A. and L. Keigwin, 1982: Deep circulation of the North Atlantic over the last 200,000 years: Geochemical evidence. *Science*, 218, p. 784.

Bradley, R.S., 1988: The explosive volcanic eruption signal in the Northern Hemisphere: Continental temperature records. *Climatic Change*, 12, pp. 221-243.

Bradley, R.S., H.F. Diaz, J.K. Eischeid, P.D. Jones, P.M. Kelly, and C.M. Goodess, 1987: Precipitation fluctuations over Northern Hemisphere land areas since the mid-19th century. *Science*, 237, pp. 171-175.

Bretherton, F.P., K. Bryan, and J.D. Woods, 1990: Time-dependent greenhouse gas-induced climate change. In *Climate Change: The IPCC Scientific Assessment*. Edited by J.T. Houghton, G.J. Jenkins, and J.J. Ephraums. Cambridge University Press, Cambridge, pp. 173-193.

Briffa, K.R., P.D. Jones, and F.H. Schweingruber, 1992: Tree-ring density reconstructions of summer temperature patterns across western North America since 1600. *Journal of Climate*, 5, pp. 735-754.

Broecker, W.S. and G.H. Denton, 1990: What drives the glacial cycles? *Scientific American*, 262, pp. 49-56.

Broecker, W.S. and G.H. Denton, 1989: The role of the ocean-atmosphere reorganizations in glacial cycles. *Geochimica et Cosmochimica Acta*, 53, pp. 2465-2501.

Broecker, W.S., J.P. Kennett, B.P. Flowers, J. Teller, S. Trumbore, G. Bonani, and W. Wolfli, 1989: The routing of Laurentide ice-sheet meltwater during the Younger Dryas cold event. *Nature*, 341, pp. 318-321.

Broecker, W.S., D. Peteet, and D. Rind, 1985: Does the ocean-atmosphere system have more than one stable mode of operation? *Nature*, 315, pp. 21-26.

Broecker, W.S., 1982: Ocean chemistry during glacial time. *Geochimica et Cosmochimica Acta*, 46, pp. 1689-1705.

Broecker, W.S. and T.H. Peng, 1982: *Tracers in the Sea*. Lamont-Doherty Geological Observatory, New York.

Bryan, K. and R. Stouffer, 1991: A note on Bjerknes' hypothesis for North Atlantic variability. *Journal of Marine Systems*, 1, pp. 229-241.

Bryan, K. and M.J. Spelman, 1989: The oceanic response to $CO_2$-induced warming. *Journal of Geophysical Research*, 90, pp. 11679-11688.

Budyko, M.I., 1980: *Climate of the Past and Future* [in Russian]. Leningrad, Gidrometeorizdat, 352 pp.

Cane, M.A., 1984: Modeling sea level during El Niño. *Journal of Physical Oceanography*, 14, pp. 1864-1874.

Carissimo, B.C., A.H. Oort, and T.H. von der Haar, 1985: Estimating the meridional energy transports in the atmosphere and ocean. *Journal of Physical Oceanography*, 15, pp. 82-91.

Carpenter Jr., R.L., C.E. Hane, K.K. Droegemeier, and P.R. Woodward, 1984: Application of the piecewise parabolic method (PPM) to meteorological modeling. *Monthly Weather Review*, 118, pp. 586-612.

Cavalieri, D.J. and C.L. Parkinson, 1981: Large variations in observed Antarctic sea ice extent and associated atmospheric circulation. *Monthly Weather Review*, 109, pp. 2323-2336.

Cess, R.D., 1989: Gauging water vapour feedback. *Nature*, 342, pp. 736-737.

Cess, R.D., et al., 1989: Interpretation of cloud-climate feedback as produced by 14 atmospheric generic circulation models. *Science*, 245, pp. 513-516.

Cess, R.D. and G.L. Potter, 1988: A methodology for understanding and intercomparing atmospheric climate feedback processes in general circulation models. *Journal of Geophysical Research*, 93, pp. 8305-8314.

Cess, R.D. and G.L. Potter, 1987: Exploratory studies of cloud radiative forcing with a general circulation model. *Tellus*, 39A, pp. 460-473.

Cess, R.D., 1976: Climate change: An appraisal of atmospheric feedback mechanisms employing zonal climatology. *Journal of the Atmospheric Sciences*, 33, pp. 1831-1843.

Chaen, M. and K. Wyrtki, 1981: The 20°C isotherm and sea level in the western equatorial Pacific. *Journal of the Oceanographic Society of Japan*, 37, pp. 198-200.

Charlson, R.J., S.E. Schwartz, J.M. Hales, R.D. Cess, J.A. Coakley Jr., J.E. Hansen, and D.J. Hofmann, 1992: Climate forcing by anthropogenic aerosols. *Science*, submitted.

Charlson, R.J., J.E. Lovelock, M.O. Andreae, and S.G. Warren, 1987: Oceanic phytoplankton, atmospheric sulfur, cloud albedo, and climate. *Nature*, 326, pp. 655-661.

Charney, J.G., W.J. Quirk, S.-H. Chow, and J. Kornfield, 1977: A comparative study of the effects of albedo change on drought in semiarid regions. *Journal of the Atmospheric Sciences*, 34, pp. 1366-1385.

Charney, J.G., 1975: Dynamics of deserts and drought in the Sahel. *Quarterly Journal of Research of the Meteorology Society*, 101, pp. 193-202.

Charney, J.G., P.H. Stone, and W.J. Quirk, 1975: Drought in the Sahara: A biogeophysical feedback mechanism. *Science*, 187, pp. 434-435.

Charney, J.G., 1969: A further note on large-scale motions in the tropics. *Journal of the Atmospheric Sciences*, 26, pp. 607-609.

Charney, J.G., R. Fjortoft, and J. von Neumann, 1950: Numerical integration of the barotropic vorticity equation. *Tellus*, 2, pp. 237-254.

Chervin, R.M., 1986: Interannual variability and seasonal climate predictability. *Journal of the Atmospheric Sciences*, 43, pp. 233-251.

Cicerone, R.J., 1988: How has the atmospheric concentration of CO changed? In *The Changing Atmosphere*. Edited by F.S. Rowland and I.S.A. Isaksen. Wiley-Interscience, pp. 49-61.

Cicerone, R.J. and J.D. Shetter, 1981: Sources of atmospheric methane: Measurements in rice paddies and a discussion. *Journal of Geophysical Research*, 86, pp. 7203-7209.

Clark, J.S., 1991: Ecosystem sensitivity to climate change and complex responses. In *Global Climate Change and Life on Earth*. Edited by R. Wyman. Chapman and Hall, New York.

CLIMAP Project, 1976: The surface of the Ice Age Earth. *Science*, 191, pp. 1131-1137.

Cline, J.D., D.P. Wisegarver, and K. Kelly-Hansen, 1987: Nitrous oxide and vertical mixing in the equatorial Pacific during the 1982-1983 El Niño. *Deep Sea Research*, 34, pp. 857-873.

Coakley Jr., J.A. and P. Chylek, 1975: The two stream approximation in radiative transfer, including the angle of the incident radiation. *Journal of the Atmospheric Sciences*, 46, pp. 249-261.

COHMAP Members, 1988: Climatic changes of the last 18,000 years: Observations and model simulations. *Science*, 241, pp. 1043-1052.

Colella, P. and P.R. Woodward, 1984: The piecewise parabolic method (PPM) for gas dynamical simulations. *Journal of Computational Physics*, 54, pp. 174-201.

Coon, M.D., 1980: A review of AIDJEX modeling. In *Sea Ice Processes and Models*. Edited by R.S. Pritchard. University of Washington Press, Seattle, pp. 12-27.

Coon, M.D., G.A. Maykut, R.S. Pritchard, D.A. Rothrock, and A.S. Thorndike, 1974: Modeling the pack ice as an elastic-plastic material. *Aidjex Bulletin*, 24, pp. 1-105.

Courant, R., K.O. Friedrichs, and H. Lewy, 1928: Über die partiellen differenzengleichungen der mathematischen physik. *Mathematischen Annalen*, 100, pp. 32-74.

Crisp, D., 1990: Infrared radiative transfer in the dust-free Martian atmosphere. *Journal of Geophysical Research*, 95, pp. 14577-14588.

Crisp, D., S.B. Fels, and M.D. Schwarzkopf, 1986: Approximate methods for finding $CO_2$ 15-μm band transmission in planetary atmospheres. *Journal of Geophysical Research*, 91, pp. 11851-11866.

Crowley, T.J. and G.R. North, 1991: *Paleoclimatology*. Oxford University Press, New York, 339 pp.

Crowley, T.J., 1989: Paleoclimate perspectives on greenhouse warming. In *Climate and Geoscience*. Edited by A. Berger et al. Kluwer Academic Publishers, pp. 179-207.

Crowley, T.J., 1983: The geological record of climatic change. *Reviews of Geophysics and Space Physics*, 21, pp. 828-877.

Crutzen, P.J., I. Aselmann, and W.S. Seiler, 1986: Methane production by domestic animals, wild ruminants, other herbivorous fauna, and humans. *Tellus*, 38B, pp. 271-284.

Crutzen, P.J. and J.W. Birks, 1982: The atmosphere after a nuclear war: Twilight at noon. *Ambio*, 11, pp. 114-125.

Deardorff, J.W., 1972: Parameterization of the planetary boundary layer for use in general circulation models. *Monthly Weather Review*, 100, pp. 93-106.

Del Genio, A.D., 1991: Convective and large-scale cloud processes in global climate models. In *Energy and Water Cycles in the Climate System*. NATO Advanced Study Institute.

Diaz, H.F., R.S. Bradley, and J.K. Eischeid, 1989: Precipitation fluctuations over global land areas since the late 1800s. *Journal of Geophysical Research*, 94, pp. 1195-1210.

Dickinson, R.E., A. Henderson-Sellers, C. Rosenzweig, and P.J. Sellers, 1991: Evapotranspiration models with canopy resistance for use in climate models: A review. *Agricultural and Forest Meteorology*, 54, pp. 373-388.

Dickinson, R.E. and A. Henderson-Sellers, 1988: Modeling tropical deforestation: A study of GCM land-surface parameterizations. *Quarterly Journal of Research of the Meteorology Society*, 114, pp. 439-462.

Dickinson, R.E., A. Henderson-Sellers, P.J. Kennedy, and M.F. Wilson, 1986: *Biosphere-Atmosphere Transfer Scheme (BATS) for the NCAR Community Climate Model*. NCAR Technical Note 275, Boulder, Colorado.

Dickinson, R.E. and R.J. Cicerone, 1986: Future global warming from atmospheric trace gases. *Nature*, 319, pp. 109-115.

Donner, L. and V. Ramanathan, 1980: Methane and nitrous oxide: Their effects on the terrestrial climate. *Journal of the Atmospheric Sciences*, 37, pp. 119-124.

Eddy, J.A., 1977: Climate and the changing sun. *Climatic Change*, 1, pp. 173-190.

Eddy, J.A., 1976: The Maunder Minimum. *Science*, 192, pp. 1189-1202.

Ehrendorfer, M. and A.H. Murphy, 1992: Evaluation of prototypical climate forecasts: The sufficiency relation. *Journal of Climate*, 5, pp. 876-887.

Ekman, V.W., 1905: On the influence of the Earth's rotation on ocean currents. *Arkiv. Matem., Astr. Fys.*, 2, 11, 53 pp.

Ellis, J.S., 1978: *Cloudiness, the Planetary Radiation Budget, and Climate*. Ph.D. thesis, Colorado State University, Fort Collins, 129 pp.

Environmental Protection Agency, 1989: *National Air Pollution Emission Estimates 1940-1987*. U.S. Environment Protection Board Report EPA/450/4/88/022. Research Triangle Park, North Carolina.

Epstein, E.S., 1982: Detecting climate change. *Journal of Applied Meteorology*, 21, pp. 1172-1182.

Erickson III, D.J., J.J. Walton, S.J. Ghan, and J.E. Penner, 1991: Three-dimensional modeling of the global atmospheric sulfur cycle: A first step. *Atmospheric Environment*, 25A, pp. 2513-2520.

Flohn, H. and A. Kapala, 1989: Changes in tropical sea-air interaction processes over a 30-year period. *Nature*, 338, pp. 244-246.

Folland C.K., D.E. Parker, and F.E. Kates, 1984: Worldwide marine temperature fluctuations, 1856-1981. *Nature*, 310, pp. 670-673.

Foukal, P. and J. Lean, 1990: An empirical model of total solar irradiance variations between 1874 and 1988. *Science*, 247, pp. 556-558.

Fox-Rabinovitz, M.S., 1991: Computational dispersion properties of horizontal staggered grids for atmospheric and ocean models. *Monthly Weather Review*, 119, pp. 1624-1639.

Frakes, L.A., 1979: *Climates Throughout Geologic Time*. Elsevier Science Publishing Company, New York, 310 pp.

Friis-Christensen, E. and K. Lassen: Length of the solar cycle: An indicator of solar activity closely associated with climate. *Science*, 254, pp. 698-700.

Gary, J.M., 1979: Nonlinear instability. In *Numerical Methods Used in Atmospheric Models, Volume II.* GARP Publication Series No. 17, World Meteorological Organization, Geneva, pp. 476-499.

Gates, W.L., 1976: Modeling the ice-age climate. *Science*, 191, pp. 1138-1144.

Gates, W.L., 1975: *The Physical Basis of Climate and Climate Modeling*. GARP Publication Series No. 16, World Meteorological Organization, Geneva.

Gordon, A.H., 1991: Global warming as a manifestation of a random walk. *Journal of Climate*, 4, pp. 589-597.

Gornitz, V., 1990: Mean sea level changes in the recent past. In *Climate and Sea Level Change: Observations, Projections, and Implications*. Edited by R.A. Warrick and T.M.L. Wigley. Cambridge University Press, Cambridge.

Gornitz, V., S. Lebedeff, and J. Hansen, 1982: Global sea level trends in the past century. *Science*, 215, pp. 1611-1614.

Goswami, B.N. and J. Shukla, 1991: Predictability of a coupled ocean-atmosphere model. *Journal of Climate*, 4, pp. 3-22.

Gray, W.M., 1984: Atlantic seasonal hurricane frequency, part I: El Niño and 30 mb quasi-biennial oscillation influences. *Monthly Weather Review*, 112, pp. 1649-1667.

Gray, W.M., 1984: Atlantic seasonal hurricane frequency, part II: Forecasting its variability. *Monthly Weather Review*, 112, pp. 1669-1683.

Grotch, S.L. and M.C. MacCracken, 1991: The use of general circulation models to predict regional climatic change. *Journal of Climate*, 4, pp. 286-304.

Grotch, S.L., 1988: *Regional Intercomparisons of General Circulation Model Predictions and Historical Climate Data*. U.S. Department of Energy, Washington, D.C., Report DOE/NBB-0084 (TR041).

Grotch, S.L., 1987: Some considerations relevant to computing average hemispheric temperature anomalies. *Monthly Weather Review*, 115, pp. 1305-1317.

Guilliland, R.L., 1982: Solar, volcanic, and $CO_2$ forcing of recent climatic changes. *Climate Change*, 4, pp. 111-131.

Haeberli, W., P. Müller, P. Alean, and H. Bösch, 1989: Glacier changes following the little ice age—A survey of the international data basis and its perspectives. In *Glacier Fluctuations and Climatic Change*. Edited by J. Oerlemans. Reidel, Dordrecht, pp. 77-101.

Halley, E., 1715: On the causes of the saltiness of the ocean, and of the several lakes that emit no rivers. *Philosophical Transactions of the Royal Society of London*, 29, pp. 296-300.

Haltiner, G.J. and R.T. Williams, 1980: *Numerical Prediction and Dynamic Meteorology*. John Wiley and Sons, New York, 477 pp.

Hansen, J., A. Lacis, R. Ruedy, and M. Sato, 1992: Potential climate impact of Mount Pinatubo eruption. *Geophysical Research Letters*, 19, pp. 215-218.

Hansen, J.E. and A.A. Lacis, 1990: Sun and dust versus greenhouse gases: An assessment of their relative roles in global climate change. *Nature*, 346, pp. 713-719.

Hansen, J., W. Rossow, and I. Fung, 1990: The missing data on global climate change. *Issues in Science and Technology*, 7, pp. 62-69.

Hansen, J., A. Lacis, and M. Prather, 1989: Greenhouse effect of chlorofluorocarbons and other trace gases. *Journal of Geophysical Research*, 94, pp. 16417-16421.

Hansen, J.,I. Fung, A. Lacis, D. Rind, S. Lebedeff, R. Ruedy, G. Russell, and P. Stone, 1988: Global climate changes as forecast by Goddard Institute for Space Studies three-dimensional model. *Journal of Geophysical Research*, 93, pp. 9341-9364.

Hansen, J. and S. Lebedeff, 1987: Global trends of measured surface air temperature. *Journal of Geophysical Research*, 92, pp. 13345-13372.

Hansen, J.E., et al., 1985: Climate response times: Dependence on climate sensitivity and ocean mixing. *Science*, 229, pp. 857-859.

Hansen, J., A. Lacis, D. Rind, G. Russell, P. Stone, I. Fung, R. Ruedy, and J. Lerner, 1984: Climate sensitivity: Analysis of feedback effects. *Geophysical Monograph*, 29, pp. 130-163.

Hansen, J., G. Russell, D. Rind, P. Stone, A. Lacis, S. Lebedeff, R. Ruedy, and L. Travis, 1983: Efficient three-dimensional global models for climate studies: Models I and II. *Monthly Weather Review*, 111, pp. 609-662.

Hansen, J.E., W.C. Chang, and A.A. Lacis, 1978: Mount Agung provides a test of a global climatic perturbation. *Science*, 199, pp. 1065-1068.

Hanson, A.G. and W.D. Hitz, 1982: Metabolic responses of mesophytes to plant water deficits. *Annual Review of Plant Physiology*, 33, pp. 163-203.

Harms, D.E., S. Raman, and R.V. Madala, 1992: An examination of four-dimensional data-assimilation techniques for numerical weather prediction. *Bulletin of the American Meteorological Society*, 73, pp. 425-440.

Harshvardhan, D.A. Randall, and D.A. Dazlich, 1990: Relationship between the longwave cloud radiative forcing at the surface and the top of the atmosphere. *Journal of Climate*, 3, pp. 1435-1443.

Harshvardhan, D.A. Randall, T.G. Corsetti, and D.A. Dazlich, 1989: Earth radiation budget and cloudiness simulations with a general circulation model. *Journal of the Atmospheric Sciences*, 46, pp. 1922-1942.

Hartman, D.L., K.J. Kowalewsky, and M.L. Michelsen, 1991: Diurnal variations of outgoing longwave radiation and albedo from ERBE scanner data. *Journal of Climate*, 4, pp. 598-617.

Hibler III, W.D. and G.M Flato, 1992: Sea ice models. In *Climate Systems Modeling*. Edited by K. Trenberth. Cambridge University Press, Cambridge, in press.

Hibler III, W.D. and K. Bryan, 1987: A diagnostic ice-ocean model. *Journal of Physical Oceanography*, 17, pp. 987-1015.

Hibler III, W.D. and S.F. Ackley, 1983: Numerical simulation of the Weddell Sea pack ice. *Journal of Geophysical Research*, 88, pp. 2873-2887.

Hibler III, W.D., 1979: A dynamic thermodynamic sea ice model. *Journal of Physical Oceanography*, 9, pp. 815-846.

Hide, R. and J.O. Dickey, 1991: Earth's variable rotation. *Science*, 253, pp. 629-637.

Holdridge, L.R., 1964: *Life Zone Ecology*. Tropical Science Center, San Jose, Costa Rica.

Holdridge, L.R., 1947: Determination of world plant formations from simple climatic data. *Science*, 105, pp. 367-368.

Idso, S.B., 1991: The aerial fertilization effect of $CO_2$ and its implications for global carbon cycling and maximum greenhouse warming. *Bulletin of the American Meteorological Society*, 72, pp. 962-965.

Idso, S.B., B.A. Kimball, and S.G. Allen, 1991: Net photosynthesis of sour orange trees maintained in atmospheres of ambient and elevated $CO_2$ concentrations. *Agricultural and Forest Meteorology*, 54, pp. 95-101.

Imbrie, J. and K.P. Imbrie, 1979: *Ice Ages—Solving the Mystery*. Macmillan, London, 224 pp.

Intergovernmental Panel on Climate Change, 1992: *1992 IPCC Supplement: Scientific Assessment of Climate Change*. Submission from Working Group I. Cambridge University Press, Cambridge, 24 pp.

Intergovernmental Panel on Climate Change, 1990: *Climate Change: The IPCC Scientific Assessment*. Edited by J.T. Houghton, G.J. Jenkins, and J.J. Ephraums. Cambridge University Press, Cambridge, 365 pp.

Jarvis, P.G. and K.G. McNaughton, 1986: Stomatal control of transpiration: Scaling from leaf to region. *Advances in Ecological Research*, 15, pp. 1-49.

Jenne, R.L., 1992: Climate model description and impact on terrestrial climate. In *Global Climate Change: Implications, Challenges, and Mitigation Measures*. Edited by S.K. Majumdar, L.S. Kalkstein, B. Yarnal, E.W. Miller, and L.M. Rosenfeld. The Pennsylvania Academy of Science, pp. 145-164.

Jenne, R.L., 1991: Climate trends, the U.S. drought of 1988, and access to data. In *Greenhouse Gas-Induced Climatic Change: A Critical Appraisal of Simulations and Observations*. Edited by M.E. Schlesinger. Elsevier Science Publishers, Amsterdam, pp. 195-209.

Jones, P.D. and T.M.L. Wigley, 1990: Global warming trends. *Scientific American*, 263, pp. 84-91.

Jones, P.D., 1989: The influence of ENSO on global temperatures. *Climate Monitor*, 17, pp. 80-89.

Jones, P.D., P.M. Kelly, G.B. Goodess, and T.R. Karl, 1989: The effect of urban warming on the Northern Hemisphere temperature average. *Journal of Climate*, 2, pp. 285-290.

Jones, P.D., 1988: Hemispheric surface air temperature variations: Recent trends and an update to 1987. *Journal of Climate*, 1, pp. 654-660.

Jones, P.D., T.M.L. Wigley, C.K. Folland, and D.E. Parker, 1988: Spatial patterns in recent worldwide temperature trends. *Climate Monitor*, 16, pp. 175-186.

Jones, P.D., S.C.B. Raper, R.S. Bradley, H.F. Diaz, P.M. Kelly, and T.M.L. Wigley, 1986: Northern Hemisphere surface air temperature variations, 1851-1984, I. *Journal of Climate and Applied Meteorology*, 25, pp. 161-179.

Jones, P.D., S.C.B. Raper, R.S. Bradley, H.F. Diaz, P.M. Kelly, and T.M.L. Wigley, 1986: Northern Hemisphere surface air temperature variations, 1851-1984, II. *Journal of Climate and Applied Meteorology*, 25, pp. 1213-1230.

Kalnay, E., M. Kanamitsu, J. Pfaendtner, J. Sela, M. Suarez, J. Stackpole, J. Tuccillo, L. Umscheid, and D. Williamson, 1989: Rules for interchange of physical parameterizations. *Bulletin of the American Meteorological Society*, 70, pp. 620-622.

Kalnay, E., R. Balgovind, W. Chao, D. Edelmann, J. Pfaendtner, L. Takacs, and K. Takano, 1983: *Documentation of the GLAS Fourth Order General Circulation Model, Volume I: Model Documentation.* Laboratory for Atmospheric Sciences, Global Modeling and Simulation Branch, Goddard Space Flight Center, NASA Technical Memorandum 86064.

Karl, T.R., G. Kukla, and J. Gavin, 1984: Decreasing diurnal temperature range in the United States and Canada from 1941-1980. *Journal of Climate and Applied Meteorology*, 23, pp. 1489-1504.

Katsaros, K.B. and R.A. Brown, 1991: Legacy of the Seasat mission for studies of the atmosphere and air-sea-ice interactions. *Bulletin of the American Meteorological Society*, 72, pp. 967-981.

Kellogg, W.W., 1991: Response to skeptics of global warming. *Bulletin of the American Meteorological Society*, 74, pp. 499-511.

Kerr, R.A., 1991: Could the sun be warming the climate? *Science*, 254, pp. 652-653.

Kiehl, J.T. and V. Ramanathan, 1990: Comparison of cloud forcing derived from the Earth Radiation Budget Experiment with that simulated by the NCAR community climate model. *Journal of Geophysical Research*, 95, pp. 11679-11698.

Kinter, J.L. and J. Shukla, 1990: The global hydrologic and energy cycles: Suggestions for studies in the pre-Global Energy and Water Cycle Experiment (GEWEX) period. *Bulletin of the American Meteorological Society*, 71, pp. 181-189.

Kling, G.W., G.W. Kipphut, and M.C. Miller, 1991: Arctic lakes and streams as gas conduits to the atmosphere: Implications for tundra carbon budgets. *Science*, 251, pp. 298-301.

Krishnamurti, T.N., S.-L. Nam, and R. Pasch, 1983: Cumulus parameterization and rainfall rates II. *Monthly Weather Review*, 111, pp. 815-828.

Krishnamurti, T.N., V. Ramanathan, H.-L. Pan, R.J. Pasch, and J. Molinari, 1980: Cumulus parameterization and rainfall rates I. *Monthly Weather Review*, 108, pp. 465-472.

Kuo, H.L., 1974: Further studies of the parameterization of the influence of cumulus convection on large-scale flow. *Journal of the Atmospheric Sciences*, 31, pp. 1232-1240.

Kutzbach, J.E. and R.G. Gallimore, 1988: Sensitivity of a coupled atmosphere/mixed-layer ocean model to changes in orbital forcing at 9000 years BP. *Journal of Geophysical Research*, 93, pp. 803-821.

Kutzbach, J.E. and P.J. Guetter, 1986: The influence of changing orbital parameters and surface boundary conditions on climate simulations for the past 18,000 years. *Journal of the Atmospheric Sciences*, 43, pp. 1726-1759.

Kutzbach, J.E. and F.A. Street-Perrott, 1985: Milankovitch forcing of fluctuations in the level of tropical lakes from 18 to 0 kyr BP. *Nature*, 317, pp. 130-134.

Labitzke, K. and H. Van Loon, 1992: Association between the 11-year solar cycle and the atmosphere, part V: Summer. *Journal of Climate*, 5, pp. 240-251.

Lacis, A.A., D.J. Wuebbles, and J.A. Logan, 1990: Radiative forcing of climate by changes in the vertical distribution of ozone. *Journal of Geophysical Research*, 95, pp. 9971-9981.

Lacis, A.A., J. Hansen, P. Lee, T. Mitchell, and S. Lebedeff, 1981: Greenhouse effect of trace gases, 1970-1980. *Geophysical Research Letters*, 8, pp. 1035-1038.

Lacis, A.A. and J.E. Hansen, 1974: A parameterization for the absorption of solar radiation in the Earth's atmosphere. *Journal of the Atmospheric Sciences*, 31, pp. 118-133.

Lamb P.J. and R.A. Peppler, 1992: Further case studies of tropical Atlantic surface atmospheric and oceanic patterns associated with sub-Saharan drought. *Journal of Climate*, 5, pp. 476-488.

Landsea, C.W. and W.M. Gray, 1992: The strong association between western Sahelian monsoon rainfall and intense Atlantic hurricanes. *Journal of Climate*, 5, pp. 435-453.

Laprise, R., 1992: The resolution of global spectral models. *Bulletin of the American Meteorological Society*, 73, pp. 1453-1454.

Lau, N.-C., S.G.H. Philander, and M.J. Nath, 1992: Simulation of ENSO-like phenomena with a low-resolution coupled GCM of the global ocean and atmosphere. *Journal of Climate*, 5, pp. 284-307.

Lindzen, R.S., 1991: Letter to the editor: Response to AMS policy statement on global climate change. *Bulletin of the American Meteorological Society*, 72, p. 515.

Lindzen, R.S., 1990: Some coolness concerning global warming. *Bulletin American Meteorological Society*, 71, pp. 288-299.

Lindzen, R.S. and A.Y. Hou, 1988: Hadley circulations for zonally averaged heating centered off the equator. *Journal of the Atmospheric Sciences*, 45, pp. 2416-2427.

Lindzen, R.S. and J.R. Holton, 1968: A theory of the quasi-biennial oscillation. *Journal of the Atmospheric Sciences*, 25, pp. 1095-1107.

Livezey, R.E., 1985: Statistical analysis of general circulation model climate simulations: Sensitivity and prediction experiments. *Journal of the Atmospheric Sciences*, 42, pp. 1139-1149.

Lorenz, E.N., 1984: Irregularity: A fundamental property of the atmosphere. *Tellus*, 36A, pp. 98-110.

Lovelock, J.E., 1988: *The Ages of Gaia: A Biography of Our Living Earth*. W.W. Norton and Co., New York, 252 pp.

MacCracken, M.C., 1992: The challenge of identifying greenhouse gas-induced climatic change. In *Modeling the Earth System*. Edited by D. Ojima. University Corporation for Atmospheric Research/Office for Interdisciplinary Earth Studies, Boulder, Colorado, pp. 359-376.

Madden, R.A. and V. Ramanathan, 1980: Detecting climate change due to increasing carbon dioxide. *Science*, 209, pp. 763-768.

Madden, R.A. and P.R. Julian, 1971: Detection of a 40-50 day oscillation in the zonal wind in the tropical Pacific. *Journal of the Atmospheric Sciences*, 28, pp. 702-708.

Manabe, S., R.J. Stouffer, M.J. Spelman, and K. Bryan, 1991: Transient responses of a coupled ocean-atmosphere model to gradual changes of atmospheric $CO_2$, part I: Annual mean response. *Journal of Climate*, 4, pp. 785-818.

Manabe, S., K. Bryan, and M.D. Spelman, 1990: Transient response of a global ocean-atmosphere model to a doubling of atmospheric carbon dioxide. *Journal of Physical Oceanography*,120, pp. 722-749.

Manabe, S. and R.J. Stouffer, 1988: Two stable equilibria of a coupled ocean-atmosphere model. *Journal of Climate*, 1, pp. 841-866.

Manabe, S. and A.J. Broccoli, 1985: The influence of continental ice sheets on the climate of an ice age. *Journal of Geophysical Research*, 90, pp. 2167-2190.

Manabe, S. and K. Bryan, 1985: $CO_2$-induced change in a coupled ocean-atmosphere model and its paleoclimatic implications. *Journal of Geophysical Research*, 90, pp. 11689-11707.

Manabe, S. and K. Bryan, 1969: Climate calculations with a combined ocean-atmosphere model. *Journal of the Atmospheric Sciences*, 26, pp. 786-789.

Manabe, S. and R.F. Strickler, 1964: On the thermal equilibrium of the atmosphere with a convective adjustment. *Journal of the Atmospheric Sciences*, 21, pp. 361-385.

Marshall Institute, 1989: *Scientific Perspectives on the Greenhouse Problem*. Edited by F. Seitz. Washington, D.C.

Martinson, D.G., 1991: Open ocean convection in the Southern Ocean. In *Deep Convection and Deep Water Formation in the Oceans*. Edited by P.C. Chu and J.C. Gascard. Elsevier Science Publishers.

Mass, C.F. and D.A. Portman, 1989: Major volcanic eruptions and climate: A critical evaluation. *Journal of Climate*, 2, pp. 566-593.

Mass, C. and S. Schneider, 1977: Statistical evidence on the influence of sunspots and volcanic dust on long-term temperature records. *Journal of the Atmospheric Sciences*, 34, pp. 1995-2004.

Maykut, G.A. and N. Untersteiner, 1971: Some results from a time-dependent thermodynamic model of sea ice. *Journal of Geophysical Research*, 76, pp. 1550-1575.

McCarthy, D.D., 1984: Variations in the rotation of the Earth. *Journal of Geomagnetics and Geoelectricity*, 36.

McDonald, A. and J.R. Bates, 1989: Semi-Lagrangian integration of a gridpoint shallow water model on the sphere. *Monthly Weather Review*, 117, pp. 130-137.

McLaren, A.S., 1989: The under-ice thickness distribution of the Arctic Basin as recorded in 1958 and 1970. *Journal of Geophysical Research*, 94, pp. 4971-4983.

Mearns, L.O., R.W. Katz, and S.H. Schneider, 1984: Extreme high-temperature events: Changes in their probabilities with changes in mean temperature. *Journal of Climate and Applied Meteorology*, 23, pp. 1601-1613.

Meehl, G.A. and W.M. Washington, 1990: $CO_2$ climate sensitivity and snow-sea-ice albedo parameterization in an atmospheric GCM coupled to a mixed-layer ocean model. *Climatic Change*, 16, pp. 283-306.

Merle, J., 1985: *Diagnostic Studies of the Thermal Structure of the Tropical Atlantic Ocean*. International Conference on the TOGA Scientific Programme. WCRP Report No. 4, section V.

Messinger, F. and T.L. Black, 1992: On the impact on forecast accuracy of the step-mountain (Eta) versus sigma coordinate. *Meteorology and Atmospheric Physics*, submitted.

Miller, M.J., A.C.M. Beljaars, and T.N. Palmer, 1992: The sensitivity of the ECMWF model to the parameterization of evaporation from the tropical oceans. *Journal of Climate*, 5, pp. 418-434.

Miller, T.L. and J.D. Fehribach, 1990: A numerical study of the onset of baroclinic instabilities in spherical geometry. *Geophysical and Astrophysical Fluid Dynamics*, 52, pp. 25-43.

Milly, P.C.D., 1992: Potential evaporation and soil moisture in general circulation models. *Journal of Climate*, 5, pp. 209-226.

Mintz, Y., 1984: The sensitivity of numerically simulated climates to land-surface boundary conditions. In *The Global Climate*. Edited by J.T. Houghton. Cambridge University Press, New York, pp. 79-103.

Molnar, G. and W.-C. Wang, 1992: Effects of cloud optical property feedbacks on the greenhouse warming. *Journal of Climate*, 5, pp. 814-821.

Monastersky, R., 1993: Fire beneath the ice. *Science News*, 143, pp. 104-107.

National Academy of Sciences, 1991: *Policy Implications of Greenhouse Warming*. National Academy Press, Washington, D.C., 127 pp.

National Academy of Sciences, 1974: *The Ocean's Role in Climate Prediction*. Workshop Report, Washington, D.C., p. 10.

National Aeronautics and Space Administration, 1988: *Earth System Science: A Closer View*. Report of the Earth System Sciences Committee, NASA Advisory Council, Washington, D.C., 208 pp.

National Research Council, 1991: *Opportunities in the Hydrologic Sciences*. National Academy Press, Washington, D.C.

National Research Council, 1990: *Global Climate Change: Assessing the Evidence, Reducing the Uncertainty*. National Academy Press, Washington, D.C.

National Research Council, 1986: *Global Change in the Geosphere-Biosphere—Initial Priorities for an IGBP*.

National Research Council, 1983: *Changing Climate*. Report of the Carbon Dioxide Assessment Committee. National Academy Press, Washington, D.C.

National Research Council, 1982: *Carbon Dioxide and Climate: A Second Assessment.* Report of the $CO_2$/Climate Review Panel. National Academy Press, Washington, D.C.

National Research Council, 1975: *Understanding Climatic Change: A Program for Action.* U.S. Committee for GARP. National Academy of Sciences, Washington, D.C., 239 pp.

Navon, I.M., X. Zou, J. Derber, and J. Sela, 1992: Variational data assimilation with an adiabatic version of the NMC spectral model. *Monthly Weather Review*, 120, pp. 1433-1446.

Nicholls, N., 1984: The Southern Oscillation, sea surface temperature, and interannual fluctuations in Australian tropical cyclone activity. *Journal of Climatology*, 4, pp. 661-670.

Nicholson, S.E., 1989: African drought: Characteristics, causal theories, and global teleconnections. *Geophysical Monograph*, 52, pp. 79-100.

Nobre, C., J. Shukla, and P. Sellers, 1990: Amazon deforestation and climate change. *Science*, 247, pp. 1322-1325.

Noilham, J. and S. Planton, 1989: A simple parameterization of land surface processes for meteorological models. *Monthly Weather Review*, 117, pp. 536-549.

North, G.R., K.-J.J. Yip, L.-Y. Leung, and R.M. Chervin, 1992: Forced and free variations of the surface temperature field in a general circulation model. *Journal of Climate*, 5, pp. 227-239.

North, G.R., J.G. Mengel, and D.A. Short, 1983: A simple energy balance model resolving the seasons and the continents: Application to the astronomical theory of the Ice Ages. *Journal of Geophysical Research*, 88, pp. 6576-6586.

North, G.R., R.F. Calahan, and J.A. Coakley, Jr., 1981: Energy balance climate models. *Review of Geophysics and Space Physics*, 19, pp. 91-121.

Ohring, G., K. Gallo, A. Gruber, W. Planet, L. Stowe, and J.D. Tarpley, 1989: Climate and global change. *EOS Transactions, American Geophysical Union*, 70, pp. 889, 891, 894, 901.

Ohring, G. and P.F. Clapp, 1980: The effect of changes in cloud amount on the net radiation at the top of the atmosphere, *Journal of the Atmospheric Sciences*, 37, pp. 447-454.

Olson, J.S., J.A. Watts, and L.J., Allison, 1983: *Carbon in Live Vegetation of Major World Ecosystems.* United States Department of Energy, TR004, 164 pp.

Oort, A.H., Y.-H. Pan, R.W. Reynolds, and C.F. Ropelewski, 1987: Historical trends in the surface temperature over the oceans based on the COADS. *Climate Dynamics*, 2, pp. 29-38.

Oort, A.H., 1985: Balance conditions in the Earth's climate system. *Advances in Geophysics*, 28A, pp. 75-98.

Oort, A.H., 1983: *Global Atmospheric Circulation Statistics, 1958-1973.* NOAA Professional Paper 14, U.S. Department of Commerce.

Overpeck, J.T., P.J. Bartlein, and T. Webb III, 1991: Potential magnitude of future vegetation change in eastern North America: Comparisons with the past. *Science*, 254, pp. 692-695.

Overpeck, J.T. and P.J. Bartlein, 1989: Assessing the response of vegetation to future climate change: Ecological response surfaces and paleoecological model validation. In *The Potential Effects of Global Climate Change on the United States.* U.S. Environmental Protection Agency, EPA-230-05-89-054, Washington, D.C., pp. 1-32.

Pacanowski, R.C. and S.H. Philander, 1981: Parameterization of vertical mixing in numerical models of tropical oceans. *Journal of Physical Oceanography*, 11, pp. 1443-1451.

Palmer, T.N., 1986: Influence of the Atlantic, Pacific, and Indian Oceans on Sahel rainfall. *Nature*, 322, pp. 236-238.

Paltridge, G.W. and C.M.R. Platt, 1976: *Radiative Process in Meteorology and Climatology.* Elsevier Science Publishers, Amsterdam, 318 pp.

Parkinson, C.L., 1983: On the development and cause of the Weddell polynya in a sea ice simulation. *Journal of Physical Oceanography*, 13, pp. 501-511.

Parkinson, C.L. and W.M. Washington, 1979: A large-scale numerical model of sea ice. *Journal of Geophysical Research*, 84, pp. 311-337.

Parton, W.J., et al., 1992: Development of simplified ecosystem models for applications in Earth system studies: The century experience. In *Modeling the Earth System*. Edited by D. Ojima. University Corporation for Atmospheric Research/Office for Interdisciplinary Earth Studies, Boulder, Colorado, pp. 281-302.

Pastor, J. and W.M. Post, 1988: Response of northern forests to $CO_2$-induced climate change. *Nature*, 334, pp. 55-58.

Peixoto, J.P. and A.H. Oort, 1984: Physics of climate. *Reviews of Modern Physics*, 56, pp. 365-430.

Penner, J.E., S.J. Ghan, and J.J. Walton, 1990: The role of biomass burning in the budget and cycle of carbonaceous soot aerosols and their climate impact. *Proceedings of the Chapman Conference on Global Biomass Burning*. MIT Press, draft.

Philander, S.G.H., 1992: Ocean-atmosphere interactions in the tropics: A review of recent theories and models. *Journal of Applied Meteorology*, 31, pp. 938-945.

Philander, S.G.H., R.C. Pacanowski, N.-C. Lau, and M.J. Nath, 1992: Simulation of ENSO with a global atmospheric GCM coupled to a high-resolution, tropical Pacific Ocean GCM. *Journal of Climate*, 5, pp. 308-329.

Philander, S.G.H., 1985: *El Niño and La Niña*. Journal of the Atmospheric Sciences, 42, pp. 2562-2662.

Philander, S.G.H. and E.M. Rasmusson, 1985: The Southern Oscillation and El Niño. *Advances in Geophysics*, 28A, pp. 197-215.

Phillips, N.A., 1959: An example of nonlinear sea computational instability. In *The Atmosphere and Sea in Motion, Rossby Memorial Volume*. Rockefeller Institute Press, New York, pp. 501-504.

Ramanathan, V. and W. Collins, 1991: Thermodynamic regulation of ocean warming by cirrus clouds deduced from observations of the 1987 El Niño. *Nature*, 351, pp. 27-32.

Ramanathan, V., B.B. Barkstrom, and E.F. Harrison, 1989: Clouds and the Earth's radiation budget. *Physics Today*, 42, pp. 22-32.

Ramanathan, V., R.D. Cess, E.F. Harrison, P. Minnis, B.R. Barkstrom, E. Ahmad, and D. Hartmann, 1989: Cloud-radiative forcing and climate: Results from the Earth Radiation Budget Experiment (ERBE). *Science*, 243, pp. 57-63.

Ramanathan, V., 1988: The greenhouse theory of climate change: A test by inadvertent global experiment. *Science*, 240, pp. 293-299.

Ramanathan, V., L. Callis, R. Cess, J. Hansen, I. Isaksen, W. Kuhn, A. Lacis, F. Luther, J. Mahlman, R. Reck, and M. Schlesinger, 1987: Climate-chemical interactions and effects of changing atmospheric trace gases. *Geophysics Review*, 25, pp. 1441-1482.

Ramanathan, V., R.J. Cicerone, H.B. Singh, and J.T. Kiehl, 1985: Trace gas trends and their potential role in climate change. *Journal of Geophysical Research*, 90, pp. 5547-5566.

Ramanathan, V., H.B. Singh, R.J. Cicerone, and J.T. Kiehl, 1984: *Trace Gas Trends and Their Potential Role in Climate Change*. NCAR Technical Report 0304/84-9.

Ramanathan, V., 1981: The role of ocean-atmospheric interactions in the $CO_2$ climate problem. *Journal of the Atmospheric Sciences*, 38. pp. 918-930.

Ramanathan, V. and R.E. Dickinson, 1979: The role of stratospheric ozone in the zonal and seasonal energy balance of the Earth-troposphere system. *Journal of the Atmospheric Sciences*, 36, pp. 1084-1104.

Rancic, M., 1992: Semi-Lagrangian piecewise biparabolic scheme for two-dimensional horizontal advection of a passive scalar. *Monthly Weather Review*, 120, pp. 1394-1406.

Randall, D.A., Harshvardhan, and D.A. Dazlich, 1991: Diurnal variability of the hydrologic cycle in a general circulation model. *Journal of the Atmospheric Sciences*, 48, pp. 40-62.

Randall, D.A. and S. Tjemkes, 1991: Clouds, the Earth's radiation budget, and the hydrologic cycle. *Palaeogeography, Palaeoclimatology, Palaeoecology (Global and Planetary Change Section)*, 90, pp. 3-9.

Randall, D.A., 1989: Cloud parameterization for climate modeling: Status and prospects. *Atmospheric Research*, 23, pp. 345-361.

Rasmussen, R.A. and M.A.K. Khalil, 1986: Atmospheric trace gases: Trends and distributions over the last decade. *Science*, 232, pp. 1623-1624.

Rasmusson, E.M. and J.M. Wallace, 1983: Meteorological aspects of the El Niño/Southern Oscillation. *Science*, 222, pp. 1195-1203.

Rasmusson, E.M. and T.H. Carpenter, 1982: Variations in the tropical sea surface temperature and surface wind fields associated with the Southern Oscillation/El Niño. *Monthly Weather Review*, 110, pp. 354-384.

Raval, A. and V. Ramanathan, 1989: Observational determination of the greenhouse effect. *Nature*, 342, pp. 758-761.

Retallack, G.J., D.P. Dugas, and E.A. Bestland, 1990: Fossil soils and grasses of a middle miocene east African grassland. *Science*, 247, pp. 1325-1328.

Rind, D., N.K. Balachandran, and R. Suozzo, 1992: Climate change and the middle atmosphere, part II: The impact of volcanic aerosols. *Journal of Climate*, 5, pp. 189-208.

Rind, D., 1988: The doubled $CO_2$ climate and the sensitivity of the modeled hydrologic cycle. *Journal of Geophysical Research*, 93, pp. 5385-5412.

Rind, D., 1987: Components of the Ice Age circulation. *Journal of Geophysical Research*, 92, pp. 4241-4281.

Robock, A., 1991: The volcanic contribution to climate change of the past 100 years. In *Greenhouse Gas-Induced Climatic Change*. Edited by M.E. Schlesinger. Elsevier Science Publishers, New York.

Robock, A., 1979: The "Little Ice Age:" Northern Hemisphere average observations and model calculations. *Science*, 26, pp. 1402-1404.

Robock, A., 1978: Internally and externally caused climate change. *Journal of the Atmospheric Sciences*, 35, pp. 1111-1122.

Ropelewski, C.F. and M.S. Halpert, 1987: Global and regional scale precipitation patterns associated with the El Niño Southern Oscillation. *Monthly Weather Review*, 115, pp. 1606-1626.

Ropelewski, C.F., 1983: Spatial and temporal variations in Antarctic sea ice (1973-1982). *Journal of Climate and Applied Meteorology*, 22, pp. 470-473.

Rosen, R.D. and D.A. Salstein, 1985: Contribution of stratospheric winds to annual and semiannual fluctuations in atmospheric angular momentum and the length of day. *Journal of Geophysical Research*, 88, pp. 5451-5470.

Rosen, R.D. and D.A. Salstein, 1983: Variations in atmospheric angular momentum on global and regional scales and the length of day. *Journal of Geophysical Research*, 88, pp. 5451-5470.

Rosenberg, N., 1986: *Climate Change: A Primer*. Resources for the Future, Washington, D.C.

Running, S.W. and R.R. Nemani, 1988: Relating seasonal patterns of the AVHRR vegetation index to simulated photosynthesis and transpiration of forests in different climates. *Remote Sensing of Environment*, 24, pp. 347-367.

Sagan, C., O.B. Toon, and J.B. Pollack, 1979: Anthropogenic albedo changes and the Earth's climate. *Science*, 206, pp. 1363-1368.

Saltzman, B., 1985: Paleoclimate modeling. In *Paleoclimate Analysis and Modeling*. Edited by A.D. Hecht. John Wiley and Sons, New York, 445 pp.

Santer, B. and T.M.L. Wigley, 1990: Regional validation of means, variances, and spatial patterns in general circulation model control runs. *Journal of Geophysical Research*, 95, pp. 829-850.

Sato, N., P.J. Sellers, D.A. Randall, E.K. Schneider, J. Shukla, J.L. Kinter III, Y.-T. Hou, and E. Albertazzi, 1989: Effects of implementing the simple biosphere model in a general circulation model. *Journal of the Atmospheric Sciences*, 46, pp. 2757-2769.

Sausen, R., K. Barthel, and K. Hasselmann, 1988: Coupled ocean-atmosphere models with flux correction. *Climate Dynamics*, 2, pp. 145-163.

Schiffer, R.A. and S. Unninayer, 1991: *The Detection of Climate Change due to the Enhanced Greenhouse Effect: A Synthesis of Findings based on the GEDEX Atmospheric Temperature Workshop*. National Aeronautics and Space Administration, Washington, D.C., 52 pp.

Schimel, D.S., T.G.F. Kittel, and W.J. Parton, 1991: Terrestrial biogeochemical cycles: Global interactions with the atmosphere and hydrology. *Tellus*, 43, pp. 188-203.

Schlesinger, W.H., 1984: Soil organic matter: A source of atmospheric carbon dioxide. In *The Role of Terrestrial Vegetation in the Global Carbon Cycle*. Edited by G.M. Woodwell. SCOPE 23, John Wiley and Sons, Chichester, pp. 111-127.

Schlosser, P., G. Bonisch, M. Rhein, and R. Bayer, 1991: Reduction of deep water formation in the Greenland Sea during the 1980s: Evidence from tracer data. *Science*, 251, pp. 1054-1056.

Schmitt, C. and D.A. Randall, 1991: Effects of surface temperature and clouds on the $CO_2$ forcing. *Journal of Geophysical Research*, 96, pp. 9159-9168.

Schneider, S.H., 1990: The global warming debate heats up: An analysis and perspective. *Bulletin of the American Meteorological Society*, 71, pp. 1292-1304.

Schneider, S.H., 1988: The whole Earth dialogue. *Issues in Science and Technology*, IV, pp. 93-99.

Schneider, S.H. and R.L. Temkin, 1977: Water supply and the future climate: Climate, climatic change, and water supply. *Studies in Geophysics*, pp. 25-33.

Schneider, S.H., 1972: Cloudiness as a global feedback mechanism: The effects of the radiation balance and surface temperature of variations in cloudiness. *Journal of the Atmospheric Sciences*, 29, pp. 1413-1422.

SCOPE, 1986: *The Greenhouse Effect, Climatic Change, and Exosystems*. Edited by B. Bolin, B.R. Döös, J. Jäger, and R.A. Warrick. John Wiley and Sons, Chichester.

Sellers, P.J., 1987: Modeling effects of vegetation on climate. In *The Geophysiology of Amazonia*. Edited by R.E. Dickinson. Wiley and Sons, pp. 133-162.

Sellers, P.J., Y. Mintz, Y.C. Sud, and A. Dalcher, 1986: A simple biosphere model (SiB) for use within general circulation models. *Journal of the Atmospheric Sciences*, 43, pp. 505-531.

Semtner Jr., A.J. and R.M. Chervin, 1988: A simulation of the global ocean circulation with resolved eddies. *Journal of Geophysical Research*, 93, pp. 15502-15522.

Shine, K.P., R.G. Derwent, D.J. Wuebbles, and J.-J. Morcrette, 1990: Radiative forcing of climate. In *Climate Change: The IPCC Scientific Assessment*. Edited by J.T. Houghton, G.J. Jenkins, and J.J. Ephraums. Cambridge University Press, Cambridge, pp. 41-68.

Shukla, J., C. Nobre, and P.J. Sellers, 1990: Amazon deforestation and climate change. *Science*, 247, pp. 1322-1325.

Shukla, J. and J.M. Wallace, 1983: Numerical simulation of the atmospheric response to equatorial Pacific sea surface temperature anomalies. *Journal of the Atmospheric Sciences*, 40, pp. 1613-1630.

Slingo, A., 1989: A GCM parameterization for the shortwave radiative properties of water clouds. *Journal of the Atmospheric Sciences*, 46, pp. 1419-1427.

Slingo, A. and D.W. Pearson, 1987: A comparison of the impact of an envelope orography and of a parameterization of orographic gravity wave drag on model simulations. *Quarterly Journal of the Royal Meteorological Society*, 113, pp. 847-870.

Slingo, J.M., 1987: The development and verification of a cloud parameterization scheme for the ECMWF model. *Quarterly Journal of the Royal Meteorological Society*, 113, pp. 899-927.

Slingo, J.M., 1980: A cloud parameterization scheme derived from GATE data for use with a numerical model. *Quarterly Journal of the Royal Meteorological Society*, 108, pp. 747-770.

Smagorinsky, J., 1963: General circulation experiments with the primitive equations, 1: The basic experiment. *Monthly Weather Review*, 91, pp. 98-164.

Smith, E.A., T.H. Von der Haar, J.R. Hickey, and R. Maschhoff, 1986(b): The nature of the short period fluctuations in solar irradiance received by the Earth. *Climatic Change*, 5, pp. 211-235.

Sommerville, R.J. and L.A. Remer, 1984: Cloud optical thickness feedbacks in the $CO_2$ climate problem. *Journal of Geophysical Research*, 89, pp. 9668-9672.

Spencer, R.W. and J.R. Christy, 1990: Precise monitoring of global temperature trends from satellites. *Science*, 247, pp. 1558-1562.

Stern, W.F. and J.J. Ploshay, 1992: A scheme for continuous data assimilation. *Monthly Weather Review*, 120, pp. 1417-1432.

Stevens, C.M., A.E. Engelkeimer, and R.A. Rasmussen, 1990: The contribution of increasing fluxes of $CH_4$ from biomass burning in the southern hemisphere based on measurements of the temporal trends of the isotopic concentrations of atmospheric $CH_4$. In *Chapman Conference on Global Biomass Burning*. Edited by J.S. Levine. Williamsburg, Virginia.

Stocker, T.F., D.G. Wright, and L.A. Mysak, 1992: A zonally averaged, coupled ocean-atmosphere model for paleoclimate studies. *Journal of Climate*, 5, pp. 773-797.

Stommel, H. and E. Stommel, 1983: *Volcano Weather*. Seven Seas Press, Newport, Rhode Island, 177 pp.

Stouffer, R.J., S. Manabe, and K. Bryan, 1989: On the climate change induced by a gradual increase of atmospheric carbon dioxide. *Nature*, 342, pp. 660-662.

Suarez, M.J., 1985: A GCM study of the atmospheric response to tropical SST anomalies. In *Coupled Ocean-Atmosphere Models*. Edited by J.C.J. Nihoul. Elsevier Oceanography Series No. 40. Elsevier Science Publishers, Amsterdam, pp. 749-764.

Suarez, M.J., A. Arakawa, and D.A. Randall, 1983: The parameterization of the planetary boundary layer in the UCLA general circulation model: Formulation and results. *Monthly Weather Review*, 111, pp. 2224-2243.

Sud, Y.C. and M. Fennessy, 1982: A study of the influence of surface albedo on July circulation in semi-arid regions using the GLAS GCM. *Journal of Climate*, 2, pp. 105-125.

Tarpley, J.D., S.R. Schneider, and R.L. Money, 1984: Global vegetation indices from the NOAA-7 meteorological satellite. *Journal of Climate and Applied Meteorology*, 23, pp. 491-494.

Thornthwaite, C.W., 1948: An approach toward a rational classification of climate. *Geographical Review*, 38, pp. 55-74.

Tibaldi, S., T. Palmer, C. Brankovic, and U. Cubasch, 1989: Extended-range predictions with ECMWF models, II: Influence of horizontal resolution on systematic error and forecast skill. *ECMWF Technical Memorandum*, 152, pp. 1-39.

Tucker, C.J., I.Y. Fung, C.D. Keeling, and R.H. Gammon, 1986: Relationship between atmospheric $CO_2$ variations and satellite-derived vegetation index. *Nature*, 319, p. 195

Trepte, C.R. and M.H. Hitchman, 1992: Tropical stratospheric circulation deduced from satellite aerosol data. *Nature*, in press.

Twomey, S.A., 1977: *Atmospheric Aerosols*. Elsevier Science Publishers, Amsterdam.

Unninayar, S., 1986: Climate system monitoring. *The Science of the Total Environment*. Elsevier Science Publishers B.V., Amsterdam, pp. 55-65.

Unninayar, S., 1992: Personal communication.

Van Loon, H. and K. Labitzke, 1990: Association between the 11-year solar cycle and the atmosphere, part IV: The stratosphere, not grouped by the phase of the QBO. *Journal of Climate*, 3, pp. 827-837.

Van Loon, H. and K. Labitzke, 1988: Association between the 11-year solar cycle, the QBO, and the atmosphere, part II: Surface and 700mb in the Northern Hemisphere winter. *Journal of Climate*, 1, pp. 905-920.

Vinnikov, K.Ya., P.Ya. Groisman, K.M. Lugina, and A.A. Golubev, 1987: Variations in Northern Hemisphere mean surface air temperature over 1881-1985. In Russian. *Meteorology and Hydrology*, 1, pp. 45-53.

Walker, G.T. and E. Bliss, 1931: *World Weather V*. Royal Meteorological Society, IV, pp. 54-84.

Walker, G.T., 1923: *Correlation in Seasonal Variations of Weather, VIII: A Preliminary Study of World Weather*. Indian Meteorology Deposition, 24, pp. 75-131.

Walsh, J.E. and B. Ross, 1988: Sensitivity of 30-day dynamical forecasts to continental snow cover. *Journal of Climate*, 1, pp. 739-753.

Wang, W.-C., G.-Y. Shi, and J.T. Kiehl, 1991: Incorporation of the thermal radiative effect of $CH_4$, $N_2O$, $CF_2Cl_2$, and $CFCl_3$ into the National Center for Atmospheric Research community climate model. *Journal of Geophysical Research*, 96, pp. 9097-9103.

Wang, W.-C., M.P. Dudek, X.-Z. Liang, and J.T. Kiehl, 1991: Inadequacy of effective $CO_2$ as a proxy in simulating the greenhouse effect of other radiatively active gases. *Nature*, 350, pp. 573-577.

Warrick, R.A., H.H. Shugart, M.Ja. Antonovsky, J.R. Tarrant, and C.J. Tucker, 1986: The effects of increased $CO_2$ and climate change on terrestrial ecosystems. In *The Greenhouse Effect, Climate Change, and Ecosystems*. Edited by B. Bolin, B. Doos, J. Jager, and R. Warrick. SCOPE 29, John Wiley and Sons, London, pp. 363-392.

Washington, W.M. and G.A. Meehl, 1989: Climate sensitivity due to increased $CO_2$: Experiments with a coupled atmosphere-ocean general circulation model. *Climate Dynamics*, 4, pp. 1-38.

Washington, W.M. and C.L. Parkinson, 1986: *An Introduction to Three-Dimensional Climate Modeling*. University Science Books, Mill Valley, 422 pp.

Washington, W.M. and L. VerPlank, 1986: *A Description of Coupled General Circulation Models of the Atmosphere and Oceans Used for $CO_2$ Studies*. NCAR Technical Note, Boulder, Colorado.

Washington, W.M., A.J. Semtner, Jr., C.L. Parkinson, and L. Morrison, 1976: On the development of a seasonal change sea-ice model. *Journal of Physical Oceanography*, 6, pp. 679-685.

Washington, W.M., 1968: Computer simulation of the Earth's atmosphere. *Science Journal*, pp. 36-41.

Watts, R.G. and M. Morantine, 1990: Rapid climatic change and the deep ocean. *Climatic Change*, 16, pp. 83-97.

Webster, P.J. and R. Lucas, 1992: TOGA-COARE: The Coupled Ocean-Atmosphere Response Experiment. *Bulletin of the American Meteorological Society*, 73, pp. 1377-1416.

Webster, P.J., 1985: Great events, grand experiments: Man's study of the variable climate, part II: Prospects of a warming Earth. *Earth and Mineral Sciences*, 55, pp. 21-24.

Wigley, T.M.L. and P.M. Kelly, 1990: Holocene climatic change, $^{14}C$ wiggles, and variations in solar irradiance. *Philosophical Transactions of the Royal Society of London*, A330, pp. 547-560.

Wigley, T.M.L. and S.C.B. Raper, 1990: Future changes in global mean temperature and thermal expansion-related sea level rise. In *Climate and Sea Level Change: Observations, Projections, and Implications*. Edited by R.A. Warrick and T.M.L. Wigley. Cambridge University Press, Cambridge.

Wigley, T.M.L., 1989: Possible climatic change due to $SO_2$-derived cloud condensation nuclei. *Nature*, 339, pp. 365-367.

Wigley, T.M.L., 1988: The climate of the past 10,000 years and the role of the Sun. In *Secular Solar and Geomagnetic Variations in the Last 10,000 Years*. Edited by F.R. Stephenson and A.W. Wolfendale. Kluwer Publishers, pp. 209-224.

Wigley, T.M.L, P.D. Jones, and P.M. Kelly, 1986: Warm world scenarios and the detection of climate change induced by radiatively active gases. In *The Greenhouse Effect, Climate Change, and Ecosystems (SCOPE 29)*. Edited by B. Bolin, B.R. Doos, J. Jager, and R.A. Warrick. John Wiley and Sons, Chichester.

Wilks, D.S. and K.L. Eggleston, 1992: Estimating monthly and seasonal precipitation distributions using the 30- and 90-day outlooks. *Journal of Climate*, 5, pp. 252-259.

Williams, P.J.L., 1975: Biological and chemical aspects of dissolved organic matter in sea water. In *Chemical Oceanography*. Edited by J.P. Riley and G. Skirrow. Academic Press, London, pp. 301-363.

Williamson, D.L. and P.N. Swarztrauber, 1984: A numerical weather prediction model—Computational aspects of the CRAY-1. *Proceedings of IEEE*, 72, pp. 56-67.

Williamson, D.L., 1983: *Description of the NCAR Community Climate Model (CCMØB)*. NCAR Technical Report, NCAR/TN-210+STR, 88 pp.

Winkler, M.G., A.M. Swain, and J.E. Kutzbach, 1986: Middle holocene dry period in the northern midwestern United States: Lake levels and pollen stratigraphy. *Quaternary Research*, 25, pp. 235-250.

Working Group on Numerical Experimentation, 1988: *Proceedings of the Workshop on Systematic Errors in Models of the Atmosphere, Toronto, 19-23 September 1988*. WNN/TD Nos. 2 and 3, 382 pp.

World Meteorological Organization, 1991: *CAS/JSC Working Group on Numerical Experimentation: An Intercomparison of the Climates Simulated by 14 Atmospheric General Circulation Models*. World Climate Research Programme, 180 pp.

World Meteorological Organization, 1989: *Report of the NASA/WMO Ozone Trends Panel*. Global Ozone Research and Monitoring Project, Report No. 16, Geneva.

World Meteorological Organization, 1987: *Climate System Monitoring: The Global Climate System 1984-1986*. World Climate Data Programme contribution to the Global Environmental Monitoring System (GEMS), 87 pp.

World Meteorological Organization, 1985: *Atmospheric Ozone 1985: Assessment of Our Understanding of the Processes Controlling its Present Distribution and Change*. Report No. 16, Global Ozone Research and Monitoring Project.

World Meteorological Organization, 1985: *Climate System Monitoring: The Global Climate System 1982-1984*. World Climate Data Programme contribution to the Global Environmental Monitoring System (GEMS), 52 pp.

World Meteorological Organization, 1975: *The Physical Basis of Climate and Climate Modeling*. GARP Publication Series No. 16, reprint 1982, 265 pp.

World Meteorological Organization, 1972: *Parameterization of Sub-Grid Scale Processes*. GARP Publication Series No. 8, Geneva, 101 pp.

Wu, Xiangqian and W.L. Smith, 1992: Assimilation of ERBE data with a nonlinear programming technique to improve cloud-cover diagnosis. *Monthly Weather Review*, 120, pp. 2009-2024.

Wuebbles, D.J., 1992: Global climate change due to radiatively active gases. In *Global Atmospheric Chemical Change*. Edited by C.H. Hewitt and W.T. Sturges. Elsevier Science Publishers, Essex.

Wuebbles, D.J., K.E. Grant, P.S. Connell, and J.E. Penner, 1989: The role of atmospheric chemistry in climate change. *APCA Journal*, 39, pp. 22-28.

Wyrtki, K., 1986: Fluctuations in upper layer volume or near surface upper oceanic heat content. *WMO/CSM Bulletin*, 1986-3.

Wyrtki, K., 1985: *Water Displacements during 1982-83 and the Genesis of El Niño and the Southern Oscillation*. International Conference on the TOGA Scientific Programme. WCRP Report No. 4, section III, pp. 1-10.

Xue, Y., P.J. Sellers, J.L. Kinter, and J. Shukla, 1991: A simplified biosphere model for global climate studies. *Journal of Climate*, 4, pp. 345-364.

Zebiak, S.E. and M.A. Cane, 1987: A model El Niño-Southern Oscillation. *Monthly Weather Review*, 115, pp. 2262-2278.

Zimmerman, P.R., J.P. Greenberg, S.O. Wandiga, and P.J. Crutzen, 1982: Termites: A potentially large source of atmospheric methane, carbon dioxide, and molecular hydrogen. *Science*, 218, pp. 563-565.

Zwally, H.J., 1989: Growth of the Greenland ice sheet: Interpretation. *Science*, 246, pp. 1589-1591.

# *Global Climate Modeling Workshop Participants List November 13-15, 1991*

James Albritton
Lawrence Livermore National Laboratory
Livermore, California 94550
(510) 422-5446

Robert M. Atlas
NASA/Goddard Space Flight Center
Code 910.4
Greenbelt, Maryland 20771
(301) 286 3604

David Bader
PNL/Department of Energy
ER-76
Washington, DC 20545
(301) 903-4328

Wayman Baker
NOAA/NMC
Development Division
World Weather Building, Rm 204
5220 Auth Road
Camp Springs, Maryland 20746
(301) 763-8005

John R. Bates
NASA/Goddard Space Flight Center
Code 910.3
Greenbelt, Maryland 20771
(301) 286-1445

Thomas Bell
NASA/Goddard Space Flight Center
Code 913
Greenbelt, Maryland 20771
(301) 286-8805

Kenneth Bergman
NASA Headquarters
Code YSM
Washington, DC 20546
(202) 358-0765

Kirk Bryan
GFDL/NOAA
Princeton University
Forrestal Campus
US Route 1, Box 308
Princeton, New Jersey 08542
(609) 452-6530

Antonio Busalacchi
NASA/Goddard Space Flight Center
Code 970
Greenbelt. Maryland 20771
(301) 286-6171

Dennis Chesters
NASA/Goddard Space Flight Center
Code 913
Greenbelt. Maryland 20771
(301) 286-9007

David Crisp
Jet Propulsion Laboratory
California Institute of Technology
4800 Oak Grove Drive
Mail Stop 169-237
Pasadena, California 91109
(818) 354-2224

J. Cullen
General Accounting Office
Washington, DC
(202) 275-3644

Robert E. Dickinson
University of Arizona
Dept. of Atmospheric Sciences
Room 542, PAS Building
Tucson, Arizona 85721
(609) 621-2810

Franco Einaudi
NASA/Goddard Space Flight Center
Code 910
Greenbelt, Maryland 20771
(301) 286-5002

Dara Entekhabi
Massachusetts Institute of Technology
Department of Civil Engineering
Building 48-321
Cambridge, Massachusetts 02139
(617) 253-9698